UNIVERSITÀ DEGLI STUDI DI PADOVA

Dipartimento di Scienze Farmaceutiche

Scuola di Dottorato in Scienze Molecolari
Indirizzo Scienze Farmaceutiche

XXII Ciclo

Plant Food Allergens

Purification and Characterisation of the Ses i 2 Major Allergen from *Sesamum indicum*
Structure-Stability-Allergenicity Relationships of Native and Methionine-Oxidised Species

Direttore della Scuola: Ch.mo Prof. Maurizio CASARIN
Coordinatore di indirizzo: Ch.mo Prof.ssa Adriana CHILIN
Supervisore:Ch.mo Prof. Vincenzo DE FILIPPIS

Dottoranda: Daniela Galla

UNIVERSITY OF PADUA

Department of Pharmaceutical Sciences

Ph.D. School in Molecular Sciences
Pharmaceutical Sciences Curriculum

XXII Cycle

Plant Food Allergens

Purification and Characterisation of the Ses i 2 Major Allergen from *Sesamum indicum*
Structure-Stability-Allergenicity Relationships of Native and Methionine-Oxidised Species

School Director: Prof. Maurizio CASARIN
Curriculum Coordinator: Prof. Adriana CHILIN
Supervisor: Prof. Vincenzo DE FILIPPIS

Ph.D Student: Daniela Galla

Ai miei genitori

Contents

Riassunto

Il termine allergia viene utilizzato per indicare una reazione immunitaria esagerata dell'organismo contro una sostanza innocua presente nell'ambiente, (quali sono gli allergeni da contatto, da ingestione e da inalazione), la quale causa sintomi patologici in soggetti predisposti. La fisiopatologia della risposta allergica coinvolge una fase detta di sensibilizzazione che si sviluppa immediatamente dopo la prima esposizione all'allergene ed una fase tardiva nella quale vengono sostanzialmente prolungati i sintomi della risposta allergica con conseguente danno tissutale.

I dati epidemiologici indicano che più del 20% della popolazione mondiale soffre di malattie allergiche IgE-mediate causate da allergeni di diversa origine. In particolare, l'allergia alimentare affligge il 2% della popolazione mondiale adulta e circa l'8% della popolazione mondiale al di sotto dei tre anni di vita.

Gli allergeni da piante sono classificati in famiglie e superfamiglie proteiche sulla base delle loro caratteristiche strutturali e conformazionali. Il gruppo più diffuso di proteine vegetali è classificato nelle *seed storage proteins* in cui si possono ritrovare gli allergeni della superfamiglia delle cupine e delle prolamine. La superfamiglia delle cupine include le proteine allergeniche di accumulo nei semi della classe delle viciline e legumine presenti nella soia, nelle arachidi e noci. La superfamiglia delle prolamine include molti importanti allergeni nei legumi, nelle noci, cereali, frutta e verdura, i quali sono suddivisi nelle classi delle: 2S albumine, *nonspecific lipid transfer protein*, α-amilasi dei cereali e inibitori delle proteasi. La ricerca clinica ha dimostrato interesse crescente per la classe delle 2S albumine le quali sono state descritte come allergeni maggiori in un numero elevato di piante alimentari.

Chiaramente gli allergeni alimentari, per indurre risposta allergica, devono evitare i processi proteolitici intraluminali ed intracellulari e raggiungere le cellule immunocompetenti nella lamina propria, ma i meccanismi mediante i quali gli allergeni aggirano il fenomeno di tolleranza e inducono la produzione di IgE specifiche sono ancora sconosciuti. Inoltre, mancano informazioni chiave sulle caratteristiche strutturali degli allergeni alimentari che risultano essere determinanti nello sviluppo di una risposta immunitaria piuttosto che dei meccanismi di tolleranza.

Esiste una sostanziale differenza nella capacità di indurre una risposta immunitaria specifica tra un antigene ed un immunogeno. L'antigenicità è l'abilità di una sostanza di combinarsi in modo specifico con i prodotti finali del sistema immunitario (anticorpi e/o recettori di

membrana). Sebbene tutte le molecole immunogene possiedano proprietà antigeniche non è possibile affermare il contrario, infatti, l'immunogenicità è definita come l'abilità di una sostanza detta immunogeno di indurre una risposta specifica umorale e/o cellulo-mediata. L'immunogenicità non è una proprietà intrinseca di un antigene, ma dipende dal sistema biologico con cui l'antigene stesso entra in contatto.

In questo lavoro abbiamo studiato l'allergene maggiore da semi di sesamo Ses i 2 (Q9XHP1) che rappresenta un modello adeguato per investigare le caratteristiche strutturali e conformazionali associate agli allergeni alimentari

In questo lavoro, abbiamo purificato in quantità sufficiente (10-30 mg) l'allergene maggiore da semi di sesamo (*S. indicum*) Ses i 2 per successivi studi strutturali e conformazionali. Durante i nostri studi sono stati ottenuti una grande quantità di dati chimici e strutturali che sono confluiti in un modello strutturale per omologia di Ses i 2. Il modello mostra la tipica struttura delle 2S albumine con quattro segmenti alpha-elicoidali a formare un *core* idrofobico compatto organizzato in una architettura *up-and-down*. La struttura globulare di Ses i 2 è stabilizzata da cinque ponti disolfuro, in particolare otto residui di Cys sono conservati nella famiglia delle prolamine. Ses i 2 mostra, inoltre una straordinaria stabilità verso la denaturazione chimica e termica, associata a una forte resistenza alla proteolisi dei principali enzimi gastrointestinali, lisosomiali, di matrice e della coagulazione. Queste osservazioni permettono di ipotizzare un assorbimento della proteina in forma intatta a livello intestinale. Alla luce di queste considerazioni la derivatizzazione chimica di Ses i 2 con un *label* fluorescente come la fluoresceina isotiocianato è stata eseguita con l'intento di esplorare l'internalizzazione cellulare dell'allergene mediante analisi di immunofluorescenza. Per evidenziare l'internalizzazione cellulare, il coniugato Ses i 2-[F] è stato incubato con cellule Caco-2, che in specifiche condizioni formano un mostrato simile all'epitelio intestinale. I dati raccolti dimostrano che Ses i 2 viene assorbito attraverso un processo endocitotico e questa informazione associata alla resistenza agli enzimi lisosomiali permette di ipotizzare una interazione di Ses i 2 in forma intatta con le cellule dendritiche nella lamina propria.

L'immunogenicità è fortemente dipendente dagli effettori che l'antigene incontra, in particolare nei siti di infiammazione i processi ossidativi giocano un ruolo fondamentale nella degradazione dell'antigene. Nei siti dell'infiammazione, H_2O_2 e HOCl sono i principali ossidanti prodotti e possiedono l'abilità di reagire con una vasta gamma di macromolecole e nelle proteine il residuo amminoacidico più sensibile all'ossidazione è la metionina. Sorprendentemente, la sequenza amminoacidica di Ses i 2 è particolarmente abbondante in Met (circa 16%), quindi in questo lavoro abbiamo investigato le conseguenze strutturali del

danno ossidativo che si sviluppa in molte condizioni patologiche nelle quali è coinvolta l'infiammazione. I residui di metionina sono stati selettivamente ossidati in presenza di H_2O_2 ed del sistema mieloperossidasico. In questo lavoro, abbiamo dimostrato che Ses i 2 è fortemente stabilizzata da un *core* idrofobico di 9 Met, questa osservazione è risultata essere in stretto accordo con la drammatica alterazione strutturale e conformazionale indotta dall'ossidazione selettiva dei residui di Met in Ses i 2. Il forte effetto dell'ossidazione sulla stabilità di Ses i 2 ha suggerito un coinvolgimento del meccanismo ossidativo nella modulazione della risposta immunitaria. Nel sito della risposta immunitaria, l'ossidazione delle proteine allergeniche può rappresentare un passaggio critico nella difesa tissutale, nella risposta immunospecifica e nella risposta allergica. Alterazioni in questo meccanismo a livello dei processi ossidativi seguiti dai processi proteolitici operati dalle cellule immunocompetenti potrebbero giocare un ruolo chiave nell'indurre la risposta allergica. Per confermare questa ipotesi abbiamo studiato l'effetto di Ses i 2 e Ses i 2-ox su cellule dendritiche umane. Sorprendentemente, Ses i 2 induce una forte produzione di IL-10 con una diminuzione nell'espressione di IL-12p70, la più importante citochina nello sviluppo della risposta Th1. Contrariamente, Ses i 2-ox non è in grado di aumentare l'espressione di IL-10 e questo è correlato con la forte produzione di IL-12p70 da parte delle DCs. Ses i 2 e Ses i 2-ox hanno dimostrato un scarsa capacità di stimolare l'espressione delle molecole co-stimolatorie CD80 e CD86, mentre HLA è aumentato in presenza di Ses i 2-ox. Nell'insieme questi dati suggeriscono che Ses i 2 non è in grado di indurre una risposta Th1, mentre Ses i 2-ox, stimolando la produzione di IL-12p70 e l'espressione di HLA è capace di indurre una risposta Th1-self. Questi risultati sostengono l'ipotesi che il danno ossidativo e la processazione proteolitica di una antigene siano fortemente correlati nel determinarne l'immunogenicità.

Da ultimo, abbiamo utilizzato la cristallografia a raggi-X con l'intento di risolvere la struttura di Ses i 2. Durante i nostri studi sono stati ottenuti cristalli che sottoposti a misurazione hanno fornito dei set di dati di diffrazione, ma al momento non hanno permesso una analisi strutturale completa della proteina.

Abstract

The term allergy is used to describe an abnormal immune response to harmless environmental substance (i.e., contact, ingestion and airborne allergens), that causes pathological symptoms in a predisposed subject. The pathophysiology of allergic responses involves a “sensitization phase”, that occurs immediately after exposure to the allergen, and "late phase reaction", which can substantially prolong the symptoms of the allergic response and result in tissue damage. Epidemiological data indicate that over 20% of the world population suffers from IgE-mediated allergic diseases caused by allergens from different sources. In particular, food allergies affect 2% of adults and up to 8% of the children under three years.

Plant food allergens can be classified into families and superfamilies on the basis of their structural and functional properties. The most widespread groups of plant proteins is classified into seed storage proteins, that contain allergens are the cupin and prolamin superfamilies. The cupin superfamily includes allergenic seed storage proteins of the vicilin and legumin type present in soybeans, peanuts, and tree nuts. The prolamin superfamily includes several important types of allergens of legumes, tree nuts, cereals, fruits, and vegetables, such as the 2S albumin, the nonspecific lipid transfer proteins, and the cereal α-amylase and protease inhibitors. The 2S albumins are becoming of increasing interest in clinical research as they have been described as the major allergen in a number of plant foods.

Although it is clear that food antigens, to produce allergy, must avoid intraluminal and intracellular degradation by proteases, reach immuno-competent cells in the intestinal lamina propria, circumvent immunological unresponsiveness and trigger specific IgE production, the path followed by many food allergens remains elusive. In addition we are lacking key information on the structural characteristic of food allergens that favour the development of an immune response rather than inducing tolerance (i.e., a T_{H1}-type response). A substantial difference in the capacity to induce a specific immune response exists among antigen and immunogen. Antigenicity is the ability to combine specifically with the final products of the immune system (i.e., antibodies, and/or cell-surface receptor). Although all molecules that have the property of immunogenicity also have the property of antigenicity, the reverse is not true. Immunogenity is the ability to induce a humoral and/or cell-mediated specific response. Immunogenicity is not an intrinsic property of an antigen but rather depends on the particular biological system that the antigen encounters.

In this work, we have studied the major allergen from sesame seed Ses i 2 (SwissProt code Q9XHP1), this allergen represents a suitable model to investigate the structural and conformational features associated to food allergens.

In this study, we have purified sufficiently large amounts (10-30 mg) of Ses i 2 the major allergen from sesame seed (*S. indicum*) for subsequent chemical, conformational and stability characterization.

Overall, we have collected great ensemble of chemical and structural data that were combined to define an homology structural model of Ses i 2. Our model shows a typical structural features of 2S albumins such as a four helical segments forming a compact hydrophobic core organised in a “up and down” architecture. The globular fold of Ses i 2 is stabilised by five disulfide bridges in particular, eight of the ten Cys-residues of Ses i 2 are conserved in prolamin superfamily. Ses i 2 manifests an extraordinary stability towards chemical and thermal denaturation, associated with a strong resistance to proteolysis to the main gastrointestinal, blood, lysosomal and matrix proteases. These observations suggest that Ses i 2 can be absorbed in gut epithelium in intact form. At the light of these considerations the chemical derivatization of Ses i 2 with a fluorescent label such as fluorescein isothiocyanate was performed with the intent to explore the allergen cellular uptake by immunohistochemical analysis. Ses i 2-[F] was incubated with Caco-2 cell line that in specific culture condition is able to form a monolayer similar to gut epithelium. Collected data demonstrate that Ses i 2 is absorbed by an endocytosis uptake pathway and this finding associated with the resistance to lysosomal enzymes suggests that Ses i 2 may interact in intact form with dendritic cells in the lamina propria. Immunogenicity strongly depends by effectors of immune response that antigen encounters, in particular in the inflammation site the oxidative mechanisms play a pivotal role in antigen degradation. In inflammation sites, H_2O_2 and HOCl are the major oxidants produced and they are highly reactive with the proteins in which methionine is one of the most oxidant-sensitive amino acid residues.

Strikingly, Ses i 2 amino acids sequence is particularly abundant in Met-resiudes (~16%) thus during this work we investigated the structural consequences of oxidative damage that occurs in several pathological states in which inflammatory processes are involved. Methionine residues in Ses i 2 are selectively oxidized in the presence of H_2O_2 and the myeloperoxidase system. In our study, we demonstrated that Ses i 2 is strongly stabilized by a hydrophobic core characterised by nine methionine residues, this observation is in agreement with the dramatic structural and conformational alterations induced by the selective oxidation of Met residues of Ses i 2. The strong effect of oxidation on stability properties of Ses i 2

suggested an involvement of the oxidative mechanism in the modulation of immune response. In the site of immune response, oxidation of protein allergens may represent a critical step in tissue defence, immunospecific response and allergic reactions. Alterations in this pathway in the oxidation step, followed by the proteolytic processing operated by immunocompetent cells might play a key role to induce allergic response. In order to confirm this hypothesis we have studied the effect on human DCs in the presence of native and oxidized protein. Surprisingly, Ses i 2 induces a strong production of IL-10 with a decrease in the IL-12p70 expression, that is the most important cytokine in the develop of Th1 response. Conversely, Ses i 2-ox is not able to rise the expression of IL-10 and this behaviour is correlated with a strong enhancement of the IL-12p70 production. Ses i 2 and Ses i 2-ox demonstrated a low capacity to simulate the expression of co-stimulatory molecules CD80 and CD86, while HLA is up-regulated in the presence of Ses i 2-ox. Overall data suggest that Ses i 2 is no able to induce a Th1 response, while Ses i 2-ox through the dual stimulation of IL-12p70 and HLA expression is able to produce a Th1 “self-response”. These results corroborate the hypothesis whereby the oxidative damage and proteolytic process are strongly correlated to determine the immunogenicity of an antigen.

Finally, we used the x-ray crystallography approach with the aim to solve the crystal structure of Ses i 2. In our trials we obtained small crystals of Ses i 2 and preliminary diffraction data have been measured. Unfortunately, the quality of the data was not good enough to allow us to determine the structure of the Ses i 2 allergen.

1. INTRODUCTION

Chapter 1.1

ALLERGY

The term allergy is used to describe an abnormal immune response to harmless environmental substance (i.e., contact, ingestion and airborne allergens), that causes pathological symptoms in a predisposed subject. Allergic disorders have been described as far back as 3000 B.C., when King Menes, who ruled Egypt, was killed by a hornet. Greek scholars described the clinical symptoms of asthma, although this encompassed different types of breathing problem. The term allergy, meaning 'changed reactivity', was originally defined by Clemens von Priquet in 1906 as an altered capacity of the body to react to foreign substances. In the subsequent years, the mechanisms of anaphylactic reaction were further expanded by the experiments of Shultz and Dale on intestinal and uterine smooth muscles. Cellular involvement in the process of anaphylaxis was proposed; it was stated that the small amounts of antibody required were in fact affixed to the surface of appropriate target cells, and any subsequent interaction would result in cell damage and a consequent shock-like syndrome (Ahrsad et al., 2001).

More than 25% of the population in industrialized countries suffers from immunoglobulin-E-mediated allergies. Generally, allergic diseases are caused by altered immunological defences and tolerance mechanisms, and unleash pathological responses ranging from vasodilatation to severe anaphylactic shock. Effectors that act to remove antigen by various mechanisms induce a localized inflammatory response without extensively damaging the host's tissue. Under certain circumstances, however, this inflammatory response can have deleterious effects, resulting in significant tissue damage or even death. This inappropriate immune response is termed hypersensitivity or allergy**.** Although the word *hypersensitivity* implies an increased response, the response is not always heightened but may, instead, be an inappropriate immune response to an antigen. Hypersensitive reactions may develop in the course of either humoral or cell-mediated responses. We currently refer to anaphylactic reactions within the humoral branch initiated by antibody or antigen-antibody complexes as immediate hypersensitivity, because the symptoms are manifest within minutes or hours after a sensitized recipient encounters antigen. Delayed-type hypersensitivity (DTH) is so named in recognition of the delay of symptoms until days after exposure.

A type I hypersensitive reaction is induced by certain types of antigens referred to as allergens, and has all the hallmarks of a normal humoral response. That is, an allergen induces a humoral antibody response by the same mechanisms for other soluble antigens, resulting in the generation of antibody-secreting plasma cells and memory cells. What distinguishes a type I hypersensitive response from a normal humoral response is that the plasma cells secrete IgE. The majority of humans mount significant IgE responses only as a defense against parasitic infections. After an individual has been exposed to a parasite, serum IgE levels increase and remain high until the parasite is successfully cleared from the body. Some persons, however, may have an abnormality called atopy, a hereditary predisposition to the development of immediate hypersensitivity reactions against common environmental antigens. The IgE regulatory defects suffered by atopic individuals allow nonparasitic antigens to stimulate inappropriate IgE production, leading to tissue damaging type I hypersensitivity. Most allergic IgE responses occur on mucous membrane surfaces in response to allergens that enter the body by either inhalation or ingestion.

The pathophysiology of allergic responses involves a “sensitization phase”, that occurs immediately after exposure to an allergen, and a “elicitation phase” reaction, which can substantially prolong the symptoms of the response and result in tissue damage. Serum IgE levels in normal individuals fall within the range of 0.1–0.4 μg/ml; even the most severely allergic individuals rarely have IgE levels greater than 1 μg/ml. IgE was found to be composed of two heavy ε and two light chains with a combined molecular weight of 190,000. The higher molecular weight as compared with IgG (150,000) is due to the presence of an additional constant-region domain. This additional domain (CH4) contributes to an altered conformation of the Fc portion of the molecule that enables it to bind to glycoprotein receptors on the surface of basophils and mast cells. Although the half-life of IgE in the serum is only 2–3 days, once IgE has been bound to its receptor on mast cells and basophils, it is stable in that state for a number of weeks.

This class of antibody binds with high affinity to Fc receptors on the surface of tissue mast cells and blood basophils. Mast cells and basophils coated by IgE are said to be sensitized. Basophils are granulocytes that circulate in the blood of most vertebrates; in humans, they account for 0.5%–1.0% of the circulating white blood cells. Mast cells are found throughout connective tissue, particularly near blood and lymphatic vessels. Some tissues, including the skin and mucous membrane surfaces of the respiratory and gastrointestinal tracts, contain high concentrations of mast cells; skin, for example, contains 10,000 mast cells per mm3. A later exposure to the same allergen cross-links the membrane-bound IgE on sensitized mast

cells and basophils, causing degranulation of these cells. The reaginic activity of IgE depends on its ability to bind to a receptor specific for the Fc region of the ε heavy chain. Two which are expressed by different cell types and differ by 1000- fold in their affinity for IgE. Mast cells and basophils express FcεRI, which binds IgE with a high affinity. The other IgE receptor, designated FcεRII (or CD23), is specific for the CH3/ CH3 domain of IgE and has a lower affinity. Allergen crosslinkage of IgE bound to FcεRII has been shown to activate B cells, alveolar macrophages, and eosinophils. When this receptor is blocked with monoclonal antibodies, IgE secretion by B cells is diminished. IgE-mediated degranulation begins when an allergen crosslinks IgE that is bound (fixed) to the Fc receptor on the surface of a mast cell or basophil. In itself, the binding of IgE to FcεRI apparently has no effect on a target cell. It is only after allergen crosslinks the fixed IgE-receptor complex that degranulation proceeds. The importance of crosslinkage is indicated by the inability of monovalent allergens, which cannot crosslink the fixed IgE, to trigger degranulation. Although crosslinkage is normally effected by the interaction of fixed IgE with divalent or multivalent allergen, it also can be effected by a variety of experimental means that bypass the need for allergen and in some cases even for IgE. The cytoplasmic domains of FcεRI are associated with protein tyrosine kinases (PTKs). Crosslinkage of the FcεRI receptors activates the associated PTKs, resulting in the phosphorylation of tyrosines within the ITAMs. These phosphorylation events induce the production of a number of second messengers that mediate the process of degranulation. The Ca^{2+} increase eventually leads to the formation of arachidonic acid, which is converted into two classes of potent mediators: prostaglandins and leukotrienes. The increase of Ca^{2+} also promotes the assembly of microtubules and the contraction of microfilaments, both of which are necessary for the movement of granules to the plasma membrane. Mast cell populations in different anatomic sites differ significantly in the types and amounts of allergic mediators they contain and in their sensitivity to activating stimuli and cytokines. Mast cells also secrete a large variety of cytokines that affect a broad spectrum of physiologic, immunologic, and pathologic processes.

The clinical manifestations of type I hypersensitive reactions are related to the biological effects of the mediators released during mast-cell or basophil degranulation. These mediators are pharmacologically active agents that act on local tissues as well as on populations of secondary effector cells, including eosinophils, neutrophils, T lymphocytes, monocytes, and platelets. The mediators thus serve as an amplifying terminal effector mechanism, much as the complement system serves interaction. The mediators can be classified as either primary or secondary. The primary mediators are produced before degranulation and are stored in the

granules. The most significant primary mediators are histamine, proteases, eosinophil chemotactic factor, neutrophil chemotactic factor, and heparin. Histamine, which is formed by decarboxylation of the amino acid histidine, is a major component of mast-cell granules, accounting for about 10% of granule weight. Because it is stored in the granules, its biological effects are observed within minutes of mast-cell activation. Once released from mast cells, histamine initially binds to specific receptors on various target cells. Three types of histamine receptors-designated H1, H2, and H3 have been identified; these receptors have different tissue distributions and mediate different effects when they bind histamine. Most of the biologic effects of histamine in allergic reactions are mediated by the binding of histamine to H1 receptors. This binding induces contraction of intestinal and bronchial smooth muscles, increased permeability of venules, and increased mucus secretion by goblet cells. Interaction of histamine with H2 receptors increases vasopermeability and dilation and stimulates exocrine glands. Binding of histamine to H2 receptors on mast cells and basophils suppresses degranulation; thus, histamine exerts negative feedback on the release of mediators.

The secondary mediators either are synthesized after target-cell activation or are released by the breakdown of membrane phospholipids during the degranulation process. The secondary mediators include platelet-activating factor, leukotrienes, prostaglandins, bradykinins, and various cytokines.

The leukotrienes mediate bronchoconstriction, increased vascular permeability, and mucus production. Prostaglandin D2 causes bronchoconstriction. The contraction of human bronchial and tracheal smooth muscles appears at first to be mediated by histamine, but, within 30–60 s, further contraction is mediated by the leukotrienes and prostaglandins. Being active at nanomole levels, the leukotrienes are as much as 1000 times more potent as bronchoconstrictors than histamine is, and they are also more potent stimulators of vascular permeability and mucus secretion.

As a type I hypersensitive reaction begins to subside, mediators released during the course of the reaction often induce localized inflammation called the late-phase reaction. Distinct from the late response seen in asthma, the late-phase reaction begins to develop 4–6 h after the initial type I reaction and persists for 1–2 days. The reaction is characterized by infiltration of neutrophils, eosinophils, macrophages, lymphocytes, and basophils. The localized late-phase response also may be mediated partly by cytokines released from mast cells. Both TNF-α and IL-1 increase the expression of cell-adhesion molecules on venular endothelial cells, thus facilitating the buildup of neutrophils, eosinophils, and monocytes that characterizes the late-phase response.

Eosinophils play a principal role in the late-phase reaction, accounting for some 30% of the cells that accumulate. Eosinophil chemotactic factor, released by mast cells during the initial reaction, attracts large numbers of eosinophils to the affected site. Various cytokines released at the site, including IL-3, IL-5, and GM-CSF, contribute to the growth and differentiation of the eosinophils. Eosinophils express Fc receptors for IgG and IgE isotypes and bind directly to antibody-coated allergen. Much as in mast-cell degranulation, binding of antibody-coated antigen activates eosinophils, leading to their degranulation and release of inflammatory mediators, including leukotrienes, major basic protein, platelet-activation factor, eosinophil cationic protein (ECP), and eosinophil-derived neurotoxin. The release of these eosinophil-derived mediators may play a protective role in parasitic infections. However, in response to allergens, these mediators contribute to extensive tissue damage in the late-phase reaction.

Neutrophils are another major participant in late-phase reactions, accounting for another 30% of the inflammatory cells. the bone marrow releases more than the usual number of neutrophils and these cells generally are the first to arrive at a site of inflammation. Neutrophils are attracted to the area of a type I reaction by neutrophil chemotactic factor, released from degranulating mast cells, that promote accumulation of neutrophils at an inflammatory site. In addition, a variety of cytokines released at the site, including IL-8, have been shown to activate neutrophils, resulting in release of their granule contents, including lytic enzymes, platelet-activating factor, and leukotrienes. Neutrophils also employ both oxygen-dependent and oxygen-independent pathways to generate antimicrobial substances.

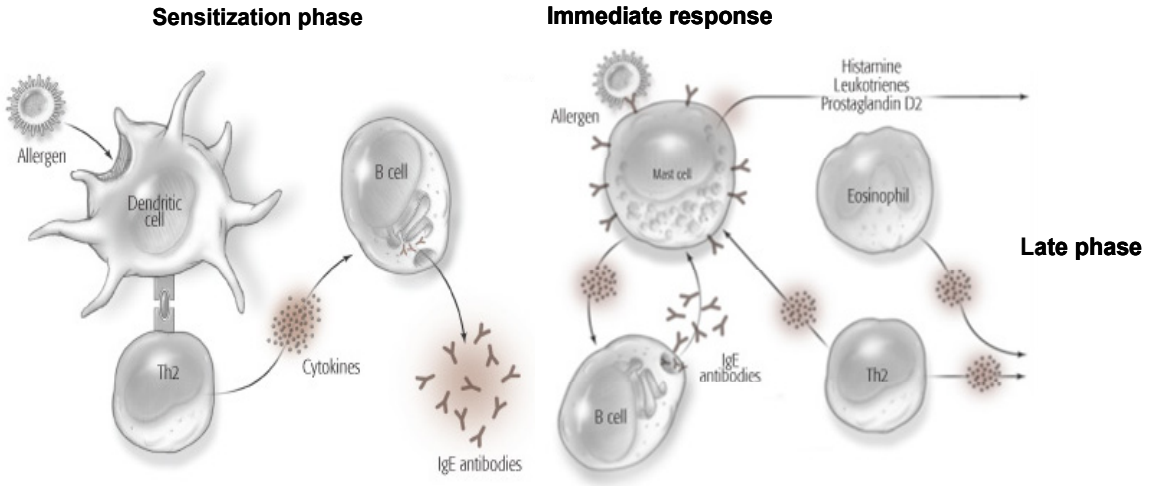

Figure 1. General mechanism underlying a allergy reaction. Exposure to an allergen activates dendritic cells that interact with lymphocytes T. the activation of Th2 subpopulation of T cells induces B cells to form IgE. The secreted IgE molecules bind to IgE specific Fc receptors on mast cells and blood basophils. (Many molecules of IgE with various specificities can bind to the IgE-Fc receptor.). Second exposure to the allergen leads to crosslinking of the bound IgE, triggering the release of pharmacologically active mediators, vasoactive amines, from mast cells and basophils. The mediators cause smooth-muscle contraction, increased vascular permeability, and vasodilation.

Neutrophils are in fact much more likely than macrophages to kill ingested microorganisms. Neutrophils exhibit a larger respiratory burst than macrophages and consequently are able to generate more reactive oxygen intermediates and reactive nitrogen intermediates.
The clinical manifestations of type I reactions can range from life-threatening conditions, such as systemic anaphylaxis and asthma, to hay fever and eczema, which are merely annoying.

Systemic Anaphylaxis and Localized Anaphylaxis (ATOPY)

Systemic anaphylaxis is a shock-like and often fatal state whose onset occurs within minutes of a type I hypersensitive reaction. A wide range of antigens have been shown to trigger this reaction in susceptible humans, including the venom from bee, wasp, hornet, and ant stings; drugs, such as penicillin, insulin, and antitoxins; and seafood and nuts. If not treated quickly, these reactions can be fatal. Epinephrine is the drug of choice for systemic anaphylactic reactions. Epinephrine counteracts the effects of mediators such as histamine and the leukotrienes by relaxing the smooth muscles and reducing vascular permeability. Epinephrine also improves cardiac output, which is necessary to prevent vascular collapse during an anaphylactic reaction. In addition, epinephrine increases cAMP levels in the mast cell, thereby blocking further degranulation.
In localized anaphylaxis, the reaction is limited to a specific target tissue or organ, often involving epithelial surfaces at the site of allergen entry. The tendency to manifest localized anaphylactic reactions is inherited and is called *atopy.* Atopic allergies, which afflict at least 20% of the population in developed countries, include a wide range of IgE-mediated disorders, including allergic rhinitis (hay fever), asthma, atopic dermatitis (eczema), and food allergies.

Chapter 1.2

ALLERGENS

The term *allergen* refers specifically to non-parasitic antigens capable of stimulating type I hypersensitive responses in allergic individuals. Although most allergens are small proteins or protein-bound substances having a molecular weight between 15,000 and 40,000, attempts to identify some common chemical property of these antigens have failed. It appears that allergenicity is a consequence of a complex series of interactions involving not only the allergen but also the dose, the sensitizing route, sometimes an adjuvant.

Semantically, the concept of allergenicity is ill defined. To a clinical allergist, allergenicity reflects the capacity of an antigen to induce symptoms or a skin reaction, whereas to an immunologist, it reflects either a peculiar type of immunogenicity (ie, the capacity of a protein to induce IgE antibodies) or simply the capacity to bind IgE antibodies. Similarly, the term *allergen* is used to describe two or three distinct molecular properties: the property to sensitize (ie, induce the immune system to produce high-affinity antibodies, particularly of the IgE class) and the property to elicit an allergic reaction (ie, to trigger allergic symptoms in a sensitized subject). Moreover, it is also used to indicate the property to bind IgE antibodies. Complete allergens have all these properties. Some proteins, however, are known to elicit allergic symptoms but do not usually sensitize.

Determinants of Allerginicity

Aspects of protein structure likely to be relevant for allergenicity are solubility, stability, size, and the compactness of the overall fold. These aspects reflect dependency

of allergenicity on transport over mucosal barriers and susceptibility to proteases. Size and solubility of the intact protein would be relevant factors for airborne allergens more than for food allergens (for which limited proteolysis might enhance mucosal transport and hence allergenicity) or parenteral antigens, such as insect venoms, insect salivary allergens, invasive organisms (helminths and fungi), vaccines, or therapeutic proteins.

Posttranslational modification may affect allergenicity in different ways. It may induce new epitopes and it may affect solubility, stability, size, and susceptibility toward proteases. Moreover, uptake and processing by antigen-presenting cells are also known to be markedly

influenced. Although glycosylation affects many of these processes, it is not a critical factor for allergenicity in general. Many allergens are not glycosylated, whereas some important allergens (eg, Gal d 1 [ovomucoid]) are heavily glycosylated.

It will become clear from this overview that few, if any, structural features are currently known to be common for allergens in general, even though most allergens can be grouped into a small number of structural classes.

Since the identification and cloning of the first allergenic proteins in the late 1980s, hundreds of allergens have been identified and their sequences determined. A number of databases that provide molecular, biochemical, and clinical data of allergens were established and the growing number of available allergen sequences together with the advancements of bioinformatics tools and methods enabled scientists to shed light on evolutionary and structural relationships between allergens from different sources. In particular, protein family databases that are linked to protein sequence databases, such as the Pfam database, provided the basis of a novel classification of allergens. Several studies revealed that most allergens can be found in a limited number of protein families. Records of most allergen databases are organized by type of allergen source and route of exposure. Likewise, allergen designations according to the official allergen nomenclature are derived from the scientific name of the allergen source species and a sequential number that in most cases does not reflect evolutionary relationships between allergens. To bring together allergen data stored in allergen databases and evolutionary and structural relationships between allergens established from protein family databases, Breiteneder and co-workers (Radauer et al., 2008) co-constructed AllFam, a database of allergen families.

The identification of a large number of allergens from diverse sources has triggered the search for common properties of allergens. The discovery of such features would be a step toward the prediction of allergenicity from protein sequence, structure, or function, a procedure that is essential for risk assessment of novel foods. Knowledge of features that make proteins allergenic would also shed light on the mechanism of the initiation of an allergic immune response, thus paving the way for novel therapeutic concepts. There is an ongoing discussion on whether common properties of allergens exist. One view claims that any protein that comes into contact with the immune system of an atopic individual in sufficient amounts and in the appropriate context can elicit an allergic immune response. Radauer and co-workers supported the view that allergens possess special features and not every protein can become allergenic, this consideration is based on: 1) the small number of protein families in which allergens were found and 2) the frequent occurrence of certain biochemical functions among

allergens. Allergens were found in only 2% of all sequence-based and 5% of all structural protein families (Tables I and II).

Table I. Numbers of sequences and protein families of allergens in AllFam

	Sequences	Sequences from known protein families	AllFam families	AllFam families with >1 allergen
All allergens	847	707	134	81
Sources				
Plants	369	338	58	34
Animals	305	268	60	36
Fungi	163	91	37	16
Bacteria	10	10	5	1
Routes of exposure				
Inhalation	479	377	99	59
Ingestion	257	240	48	29
Sting, bite	66	52	14	7
Contact	58	50	35	10
Autoallergen	14	14	14	0
Iatrogenic	11	10	7	2

Biochemical functions of allergens showed a bias toward certain classes, such as hydrolysis of proteins, polysaccharides, and lipids; binding of metal ions and lipids; transport; storage; and cytoskeleton association (Table III). A possible connection between biochemical function and allergenicity is best understood in the case of proteases. The major house dust mite allergen Der p 1, a cysteine protease, was shown to cleave the tight junction protein occludin, thus increasing epithelial permeability and facilitating its entry into the tissue (Wan et al.1999). Furthermore, several studies demonstrated that Der p 1 acts directly on cells of the human immune system by cleaving cell-surface proteins, such as CD23, CD25, CD40, and dendritic cell–specific intercellular adhesion molecule–grabbing nonintegrin (Furmonaviciene at al., 2007). The link between other biochemical functions and allergenicity is less clear. Interestingly, many families of allergens are involved in defense against pathogens and predators, such as several groups of plant pathogenesis–related proteins, cereal bifunctional inhibitors (Breteineder at al., 2004), and enzymes from insect venoms. The assumption that allergens do not possess special features that render them allergenic was based on the observation that allergens fold into highly diverse structures and no ‘‘allergenic’’ folds could be detected. With the much larger number of structures of allergens and allergen homologues available today, we showed that the structural repertoire of allergens was restricted to only 5% of all structural families, but most of these families were grouped into different

superfamilies and folds (Table II). Thus most folds and superfamilies contained either no or only a single allergen family. These data argue against the hypothesis that it is a single structure that makes a protein allergenic. In contrast, common structural features have been established for food allergens that sensitize through the gastrointestinal tract (Breteineder at al., 2005). These features, such as high numbers of disulfide bonds, repetitive structures, binding of lipid or metal ions, and formation of stable oligomers, confer stability toward heat, acid, and proteolysis. However, these general features cannot be traced back to certain folds, making this observation compatible with the lack of specific allergenic folds.

The AllFam database, an Internet resource for classifying allergens into protein families. Analysis of allergen families confirmed that allergens are distributed among a small number of protein families and possess a limited range of biologic functions.

The AllFam database can be used to test hypotheses on factors that determine allergenicity by comparing allergen-containing protein families with respect to the features. This hypothesis was based on database similarity searches using a sample of only 30 allergen sequences from an even smaller number of protein families. In contrast, an overview of the most important protein families of all allergens shows that members of many of these families are found in bacteria, such as EF-hand proteins (fourth rank), cupins (fifth rank), PR-1 proteins (ninth rank), subtilisin-like serine proteases (tenth rank), and trypsin-like serine proteases (eleventh rank). Sequence comparison of allergenic members of the 3 most important protein families of allergens showed a wide range of the degree of sequence conservation. Allergenic tropomyosins from invertebrates and profilins from higher plants show sequence identities between homologues from unrelated species of more than 50%. This sequence conservation is reflected by the high extent of IgE cross-reactivity observed within these families. On the other end of the spectrum are the 2S albumins, important food allergens from legumes, nuts, and other seeds. 2S albumins from different plant families show sequence identities of less than 40%. Cross-reactivity was thought to be low or even absent between 2S albumins from different plant orders. Recently, considerable cross-reactivity between Ara h 2 from peanut and yet unidentified allergens from almond and Brazil nut was demonstrated. Furthermore, high sequence similarity between linear IgE epitopes, despite low global sequence similarity of 2S albumins from cashew and walnut, was shown. The situation seems to be different for food allergens, which come into contact with the human immune system after partial denaturation in the digestive tract, leading to significant IgE binding to linear epitopes. Thus global sequence similarity seems not to be suitable to predict cross-reactivity among these allergens.

The AllFam database contained 847 (2008) allergens with known partial or total sequences (Table I). Of these, 707 allergens were classified into 134 AllFam families that contained 184 different Pfam domains. The distribution of allergens was highly biased toward a few protein families. Although the protein family with the highest number of allergens, the prolamin superfamily, contained 59 allergens (8% of all allergens with known protein family) and the 10 most abundant families contained 300 allergens (42%; Figure 2A and B), there were 53 families that contained only a single allergen. Figure 2A and B, shows the 15 most important families of allergens itemized by source and route of exposure. Most allergen families were confined to a single source kingdom, such as prolamins, profilins, and cupins from plants and tropomyosins, lipocalins, and caseins from animals. A minority of protein families, such as the EF-hand family and the pathogenesis-related proteins (PR-1), contained allergens from multiple kingdoms. Most protein families contained allergens that sensitize human subjects through different routes. Among these are allergens responsible for cross-reactivity between inhalative allergen sources and foods, such as profilins, Bet v 1–related allergens, and tropomyosins.

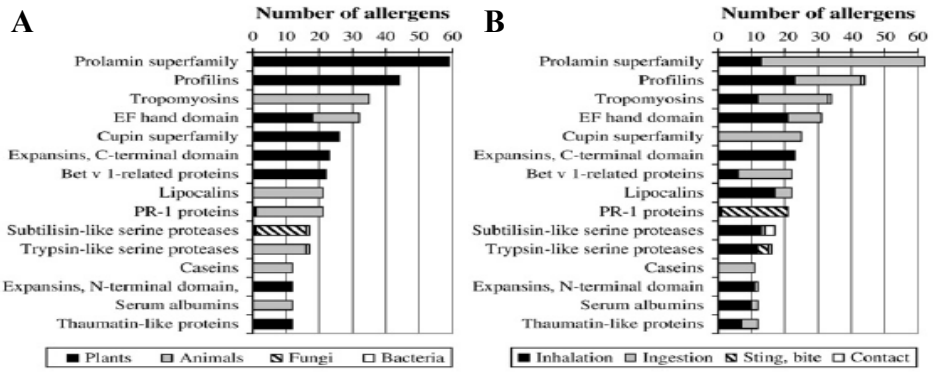

Figure 2. The 15 protein families with the highest number of allergens classified by source (A) and route of exposure (B). Numbers in Figure 1 B, differ because of multiple or missing routes of exposure for some allergens (Radauer et al., 2008).

Structural Classification of Allergens

A structural classification of allergens whose 3-dimensional structures have been experimentally determined or inferred from sequence similarity showed a restricted distribution similar to the distribution of allergens into sequence-based Pfam families (Table II). Allergens were found in all structural classes, as defined by SCOP. However, all members of protein families that contained allergens could be grouped into only 138 structural families (5% of all families in the SCOP database). A comparison of the numbers of structural families, superfamilies, and folds that contain allergens showed that structural allergen

families did not cluster in certain folds. All 3012 families in the SCOP database were grouped into 1639 superfamilies and 978 folds, whereas the 138 structural families that contained allergens were grouped into 108 superfamilies and 97 folds (Table II). The folds that contained the greatest numbers of allergen families were the TIM β/α-barrel fold (SCOP accession no. c.1), with 9 allergen families, and the concanavalin-like lectins/glucanases fold (SCOP accession no. b.29), with 7 allergen families.

Table II. Structural classes of all protein families that contain allergens.

	All structures in SCOP			Structures of allergens and allergen homologs*		
SCOP class	Folds	Superfamilies	Families	Folds	Superfamilies	Families
a: All α proteins	226	392	645	19 (8%)	20 (5%)	25 (4%)
b: All β proteins	149	300	549	22 (15%)	24 (8%)	36 (7%)
c: α and β proteins (a/b)	134	221	661	14 (10%)	18 (8%)	29 (4%)
d: α and β proteins (a+b)	286	424	753	28 (10%)	29 (7%)	31 (4%)
e: Multidomain proteins	48	48	64	2 (4%)	2 (4%)	2 (3%)
f: Membrane and cell-surface proteins	49	90	101	2 (4%)	2 (2%)	2 (2%)
g: Small proteins	79	114	186	8 (10%)	9 (8%)	9 (5%)
h: Coiled coil proteins	7	50	53	2 (29%)	4 (8%)	4 (8%)
Totals	978	1639	3012	97 (10%)	108 (7%)	138 (5%)

Functional Classification of Allergens

The standardized, hierarchically organized terms of the GO (gene ontology) database were used to determine the biologic functions most frequently found among allergens (Table III). Of the 847 allergens listed in AllFam, 644 contained GO annotations distributed among 351 different GO terms. One sixth of all allergens in AllFam (119 allergens) were inferred to possess hydrolase activity. Half of them (58 allergens) were proteases, such as trypsin-like and subtilisin-like serine proteases (14 and 13 allergens, respectively) and papain-like cysteine proteases (10 allergens). Other hydrolytic enzymes included polygalacturonases (8 allergens), lipases (8 allergens), and ribosome-inactivating proteins (8 allergens). Many allergens bound metal ions. These included calciumbinding allergens from the EF-hand family (32 allergens), serum albumins (12 allergens), globins (9 allergens), enolases (9 allergens), and Fe/Mn superoxide dismutases (7 allergens). Allergens with lipid-binding activity comprised nonspecific lipid transfer proteins (nsLTPs) from the prolamin superfamily (28 allergens), serum albumins (12 allergens), and lipocalins (9 allergens).

The nonmetabolic biologic process associated with the greatest number of allergens was transport. This group of allergens comprised lipid-binding proteins, such as the nsLTPs (28 allergens) and lipocalins (21 allergens), as well as general carrier proteins, such as serum albumins (12 allergens) and caseins (12 allergens). Many allergens fromthe cupin and prolamin superfamilies (26 and 22 allergens, respectively) were annotated as nutrient

reservoirs. The GO terms from the category ‘‘cellular component’’ most frequently found in allergen sequence annotations were the general terms ‘‘extracellular region’’ and ‘‘cytoplasm.’’ In addition, 45 allergens (44 profilins and a single tropomyosin) were described as associated with the cytoskeleton. Of the 203 allergens without GO annotations, 112 were not assigned to a protein family, in most cases because their sequences were too short. The remaining 91 sequences were grouped into 17 AllFam families, with tropomyosins (34 allergens), group 2 mite allergens (10 allergens), thaumatin-like proteins (9 allergens), Ole e 1–related proteins (9 allergens), and pectate lyases (9 allergens) as the prevailing families.

Table III. The 15 GO terms associated with the highest number of allergens in AllFam.

GO term	Allergens
Molecular function	
Hydrolase activity (GO:0016787)	119
Peptidase activity (GO:0008233)	56
Metal ion binding (GO:0046872)	73
Calcium ion binding (GO:0005509)	56
Nutrient reservoir activity (GO:0045735)	55
Lipid binding (GO:0008289)	53
Actin binding (GO:0003779)	48
Biologic process	
Transport (GO:0006810)	105
Metabolic process (GO:0008152)	45
Proteolysis (GO:0006508)	58
Carbohydrate metabolic process (GO:0005975)	45
Cytoskeleton organization and biogenesis (GO: 0007010)	45
Cellular component	
Extracellular region (GO:0005576)	109
Cytoplasm (GO:0005737)	76
Cytoskeleton (GO:0005856)	45

The extent of sequence conservation among members of these families showed considerable differences. nsLTPs from the prolamin superfamily showed a moderate degree of sequence identity between allergens from different plant families (25% to 67%) and considerable sequence conservation only among proteins from botanically related species (at least 69% sequence identity among nsLTPs from Rosaceae fruits). In contrast, sequence identities between 2S albumin allergens from different plant families were generally low (18% to 39%) 2S albumins shared only 7% to 25% of their sequences with nsLTPs.

When is a Protein Considered to be a Major Allergen?

The distinction between major and minor allergens is relevant for various reasons but also in relation to the issue of allergenicity. The current definition of major allergen is based on the prevalence of IgE or skin reactivity in subjects that are sensitized (usually very strongly) to the total extract. This definition is unsatisfactory in that it does not reflect the contribution of

the allergen to the overall reactivity of the extract. Intuitively, removal of a truly major allergen from an extract is expected to have a noticeable effect on the overall reactivity of that extract: a major allergen should make a difference. Such an interpretation invites a different type of definition. For example, a major allergen is responsible for more than 20% of the allergenic reactivity in more than 20% of the sensitized patients. This requires testing with extracts from which the allergen in question has been selectively removed (eg, with monospecific antibodies). Alternatively, it could be tested serologically by absorbing out all IgE antibodies to the allergen and then testing the residual activity of the absorbed serum. For most allergens, this aspect has not been studied.

Allergens and Immune System

Immunogenicity and antigenicity are related but distinct immunologic properties that sometimes are confused. Immunogenicity is the ability to induce a humoral and/or cell mediated immune response. Although a substance that induces a specific immune response is usually called an antigen, it is more appropriately called an immunogen. Antigenicity is the ability to combine specifically with the final products of the above responses (i.e., antibodies and/or cell-surface receptors). Although all molecules that have the property of immunogenicity also have the property of antigenicity, the reverse is not true. Some small molecules, called *haptens,* are antigenic but incapable, by themselves, of inducing a specific immune response. In other words, they lack immunogenicity. Proteins, thus, allergens are the most potent immunogen.

Antigen Processing and Presentation

Antigens, as allergens, which are generally very large and complex, are not recognized in their entirety by lymphocytes. Instead, both B and T lymphocytes recognize discrete sites on the antigen called antigenic determinants, or epitopes. Epitopes are the immunologically active regions on a complex antigen, the regions that actually bind to B-cell or T-cell receptors. Although B cells can recognize an epitope alone, T cells can recognize an epitope only when it is associated with an MHC molecule on the surface of a self-cell (either an antigen-presenting cell or an altered self-cell). Each branch of the immune system is therefore uniquely suited to recognize antigen in a different milieu. The humoral branch (B cells) recognizes an enormous variety of epitopes: those displayed on the surfaces of bacteria or viral particles, as well as those displayed on soluble proteins, glycoproteins, polysaccharides,

or lipopolysaccharides that have been released from invading pathogens. The cell-mediated branch (T cells) recognizes protein epitopes displayed together with MHC molecules on self-cells, including altered self-cells such as virus-infected self-cells and cancerous cells. Thus, four related but distinct cell-membrane molecules are responsible for antigen recognition by the immune system, are:

- Membrane-bound antibodies on B cells
- T-cell receptors
- Class I MHC molecules
- Class II MHC molecules

Each of these molecules plays a unique role in antigen recognition, ensuring that the immune system can recognize and respond to the different types of antigen that it encounters.

Antigen Presenting Cell (APCs)

Recognition of foreign protein antigen by a T cell requires that peptides derived from the antigen be displayed within the cleft of an MHC molecule on the membrane of a cell. The formation of these peptide-MHC complexes requires that a protein antigen be degraded into peptides by a sequence of events called antigen processing. The degraded peptides then associate with MHC molecules within the cell interior, and the peptide-MHC complexes are transported to the membrane, where they are displayed (antigen presentation). MHC molecules that function in this recognition event are polymorphic (genetically diverse) glycoproteins found on cell membranes. There are two major types of MHC molecules: Class I MHC molecules, which are expressed by nearly all nucleated cells of vertebrate species, consist of a heavy chain linked to a small invariant protein called β_2-microglobulin. Class II MHC molecules, which consist of an alpha and a beta glycoprotein chain, are expressed only by antigen-presenting cells. When a naive T cell encounters antigen combined with a MHC molecule on a cell, the T cell proliferates and differentiates into memory T cells and various effector T cells.

Class I and class II MHC molecules associate with peptides that have been processed in different intracellular compartments.

Class I MHC molecules bind peptides derived from endogenous antigens that have been processed within the cytoplasm of the cell (e.g., normal cellular proteins, tumor proteins, or

viral and bacterial proteins produced within infected cells). Class II MHC molecules bind peptides derived from exogenous antigens that are internalized by phagocytosis or endocytosis and processed within the endocytic pathway.

Most cells can present antigen with class I MHC but presentation of antigen by class II MHC is a unique characteristic of APCs. Since all cells expressing either class I or class II MHC molecules can present peptides to T cells, by convention, cells that display peptides associated with class I MHC molecules to $CD8^+$TC cells are referred to as *target cells;* cells that display peptides associated with class II MHC molecules to $CD4^+$TH cells are called *antigen-presenting cells (APCs).*

A variety of cells can function as antigen-presenting cells. Their distinguishing feature is their ability to express class II MHC molecules and to deliver a co-stimulatory signal. Three cell types are classified as *professional* antigen-presenting cells: dendritic cells, macrophages, and B lymphocytes. These cells differ from each other in their mechanisms of antigen uptake, in whether they constitutively express class II MHC molecules, and in their co-stimulatory activity:

- Dendritic cells (DCs) are the most effective of the antigen presenting cells. Because these cells constitutively express a high level of class II MHC molecules and costimulatory activity, they can activate naive TH cells.
- Macrophages must be activated by phagocytosis of particulate antigens before they express class II MHC molecules or the co-stimulatory B7 membrane molecule.
- B cells constitutively express class II MHC molecules but must be activated before they express the co-stimulatory B7 molecule.

Several other cell types, classified as *nonprofessional* antigen-presenting cells, can be induced to express class II MHC molecules or a co-stimulatory signal. Many of these cells function in antigen presentation only for short periods of time during a sustained inflammatory response.

Because nearly all nucleated cells express class I MHC molecules, virtually any nucleated cell is able to function as a target cell presenting endogenous antigens to TC cells. Most often, target cells are cells that have been infected by a virus or some other intracellular microorganism. However, altered self-cells such as cancer cells, aging body cells, or allogeneic cells from a graft can also serve as targets.

Only professional antigen-presenting cells (dendritic cells, macrophages, and B cells) are able to present antigen together with class II MHC molecules and deliver the co-stimulatory signal necessary for complete T-cell activation that leads to proliferation and differentiation. The principal costimulatory molecules expressed on antigen-presenting cells are the glycoproteins

B7-1 and B7-2. The professional antigen-presenting cells differ in their ability to display antigen and also differ in their ability to deliver the co-stimulatory signal. Dendritic cells constitutively express high levels of class I and class II MHC molecules as well as high levels of B7-1 and B7-2. For this reason, dendritic cells are very potent activators of native, memory, and effector T cells. In contrast, all other professional APCs require activation for expression of co-stimulatory B7 molecules on their membranes; consequently, resting macrophages are not able to activate naive T cells and are poor activators of memory and effector T cells. Macrophages can be activated by phagocytosis of bacteria or by bacterial products such as LPS or by IFN-γ, a TH1-derived cytokine. Activated macrophages up-regulate their expression of class II MHC molecules and co-stimulatory B7 molecules. Thus, activated macrophages are common activators of memory and effector T cells, but their effectiveness in activating naive T cells is considered minimal. B cells also serve as antigen-presenting cells in T-cell activation. Resting B cells express class II MHC molecules but fail to express co-stimulatory B7 molecules. Consequently, resting B cells cannot activate naive T cells, although they can activate the effector and memory T-cell populations. Upon activation, B cells up-regulate their expression of class II MHC molecules and begin expressing B7. These activated B cells can now activate naive T cells as well as the memory and effector populations

Whether an antigenic peptide associates with class I or with class II molecules is dictated by the mode of entry into the cell, either exogenous or endogenous, and by the site of processing. Once an antigen is internalized, it is degraded into peptides within compartments of the endocytic processing pathway. Internalized antigen takes 1–3 h to transverse the endocytic pathway and appear at the cell surface in the form of peptide–class II MHC complexes. The endocytic pathway appears to involve three increasingly acidic compartments: early endosomes (pH 6.0–6.5); late endosomes, or endolysosomes (pH 5.0–6.0); and lysosomes (pH 4.5–5.0). Internalized antigen moves from early to late endosomes and finally to lysosomes, encountering hydrolytic enzymes and a lower pH in each compartment. Lysosomes, for example, contain a unique collection of more than 40 acid-dependent hydrolases (hydrolytic enzymes are optimally active under acidic conditions), including proteases, nucleases, glycosidases, lipases, phospholipases, and phosphatases. Within the compartments of the endocytic pathway, antigen is degraded into oligopeptides of about 13–18 residues, which bind to class II MHC molecules. The mechanism by which internalized antigen moves from one endocytic compartment to the next has not been conclusively demonstrated. It has been

suggested that early endosomes from the periphery move inward to become late endosomes and finally lysosomes.
Once a peptide has bound, the peptide–class II complex is transported to the plasma membrane, where the neutral pH appears to enable the complex to assume a compact, stable form. Peptide is bound so strongly in this compact form that it is difficult to replace a class II–bound peptide on the membrane with another peptide at physiologic conditions.

TH-Cell Activation

The central event in the generation of both humoral and cell mediated immune responses is the activation and clonal expansion of TH cells. T_H cell activation is initiated by interaction of the TCR-CD3 complex with a processed antigenic peptide bound to a class II MHC molecule on the surface of an antigen-presenting cell. This interaction and the resulting activating signals also involve various accessory membrane molecules on the TH cell and the antigen-presenting cell. Interaction of a TH cell with antigen initiates a cascade of biochemical events that induces the resting TH cell to enter the cell cycle, proliferating and differentiating into memory cells or effector cells.
These profound changes are the result of signal-transduction pathways that are activated by the encounter between the TCR and MHC-peptide complexes.
T-cell activation requires the dynamic interaction of multiple membrane molecules, but this interaction, by itself, is not sufficient to fully activate naive T cells. Native T cells require more than one signal for activation and subsequent proliferation into effector cells:

- *Signal 1,* the initial signal, is generated by interaction of an antigenic peptide with the TCR-CD3 complex,
- A subsequent antigen-nonspecific co-stimulatory signal, *signal 2,* is provided primarily by interactions between CD28 on the T cell and members of the B7 family on the APC.

There are two related forms of B7, B7-1 and B7-2. These molecules are members of the immunoglobulin superfamily and have a similar organization of extracellular domains but markedly different cytosolic domains. Both B7 molecules are constitutively expressed on dendritic cells and induced on activated macrophages and activated B cells. The ligands for B7 are CD28 and CTLA-4 (also known as CD152), both of which are expressed on the T-cell membrane as disulfide-linked homodimers; like B7, they are members of the immunoglobulin superfamily. Although CD28 and CTLA-4 are structurally similar glycoproteins, they act

antagonistically. Signaling through CD28 delivers a positive co-stimulatory signal to the T cell; signaling through CTLA-4 is inhibitory and down-regulates the activation of the T cell. CD28 is expressed by both resting and activated T cells, but CTLA-4 is virtually undetectable on resting cells. Typically, engagement of the TCR causes the induction of CTLA-4 expression, and CTLA-4 is readily de-tectable within 24 hours of stimulation, with maximal expression within 2 or 3 days post-stimulation. Even though the peak surface levels of CTLA-4 are lower than those of CD28, it still competes favorably for B7 molecules because it has a significantly higher avidity for these molecules than CD28 does. Interestingly, the level of CTLA-4 expression is increased by CD28-generated co-stimulatory signals. This provides regulatory braking via CTLA-4 in proportion to the acceleration received from CD28. CTLA-4 can effectively block CD28 co-stimulation by competitive inhibition at the B7 binding site, an ability that holds promise for clinical use in autoimmune diseases and transplantation.

TH-cell recognition of an antigenic peptide–MHC complex sometimes results in a state of nonresponsiveness called **clonal anergy,** marked by the inability of cells to proliferate in response to a peptide-MHC complex. Whether clonal expansion or clonal anergy ensues is determined by the presence or absence of a co-stimulatory signal (signal 2), such as that produced by interaction of CD28 on TH cells with B7 on antigen-presenting cells. Experiments with cultured cells show that, if a resting TH cell receives the TCR-mediated signal (signal 1) in the absence of a suitable co-stimulatory signal, then the TH cell will become anergic. Specifically, if resting TH cells are incubated with glutaraldehyde-fixed APCs, which do not express B7, the fixed APCs are able to present peptides together with class II MHC molecules, thereby providing signal 1, but they are unable to provide the necessary co-stimulatory signal 2. In the absence of a co-stimulatory signal, there is minimal production of cytokines, especially of IL-2. Anergy can also be induced by incubating TH cells with normal APCs in the presence of the Fab portion of anti-CD28, which blocks the interaction of CD28 with B7.

T-Cell Differentiation

CD4+ and CD8+ T cells leave the thymus and enter the circulation as resting cells in the G0 stage of the cell cycle. There are about twice as many CD4+T cells as CD8+ T cells in the periphery. T cells that have not yet encountered antigen (naive T cells) are characterized by condensed chromatin, very little cytoplasm, and little transcriptional activity. Naive T cells continually recirculate between the blood and lymph systems. During recirculation, naive T

cells reside in secondary lymphoid tissues such as lymph nodes. If a native cell does not encounter antigen in a lymph node, it exits through the efferent lymphatics, ultimately draining into the thoracic duct and rejoining the blood. It is estimated that each naive T cell recirculates from the blood to the lymph nodes and back again every 12–24 hours. Because only about 1 in 105 naive T cells is specific for any given antigen, this large-scale recirculation increases the chances that a naive T cell will encounter appropriate antigen.

If a naive T cell recognizes an antigen-MHC complex on an appropriate antigen-presenting cell or target cell, it will be activated, initiating a *primary response*. About 48 hours after activation, the naive T cell enlarges into a blast cell and begins undergoing repeated rounds of cell division. Activation depends on a signal induced by engagement of the TCR complex and a co-stimulatory signal induced by the CD28-B7 interaction. These signals trigger entry of the T cell into the G1 phase of the cell cycle and, at the same time, induce transcription of the gene for IL-2. In addition, the co-stimulatory signal increases the half-life of the IL-2 mRNA. The increase in IL-2 transcription, together with stabilization of the IL-2 mRNA, increases IL-2 production by 100-fold in the activated T cell. Secretion of IL-2 and its subsequent binding to the high-affinity IL-2 receptor induces the activated naive T cell to proliferate and differentiate. T cells activated in this way divide 2–3 times per day for 4–5 days, generating a large clone of progeny cells, which differentiate into memory or effector T-cell populations.

The various *effector T cells* carry out specialized functions such as cytokine secretion and B-cell help (activated CD4+ TH cells) and cytotoxic killing activity (CD8+ CTLs). Effector cells are derived from both naive and memory cells after antigen activation. Effector cells are short-lived cells, whose life spans range from a few days to a few weeks. The effector and naive populations express different cell-membrane molecules,which contribute to different recirculation patterns.

CD4+ effector T cells form two subpopulations distinguished by the different panels of cytokines they secrete. One population, called the TH1 subset, secretes IL-2, IFN-γ, and TNF-β. The TH1 subset is responsible for classic cell-mediated functions, such as delayed-type hypersensitivity and the activation of cytotoxic T lymphocytes. The other subset, called the TH2 subset, secretes IL-4, IL-5, IL-6, and IL-10. This subset functions more effectively as a helper for B-cell activation. The *memory T-cell* population is derived from both naive T cells and from effector cells after they have encountered antigen. Memory T cells are antigen-generated, generally long-lived, quiescent cells that respond with heightened reactivity to a subsequent challenge with the same antigen, generating a *secondary response.* An expanded population of memory T cells appears to remain long after the population of effector T cells

has declined. In general, memory T cells express many of the same cell-surface markers as effector T cells; no cell-surface markers definitively identify them as memory cells. Like naive T cells, most memory T cells are resting cells in the G0 stage of the cell cycle, but they appear to have less stringent requirements for activation than naive T cells do. For example, naive TH cells are activated only by dendritic cells, whereas memory TH cells can be activated by macrophages, dendritic cells, and B cells. It is thought that the expression of high levels of numerous adhesion molecules by memory TH cells enables these cells to adhere to a broad spectrum of antigen-presenting cells. Memory cells also display recirculation patterns that differ from those of naive or effector T cells.

Chapter 1.3

FOOD ALLERGY

Food allergies and other food sensitivities are *individualistic* adverse reactions to foods (Taylor et al., 1987). These food-related illnesses are individualistic because they affect only a few people in the population; most consumers can eat the same foods with no ill effects. Adverse food reactions can include IgE and non-IgE-mediated primary immunological sensitivities, non-immunological food intolerances, and secondary sensitivities. While these various types of reactions are often considered collectively as food allergies, true food allergies represent only a fraction of the individualistic adverse reactions to foods. Adverse reactions to foods have been reported in up to 25% of the population at some point in their lives, with the highest prevalence observed during infancy and early childhood. Such reactions are generally divided on a basis of the underlying pathophysiologic changes that produced the reaction, eg, food allergy, food intolerance, pharmacologic reactions, food poisoning, and toxic. Although adverse reactions to foods are common, food allergy, defined as an IgE-mediated response to a food, represents only a small percentage of all adverse reactions to foods.

True food allergies are abnormal (heightened) responses of the immune system to components of certain foods. The components of foods that elicit these abnormal immune responses are typically naturally-occurring proteins in the foods. True food allergies can be divided into two categories based upon the nature of the immune response immediate hypersensitivity reactions and delayed hypersensitivity reactions. In immediate hypersensitivity reactions, symptoms begin to develop within minutes to an hour or so after ingestion of the offending food. Immediate hypersensitivity reactions have been noted with many foods and can sometimes be quite severe (Hefle et al., 1996). Immediate hypersensitivity reactions involve abnormal responses of the humoral immune system with the formation of allergen-specific immunoglobulinE (IgE) antibodies. In delayed hypersensitivity reactions, symptoms do not begin to appear until 24 hours or longer after the ingestion of the offending food. With the exception of celiac disease, which involves an abnormal immunological response to wheat and related grains, the role of delayed hypersensitivity reactions to foods remains poorly defined. Delayed hypersensitivity reactions involve abnormal responses of the cellular immune system with the development of sensitized T cells.

The mechanism of IgE-mediated allergic reactions is depicted the allergen must occur. In the sensitization phase of the response, the allergen stimulates production of specific IgE antibodies. While sensitization can occur with the first exposure to the allergen, that is not always the case. With respect to food allergens, sensitization does occur most commonly among young infants where the immune response seems to be more likely to be oriented toward an IgE response. However, even in susceptible infants exposure to most dietary proteins results in oral tolerance, a normal immunologic response that is not associated with adverse reactions, rather than sensitization (Strobel et al., 1995). The specific IgE antibodies then attach to mast cells in various tissues and basophils in the blood. On subsequent exposure to the allergenic substance, the allergen cross-links two IgE antibodies on the surface of the mast cell or basophil membrane, stimulating the release into tissues and blood of a host of allergic response mediators. Although many mediators have been described, histamine is one of the primary mediators responsible for many of the immediate symptoms that occur in IgE-mediated allergic reactions. Other important mediators include the various leukotrienes and prostaglandins, some of which are associated with more delayed symptoms that can occur in IgE-mediated, immediate hypersensitivity reactions, the so-called late-phase responses (Lenzner et al., 1998).

Food Allergy and Gut-Associated Lymphoid Tissue (GALT)

Food allergy represents an abnormal response of the mucosal immune system to antigens delivered through the oral route. Unlike the systemic immune system, which sees relatively small quantities of antigen and mounts a brisk inflammatory response, the mucosal immune system encounters enormous quantities of antigen on a daily basis and generally suppresses immune reactivity to harmless foreign antigens (eg, food proteins and commensal organisms), although it is fully capable of mounting a brisk protective response to dangerous pathogens. The gastrointestinal mucosal barrier is a complex structure that provides an enormous surface area for processing and absorbing ingested food and discharging waste products (Mayer L., 2003). This barrier uses both physicochemical and cellular factors to prevent the penetration of foreign antigens. The physical barrier is comprised of the epithelial cells joined by tight junctions and covered with a thick mucus layer that traps particles, bacteria, and viruses, trefoil factors that help strengthen and promote restoration of the barrier, and lumenal and brush border enzymes, bile salts, and extremes of pH, which all serve to destroy pathogens and render antigens non-immunogenic. Innate (natural killer cells, polymorphonuclear leukocytes, macrophages, epithelial cells, and toll-like receptors) and adaptive immune

(intraepithelial and lamina propria lymphocytes, Peyer's patches, sIgA, and cytokines) responses provide an active barrier to foreign antigens. However, developmental immaturity of various components of the gut barrier and immune system reduces the efficiency of the infant mucosal barrier. For example, enzymatic activity is suboptimal in the newborn period, and the sIgA system is not fully mature until 4 years of age. Consequently, this immature state of the mucosal barrier might play a role in the increased prevalence of gastrointestinal infections and food allergy seen in the first few years of life (Sampson H.A., 1999). Despite the evolution of this complex mucosal barrier, about 2% of ingested food antigens are absorbed and transported throughout the body in an immunologically intact form, even through the normal mature gut. In an elegant series of experiments more than 75 years ago, Walzer and colleagues (Brunner et al., 1928 and Walzer M., 1941) used sera from patients with food allergy to passively sensitize volunteers and demonstrate that immunologically intact antigens cross the mucosal barrier and disseminate rapidly throughout the body.

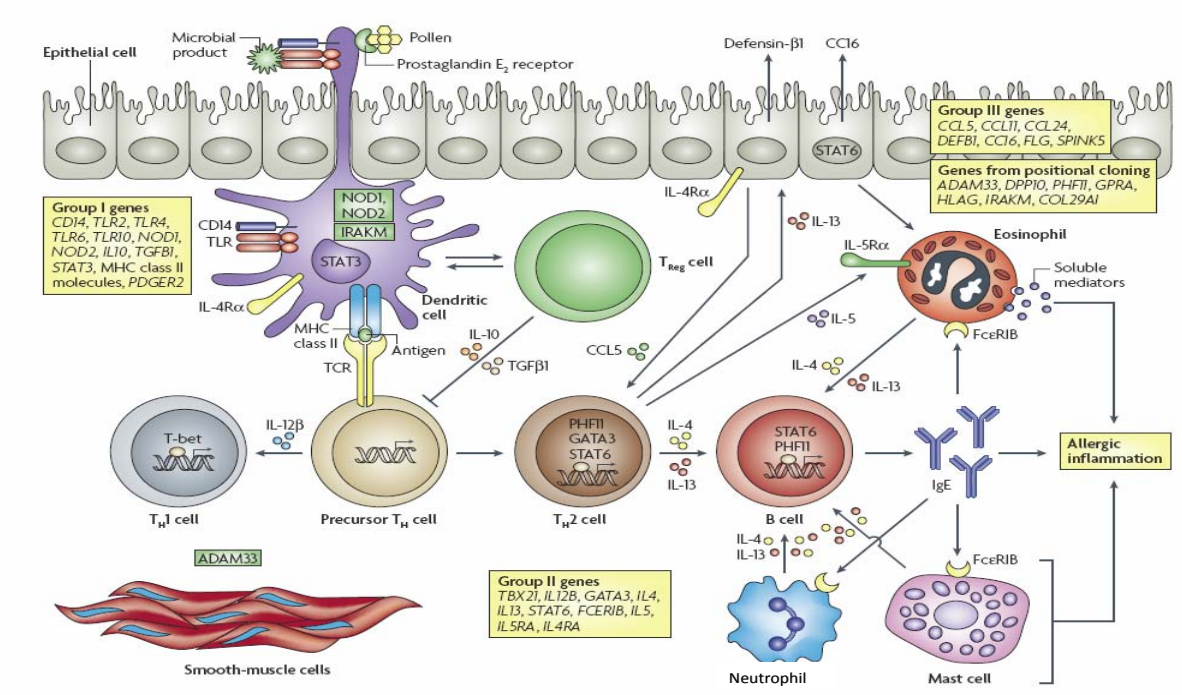

Figure 3. Schematic representation of mucosal immune system in allergy response.

Clinical Features of IgE Mediated Food Allergy

IgE-mediated food allergies are associated with a wide variety of symptoms can involve the gastrointestinal tract, skin, or respiratory tract. The nature and severity of the symptoms

experienced by a food-allergic individual may also vary from one episode to the next depending on the dose of the offending food that has been inadvertently ingested, the degree of sensitization to the offending food at the time of the episode, and probably other factors. Because foods are ingested, gastrointestinal symptoms are often encountered. However, these symptoms can also be involved in other illnesses so their association with food allergies is often difficult to decipher. Cutaneous symptoms such as urticaria (hives) and dermatitis (eczema) are also common manifestations of food allergies. Although few asthmatic individuals experience food-induced asthma, asthma is among the most severe symptoms associated with food allergies. Food-induced asthma is a risk factor for severe, life-threatening reactions to the offending foods (Sampson et al., 1992). Oral allergy syndrome is perhaps the most common manifestation of food allergy (Ortolani et al., 1998) involves symptoms confined to the oropharyngeal area including hives, itching, and swelling (Pastorello et al., 1997). Fresh fruits and vegetables are the foods most frequently associated with oral allergy syndrome (Pastorello at al., 1997). Individuals with oral allergy syndrome are usually sensitized to one or more pollens, and react to proteins in specific fresh fruits and vegetables that cross-react with the pollen allergens (Ebner et al., 1995). The most frightening symptom associated with food allergies is anaphylactic shock, which usually involves multiple systems including the gastrointestinal tract, the skin, the respiratory tract, and the cardiovascular system. Symptoms occur in combination and develop rapidly. Death can occur from cardiovascular and/or respiratory collapse within minutes of ingestion of the offending food. Only a few of the many people with IgE mediated food allergies are at risk for such serious manifestations. However, numerous deaths have been attributed to inadvertent exposure to the offending food among individuals with food allergies (Sampson et al., 1992). These deaths have involved asthma and/or anaphylactic shock.

Prevalence

IgE-mediated food allergies likely affect between 2 and 2.5% of the total population. For many years, the overall prevalence estimate for IgE mediated food allergies has been between 1 and 2% of the total population (Lemke and Taylor, 1994). Infants (1–3 years of age) and children are more commonly affected by food allergies than other age groups (Taylor et al., 1999). Among infants younger than 3 years, the prevalence of food allergies appears to be in the range of 5% to 8% (Sampson, 1990). The prevalence of food allergy among young infants

(<1 year of age) has been studied more thoroughly than has the prevalence among older children and adults.

Most Common Allergenic Foods

The prevalence of allergies to specific foods is not precisely known. Cows' milk allergy appears to be among the more prevalent food allergies in infants. This is not surprising given the importance of milk in infant feeding practices. The prevalence of cows' milk allergy among infants under the age of two in Sweden, Denmark, and Australia has been studied and found to be approximately 2% in all three countries in well-conducted clinical studies involving groups of unselected infants followed from birth to the age of two years. The prevalence of milk allergy is known to diminish with age, but the exact prevalence of milk allergy among other age groups is unknown. The prevalence of other specific food allergies has not been established in controlled clinical trials using unselected population groups. The comparative prevalence of various specific food allergies can be discerned from studies involving groups of individuals with probable food allergies. In the U.S., eggs and peanuts are also common allergenic foods for infants, along with soybeans, tree nuts, fish, and wheat (Bock and Atkins, 1990). Among adults in the U.S., peanuts are probably the most common allergenic food. Seafood allergies, especially to crustaceans (shrimp, crab, lobster), are also rather common among adults. Fewer studies have been conducted on the prevalence of specific types of food allergies in adults in the U.S. or other countries. The prevalence of specific types of food allergies may vary among population groups based upon their eating habits. Peanut allergy appears to be more common in North America than in other parts of the world.

Eight foods or food groups are thought to account for more than 90% of all IgE-mediated food allergies on a worldwide basis (Bousquet et al., 1998). These foods or food groups are milk, eggs, fish (all species of finfish), crustacea (shrimp, crab, lobster, crayfish), peanuts, soybeans, tree nuts (almonds, walnuts, pecans, cashews, Brazil nuts, pistachios, hazelnuts also known as filberts, pine nuts also known as pinyon nuts, macadamia nuts, chestnuts, and hickory nuts), and wheat. In 1995, an expert consultation of the Food and Agriculture Organization of the United Nations determined that these eight foods or food groups were the most common causes of food allergy on a worldwide basis. Subsequently this list was adopted by the Codex Alimentarius Commission in 1999 (CAC, 1999). These foods and food groups have come to be known as the "Big Eight" (wheat, crustacea, eggs, milk, peanut, tree nut,

soybean and fish). More than 160 other foods have been documented as causing food allergies less frequently (Hefle et al., 1996). Basically, any food that has protein has the potential to elicit an allergic reaction among susceptible individuals. Beyond the Big Eight, in certain geographic regions other foods or food groups may frequently cause IgE-mediated food allergies. Celery allergy, for example, is rather common in some European countries (Wuthrich et al., 1990). The prevalence of buckwheat allergy in southeast Asia has already been mentioned. And, sesame seed allergy is very common in middle Eastern countries and countries where the ethnic population of middle Easterners is high; this may be due to the popularity of tahini, a paste made from sesame seeds, in the diets. Several countries including Canada have decided to add sesame seeds to the list of commonly allergenic foods for that country.

The allergens in foods are almost always naturally occurring proteins. Foods contain millions of individual proteins, but only a comparative few of the proteins have been documented to be allergens (Hefle et al., 1996). Some foods such as milk, eggs, and peanuts are known to contain multiple allergenic proteins (Hefle et al., 1996). Other foods such as Brazil nuts, shrimp, and codfish contain only one major allergenic protein (Hefle et al., 1996). However, the majority of the proteins, even those from commonly allergenic foods, are incapable of eliciting IgE production. Although the common allergenic foods listed above tend to be good sources of protein, other common protein-rich foods such as beef, pork, chicken, and turkey are rarely allergenic. No common structural features have allowed distinctions to be made between those proteins that are capable of eliciting IgE production and those that are not. Allergenic proteins, however, tend to be major proteins in the implicated foods, resistant to digestion, and stable to processing operations, particularly heat processing (Taylor and Lehrer, 1996).

Allergy to Sesame

Sesame seeds represent a potent food allergen. Over the past few years, the number and severity of reactions to dietary sesame has increased, probably because of a growing use of sesame seeds and sesame oil in foods. Sesame allergy is common in Eastern countries like Israel, where it is the third most common cause of IgE-mediated food allergy, and is becoming frequent also in European countries. Its prevalence ranges from 0.7% to 1.2%.

Allergy to sesame seeds starts early in childhood, due to the use of sesame-containing foods in the diet of infants as a source of protein and iron. Sesame allergens are often associated

with particularly severe reactions with a high risk of anaphylaxis. Sesame has also been described as an occupational sensitiser for bakers and other exposed workers.

Sesame allergens were only recently identified. Ses i 1 (Pastorello et al., 2001), a sulphur-poor 2S albumin with about 40% homology to allergens of sunflower seeds, Brazil nut and castor bean was the first identified allergen in sesame seeds. Recently, 4 other allergens have been identified: Ses i 2, a sulphur-rich 2S albumin; Ses i 3 (Navuluri et al, 2006), a 7S vicillin-type globulin; a 34 kDa allergen, homologous to seed maturation protein and a 78 kDa allergen, homologous to embryonic abundant protein (Tai et al., 1999).

Oral challenge-based studies revealed that both sesame seeds and sesame oil can cause allergic reactions in sensitised patients, with threshold doses ranging from 30 mg to 10 g of sesame seed, and few millilitres (1-5 mL) of sesame oil. The interaction between sesame allergens and the lipid matrix in sesame oil may increase allergenicity and may cause reactions to few milligrams of sesame proteins.

Sesamum indicum is a plant originally from tropical Africa, which is now universally cultivated for its seeds. It is the most important species in the *Sesamum* genus of the *Pedialaceae* family; the annual worldwide production is around 2 million tons. The seeds are used in several food products, especially in bakery products, fast-foods, “health foods”, vegetarian and ethnic dishes; the oil obtained from the seeds is used for cooking and salad dressing in Oriental, Chinese and South American cuisines, and is also employed by the pharmaceutical industry as a vehicle of medications for intramuscular injection. Allergy to sesame seeds has been increasingly reported in recent years, maybe because of their increasing consumption. In some countries sesame is one of the major causes of food allergy: in Israel, where sesame seed-based foods (halva and tehina) are included in the diet of infants and young children as a source of proteins and iron, sesame is the third common cause of IgE-mediated food allergy and the second most common cause of anaphylaxis (Dalal et al., 2002 and 2003).

Identified Allergens (FAO, 2004)

Sesame seeds contain about 50% oil and 20% proteins. The major protein of sesame, alpha-globulin, is the insoluble 11S globulin, which constitutes 60-70% of the seed protein, while the major soluble protein fraction is represented by the 2S albumins, which account for 25% of the total protein content. The 7S vicillin, a less abundant protein in sesame, constitutes, together with the 11S protein, the Osborne globulin fraction (Tai et al., 1999). Two studies compared the allergenicity of different varieties of sesame seeds (white, brown and black

sesame). The first by Kolopp-Sarda (Kolopp-Sada et al., 1997) used sera from 10 sesame sensitised individuals and found that six of them recognised a 25 kDa allergen of brown sesame; other allergens of 30 and 14 kDa were recognised by a minority of patients. The second by Fremont (Fremont et al., 2002) used sera from 6 sesame sensitised patients, with or without clinical reactivity, for an immunoblotting experiment with white sesame. The allergenic pattern was similar for symptomatic and asymptomatic subjects; ten allergens were revealed, with more intense IgE-binding to those around 12-13 and 22-23.5 kDa. None of these allergens were characterised. The first allergen identified and sequenced in sesame seeds by Pastorello (Pastorello et al., 2001) was a 2S albumin with about 40% homology to allergens of sunflower seeds, Brazil nut and castor bean. This seed storage protein was recognised as a major allergen by ten patients with severe systemic reactions to sesame seeds (urticaria/angio-edema, laryngeal oedema, gastrointestinal symptoms, asthma, hypotension or anaphylactic shock). All ten patients showed high levels of sesame specific IgE and highly positive skin prick tests with both fresh seeds and commercial extracts. An Israelian study evaluating 24 subjects with symptoms and specific IgE to sesame, confirmed the previous findings: 22 out of 24 patients recognised the 14 kDa 2S albumin precursor, which was the only major allergen identified (Wolff et al.,2003). The reacting epitope was found on the peptide corresponding to the residues 24-94. Some minor sesame allergens, of higher molecular weight, were also revealed.

A study by Beyer (Beyer et al., 2002) confirmed the allergenicity of sesame 2S albumins. In the Beyer's study the sulphur-rich protein is a major allergen while the sulphur-poor behaved like a minor one. In the same study, the authors demonstrated that a 7S vicillin-like globulin is a major allergen of sesame, recognised by 75% of patients; this protein showed 41% homology to the walnut allergen Jug r 2 and 36% homology to the peanut allergen Ara h 1. Moreover, it seemed to share an IgE-binding site with Ara h 1, as one of the 22 known IgE-binding epitopes of Ara h 1 showed 80% homology with the corresponding area of the sesame vicillin. Lastly, the authors identified two high-molecular weight allergens homologous to a seed maturation protein and to an embryonic abundant protein of soybean; neither protein was previously described as a food allergen in other plants.

Chapter 1.4

2S ALBUMIN SEED STORAGE PROTEINS

The prolamin superfamily is an excellent example of a superfamily of proteins with limited sequence identity, the existence of the superfamily was first proposed (Kreis et al., 1989), based on visual comparisons of amino acid sequences which showed a conserved `skeleton' of eight cysteine residues spaced as follows: C-X*n*-CX *n*-CC-X*n*-CXC-X*n*-C-X*n*-C. The presence of CC and CXC motifs is particularly unusual and has since facilitated the identification of further members of the superfamily that show little or no other sequence identity.

The vast majority of the characterized members of the prolamin superfamily are seed proteins, which can be broadly divided into two types. Low-molecular-mass sulphur-rich seed proteins include 2S storage albumins from dicotyledonous seeds (Shewry and Pandya 1999), inhibitors of α-amylase and trypsin, puroindolines (Douliez et al., 2000) and grain softness proteins from cereal seeds (Rahman et al., 1994), hydrophobic protein from soybean (Baud et al., 1993), and nonspecific lipid transfer proteins (Douliez et al., 2000), although many examples of the latter have also been isolated from non-seed tissues. These proteins all have molecular masses of below about 15000 Da and have eight or more conserved cysteine residues. Available structures (Figure 4) show that they have a similar fold, comprising bundles of α-helices stabilized by disulphide bonds, and are classified in the SCOP protein database (Murzin et al. 1995) as ``4 helices; folded leaf ; right-handed superhelix; disulphide-rich". Although there is high conservation of cysteine residues, these may form different patterns of disulphide bonds in the different protein groups. 2S albumins, defined on the basis of their sedimentation coefficient, are a major group of seed storage proteins widely distributed in both mono- and di-cotyledonous plants. As storage proteins, they are deposited in protein bodies of developing seeds and are utilized by the plant as a source of nutrients (amino acids and carbon skeletons) during subsequent germination and seedling growth. Recent findings have demonstrated that 2S albumins can also play a protective role in plants as defensive weapons against fungal attack (Agizzio et al., 2003) In addition to their physiological role in plants, these small globular proteins are becoming of increasing interest in nutritional and clinical studies. The amino acid composition of 2S albumin proteins from many plant species has revealed their high content of sulphur-containing amino acids.

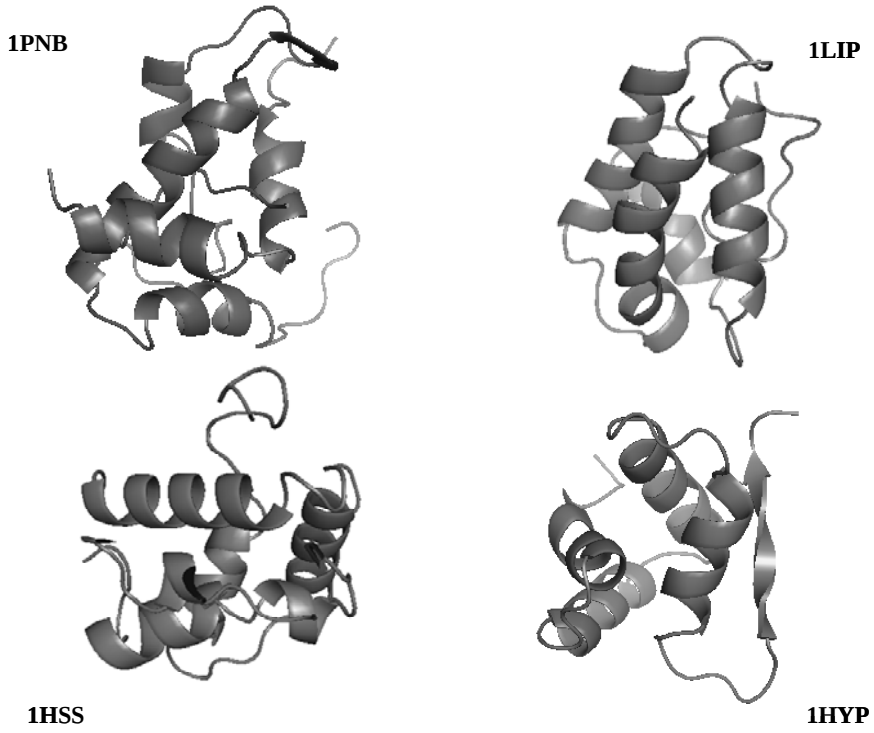

Figure 4. Secondary structures of allergens from the prolamin superfamily. Rapeseed 2S albumin (napin BNIb, Protein Data Bank accession no. 1PNB). Barley nsLTP (1LIP). C, Wheat α-amylase inhibitor (1HSS). Soybean hydrophobic seed protein (1HYP).

Typically, 2S albumins show high levels of cysteine residues, ranging from 6 to 13 mol %; in some cases, the content of methionine is relatively high, as occur with 2S proteins from Brazil nut (*Bertholletia excelsa*) reaching values of 17 mol %. To improve the nutritional quality of legume seeds, usually compromised by a relative deficiency of sulphurcontaining amino acids, some attempts to transfer 2S albumin genes from different sources by genetic engineering were carried out. However, some disappointed results were obtained; when a 2S Brazil nut albumin gene was transferred into soybean, the recombinant 2S protein kept its intrinsic allergenicity (Pastorello et al., 1998). It was clearly shown that people who reacted to Brazil nut extracts on standard skin-prick tests had similar reactions in response to extracts of transgenic soybean that contained recombinant 2S Brazil nut albumins. Consequently, the transgenic soybean was considered unsafe for human and animal nutrition. These studies revealed that prior gene transfer into food plants.

In recent years, some members of this protein family have been described as major food allergens demonstrating their ability to bind IgE from allergic patients´ sera. Allergenic proteins from yellow (*Sinapis alba*, Sin a 1) and oriental mustard (*Brassica juncea*, Bra j 1),

Brazil nut (Ber e 1), castor bean (*Ricinus communis*, Ric c 1) or white sesame seeds (*Sesamum indicum*, Ses i 1) have been classified as 2S albumins.

Several attempts to categorize plant food allergens on the basis of their three-dimensional structure (Aalbarese et al., 2000), biological function or protein families have been carried out.

In particular, 2S albumins are grouped in the prolamin superfamily; other allergenic proteins included in this superfamily are the non-specific lipid transfer proteins, the amylase/trypsin inhibitors and the prolamin storage proteins of cereals [9]. Typically, members of this superfamily are characterized by the presence of a well-conserved skeleton of eight cysteine residues and a similar three dimensional structure enriched in α-helices (Murzin et al., 1995). In addition to the global folding, other structural and biochemical properties are shared by this protein superfamily and could be involved in the intrinsic allergenicity of some of their members, including the 2S albumins. This review deals with those features thought to play a potential role in promoting allergenicity within the 2S protein family.

Structural Features of 2S Albumins

Primary Structure

As occurs with other groups of storage proteins, the 2S albumins show a high level of polymorphism. These proteins are generally encoded by a multigene family leading to numerous isoforms subjected to post-translational modifications, mainly derived from proteolytic processing; these isoforms may show considerable differences in their structures and biological properties. Nevertheless, it is possible to define the protein structure of a “typical” 2S albumin. These proteins are synthesized as a single larger precursor polypeptide of Mr~18-21 kD, which is co-translationally transported into the lumen of the endoplasmic reticulum. After the formation of four intra-chain disulphide bonds, involving eight conserved cysteine residues, the folded protein is transported into the vacuole where is subsequently processed to a polypeptide of Mr ~12-14 kD and eventually to the large and small subunits of Mr~8-10 and 3-4 kD, respectively (Shewry P.R., 1995).

Owing to the conserved skeleton of cysteine residues, the small and large subunits remain associated by two intermolecular disulphide bonds in the mature form; other two intra-chain disulphide bonds are present within the large subunit. Figure 5 depicts the typical disulphide bond mapping of the 2S albumins. The conserved scaffold includes that the third

and fourth cysteine residues are consecutive in the polypeptide chain (large subunit) and the fifth and sixth cysteine residues are separated by only one residue. The interchain disulphide bonds are those formed between cysteine residues 1-5 and 2-3 whereas the intra-chain bridges are formed by the cysteine residues 4-7 and 6-8.

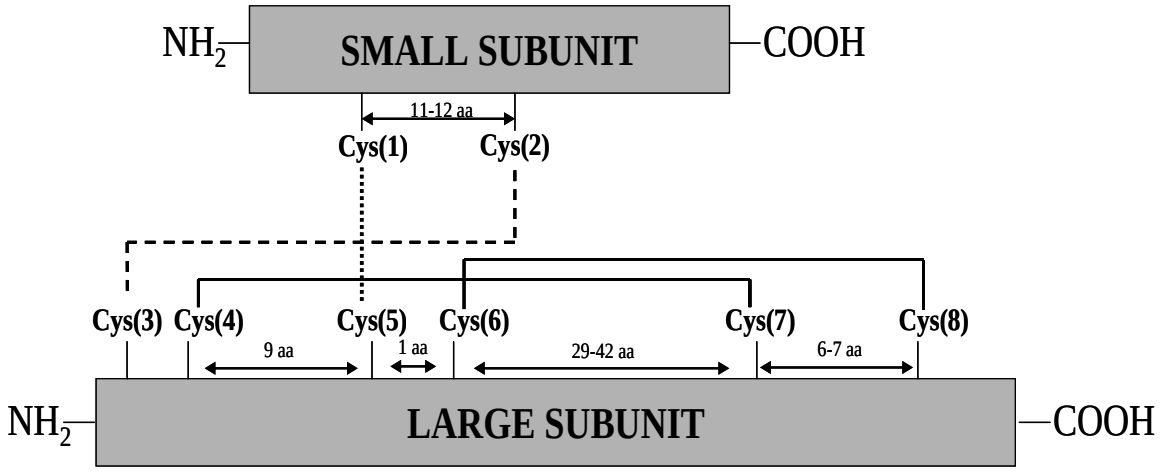

Figure 5. Schematic representation of the disulphide bond patterns formed between the eight conserved cysteine in the 2S family.

A range of variants differing from the "typical" 2S albumins in their structure or mode of biosynthesis has been reported. Such is the case of the major methionine-rich albumin, SFA8, from sunflower (*Helianthus annuus*) in which post-translational processing seems to be limited to the removal of the signal peptide and the pro-region with no further proteolytic cleavage of the polypeptide chain into large and small subunits. SFA8 is the only 2S albumin isolated and characterized to date that is composed of a single polypeptide chain (Kortt et al., 1991).

A characteristic post-translational modification of 2S albumin proteins is the clipping observed at the C-terminal side of both subunits. C-terminal microheterogeneity has been described in 2S albumins from different plant species, including Brazil nut (Moreno et al., 2004), rapeseed (*Brassica napus*) (Monsalve et al., 1990), castor bean and sesame (Moreno et al., 2005). This heterogeneity could either be due to the presence of different precursors, a shift in the position of the cleavage site during the maturation process, or due to the presence of carboxypeptidases in the protein bodies of the seeds, as reported for the α-chains of pea

seed isolectins. However, the precise number and characteristics of the proteolytic enzymes involved in these post-translational modifications still remains unclear.

Despite the skeleton of cysteine residues of 2S albumins being highly conserved, a relatively low amino acid sequence homology, within and among plant species, can be observed. As expected, regions spanning the cysteine residues showed the highest amino acid sequence homology whereas the regions showing the lowest amino acid sequence homology corresponded to i) the C-terminal of the small subunit, ii) the NH2-terminal of the large subunit and iii) that contained between the sixth and seventh cysteine residues within the large subunit. Overall, the degree of sequence homology of 2S allergens is low, ranging from 14 to 40 %, and does not reflect phylogenetic relationships, with the exception of 2S albumins belonging to the Brassicaceae family (i.e., Bra j 1, BnIa, Bra n 1 and Sin a 1). A high amino acid sequence polymorphism has been also found in 2S albumins belonging to the same specie, as occur with allergens from sesame (Ses i 1 and Ses i 2) or castor bean (Ric c 1 and Ric c 3).

Secondary and Tertiary Structure

2S albumins adopt a common and compact three dimensional structural scaffold comprising a bundle of five α-helices displayed in different regions (helices Ia, Ib, II, III and IV) and a C-terminal loop folded in a right-handed superhelix stabilized by four conserved disulphide bonds. Connecting the α-helices III and IV, there is an exposed and relatively short segment known as “hypervariable region” which has been described to be the most important antigenic region of the 2S albumins. However, its variability in length and amino acid composition observed in 2S albumins from different plant species suggests that it does not play any role in determining the folded structure (Pantoja-Uceda etal., 2003). The structural homology within the protein family is high and such similarities have recently been exploited in protein modelling studies. Using the 2S albumin structures from rapeseed and castor bean as templates, structural models for the 2S albumins from Brazil nut and English walnut, and those from pecan nut (*Carya illinoinensis*) and peanut have been reported (Alcocer et al., 2002). Strikingly, the global fold is shown to be similar to that of other sulphur rich proteins from the prolamin superfamily like the non-specific lipid transfer proteins from wheat (various species of the genus *Triticum*) or the bifunctional α-amylase/trypsin inhibitor from ragi (*Eleusine coranaca*) (Strobl et al., 1995). The pattern of eight cysteines in specific order

appears to be a structural scaffold of conserved helical regions that would form a network of disulphide bridges necessary for the maintenance of the tertiary structure.

2.RESULTS

Ses i 2 The Major Allergen from Sesame Seed

Chapter 2.1

The Major Allergen *Ses i 2* from *Sesamum indicum*: Purification, Structure, Stability and Function

INTRODUCTION

Atopic allergy disease (type I allergies) are common clinical disorders in developed countries, food begin on of the most relevant biological sources of type I allergens. The analysis of plant proteins has a long and distinguished history, with work dating back over 250 years. Much of the work has focused on seed proteins and early studies classified plant proteins into groups based on structural and evolutionary relationships. Many of food allergens are plant proteins. A majority of plant food allergens belongs to four protein families, the prolamin superfamily, the cupin superfamily, the porfilins and the homologues of the major birch pollen allergen (Shewry et al., 1995).One of the most widespread groups of plant proteins is the prolamin superfamily, which comprises cereal seed storage proteins, a range of low-molecular-mass sulphur rich proteins (many of which are located in seeds) and some cell wall glycoproteins. This superfamily includes several major types of plant allergen: non-specific lipid transfer proteins, cereal seed, inhibitors of α-amylase and/or trypsin, and 2 S albumin storage proteins of dicotyledonous seeds (Shewry et al., 2002).

2S albumins, defined on the basis of their sedimentation coefficient, are a major group of seed storage proteins widely distributed in both mono- and di-cotyledonous plants. As storage proteins, they are deposited in protein bodies of developing seeds and are utilized by the plant as a source of nutrients (amino acids and carbon skeletons) during subsequent germination and seedling growth. Recent findings have demonstrated that 2S albumins can also play a protective role in plants as defensive weapons against fungal attack. In recent years, some members of this protein family have been described as major food allergens demonstrating their ability to bind IgE from allergic patients´ sera. Allergenic proteins from yellow (*Sinapis alba*, Sin a 1) and oriental mustard (*Brassica juncea*, Bra j 1), Brazil nut (Ber e 1), castor bean (*Ricinus communis,* Ric c 1) or white sesame seeds (*Sesamum indicum,* Ses i 1) have been classified as 2S albumins (Moreno and Clemente, 2008). These proteins are synthesized as a

single larger precursor polypeptide of Mr~18-21 kD, which is co-translationally transported into the lumen of the endoplasmic reticulum. After the formation of four intra-chain disulphide bonds, involving eight conserved cysteine residues, the folded protein is transported into the vacuole where is subsequently processed to a poly-peptide of Mr~12-14 kD and eventually to the large and small subunits of Mr~8-10 and 3-4 kD, respectively. Owing to the conserved skeleton of cysteine residues, the small and large subunits remain associated by two intermolecular disulphide bonds in the mature form; other two intra-chain disulphide bonds are present within the large subunit. The conserved scaffold includes that the third and fourth cysteine residues are consecutive in the polypeptide chain (large subunit) and the fifth and sixth cysteine residues are separated by only one residue.

2S albumins adopt a common and compact three dimensional structural scaffold comprising a bundle of five α-helices displayed in different regions (helices Ia, Ib, II, III and IV) and a C-terminal loop folded in a right-handed superhelix stabilized by four conserved disulphide bonds. Connecting the α-helices III and IV, there is an exposed and relatively short segment known as “hypervariable region” which has been described to be the most important antigenic region of the 2S albumins. However, its variability in length and amino acid composition observed in 2S albumins from different plant species suggests that it does not play any role in determining the folded structure (Pantoja-Uceda et al., 2003). Many 2S albumins have been classified as major allergens in plant food species, including sesame seeds (Mills et al., 2003).

In this chapter, we have focused our studies on Ses i 2 the major allergen from sesame seed. Sesame is associated with immunoglobulin E (IgE) mediated food allergy (Beyer et al., 2002) and is a cause for concern because of the severity of reactions it elicits. The cDNAs of two 2S albumin precursors from sesame seeds have been sequenced (Tai et al., 2001), and the corresponding mature proteins, known as Ses i 1 and Ses i 2, have been reported to be major allergens (Pastorello et al., 2001). Although the skeleton of cysteine residues is conserved, the proteins show a low sequence homology (46%), Ses i 1 being a sulphur-poor protein whilst Ses i 2 is rich in methionine.

Despite its potential importance, Ses i 2 has not been characterized, while Ses i 1 has been purified and extensively characterised.

In this work, we have purified Ses i 2 in sufficiently large amounts (10-30 mg) for subsequent chemical, conformational and stability characterization. Ses i 2 was purified to homogeneity (> 98%) in two consecutive chromatographic steps, involving size-exclusion chromatography on a sephacryl HR-100 column and semi-preparative RP-HPLC on a C18

coulmn. Reduction and carboxamidomethylation of Cys-residues allowed us to establish that mature Ses i 2 is composed of a light (LC) and heavy (HC) chain held together by three disulfides, while two extra disulfides are present in the HC. Peptide mass fingerprint analysis of LC and HC with *S. aureus* V8 protease, combined with a MASCOT search, allowed us to unambiguously identify all the peptide masses of the proteolytic fragments as originating from the precursor protein of the *Ses i 2* allergen from *Sesamum indicum* (Swiss-Prot entry code: Q9XHP1). Notably, the abundance of Cys (10.6%), Arg (13.8%), Met (16%), and Gln (17%) in the mature Ses i 2 (containing 94 amino acids) is much higher than that normally observed in natural proteins. The structural model of Ses i 2, obtained by homology on the NMR structure of napin from Brassica napus (PDB code 1SM7), revealed that Ses i 2 is arranged in a four-helix bundle topology.

Ses i 2 possess an extraordinarily high stability to heat, Gnd-HCl, low pH, and proteases. In particular, at both pH 2.0 and 7.0, Ses i 2 structure exhibits only a partial unfolding even at high temperatures (e.g., 90°C). In the presence of Gnd-HCl, Ses i 2 reversibly unfolds with a $[Gnd\text{-}HCl]_{1/2}$ of 6.8 M. Strikingly, Ses i 2 is fully resistant to the combined action of low pH and pepsin in simulated gastric fluid, while in simulated intestinal fluid it is only partially trimmed at the N- and C-termini by trypsin and chymotrypsin, leaving a compact and folded protein structure. Quite surprisingly, Ses i 2 inhibits the amidolytic activity of thrombin, a key enzyme in blood coagulation, with an IC_{50} value of 1.44±0.05 μM.

Altogether, our results indicate that Ses i 2 may preserve its structure from the degradation in the gastrointestinal tract and this behaviour may be crucial to sensitise the mucosal immune system in the gut.

This study reports the purification and characterization of Ses i 2 using a combination of chromatographic and spectroscopic techniques. The stability of the protein to thermal denaturation and proteolysis is described and compared with other allergenic proteins.

MATERIALS AND METHODS

Materials

"White" sesame seeds of Ethiopian origin were kindly supplied by Chelab s.r.l. (Resana, TV, Italy). Human α-thrombin (E.C 3.4.21.5), activated factor X (FXa) (E.C. 3.4.21.6.), activated protein C (aPC) (E.C. 3.4.21.69), and plasmin (E.C. 3.4.21.7), were purchased from

Hematologic Technologies Inc. (Essex Junction, VT). Cathepsin B (E.C. 3.4.22.1) from human liver, trypsin (E.C. 3.4.21.4), chymotrypsin (E.C.3.4.21.1) and pepsin (E.C.3.4.23.1), S. aureus V8 protease (E.C. 3.4.21.19), thermolysin (E.C. 3.4.24.27) bovine serum albumin (BSA), α-lactalbumin (α-Lact) and ovalbumin (Ovo), 2-iodoacetamide (IA) and 4-vinylpyridine (VP) were from Sigma (St. Louis, MO). Bovine spleen cathepsin D (E.C. 3.4.23.5) and human netrophil elastase (E.C. 3.4.21.37) were from Calbiochem. The chromogenic substrates D-Phe-Pro-Arg-p-NA (FPR), D-Trp-Trp-Arg-pNA (WRR), Arg-Gly-Arg-pNA (RGR), D-Val-Leu-Arg-pNA (VLR) were synthesized as previously detailed (De Filippis et al., 2002). The substrate N-[3-(2-furylacrylolyl]-glycyl-L-leucyl amide (FAGLA) was purchased from Protogen AG (Switzerland). The substrate N^{α}-glutaryl-Phe-pNA was from Fluka. Reagents for electrophoresis, buffers, and organic solvents were of analytical grade and obtained from Fluka or Merck (Darmstadt, Germany).

Extraction and purification of Ses i 2 from sesame seeds

To 1 g of coarsely ground sesame seeds were added 10 ml of 0.1 M Tris-HCl buffer, pH 8.0, containing 0.2 M NaCl. The mixture was gently stirred at room temperature for 24 h on a model 708 Asal (Milan, Italy) rotating stirred. Thereafter, the suspension was centrifuged at 13000 r.p.m. for 5 min and the supernatant filtered on 0.45-μm durapore filters (Millipore, Badford, MA, USA). Total protein concentration in the filtered solution was determined by the bicinconinic acid protein assay kit (Sigma) (Brown et al., 1989). The crude extract (100 μl) was fractionated by analytical size-exclusion chromatography on a (1 x 30 cm) HR10/30 Superose-12 (Amersham-Pharmacia, Uppsala, Sweden) eluted at a flow-rate of 0.3 ml/min in 50 mM Tris-HCl buffer, pH 7.5, containing 1 M NaCl and 10% ethanol (v/v). The absorbance of the effluent was recorded at 280 nm. For preparative purposes, 1 ml of the crude extract (~ 8 mg) was loaded onto a (1.6 x 60 cm) column (Pharmacia Fine Chemicals), packed in-house with Sephacryl HR-100 and eluted in the same Tris-HCl buffer at a flow-rate of 0.8 ml/min. In a second step, the fractions (1.5-2.0 ml each) eluted from the Sephacryl column, denoted as P5 and found to correspond to the Ses i 2 allergen (see Results), were pooled, lyophilised and further purified by reversed-phase high-performace liquid chromatography (RP-HPLC) on a Grace-Vydac (The Separation Group, Hesperia, CA, USA) C18 semi-preparative column (1 x 25 cm, 5 μm, 300 Å porosity), eluted with a linear acetonitrile-0.1% TFA gradient, at a flow rate of 1.5 ml/min. The material eluted in correspondence of the major chromatographic peak was collected, lyophilised and stored at –20°C for subsequent studies.

The homogeneity of the purified protein was established by SDS-PAGE and analytical RP-HPLC. Standard SDS-PAGE under reducing and non-reducing conditions was carried out on a 15% acrylamide gel (Laemmli, 1970). RP-HPLC analyses were carried out on a C18 analytical column (4.6 x 150 mm, 5 μm particle size, 300 Å porosity) from Grace-Vydac. The column was equilibrated with 0.1% (v/v) aqueous TFA and eluted with a linear 0.1% (w/w)-TFA-acetonitrile gradient at a flow rate of 0.8 ml/min. The absorbance of the effluent was recorded at 226 nm.

Protein identification by peptide mass fingerprint analysis

The purified protein (100 μg, 57 μM) was reduced in the dark for 2 h at 37°C under nitrogen flow in 0.1 M Tris-HCl buffer, pH 7.8, containing 7 M guanidinium chloride (Gnd-HCl) 1 mM EDTA and 0.125 M dithiotreitol (DTT). The reaction was quenched by adding a double volume of 4% (v/v) trifluoroacetic acid (TFA). The reduction products, namely the light (LC) and heavy (LC) chains, were purified by analytical RP-HPLC, lyophilised and subjected to proteolysis with Glu-C endoproteinase from *S. aureus* strain V8 for 24 h at 25°C using an enzyme:protein ratio of 1:50 (w/w) in 50 mM ammonium acetate buffer, pH 4.0. Proteolytic fragments were purified by RP-HPLC and analysed by mass spectrometry. Spectra were taken with a model Mariner electrospray(ESI)-Time-of-Flight(TOF) mass spectrometer from Perseptive Biosystems (Stafford, TX, USA). Typically, protein samples (10 μl 10 μM) were analysed by direct injection in H_2O/acetonitrile (1:1), containing 1% (v/v) formic acid, at a flow-rate of 15 μl/min. The nozzle temperature was set at 140°C and the electrostatic potential at 4.4 kV. The instrument was calibrated using the standard protein kit, according to the manufacturer's procedures. The chemical identity of the purified protein was established by peptide mass fingerprint analysis of the reduced LC and HC treated with Glu-C protease, using the MASCOT program (Perkins et al., 1999), available on-line at the site www.matrixscience.com. The search paramenters were as follows: (1) Glu-C digest was assumed to have a maximum number of one missed cleavage; (2) peptide masses were stated to be monoisotopic; (3) Cys-residues were considered in the thiol free state (i.e, –SH); (4) any other post-translational modification was considered; (5) the mass tolerance was kept at 50 ppm.

Carboxamidomethylation of Cys-residues was conducted by reacting the reduced LC ad HC with 20 mM iodoacetamide for 30 min at 30°C in the dark. The reaction products were purified by RP-HPLC and analysed by mass spectrometry. To determine the number of free Cys-residues, the purified Ses i 2 protein (25 μg, 22 μM) was reacted in the dark with

iodoacetamide (1 min at 37°C) or 4-vinylpyridine (30 min at 37°C), in 50 mM borate buffer, pH 8.5, containing 2 mM EDTA in the presence or absence of 8 M Gnd-HCl. The reaction mixture was fractionated by analytical RP-HPLC and the material eluted in correspondence of the chromatographic peaks analysed by ESI-TOF mass spectrometry. N-terminal sequence analysis was carried out on a model 477A liquid-phase automated protein sequencer (Applied Biosystems).

Analytical Size-exclusion chromatography

The apparent molecular weight of *Ses i 2* was estimated under non denaturing conditions by analytical SEC (Corbett and Roche, 1984) using on a HR 10/30 Superose-12 column (1 x 30 cm) eluted in 50mM Tris-HCl buffer, pH 7.5, containing 1 M NaCl and 10% ethanol (v/v) at a flow rate of 0.3 ml/min. Absorbance of effluent was monitored at 280 nm. The column was calibrated using the low-molecular weight gel-filtration protein calibration kit (Amerhsam-Pharmacia). The value of void volume (V_0) and interstitial volume (V_i) were determined by loading dextran blue ($2 \cdot 10^3$ kDa) and the dipeptide H-Tyr-Gly-OH, respectively. The distribution constant, K_D, was calculated by the equation $K_D = (V_e - V_0)/(V_i - V_0)$, where V_e is the elution volume of each species.

Spectroscopic methods.

All measurements were carried out at least in duplicate at 25 ± 0.2°C in 10 mM sodium phosphate buffer, pH 7.0 or at 2.0.

UV-absorption. Peptide and protein concentration was determined by UV absorbance at 280 nm on a double beam model Lambda-2 spectrophotometer from Perkin-Elmer (Cupertino, CA), using extinction coefficients (ε) calculated on the basis of the amino acid composition (Gill and von Hippel, 1989), taken as 1.35 $cm^2 \cdot mg^{-1}$ for mature *Ses i 2*, and 3840 and 11380 $M^{-1} \cdot cm^{-1}$ for the isolated light (LC) and heavy chain (HC), respectively; ε values were taken as 0.667 $cm^2 \cdot mg^{-1}$ for BSA, 2.01 $cm^2 \cdot mg^{-1}$ for α-lactalbumin and 0.741 $cm^2 \cdot mg^{-1}$ for ovoalbumin.

Circular dichroism. CD spectra were recorded on a Jasco (Tokyo, Japan) model J-810 spectropolarimeter equipped with a thermostatted cell-holder connected to a NesLab (Newington, NH) model RTE-111 water circulating bath. The instrument was calibrated with *d*-(+)10-camphorsulfonic acid. The results were expressed as mean residue ellipticity, $[\theta]_{MRW}$

$= ([\theta]_{obs}/10) \cdot (MRW/l \cdot c)$, where $[\theta]_{obs}$ is the observed ellipticity in degrees at a given wavelength, *MRW* is the mean residue weight, *l* is the cuvette pathlength in cm, and *c* is the protein concentration in g/ml. Far- and near-UV CD spectra were recorded in a 1-mm and 1-cm quartz cell, respectively, at a scan speed of 10 nm/min and with a response time of 16 sec. The final spectra were the average of four accumulations, after base line subtraction. Quantitative estimation of the secondary structure content was performed using equation 1:

$$\%\alpha\text{-Helix} = 100/\{1 + [(\theta_{obs} - \theta_H)/(\theta_C - \theta_{obs})]\} \quad (1)$$

where θ_{obs} is the mean residue ellipticity determined at 222 nm and θ_H and θ_C are the ellipticity values for the 100% helical and coil conformation at 222 nm, respectively. Figures for θ_H and θ_H at 25°C were taken as -33500 and -485 deg·cm^2·dmol$_{-1}$, respectively, according to Schlotz et al. (1991).

Fluorescence. Fluorescence spectra were carried out on a Jasco spectrofluorimeter model FP-6500, equipped with a Peltier model ETC-273T temperature control system. Spectra were taken 25.0±0.1°C in a 1-cm pathlength quartz cell, at a scan speed of 200 nm/min by exciting the protein samples at 280 nm or 295 nm with an excitation/emission slit of 5 nm. Inner filter effects were avoided by keeping the optical density of the solution at λ_{ex} always lower than 0.05 (Lakowicz, 1986). The final spectrum was the average of four accumulations, after baseline subtraction. Under these conditions, photobeaching due to photodegradation of Trp-residues was negligible (< 2%), even after prolonged light exposure.

Titration experiments were carried out at 25.0±0.1°C by recording the fluorescence intensity at 346 nm as a function of pH. Solutions of *Ses i 2* (2 ml, 0.3 μM) were prepared adding 200 μl of a *Ses i 2* stock solution (3 μM) in Milli-Q water to 1800 μl of 5 mM citrate-borate-phosphate buffer at the specified pH value in the range 2.0-9.0. Protein samples were first incubated for 10 minutes at the specified pH and then excited at 280 nm with an excitation/emission slit of 5/10 nm, at a scan speed of 200 nm. The solution pH was measured at 25±0.5°C with a Metrohm (Herisau, CH) model 632 pH-meter. Fluorescence data were fitted to the equation:

$$F_{348\,nm} = \{(F_{max} - F_0)/[1 + 10^{(pKa - pH)}]\} + F_0 \quad (2)$$

where F_{max} and F_0, are the higher and lower fluorescence limits of *Ses i 2* at 346 nm. The values of F_{max}, F_0, and pK_a were obtained as fitting parameters.

Stability measurements. Thermal denaturation of *Ses i 2* was carried out by recording the CD signal of the protein samples (100 μg/ml) at 222 nm as a function of sample temperature. The sample cuvette (200 μl, 1-mm pathlength) was heated at a rate of 50°C/hour in the range 20-85°C and the denaturation curve was obtained after base-line subtraction. Gnd-HCl-induced unfolding of *Ses i 2* was monitored at 25°C by measuring either the CD signal at 222 nm and the fluorescence change at 346 nm, after 280-nm excitation, as a function denaturant concentration. For CD measurements, solutions at different Gnd-HCl concentrations were prepared by diluting a 8-M Gnd-HCl solution in phosphate buffer at pH 7.0 or 2.0. Protein samples (100 μl, 10 μM) were added to guanidinium solutions (900 μl), up to a final protein concentration of 1 μM. For fluorescence measurements, protein samples (0.3 μM), were excited at 280 nm with an excitation/emission slit of 5/10 nm, at a scan speed of 200 nm. At each denaturant concentration, protein samples were incubated at 25°C for 1 h and the final spectra were the average of four accumulations and resulted from subtraction of the corresponding baseline spectra, recorded under identical conditions. Reversibility of denaturation process was determined by measuring the recovery of the spectroscopic signal (i.e., CD or fluorescence intensity) upon 20-fold dilution of *Ses i 2* stock solutions in 7 M Gnd-HCl with non-denaturing buffer.

The data were analyzed assuming a two-state unfolding process ($N \Leftrightarrow U$), a linear relationship between the unfolding free energy change (ΔG_U) and denaturant concentration ($[D]$), and a linear dependence of native and unfolded state fluorescence on denaturant concentration (Pace 1986). The data points were fitted to the equation (Eftink, 1994):

$$Y = \{(Y_N + S_N[D] + (Y_U + S_U[D]) \times \exp(m[D] - \Delta G_U^\circ)/RT\} / 1 + \exp(m[D] - \Delta G_U^\circ)/RT \quad (3)$$

where Y is the observed spectroscopic signal (i..e, either CD or fluorescence signal), Y_N and Y_U the intensities of the native (N) and unfolded (U) states in the absence of denaturant, S_N and S_U are the base-line slopes for the native and unfolded regions, ΔG_U° is the free energy change for the unfolding reaction in the absence of denaturant at 25°C, and m is the denaturant index ($m = -d\Delta G_U^\circ/d[D]$). Alternatively, ΔG_U° was estimated by linear

extrapolation to [Gnd-HCl] = 0 of ΔG_U values calculated in the transition region according to the equation (Pace 1986):

$$\Delta G_U = \Delta G_U^\circ - m \cdot [D] \quad (4)$$

where m is the slope of the straight line. $[D]_{1/2}$ is defined as the denaturant concentration at which $\Delta G_U = 0$ (i.e., [U] = [N]). When the unfolding of Ses i 2 was monitored by recording the fluorescence change at pH 7.0, the data points were fitted to a biphasic equation, as implemented in the computer program Origin vs. 7.5 (Microcal Inc), describing the sequential and independent unfolding of two different regions of the molecule:

$$F = Y_N + \frac{(Y_1 - Y_N)}{1+10^{(([D]-[D]_1)*m_1)}} + \frac{(Y_2 - Y_N)}{1+10^{(([D]_2-[D])*m_2)}} \quad (5)$$

where F is the fluorescent observed signal, Y_N , Y_1 and Y_2 are the fluorescence intensities, m_1 and m_2 are the denaturant index ($m = -d\Delta G_U^\circ / d[D]$). [D] is the denaturant concentration and $[D]_1$ and $[D]_2$ are the denaturant concentration of the transition midpoint.

Ses i 2 nicked was subjected to unfolding process in presence of urea at pH 2.0 and pH 7.0. In comparison, Ses i 2 was subjected to unfolding in presence of urea at pH 2.0 and pH 7.0. At neutral pH is not possible to observe a unfolding transition for Ses i 2. The fluorescence emission signal at λ_{max} of Ses i 2 and Ses i 2 nicked was recorded at function of [urea] and data of both species were fitted by the following equation (6), which assumes a two-state model in which the fluorescence of folded states and unfolded states are dependent on denaturant concentration (Clark and Fersht, 1993):

$$F = \frac{(\alpha_N + \beta_N[D] + (\alpha_D + \beta_D[D])\exp(m([D]-[D]_{50\%})/RT)}{1+\exp(m([D]-[D]_{50\%})/RT)} \quad (6)$$

F is the fluorescence at the given [denaturant] and α_N and α_D are the intercepts and β_N and β_D are the slopes of the base line at low (N) and high (D) denaturant concentrations, respectively, [D] is the concentration of denaturant, $[D]_{50\%}$ is the concentration of denaturant at which half

of the protein is denatured, m is the slope of the transition, R is the gas constant and T is the temperature in K.

Hydrogen/deuterium (H/D) exchange mass spectrometry

Hydrogen/deuterium exchange (H/D) measurements were carried out for 23 h at 25 ± 0.2°C. The number of deuterons incorporated (on-exchange) was measured in D_2O as a function of time. Lyophilized *Ses i 2* (100 μg) was dissolved in 100 μl D_2O and, at fixed time intervals, aliquots (10 μl) were taken and directly injected into the mass spectrometer, which was flushed with D_2O at a constant flow-rate of 25 μl/min, using a model Pump-11 delivery system from Harvard Apparatus (Holliston, MA). For comparison, the same measurements were carried out with apo-myoglobin, taken as a prototypical α-helical protein. Mass values were determined as the average mass by taking the centroid of the isotopic envelope and the per cent incorporation of deuterium (%D) was calculated as $\%D = [(M_D - M_{0\%})/(M_{100\%} - M_{0\%})] \times 100$ (Smith et al., 1997), where M_D is the molecular mass of the protein at a given exchange time and $M_{0\%}$ and $M_{100\%}$ are the molecular mass values of the unlabeled and fully (i.e., 100%) deuterated protein, respectively. $M_{100\%}$ was calculated assuming that all the potentially exchangable hydrogens were replaced by deuterium. For apo-myoglobin, the experimetal value of $M_{100\%}$ was obtained after heating protein solutions at 90°C for 30 min in D_2O and measuring the mass increment by direct injection as before. Experimental values of $M_{100\%}$ were found in close agreement (± 2%) with the theoretical ones.

Proteolysis

Proteolysis reaction of Ses i 2 and other selected proteins (i.e., BSA, α-lactalbumin, and ovalbumin), used as controls, were carried out in duplicate under identical and carefully controlled conditions. The reactions were conducted with Ses i 2 solutions (500 μl, 0.1 mg/ml) in the specified buffer to which were added 20 μl of the protease stock solution. At time intervals, aliquots (50 μg) were taken and proteolysis reactions were stopped by addition of acid, 100 μl of 4% (v/v) TFA, or a solution of specific protease inhibitors. Quenched aliquots were analyzed by RP-HPLC, on C18 Vydac analytical column, eluted with a linear acetonitrile-0.1% TFA gradient at a flow rate of 0.8 ml/min. At each time point, the concentration of intact proteins remained in solution was estimated by integrating the area under the chromatographic peak corresponding to the uncleaved proteins. The chemical identity of the intact protein eluted from the RP-column was established by ESI-TOF mass spectrometry.

Digestive proteases. Time course kinetics of proteolysis reaction was conducted using a protein solution (1 mg/ml) in simulated gastric fluid (SGF), containing 50 mM HCl, 30 mM NaCl and 1.4 μM bovine pepsin at 37°C (Astwood et al., 1996). After 2-h reaction, the proteolytic activity of pepsin was blocked with pepstatin A (1 mg/ ml) and by increasing the solution pH with sodium bicarbonate. Aliquots (200 μl) of the quenched reaction in SGF were taken and incubated at 37°C for 4 h in 200 μl simulated intestinal fluid (SIF), containing 50 mM Tris-HCl buffer, pH 7.0, containing 30 mM $CaCl_2$, 5 mM bile salts, 1.25 μM trypsin and 3.9 μM chymotrypsin (Moreno et al., 2004).

Coagulation and fibrinolysis proteases. Proteolysis of Ses i 2 (32 μM) with thrombin (10 nM) and plasmin (44 nM) was conducted for 3 hour at 25°C in 5 mM Tris-HCl buffer, pH 8.0, 0.1% PEG 6000 and 0.2 M NaCl.

Bacterial proteases. Proteolysis with Glu-C proteinase V8 from *S. aureus* was conducted for 3 h at 37°C in 50 mM ammonium acetate buffer, pH 4.0, at a substrate:protease ratio of 100:1 (w/w). Proteolysis with thermolysin from *B. thermoproteolyticus* was conducted for 3 h at 70 or 90°C in 50 mM Tris-HCl buffer, pH 7.8, containing 5 mM $CaCl_2$ and 10μM $ZnCl_2$, at a substrate:protease ratio of 100:1 (w/w).

Protease inhibition assays

Digestive proteases (trypsin, chymtrypsin and pepsin). For trypsin and chymotrypsin, inhibition by Ses i 2 was estimated by measuring the release of *p*-nitroaniline (pNA) from suitable chromogenic substrates, monitored by recording the increase of absorbance at 405 nm [Lottenberg and Jackson, 1983]. The concentration of pNA-substartes was determined at 342 nm, using an extinction coefficient of 8270 $M^{-1}\cdot cm^{-1}$. Experimental conditions were as follows: 0.2 nM trypsin, 26 μM FPR-pNA and 8.8 μM Ses i 2; 200 nM chymotrypsin, 430 μM GPNA and 7.2 μM Ses i 2. Assays were conducted at 25±0.2°C in 5 mM Tris-HCl buffer, pH 8.0, containing 0.15 M NaCl and 5 mM $CaCl_2$. Pepsin inhibition assays were conducted at 25±0.2°C in 10 mM sodium phosphate buffer, pH 2.0, with 22 nM pepsin, 9.5 μM Ses i 2, and using apo-myoglobin (43.2 μM) as a substrate. The values of s_I and s_0 were determined by RP-HPLC. At each time point, the concentration of residual apo-myoglobin was estimated by integrating the area under the chromatographic peak corresponding to the uncleaved protein. The concentration of apo-myoglobin, $[apo]_t$, measured as a function of time, t, was analyzed under pseudo-first-order conditions (Copeland, 2000) and fitted to the kinetic equation $[apo]_t = [apo]_0 \cdot exp(-k_{obs} \cdot t)$, where $[apo]_0$ is the initial apo-myoglobin concentration

and $k_{obs} = e_o \cdot s$ is the observed rate constant of substrate hydrolysis, s is the specificity constant, and e_o is the concentration of pepsin. The per cent residual activity was calculated as $\%R.A. = (s_I/s_0)\ x\ 100$, where s_I and s_0 are the specificity constants, $s = k_{cat}/K_m$, for the hydrolysis of apo-myoglobin in the presence or absence of inhibitor, I.

Coagulation (thrombin, factorXa, and aPC) and fibrinolysis (plasmin) proteases. Experimental conditions were as follows: 200 pM thrombin, 21.6 μM FPR-pNA and 4.6 μM Ses i 2; 0.5 nM factor Xa, 300 μM RGR-pNA and 9.4 μM Ses i 2; 1 nM aPC, 60 μM WRR-pNA and 7.2 μM Ses i 2; 1 nM plasmin, 102 μM VLR-pNA and 9.6 μM Ses i 2. For thrombin inhibition, the IC_{50} value (i.e., the inhibitor concentration reducing by 50% the rate of substrate hydrolysis) was determined by using 100 pM thrombin, 20 μM FPR-pNA and increasing Ses i 2 concentrations from 0 to 7.5 μM. The data points were fitted to a dose-response equation of the type (Copeland, 2000):

$$v_i/v_0 = \{1/[1 + 10^{(\log[I] - \log IC50)}]\} \quad (5)$$

where v_0 and v_i are the initial velocities of substrate hydrolysis in the absence and presence of the inhibitor, I (i.e., Ses i 2).

Bacterial proteases (thermolysin). Inhibition assays were conducted by measuring the effect of Ses i 2 (10 μM) on the initial velocity of FAGLA (660 μM) hydrolysis by thermolysin (22 nM). The concentration of FAGLA was determined at 345 nm, using an extinction coefficient of 766 $M^{-1} \cdot cm^{-1}$ and the substrate hydrolysis by thermolysin was determined using the molar absorption difference $\Delta\varepsilon_{345nm}$ = - 310 $M^{-1} \cdot cm^{-1}$ 8Feder, 1968; Yasukawa and Inouye, 2007).

Computational methods

The structure of Ses i 2 (Swiss-Prot entry code: Q9XHP1) was modelled by homology on the NMR structure (PDB entry code: 1SM7) (Pantoja-Uceda et al., 2004) of the recombinant precursor of the 2S albumin BnIb from *Brassica napus* (Swiss-Prot entry code: Q8GT96). The best-representative model in the NMR ensemble was selected using the program OLDERADO (http://neon.ce.umist.ac.uk/) (Kelley and Sutcliffe, 1997). Pairwise sequence alignments were performed with the program LALIGN (http://www.ch.embnet.org/software/LALIGN_form.html), while for multiple sequence alignments, the T-COFFEE program (http://www.ebi.ac.uk/t-coffee/) was used (Notredame et al. 2000). Secondary structure predictions were performed using the PHD program (Rost,

1996) as implemented in the PredictProtein server (http://www.predictprotein.org/main.php). The Structural model of Ses i 2 was built by keeping the secondary structure segments of rproBnIb (1SM7) fixed and manually replacing the non-conserved amino acids by using the program Insight-II (Accelrys Inc., CA). Side-chains conformation was modeled by selecting the most probable rotamer, as identified with the SCWRL-3.0 program (Canutescu et al., 2003). Segments of non regular secondary structure (i.e., loops and turns) were modelled using the ArchPRED program (http://manaslu.aecom.yu.edu/loopred/) (Fernandez-Fuentes et al., 2006). Model refinement was carried out by energy minimisation using the program CNS. Quality control of the resulting model was performed using the Structure Validation option (http://swift.cmbi.ru.nl/servers/html/index.html), as implemented in the WHAT IF software package (Hooft et al., 1996). Accessible surface area (ASA) calculations were carried out using the program available on-line at the site http://molbio.info.nih.gov/structbio/basic.html and a water probe radius of 1.4 Å.

RESULTS AND DISCUSSION

Identification, purification and chemical characterization of Ses i 2

Protein extraction from coarsely ground sesame seeds with Tris-HCl buffer, pH 8.0 (10% w/v; see Methods), resulted in a crude extract with a total proteins content of about 8 mg/ml. For analytical purposes, this extract was fractionated on a Superose 12 gel filtration column. P1-P5 fractions were collected as indicated in Figure 1A and analysed by SDS-PAGE (Figure 1A, Inset). Fractions P1 and P2 do not seem to contain any protein material. Indeed, the corresponding lanes in the gel do not stain with Coumassie, even though the amount of material estimated from the peaks absorbance is not too low. As shown by SEC experiments (Figure 1C), P3 elutes with an apparent molecular weight of 120 kDa (Figure 1C) and, when analysed by SDS-PAGE, displays two major bands at ~50 kDa, likely corresponding to isoforms of the 11S α-globulin, earlier identified is sesame seeds (Tai et al., 1999; 2001). P4 and P5 have an apparent molecular weight of 14 and 6 kDa (Figure 1C), respectively, within the mass range of 2S albumins, seed storage proteins widely distributed in dicotyledonous plants (Shewry et al., 2002) and representing about 25% of the protein content in sesame seeds (Tai et al., 1999; Pastorello et al., 2001; Wolff et al., 2003). Both fractions were desalted by RP-HPLC and analysed by ESI-TOF mass spectrometry, yielding mass values of 15595.8±0.8 a.m.u. for P4 and 11726.4±0.7 a.m.u. for P5. Of interest, both P4 and P5 migrate at 14 kDa when run on a non-reducing polyacrylamide gel (Figure 1A, Inset), thus suggesting

that this latter protein is composed of a larger and smaller chain held together by at least one disulfide bond. With this in mind, we decided to focus our attention on the protein fraction P5, corresponding to the most abundant component among the low-molecular weight proteins in the crude extract. P5 was purified in two steps, including gel-filtration chromatography on a Sephacryl HR 100 column and semi-preparative RP-HPLC. The homogeneity of the purified protein was established by analytical RP-HPLC, SDS-PAGE and mass spectrometry (Figure 1B).

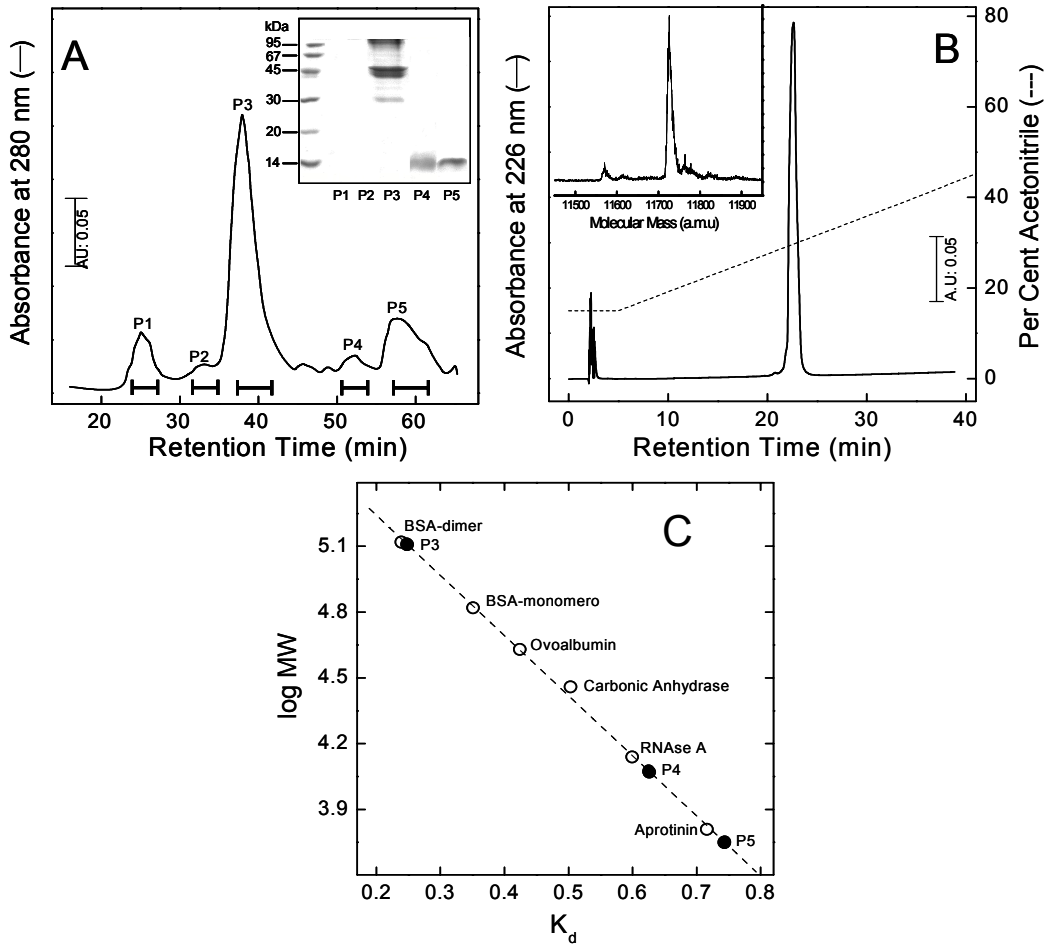

Figure 1. Purification of the major protein components from the sesame seeds extract. (A) Fractionation of the clarified extract by gel-filtration chromatography. An aliquot (100 µl, 800 µg of total proteins) of the crude extract was loaded onto a Superose 12 column, eluted at a flow-rate of 0.3 ml/min in 50 mM Tris-HCl buffer, pH 7.5, containing 1 M NaCl and 10% ethanol (v/v). (Inset) Fractions P1-P5 were collected, as indicated, and analysed (15-µl aliquots) by SDS-PAGE on a 14%-acrylamide gel, in the absence of β-mercaptoethanol. Molecular weight standards are reported on the left hand lane. **(B)** Purity check of P5. An aliquot (30 µg) of P5, previously purified by semi-preparative RP-HPLC (see text), was loaded onto an analytical C18 column, eluted at a flow rate of 0.8 ml/min with a linear 0.1% (v/v)-TFA-acetonitrile gradient (---). **(Inset)** Deconvoluted ESI-TOF mass spectrum of the RP-HPLC purified P5. **(C) Determination of the apparent molecular weight of the major protein components of sesame seeds by size-exclusion chromatography.** The column was calibrated using protein standards (empty cyrcles) of known molecular weight and the distribution constant, K_D, calculated according to Corbett and Roche (1984). For the components P3-P5 (filled cyrcles), the estimated molecular weight was as follows: P3, 120±10 kDa; P4, 12±2 kDa; P5, 6±1 kDa.

The strategy we exploited for the chemical identification of the protein fraction P5 is highlighted in Figure 2. The purified protein was first reduced with DTT (Figure 2A), yielding two species with masses 3312.8±0.4 and 8424.6±0.3 a.m.u. for the light (LC) and heavy (HC) chain, respectively. The reduced LC and HC were derivatised with iodoacetamide (Figure 2B) and the mass values of the resulting carboxamidomethylated products are compatible with the incorporation of three and seven $–CH_2$-CO-NH_2 groups at the level of the Cys-residues in the LC and HC, respectively. Interestingly, when P5 was reacted with iodoacetamide or 4-vinylpyridine in the absence of DTT, under strongly denaturing (i.e, 8 M Gnd-HCl) or non-denaturing (ie., Tris buffer, pH 8.0) conditions, any change in the RP-HPLC plot or in the mass values of the material eluted from the column could be detected. The lack of reactivity with iodoacetamide and 4-vinylpyridine prides evidence that that all Cys residues in the P5 protein fraction form intramolecular disulfide bonds.

Peptide mass fingerprint analysis of LC (Figure 2C) and HC (Figure 2D) with *S. aureus* V8 protease, combined with a MASCOT search (Perkins et al., 1999), allowed us to unambiguously identify all the peptide masses (see Table 1) of the proteolytic fragments as originating from the precursor protein of the *Ses i 2* allergen from *Sesamum indicum* (Swiss-Prot entry code: Q9XHP1) (Figure 2E) (Tai et al., 1999). In total, 12 peptide fragments were isolated and of these, 9 have mass values that could be easily assigned to the corresponding segments in the *Ses i 2* sequence. Only three masses did not match with any of the Glu-C derived fragments of *Ses i 2*: the mass value at 890.3±0.03 a.m.u. for the LC, and those at 591.2±0.02 and 1159.5±0.08 a.m.u. for the HC. A closer analysis of data reveals all these values always differ by –17 a.m.u. from the theoretical masses of the fragments 18-24 (907.9 a.m.u.) in the LC, and 56-60 (607.6 a.m.u.) and 56-64 (1177.2 a.m.u.) in the HC. These differences can be assigned to the loss of ammonia resulting form the conversion of the N-terminal Gln18 in the LC and Gln56 in the HC to pyroglutamic acid (Pyr-Glu).

The nonenzymatic Gln $\rightarrow$ Pyr-Glu reaction occurs spontaneously and quantitatively when Gln is at the N-terminal end (for a review, see Abraham and Podell, 1981) and, in our case, it well explains the failure of N-terminal sequencing carried out by Edman chemistry on the LC and HC of Ses i 2.

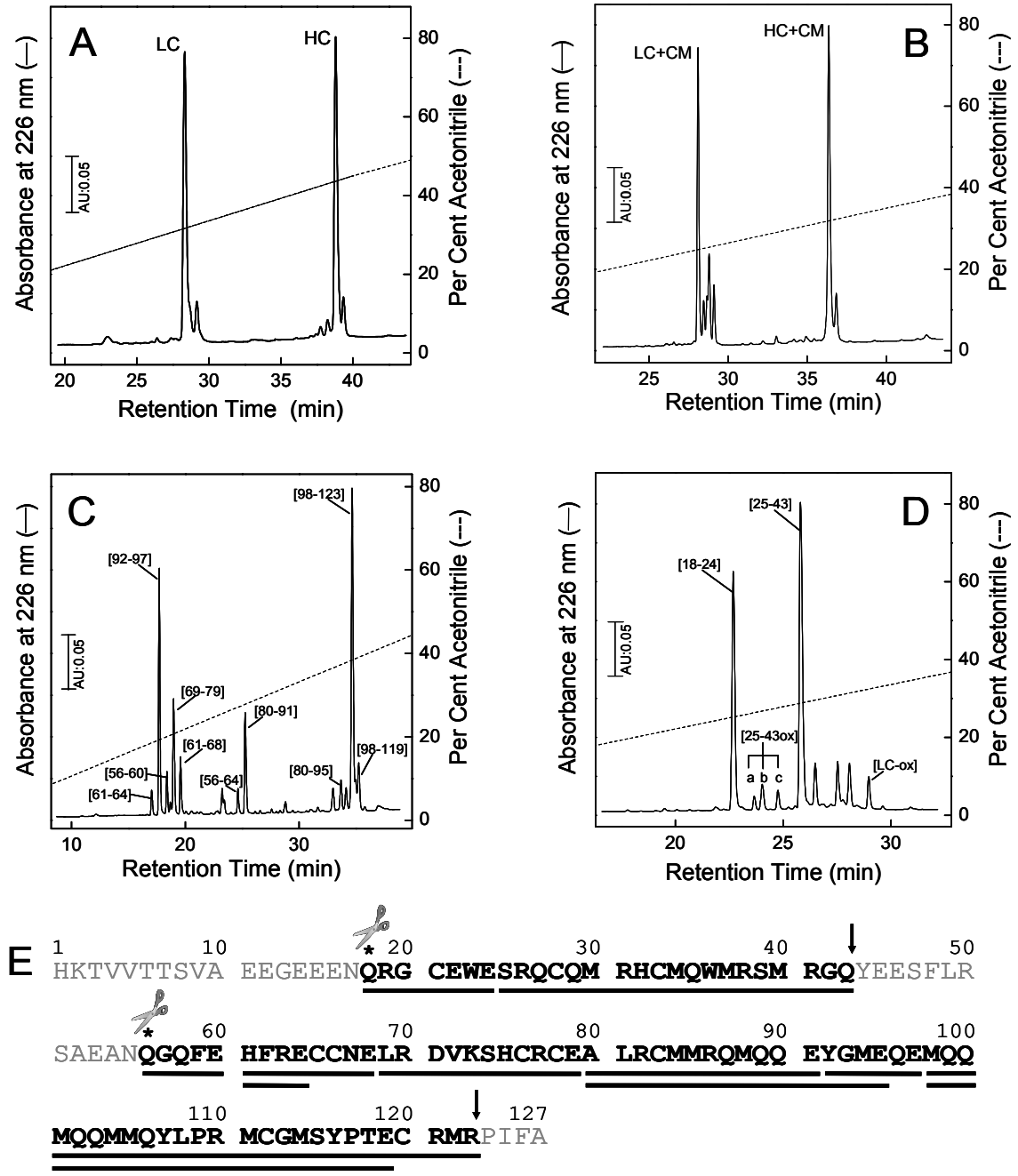

Figure 2. Chemical characterization of fraction P5. (**A**) RP-HPLC analysis of the disulfide reduction reaction of P5. The reaction products, denoted as LC and HC, were separated on a C18 column and analysed by ESI-TOF mass spectrometry. (**B**) RP-HPLC analysis of the carboxamidomethylation reaction of P5. Mass spectrometric analysis of the material eluted in correspondence of the major peaks, denoted as LC-CM and HC-CM, gave mass values of 3483.8±0.4 and 8823.6±0.3 a.m.u. RP-HPLC analyses of the proteolysis reaction of purified LC (**C**) and HC (**D**) with Glu-C protease. The numbers next to the chromatographic peaks refer to the peptide segments of Ses i 2, as identified by ESI-TOF mass spectrometry (**see Table 1S in the Supplementary Materials**). (**E**) Amino acid sequence of the precursor Ses i 2 protein allergen lacking the signal peptide (SwissProt entry code: Q9XHP1). In bold is reported the sequence of the mature protein, as identified by the molecular masses of the proteolytic fragments. (*) indicates that Q18 and Q56 are in the form of Pyr-Glu.

Mass spectrometry analysis of the material eluted in correspondence of the minor peaks in Figure 2C shows the presence of mono-oxidized species of LC (Δm = + 16 a.m.u.), likely generated by the acid-catalysed air oxidation of methionine (Met) to Met sulfoxide (MetSO) (Glazer A.N., 1970), occurring during RP-HPLC purification and lyophilisation of the LC. Ses i 2 is highly stable to physical and chemical denaturants as well as to proteolytic degradation by several different proteases (see below), and therefore (despite many attempts) we failed to obtain Ses i 2 fragments suitable for disulfide pairing assignment. For this reason, the disulfide bond topology was inferred from that usually observed in other 2S albumins of known three-dimensional structure (for a review see Pantoja-Uceda et al., 2002). Notably, 74% of the entire Ses i 2 precursor sequence was covered by peptide mass fingerprint analysis. However, we could not identify any fragment within (or encompassing) the segments 1-17, 44-55, and 124-127, in agreement with earlier studies showing that, during seeds maturation, 2S albumins undergo extensive proteolytic processing by different proteases leading to the removal of the N-terminal propetide, excision of an internal loop, and trimming of the C-terminal segment (Hara-Hishimura et al., 1998; Hiraiwa et al., 1997).

Notably, second-derivative UV/Vis absorption spectra of the isolated LC and HC (Figure 3B) indicate that, among the aromatic amino acids, the light chain contains only Trp-residues, whereas the heavy chain contains only Tyr- and Phe-residues.

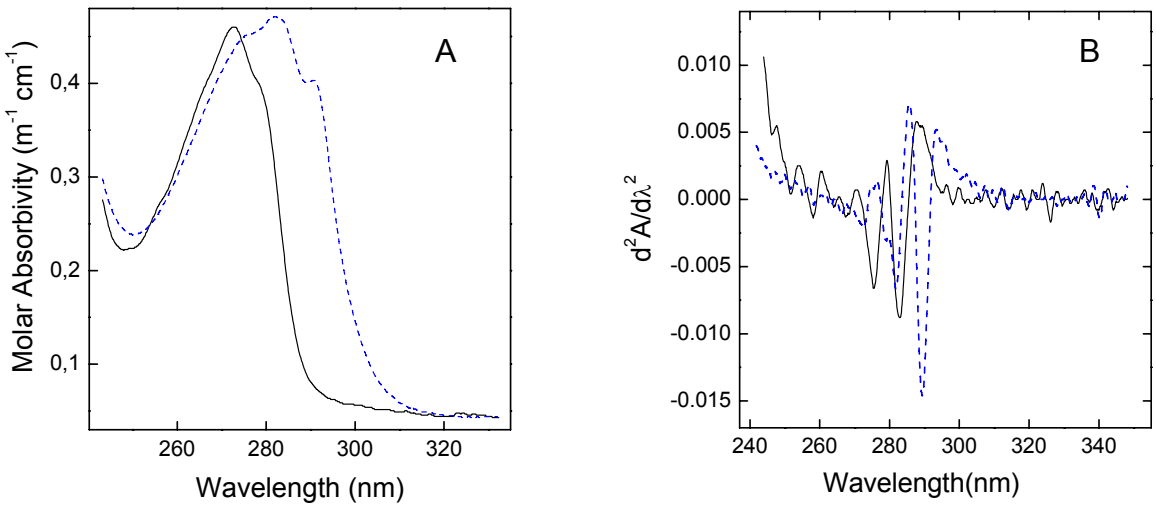

Figure 3. UV/Vis absorption spectra (A) and second derivative UV/Vis spectra (B) of LC (—) and HC (—).

Here we have shown that the mature form of the protein allergen Ses i 2 is formed by two subunits: a light chain (LC), comprising residues 18-43, and a heavy chain (LC), comprising residues 56-123, held together by three S-S bonds and with the N-terminal Gln18 and Gln56 in the Pyr-Glu form. The mature Ses i 2 sequence accounts for about 63% of the full-length

protein chain (i.e, 148 amino acids) (see Figure 2E), encoded by the corresponding sesame DNA sequence (accession no. AF091841) (Tai et al. 1999). This result indicates that, similarly to other storage proteins (Hiraiwa et al., 1997), Ses i 2 undergoes extensive proteolytic degradation at different sites along the polypeptide chain during seed development and maturation. However, to rationalize our data, a deeper knowledge of the biosynthesis and processing of seed storage proteins is required.

2S albumins are synthesized in the rough endoplasmic reticulum (ER) as pre-pro-proteins and their translocation in the ER lumen is specified by an N-terminal hydrophobic signal peptide that is cleaved from the nascent chain as it enters the lumenal space, where disulfide bonds are formed and the polypeptide chain folds into the stable pro-protein form. Next, through different trafficking pathways, the pro-proptein is translocated into the lytic (LVs) and protein storage vacuoles (PSVs). Targeting to LVs or PSVs is directed by different vacuolar sorting signals (VSS) acting as propetides and grouped into sequence specific (ssVSS) and C-terminal (ctVSS) VSSs. In particular, sequence specific VSS (ssVSS) have a consensus tetrapeptide sequence [N/L][P/I/L][I/P][R/N/S] and direct storage proteins to LVs. The route to PSVs, instead, is specified by the ctVSS, consisting of a poorly conserved short string of hydrophobic residues, located at the very C-terminus of the protein in unstructured and exposed regions, where they are removed upon vacuolar delivery (Vitale and Hinz, 2005). LVs are acidic compartments, rich in hydrolases and can be regarded as the equivalent of mammalian lysosomes. PSVs, instead, accumulate storage proteins, that will be used as a source of amino acids during seed development and germination (Müntz K., 1998). PSVs have a higher pH and lower hydrolytic activity than LVs do. It seems that during seed maturation, LVs and PSVs ultimately merge to form a large central vacuole containing several different proteases (Di Sansebastiano et al., 2001) responsible for the mobilization of storage proteins after germination. The known vacuolar proteases include 1) the vacuolar processing enzyme (VPE) (Hara-Hishimura et al., 1993), a key cysteinyl-protease cleaving many storage proteins at conserved Asn-Xxx bonds, where Xxx is preferentially a Gln or Pro; 2) an aspartyl-endopeptidase (Hiraiwa et al., 1997), cleaving peptide bonds in which one of the amino acids has a bulky hydrophobic side chain and functioning as a secondary enzyme in trimming the C-terminal propeptides that derive from the subunits newly formed by the action of the VPE; 3) amino- and carboxy-peptidases, also functioning as secondary enzymes in the production of mature 2S albumins. Hence, in the case of 2S albumin it is feasible that removal of the propeptide 1-17 is accomplished in the PSVs by the action of VPE at Asn17-Gln18 bond, while excision of the internal loop ^{44}YEESFLRSAEAN^{55} is mediated by the combined

action of VPE, at the Asn55-Gln56 bond, and of the vacuolar aspartyl-protease, at the Gln43-Tyr44 bond. Loop excision has also been demonstrated for other pro-2S albumins from Arabidopsis, Brassica, castor bean, and Brazil nut (Hiraiwa et al., 1997). Finally, an exoprotease enzyme selective for hydrophobic amino acids is responsible for the stepwise removal of the C-terminal tetrapeptide –PIFA, that likely acts as a C-terminal vacuolar sorting signal (ctVSS). Similar hydrophobic ctVSSs are released from the 2S albumin in Bertholletia excelsa (i.e., -IAGF) and from the 7S globulin in Phaseolus vulgaris (i.e., -AFVY).

Altogether, our data indicate that the protein fraction P5 corresponds to a partially proteolyzed form of the Ses i 2 precursor, composed of a light chain, comprising residues 18-43, and a heavy chain, comprising residues 56-123, held together by three S-S bonds and with the N-terminal Gln18 and Gln56 in the Pyr-Glu form. Notably, the abundance of Cys (10.6%), Arg (13.8%), Met (16%), and Gln (17%) in the mature Ses i 2 (containing 94 amino acids) is much higher than that normally observed in natural proteins for Cys (1.4%), Arg (5.4%), Met (2.4%) and Gln (3.9%) (http://expasy.org/sprot/relnotes/relstat.html), even though the frequency of the positive residues (i.e, Arg + Lys = 14.9%) is not dramatically different from that observed statistically (i.e, 11.4%). For comparison, and assuming a proteolytic processing similar to that of Ses i 2 , the mature Ses i 1 sequence contains 17 Arg and 28 Gln, but only one Met. As proposed for other 2S albumins, these amino acids represent an excellent source of nitrogen and sulphur during seed germination.

Conformational and stability properties of Ses i 2 at neutral and acidic pH

Considering the pH values of the main anatomic districts (i.e, stomach and gut) with which Ses i 2 comes into contact after oral ingestion and the pH gradient to which Ses i 2 is subjected in the seed during its translocation for final deposition, ranging from neutral in the endoplasmic reticulum to acidic in the vacuole (Tai et al., 1999), we investigated the conformational and stability properties of Ses i 2 at pH 7.0 and 2.0.

The far-UV CD spectra of Ses i 2 (Figure 5A) at both neutral and acidic pH share a common shape, with two negative bands at 222 and 210 nm, and a positive band at 193 nm, typical of proteins with a large α-helical content (Brahms and Brahms, 1980). At acidic pH, however, there is a substantial increase in the CD signal, while the $[\theta]_{222nm}/[\theta]_{210nm}$ ratio remains constant. Estimation of the secondary structure content with equation 1 (Schlotz et al., 1991) suggests that going from pH 7.0 to pH 2.0, there is a significant increase in the helix content, from 39 to 53%.

To test whether the two chains can independently fold in solution and to evaluate the role of disulfide bridges in Ses i 2 structure, the far-UV spectra of the purified LC and HC, both in the disulfide reduced state, were separately recorded at pH 2.0, a value at which disulfide shuffling is inhibited. The CD spectra (Figure 5A, Inset) indicate that the LC is largely unfolded, whereas the HC still retains significant helical structure, even though much lower than that of the parent Ses i 2. Interestingly, the spectrum of the LC and HC mixed in a 1:1 molar ratio is superimposable to the theoretical sum spectrum, obtained by adding the spectra of the isolated LC and HC. Similarly to other protein systems, these findings indicate that the integrity of disufide bonds is necessary for stabilizing the tertiary structure of Sis i 2 and that the LC and HC are not able to form a non-covalent complex, under the experimental conditions explored at least.

The near-UV CD spectrum of Ses i 2 at pH 7.0 (Figure 5B) displays two positive bands at 294 and 288 nm, assigned to the ^1L_b band superimposed to the negative ^1L_a band of Trp-residues (Strickland, 1974), while the contribution of Tyr-residues appears as two distinct bands at 278 and 282 nm. The typical 6-nm spaced fine structure of Phe-absorption is also detectable at 269 and 263 nm. A similar spectrum is obtained for the mature napin (Murèn et al., 1996). Near-UV CD is a very sensitive probe of aromatic side-chains and disulfide bonds topology and even subtle changes in protein structure can markedly affect the signal in the near-UV region (Strickland, 1974). At acidic pH, the absorption of Trp is essentially unchanged, indicating that the chemical environment surrounding Trp-residues is retained at pH 2.0. Conversely, the CD signal in the 260-278 nm range becomes more negative at low pH, suggesting that the environment of Tyr- and Phe-residues and or the chirality of the five S-S bonds in Ses i 2 are significantly altered at pH 2.0.

The properties of the chemical environment in which Trp-residues are embedded was investigated by fluorescence spectroscopy after excitation at 280 and 295 nm. After excitation at 280 nm, Ses i 2 emits fluorescence with a λ_{max} value of 346 nm (Figure 5C), typical of Trp-residues embedded in a polar environment (Vivian and Callis, 2001), while the contribution of Tyr-residues appears as a weak, but detectable, shoulder at 303 nm, indicative of inefficient Tyr-to-Trp resonance energy transfer (RET). The intensity of the 295-nm spectrum of Ses i 2 is about three-fold lower than that recorded after excitation at 280 nm, as also observed in the spectra of model compounds (Figure 2C, Inset). At pH 2.0, the λ_{max} remains constant, but the signal intensity decreases by three-fold. Such a remarkable decrease of fluorescence is not accounted for simply by acid quenching of Trp emission, caused by excited-state proton transfer to indolyl nitrogen. In fact, with model compounds the fluorescence intensity at pH

2.0 is only 10% lower than that measured at pH 7.0 (Figure 5C, Inset). Therefore, there must exist a near-neighbour effect for which protonation of a specific chemical group quenches the fluorescence of some Trp-residue nearby in the protein. The pH-dependent fluorescence signal of Ses i 2 follows a sigmoidal shape (Figure 5D) in the pH range 1-9 and, after data fitting with equation 2, a pK_a value of 3.64±0.07 was estimated. This value is fully compatible with those of the carboxyl groups of Asp and Glu side-chains at highly exposed protein sites (i.e., 3.3-4.1) (Oliveberg et al., 1995), but it is 0.5-0.7 pH units lower than those determined for model compounds in water. With respect to this, detailed spectroscopic studies have demonstrated that carboxylic acids, but not carboxylates, quench the fluorescence of Trp by a nonradiative process involving excited-state electron transfer from the indole ring to the electrophilic carboxyl group acceptor. Hence, we conclude that in the chemical environment of one or both Trp-residues in Ses i 2 there are acidic amino acids whose titration to the neutral carboxyl form is able to effectively quench Trp fluorescence. Visual inspection of Ses i 2 sequence reveals that Trp23 in the N-terminal segment of the LC is flanked by two Glu-residues, that at acidic pH may effectively quench the fluorescence of the neighbouring Trp23 (see Figure 4).

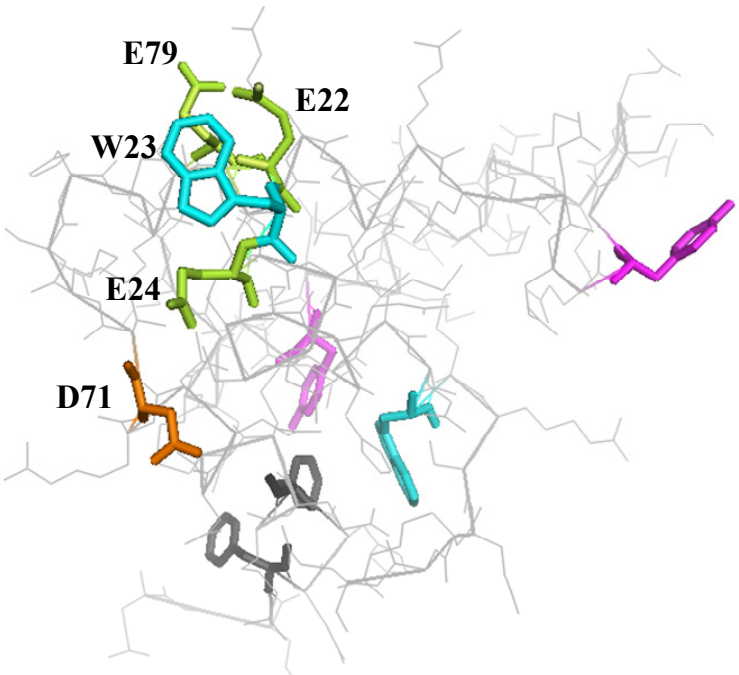

Figure 4. Schematic representation of Trp23, Glu22, Glu24,Glu79 and Asp71.

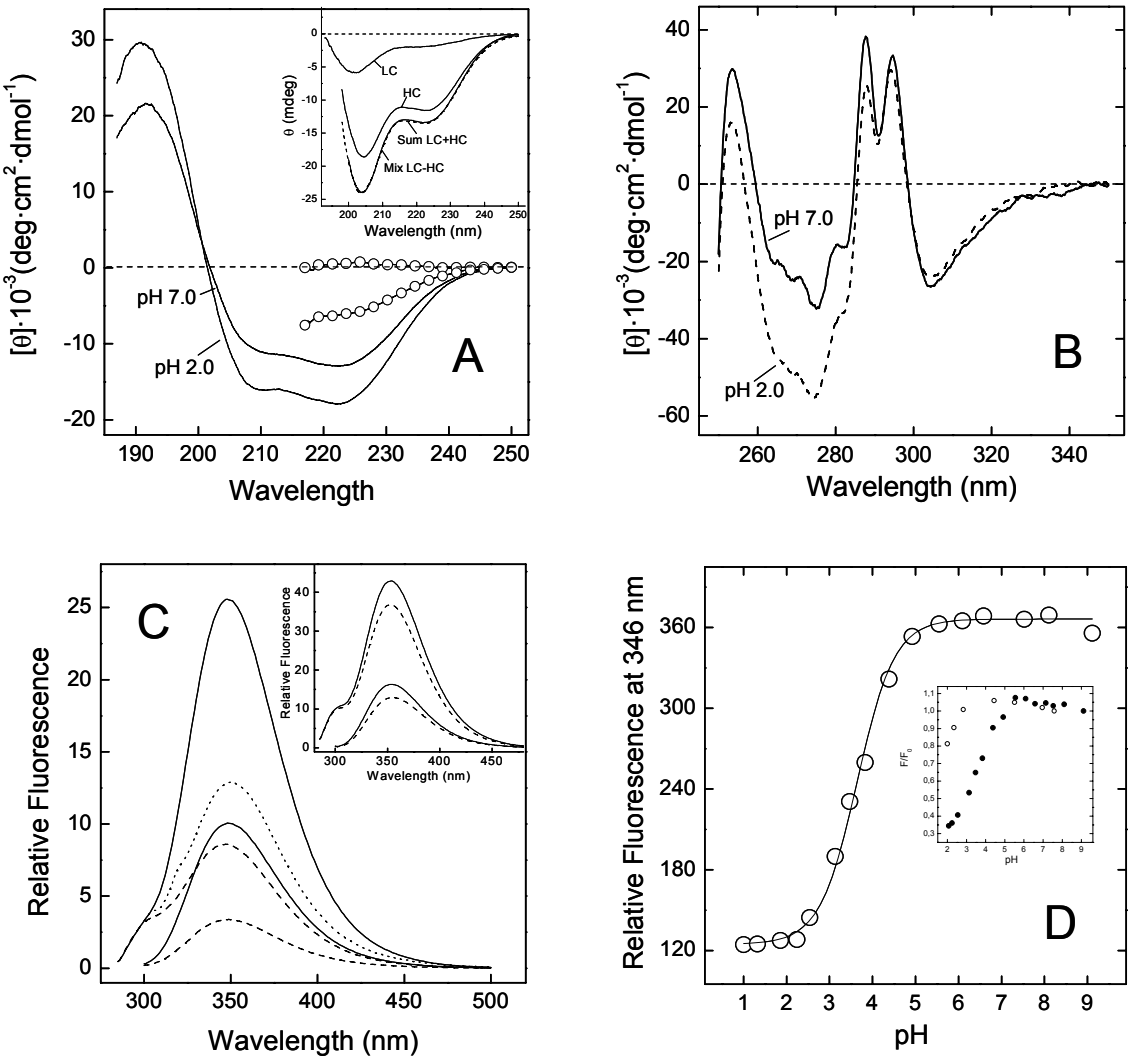

Figure 5. Conformational characterisation of Ses i 2 at pH 7.0 and 2.0. Far- (**A**) and near-UV (**B**) circular dicroism spectra of purified Ses i 2 at pH 7.0 (—) and 2.0 (---) or in the presence of 8.0 M Gnd-HCl at pH 7.0 (○). (**Inset to panel A**) Far-UV CD spectra of LC and HC at pH 2.0, isolated or in equimolar mixture. The theoretical sum spectrum of the LC and HC spectra is also reported (---). All CD spectra were recorded at 25±0.2°C in 10 mM sodium phosphate buffer, pH 7.0 or pH 2.0, at a protein concentration of 0.1 and 0.6 mg/ml, in the far- and near-UV region, respectively. (**C**) Fluorescence spectra of Ses i 2 at pH 7.0 (—) and 2.0 (---) or in the presence of 4.0 M Gnd-HCl at pH 2.0 (○). Protein samples (0.6 μM) were excited at 280 or 295 nm, as indicated. (**Inset to panel C**) Fluorescence spectra of the model compound solutions N^{α}-acetyl-Tyr-NH_2 and N^{α}-acetyl-Trp-NH_2, mixed in the same molar ratio as that present in the mature Ses i 2 sequence (i.e., Tyr/Trp = 3:2). The spectra were taken at pH 7.0 (—) and 2.0 (---). (**D**) pH-Dependence of the fluorescence intensity Ses i 2 (●). Protein samples (0.3 μM) in 5 mM citrate-borate-phosphate buffer, at the pH value indicated, were excited at 280 nm and the emission fluorescence recorded at λ_{max} (i.e., 346 nm). The data points were fitted to equation 2 with best-fit parameters: F_{max} = 373±5, F_0 = 123±8, and pK_a = 3.64±0.07. (**Inset**) For comparison, the fluorescence intensity of a solution of N^{α}-acetyl-Tyr-NH_2 and N^{α}-acetyl-Trp-NH_2 (see above), as a function of pH, is also reported (○).

Stability of Ses i 2 to temperature and Gnd-HCl at neutral and acidic pH.The thermal stability of Ses i 2 was monitored by recording the ellipticity at 222 nm, θ_{222nm}, as a function of temperature, while the stability of the sesame allergen to chemical denaturants was followed by recording both θ_{222nm} and the fluorescence intensity at λ_{max} for increasing Gnd-HCl concentration. In all cases, the denaturation process was fully reversible (>95%).

At both pH 7.0 and 2.0, the ellipticity gradually decreases (in absolute value) with a roughly linear shape by increasing the temperature (Figure 6B). Strikingly, at 87°C Ses i 2 retains 85% and 73% of the initial CD signal measured at pH 7.0 and pH 2.0, respectively, at the starting temperature (i.e., 25°C). The extraordinarily high thermal stability of secondary structure elements in Ses i 2 is paralleled by its resistance to chemical denaturation with Gnd-HCl (Figure 6). At both pH 7.0 and 2.0, the value of θ_{222nm} changes with [Gnd-HCl] according to a sigmoidal transition, suggestive of a cooperative unfolding process (Eftink, 1994), and barely reaches a plateau only at [Gnd-HCl] > 8.0 M, just below the aqueous solubility limit of the denaturant. At high [Gnd-HCl], the far-UV CD spectra of Ses i 2 is that typical of a fully unfolded protein, with a strong decrease of the θ_{222nm}-band intensity and a blue-shift of the θ_{210nm}-band towards 200 nm (see Figure 5A). The value of $[Gnd\text{-}HCl]_{1/2}$ (i.e., the concentration of half denaturation) was calculated as 6.83±0.05 and 6.23±0.05, at neutral and acidic pH, respectively. The differences in the shape of the thermal and Gnd-HCl denaturation curves may arise from the different molecular mechanisms by which these two agents unfold proteins, leading to intrinsically different denatured states (Dill and Shortle, 1991). Gnd-HCl denatures proteins by direct binding especially to polar groups and by an indirect effect, chaotropic effect, thus favouring solvation of apolar surfaces by water, whereas thermal unfolding is caused by weakening of intramolecular interactions due to diffusion of water molecules into the protein core at high temperatures (Nishii et al., 1995, Pace et al., 1995).

Since no clear transition could be detected even at highest temperatures explored (92°C), we performed thermal denaturations of Ses i 2 at pH 2.0 in the presence of increasing concentrations of Gnd-HCl, which is expected to make the experimental determination of the melting temperature, T_m, more accessible to physical measurement (Vieille and Zeikus, 2001). The data shown in Figure 6D indicate that at 5 M Gnd-HCl the denaturation curve is shallow, with a T_m value estimated as high as 75±3°C, whereas at 6 M Gnd-HCl it becomes fairly sigmoidal, suggestive of a cooperative unfolding, with a T_m of 62.5±1.0°C. At 7M Gnd-HCl, Ses i 2 is mainly unfolded and therefore no transition could be observed.

When the Gdn-HCl-mediated unfolding of Ses i 2 was monitored by recording the fluorescence change at neutral and acidic pH, two different profiles were obtained (Figure 6A). At pH 2.0, a single transition was observed. The fluorescence intensity sharply increases with a sigmoidal shape as a function of denaturant concentration, even though a plateau in the post-transition region could not be clearly identified. From these data a $[Gnd\text{-}HCl]_{1/2}$ value of 6.8±0.1 M was estimated. Enhancement of fluorescence intensity during unfolding originates from the relief of Trp quenching (Eftink, 1994), that in the folded native state may be caused by specific groups (e.g., carboxyl groups, peptide bonds, aromatics, disulfides, etc.) surrounding Trp-residues. At pH 7.0 the denaturation curve displays an unusual biphasic profile. The first transition occurs with a shallow but significant decrease of fluorescence intensity (i.e., up 40%) and with a $[Gnd\text{-}HCl]_{1/2}$ value of about 3 M. Conversely, at higher denaturant concentrations, the fluorescence signal sharply increases, reaching a maximum value similar to that recorded at pH 2.0. Form this latter transition, a figure of $[Gnd\text{-}HCl]_{1/2}$ of 6.8±0.1 M was calculated. Thus, at acidic pH both Trp23 and Trp36 are quenched in the folded protein and, upon increasing [Gnd-HCl], they denature as a single unfolding unit. At neutral pH, instead, it seems that the two Trp-residues unfold almost independently, likely because of the different effect that the carboxylate charges have on the stability of the local environment surrounding the two Trp-residues. At pH 7.0, indeed, quenching of Trp23 by the flanking Glu-residues is selectively abolished and it unfolds at low [Gnd-HCl] with a decrease in the fluorescence intensity. At higher [Gnd-HCl], quenching of Trp36 is relieved, with a concomitant fluorescence increase.

In all chemical unfolding experiments, increasing [Gnd-HCl] causes a change in the fluorescence intensity of Ses i 2 but only a negligible, if any, change in the λ_{max} value. The good coincidence of the $[Gnd\text{-}HCl]_{1/2}$ value determined by recording the CD signal at 222 nm and the fluorescence intensity at 346 nm is taken as a strong evidence that at pH 2.0, but not at pH 7.0, Ses i 2 unfolds according to a reversible two-state process ($N \Leftrightarrow U$). Linear extrapolation of the denaturation data to [Gnd-HCl] = 0 (Methods) at pH 2.0 yields a conformational stability ($\Delta G_u°$) for Ses i 2 of 11.3±1.0 kcal/mol (Figure 5B, Inset).

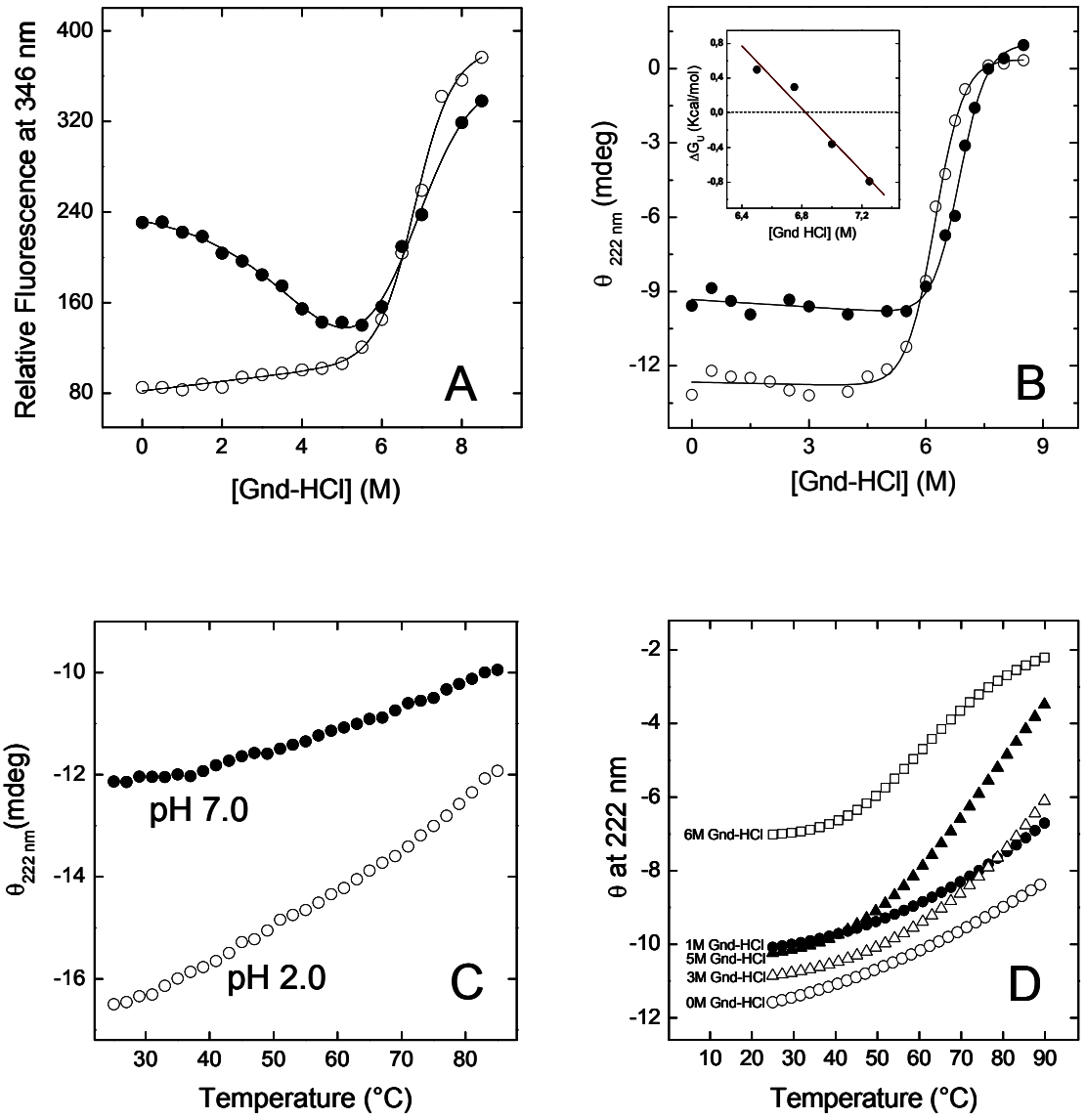

Figure 6. Stability of Ses i 2 to heat and Gnd-HCl at pH 7.0 and 2.0. (**A**) Thermal denaturation of Ses i 2 monitored by circular dichroism. The CD signal at 222 nm, θ_{222nm}, of Ses i 2 samples (1 ml, 10 μg/ml) was recorded as a function of sample temperature at pH 7.0 in the absence of denaturant and at pH 2.0 in the presence of increasing concentrations of Gnd-HCl (0–6 M), as indicated. (**B**) Gnd-HCl-induced unfolding of *Ses i 2* monitored by circular dichroism. $\theta_{222\ nm}$ values of *Ses i 2* samples (1 ml, 11.7 μg/ml) was recorded under neutral (●) and acidic (○) conditions. Continuous lines represent the best fit of data points to equation **3**, describing a single-step unfolding process. (**Inset to panel B**) Plot of the unfolding free energy change, ΔG_U, of Ses i 2 at pH 2.0 as a function of [Gnd-HCl] in the transition region. Data points were linearly fitted to equation **4**, yielding the best-fit parameters $[D]_{1/2}$ = 6.23±0.05, $\Delta G_U°$ = 11.3±1.0 kcal/mol, and m = 1.81±0.07 kcal/mol^2. (**C**) Gnd-HCl-induced unfolding of *Ses i 2* monitored by fluorescence spectroscopy. Protein samples (2ml, 0.3 μM) at pH 7.0 (●) or 2.0 (○) were excited at 280 nm and the fluorescence intensity at 346 nm was recorded as a function of [Gnd-HCl]. All spectra were taken at 25±0.2°C in 10 mM sodium phosphate buffer, at the pH value indicated. The data points obtained at pH 2.0 were fitted to equation **3**, whereas those obtained at pH 7.0 were fitted to a biphasic equation describing a two-step unfolding process. In the latter case, the denaturation midpoint for the first and second transition was estimated at 3.1±0.1 M and 6.7±0.1 M [Gnd-HCl], respectively.

Ses i 2 exhibits extraordinarily high stability against unfolding induced by chemical (i.e, low pH, urea, and Gnd-HCl) and physical (i.e., heat) denaturants, and against proteolytic degradation. Strikingly, under experimental conditions of pH 2.0, 5 M Gnd-HCl, and 60°C temperature, the Ses i 2 retains about 75% of the CD signal recorded under non denaturing conditions (i.e., pH 2.0, 25°C) (see Figure 6D). The "general" stability of Ses i 2 towards denaturants and proteases is quite common in proteins isolated from thermophilic organisms, which represent powerful, naturally occurring model systems for studying protein (thermo) stability (Jaenicke, 2000).

However, from a thermodynamic standpoint, the conformational stability of a protein, defined as the free energy gap ($\Delta G = G_D - G_N$) existing between the native (N) and denatured (D) state, may be enhanced by lowering G_N (i.e., positive design), raising G_D (i.e., negative design), or both (Berezovsky et al., 2007). Positive design may be achieved by optimising those interactions that stabilize the native state (i.e., $< G_N$), including hydrophobic and electrostatic interactions, cavity filling, and release of steric strain. On the other hand, negative design may achieved by destabilizing the denatured state (i.e., $> G_D$), by introducing mutations with sterically restricted amino acids (Gly→Ala, X→Pro, Ala→α-aminoisobutyric) or covalent cross links (i.e., disufide bonds) (De Filippis et al., 1998). The importance of S-S bonds and hydrophobic and electrostatic interactions in protein (thermo)stability has been validated very recently by large-scale proteomic analyses showing that the optimal growth temperature (OGT) of any organism in data set, ranging from psychrophiles to hyperthermophiles, is strictly correlated with the fractional content of hydrophobic (i.e., Ile, Val, Leu, Tyr, and Trp) and charged (i.e., Arg and Glu) residues (Zeldovich et al., 2007), as well as with the content of disulfide bridges (Beeby et al., 2005). Notably, the strength of both hydrophobic and electrostatic interactions show a marked increase with temperature. In particular, at low temperatures the hydrophobic effect is entropy driven, whereas at high temperatures it becomes enthalpy-driven and is maximal at about 70°C (Scheraga, 1998). On the other hand, the intensity electrostatic interactions dramatically increases with temperature mainly because the dielectric constant of water, ε, decreases at high temperatures, being 80 at 20°C and 55 at 100°C. In the following, we discuss the effects of relevant physico-chemical properties on the stability of Ses i 2 to heat and denaturants.

The effect of chain-length and S-S bonds. Despite the unusually high resistance of Ses i 2 to thermal and Gnd-HCl-induced denaturation, its conformational stability extrapolated to 0 M Gnd-HCl (ΔG = 11.3 kcal/mol) is well within the stability range determined for natural proteins (i.e., 5-15 kcal/mol) (Privalov and Gill, 1988) and, when normalized on a per residue

basis, the conformational stability of Ses i 2 coincides with the upper limit of the ΔG of folding determined for globular proteins (i.e., 120 cal/mol per residue). This behaviour is typical of small-size globular proteins (i.e., number of amino acids < 100) and arises from the fact that the values of ΔC_p (i.e., the change in heat capacity of unfolding at constant pressure) and the denaturation index m (i..e, the dependence of the free energy change on denaturant concentration, [D], m = dΔG/d[D]; see also equation 4) are both proportional to ΔASA of unfolding (i.e, the change in the protein accessible surface area that becomes exposed upon unfolding), which is in turn proportional to the polypeptide chain length and inversely related to the number of S-S bonds (Myers et al., 1995). So proteins with low ΔC_p's have shallower stability curves (Becktel and Schellman, 1987) and therefore higher T_m values. On the other hand, proteins with low *m* values have very high denaturation midpoint values, while still having average conformational stabilities (Myers et al., 1995).

In the case of Ses i 2, the experimental determination of ΔC_p was accessible only in the presence of 6M Gnd-HCl, yielding a value as low 0.7±0.1 kcal/(mol·K). The denaturation index, m, determined from the Gnd-HCl-induced unfolding of Ses i 2 at 25°C using the linear extrapolation method (Pace and Shaw, 2000), was also very low [m = 1.81±0.07 kcal/(mol·M)]. When these values were normalized on a per residue basis, we obtained a value of ΔC_p of 7.2 cal/(mol·K) per residue and *m* of 19.2 cal/(mol·M) per residue, that are significantly lower than the average values previously collected for a large set of globular proteins [ΔC_p = 14±2 cal/(mol·K) per residue; *m* = 26±7 cal/(mol·M) per residue] (Myers et al., 1995). These data allow us to conclude that the high stability of Ses i 2 is almost a mandatory consequence of its small size, an intrinsic structural property that determines the value of ΔASA of unfolding and thus of the thermodynamic quantities ΔC_p and m. The presence of five disulfide bridges, encompassing almost the entire Ses i 2 sequence (i.e., 94 amino acids), also significantly contributes to reduce the value of ΔASA by impairing complete protein unfolding even at elevated temperatures or high denaturant concentrations. With respect to this, the reduction of ΔASA *per* disulfide bridge has been estimated as high as 900 $Å^2$ (Myers et al., 1995). The effect of S-S bond on the energetics of Ses i 2 denaturation, however, manifests not only by reducing the ΔASA of denaturation. Disulfide bonds, in fact, are thought to stabilize proteins mainly by reducing the conformational entropy of the unfolded state (i.e., < S_D), with a resulting increase in ΔG (i.e., negative design) (Harrison and Sternberg, 1994). Meanwhile, S-S bonds may also stabilize the folded state on enthalpic grounds (i.e., > H_N), by stabilizing local interactions and thus increasing the compacteness of

the tertiary structure (Gekko et al., 2003). The structural rigidity imposed by the covalent crosslinks to the native state has significant effects on the stability of Ses i 2 to heat and Gnd-HCl. impairing penetration of water and denaturant molecules to a different extent in the protein core during thermal or Gnd-HCl-induced denaturation.

The role of hydrophobic interactions. In the case of Ses i 2, the structural model of reveals the presence of a large hydrophobic core that stabilizes the protein in its folded structure (i.e., positive design). The presence of nine methionines in the protein core may potentially destabilize the native state, because of the high conformational entropy of the long side-chain (Creamer and Rose, 1992). At the same time, however, the high conformational adaptability and (more importantly) the hydrophobic character of Met-residues (Fauchere and Pliska, 1987) are expected to significantly stabilize the folded structure. With respect to this, the role of Met-residues on the stability of Ses i 2 has been conformed by preliminary results form our Laboratory showing that complete oxidation of the 15 methionines to the more hydrophilic methionine sulfoxide species dramatically alters the native fold of Ses i 2 and almost abolishes the stability of this allergen towards denaturants and proteases.

Effect of electrostatic interactions on the thermal stability of Ses i 2. Electrostatic interactions (i..e, hydrogen bonds and salt bridges) have been thought to contribute little, if at all, to protein stability at room temperature because the highly favourable Coulombic interactions would be nearly offset by the large desolvation penalty incurred when bringing two oppositely charged groups together to form a salt bridge. However, more recent studies have challenged this conclusion on both theroteical and experimental grounds. In particular, it has been shown that the desolvation penalty for the formation of a salt bridge is markedly reduced in magnitude at high temperatures [Elcock, 1998], thus explaining the unique temperature dependence of the dielectric constant of water [Archer and Wang, 1990] and the higher frequency with which salt bridges occur in hyperthemophilic proteins [Ledenstein, 199x; Cambillau and Claverie, 2000]. Furthermore, recent studies have shown that isolated charged residues on the protein surface can dramatically enhance protein stability, even in the absence of salt-bridge formation (Berezovsky et al., 2007).

As reported above, Ses i 2 has a peculiar surface electrostatic potential, with a large positive region and two small negative spots (see Figure 13B). Despite the abundance of charged residues (16 positive and 13 negative at pH 7.4, comprising the N- and C-termini), only very few salt bridges could be identified with some confidence in the structural model of Ses i 2 herein reported. This is conformed by the marginal pH-dependence of Ses i 2 stability. Hence, it can be envisaged that these uncompensated charges may destabilize the folded state,

because of strong electrostatic repulsion on the protein surface. Using simple physical concepts, here we demonstrate that Ses i 2 may achieve stabilization through negative design of unfavourable electrostatic interactions. We have already emphasized that S-S bonds impose severe stereochemical constraints to the polypeptide chain mainly in the unfolded state. It is conceivable, therefore, that at high temperatures some surface loop and the fraying N- and C-terminal ends become disordered, whereas the protein core comprised in the S-S network likely remains compact, as documented by the large residual CD signal measured at high temperatures. In this scenario, the average distance between charged groups is only slightly increased in the denature state. Conversely, the Coulombic repulsion is dramatically enhanced at high temperatures where the D state is achieved, due to remarkable decrease of the dielectric constant of water (see above). Hence, the denatured state is more destabilized than the native state by increasing the temperature, with a resulting higher energy gap between the N and D state ($\Delta G = G_D - G_N$) (i.e., negative design). Likely, the same strategy might have been exploited by other Arg-rich allergens of the 2S-albumin family, including Ses i 1 from *Sesamum indicum* (Moreno et al., 2005), Ber e 1 from Brazil nut (Koppelman et al., 2005), and Ara h 2 and Ara h 6 from the peanut *Arachis hypogaea* (Lehmann et al., 2006).

Resistance of Ses i 2 to proteolysis

Digestive proteases. The susceptibility of Ses i 2 to proteolysis by the hydrolases of the gastrointestinal tract pepsin, trypsin, and chymotrypsin, was evaluated by incubating 2S albumin under *in vitro* conditions simulating the gastric (SGF) and intestinal (SIF) fluid (see Methods). For comparison, digestion experiments were conducted under carefully controlled conditions with other well known allergenic proteins, including ovalbumin (Ova), α-lactalbumin (α-Lact), and bovine serum albumin (BSA) (Astwood et al., 1996; Fu et al., 2002). As shown in Figure 7A-B, Ses i 2 is fully resistant to the action of pepsin in SGF after 2-h incubation, which is the average permanence time of ingested proteins in the stomach, whereas α-Lact and BSA are suddenly and completely degraded. Only Ova is moderately resistant to pepsin and, after 2-h reaction, about 40% of intact protein was still present. After digestion in SGF aliquots of protein samples, which had been already reacted with SGF, were incubated in SIF. The data shown in Figure 6 demonstrate that Ses i 2 is largely resistant to the combined action of trypsin and chymotrypsin in SIF. For instance, after 1h-reaction, there is about 78% of residual intact Ses i 2, whereas only 6% of Ova is still present.

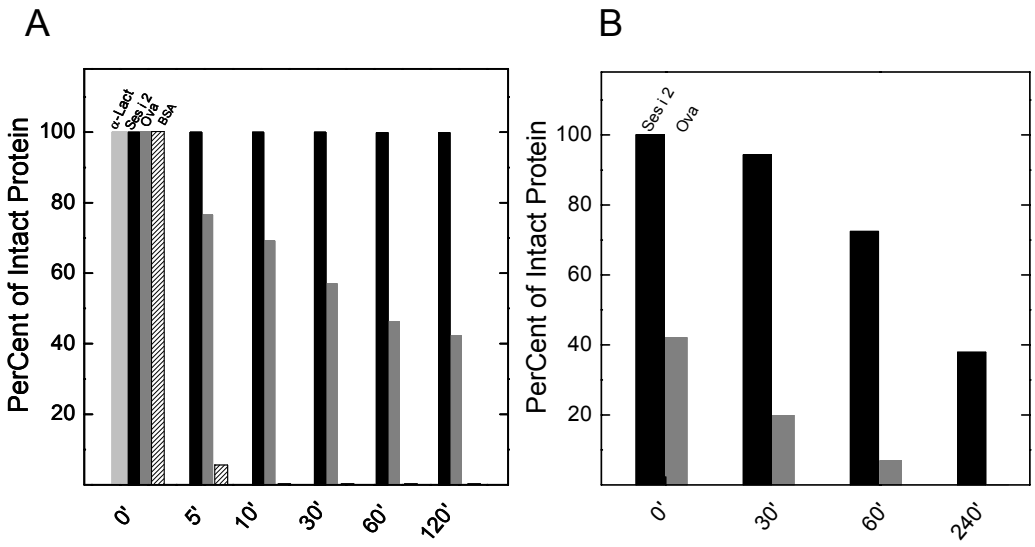

Figure 7. Stability of Ses i 2 to proteolysis in SGF (A) and in SIF (B). Time-course kinetics of proteolysis reaction of Ses i 2 in simulated gastric (**A**) and intestinal (**B**) fluid. For comparison, proteolysis was conducted under identical conditions with BSA, α-lactalbumin and ovalbumin, as indicated. Reactions were conducted as detailed in the Methods. At time intervals, inhibited aliquots (50 μg) were loaded onto a C18 RP-HPLC column and the per cent of residual intact protein was estimated by integrating the area under the chromatographic peak corresponding to the uncleaved protein, before (t = 0) and after the reaction was started. MS analyses allowed us to verify that no other peptide material co-eluted with intact Ses i 2.

The extraordinarily high resistance of Ses i 2 to poteases is probably correlated with its high conformational rigidity. H/D mass spectrometry is emerging as a powerful tool for investigating the conformational flexibility of proteins in solution (Smith et al., 1997; Hoofnagle et al., 2003). Indeed, the extent and the rate of isotope exchange of side-chain and peptide amide hydrogens is markedly affected by their solvent accessibility and hydrogen bonding within the protein. In general, highly exposed hydrogens, not involved in hydrogen bond contacts with the surrounding groups, exchange faster and to a greater extent than those hydrogens buried in the protein core and involved in strong hydrogen bonds (Hoofnagle et al., 2003). The per cent of H/D exchange, %D, is averaged over all the exchangeable hydrogens in the polypeptide chain and therefore it gives a cumulative figure of the protein flexibility.

Here we have exploited H/D exchange mass spectrometry to study the conformational flexibility of Ses i 2 in comparison with apomyoglobin, a non-allergenic protein sharing with Ses i 2 a comparable size and high α-helix content. The time course kinetics of the exchange reactions (Figure 8) indicate that Ses i 2 is conformationally more rigid than apomyoglobin in the time range explored, in keeping with the remarkably higher stability of the sesame 2S albumin to heat and Gnd-HCl compared to apomyoglobin (Regis et al., 2005).

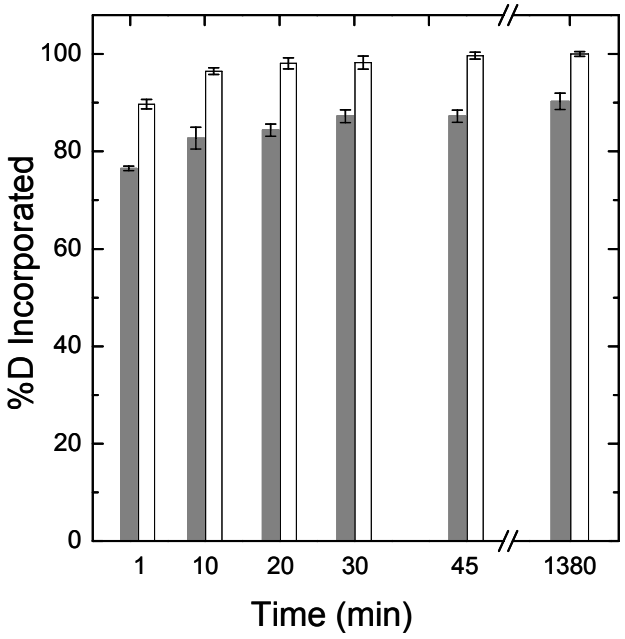

Figure 8. Conformational flexibility of Ses i 2 probed by H/D exchange mass spectrometry. Time-coarse kinetics of the H/D exchange reaction of Ses i 2 (grey bars) and apo-myogloboin (white bars) was carried out at 25±0.5°C in 9:1 (v/v) D_2O:H_2O and monitored by ESI-TOF mass spectrometry, as detailed in the Methods section. At each time point, the per cent incorporation of deuterium (%D) derived from the average of three separate experiments conducted in parallel under carefully controlled conditions. Error bars correspond to the standard deviation calculated for each set of measurements.

H/D exchange, and the stability towards heat- and guanidinium-induced denaturation are in closely agreement with high resistance toward proteolysis demonstrated by Ses i 2. Moreover, it is consistent with high α-helix content of this allergen and with the presence of S-S bonds. Proteolysis, indeed, is disfavoured at the more rigid elements of secondary structure, whereas cleavage occurs at the most flexible sites in proteins (i.e., loop regions), which are more prone to local unfolding (Fontana et al., 1997). On the other hand, S-S cross-links increase the conformational rigidity and compactness (Gekko et al., 2003) of Ses i 2 by restricting the possibility of local unfolding, thus maintaining the structural integrity of the protein against proteases. The resistance of Ses i 2 to proteolytic degradation in SGF and SIF is even higher than that recently found for the homologous Ses i 1 allergen (Moreno et al., 2005) and favourably correlates with the high allergenic potential of the Ses i 2 protein (Wolff et al., 2003). Indeed, it is thought that resistance to digestion in the gastrointestinal tract (GIT) is a major factor contributing to the allergenicity of food proteins (Astwood et al., 1996; Moreno et al., 2007) by allowing enough intact allergen to reach the intestinal mucosa where absorption and sensitization of the gut immune system can occur (Mills et al., 2004). Therefore, protein gastric resistance is taken as one of the relevant criteria for the protein

allergenicity assessmen. In a previous study aimed at identifying B-cell epitopes of Ses i 2, three linear peptides displaying strong IgE binding properties were identified (i.e., ^{10}QCQMRHCM^{17}, ^{40}GQFEHF^{45}, and ^{44}HFRECC^{49}) (Wolff et al., 2003, 2004). These linear epitopes are largely exposed on the protein surface and cluster in a region of the structural model comprising the segment connecting helix Ia and Ib, as well as helix II. Strikingly, our data indicate that after 2 h of gastric digestion, Ses i 2 remains completely uncleaved and that even after prolonged (i.e., 4 h) intestinal digestion, ~40% of the allergen may reach the gut immune system in its structurally intact and immunologically active form (Nicoletti, 2000; Temblay et al., 2007).

In the case of chymotrypsin, another species (i.e., Ch-1) is generated only at high protease:Ses i 2 ratio (i.e., 1:5 or 1:20), eluting at longer retention times and having a molecular mass of 38 a.m.u. higher than that of 2S albumin, thus suggesting that Ch-1 is a nicked Ses i 2 species with two peptide bonds cleaved (Figure 9).

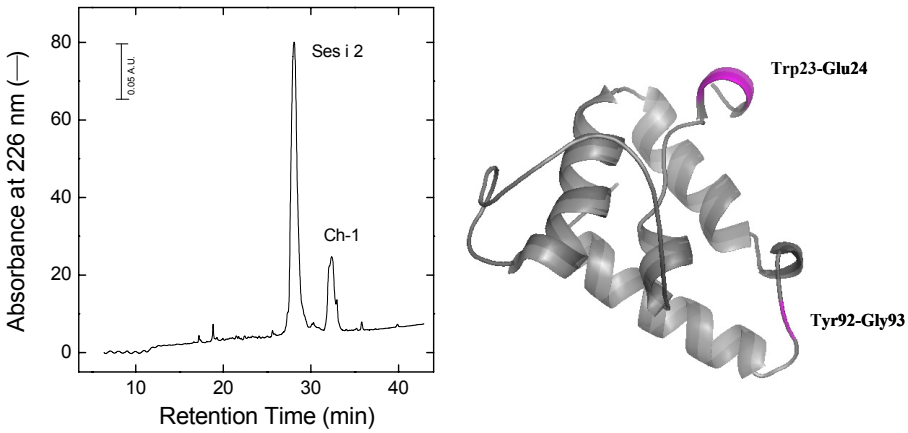

Figure 9. RP-HPLC analysis of Ses i 2 in presence of chymotripsin. Ses i 2 was digested in 50 mM Tris-HCl, pH 7.8, 5 mM $CaCl_2$ at 37°C for 3h at E/S ratio of 1:10 (w/w). **Schematic representation of cleavage sites in Ses i 2 (see Structural Model).**

Ses i 2 nicked involves in the cleavage two peptide bonds which are Trp23-Glu24 in light chain and Tyr92-Gly93 in heavy chain. Ses i 2 nicked was subjected to reduction and the mass data show a small percentage a species with molecular weight about of 3312 ± 0.3 Da that correspond to light chain. The presence of LC in the reduction mixture may suggest that the first cleavage in the formation of Ses i 2 nicked is located at Tyr92. Thus, in intestinal lumen Ses i 2 might be partially converted in the nicked form and this species could be digested by gastrointestinal enzymes as a consequence of an increase in flexibility of protein

structure. Stability of Ses i 2-nicked was studied by urea-mediated unfolding was performed at 25°C following the increase of fluorescence signal at λ_{max} after increasing the urea concentration at neutral and acidic pH. As shown in Figure 10 two different profiles were obtained. At pH 2.0 and pH 7.0 a single transition was observed. The fluorescence intensity increases with a sigmoidal shape as a function of denaturant concentration, even though a plateau in the post-transition region could not be clearly identified. The process at pH 2.0 is poorly cooperative with a midpoint denaturation at 7.5±0.3 and at pH 7.0 $[urea]_{1/2}$ values is about 9.7±0.1 M (Figure 10 shows a simulation at 12 M urea). For comparison, Ses i 2 was subjected to urea unfolding at pH 2.0 and pH 7.0, but at neutral condition was not observed a transition, while at pH 2.0 a $[urea]_{1/2}$ value of 8.8±0.3 M was calculated. These data confirmed a minor stability of Ses i 2 nicked respect Ses i 2.

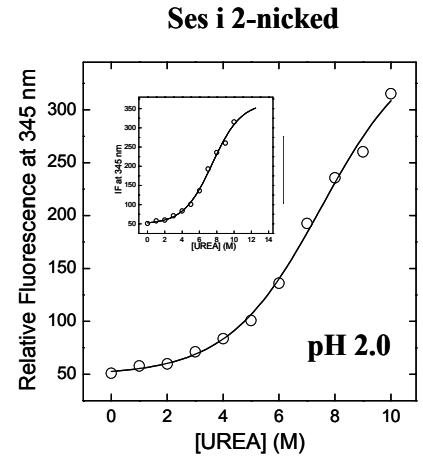

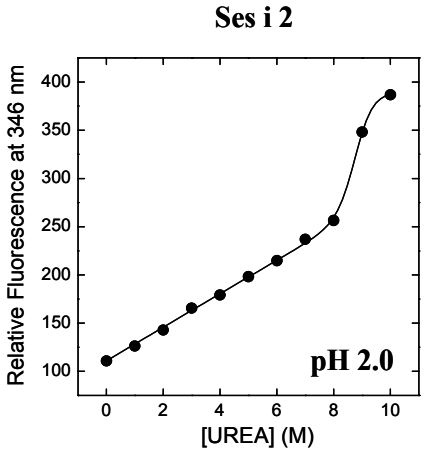

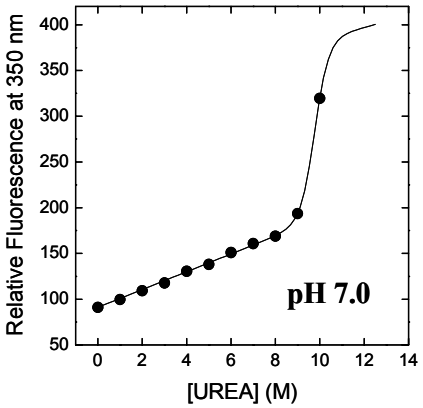

	$[UREA]_{1/2}$	
	Ses i 2	**Ses i 2-nicked**
pH 2.0	8.8 ± 0.3 M	7.5 ± 0.3 M
pH 7.0	-------	9.7 ± 0.1 M

Figure 10. Stability of Ses i 2-nicked at pH 7.0 and 2.0. Urea-induced unfolding of *Ses i 2*-nicked was monitored by fluorescence spectroscopy. Protein samples (2ml, 0.3 μM) at pH 7.0 (●) or 2.0 (○) were excited at 280 nm and the fluorescence intensity was recorded as a function of [urea]. All spectra were taken at 25±0.2°C in 10 mM sodium phosphate buffer, at the pH value indicated. The data points obtained at pH 2.0 were fitted to sigmoidal equation, whereas those obtained at pH 7.0 and data of Ses i 2 unfolding at pH 2.0 were fitted to a equation (6).

Our data suggest that Ses i 2 may be absorbed in intact form in intestinal mucosa mainly by M cells. Intestinal epithelium presents a high density of vascularisation through capillary Ses i 2 can be involved in blood circulation where are present several enzyme of coagulation pathway such as thrombin, factor Xa, protein C and plasmin. Thus, with the intent to observe a possible degradation of Ses i 2 we have performed experiments of proteolysis with proteases of the blood coagulation/fibrinolytic system (i.e., human α-thrombin, factor Xa, activated protein C, and plasmin). Our results (Figure 11) show that Ses i 2 is fully resistant to proteolytic cleavage of blood enzyme. Extraordinary stability to proteolysis of Ses i 2 was confirmed by bacterial proteases assay. After 1-h incubation at 90°C, Ses i 2 is resistant to proteolysis by thermolysin and after 1 h at 70°C, the temperature at which the enzyme is maximally active, only 10% of the protein is degraded (Figure 11), leading to the formation of a species (i.e., Th-1) having a molecular mass of 11257.9±1.0 a.m.u., corresponding to a trimmed Ses i 2 species lacking the segment ^{40}MRGQ^{43} at the C-terminal end of the LC.

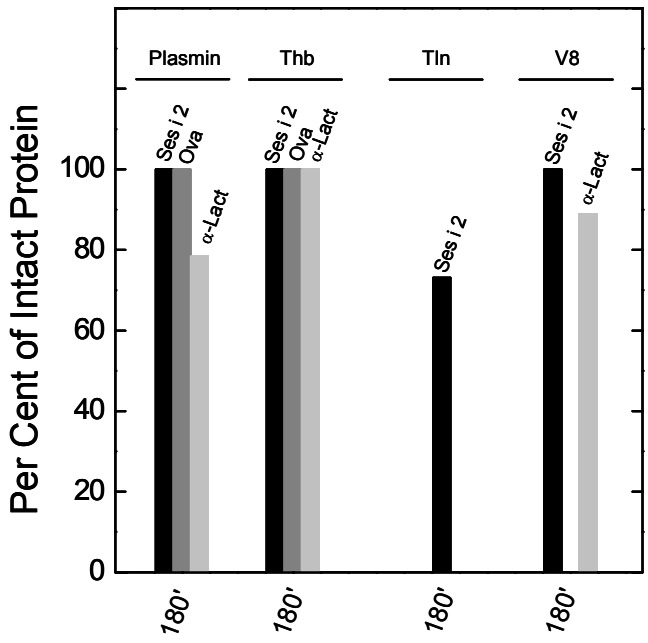

Figure 11. Stability of Ses i 2 to enzyme of blood coagulation/fibrinolytic system and bacterial enzyme. Proteolysis of Ses i 2 with coagulative (i.e., thrombin) and fibrinolytic (i.e., plasmin) proteases and with bacterial proteases (i.e., thermolysin and Glu-C protease). Reactions were conducted as detailed in the Methods. At time intervals, inhibited aliquots (50 μg) were loaded onto a C18 RP-HPLC column and the per cent of residual intact protein was estimated by integrating the area under the chromatographic peak corresponding to the uncleaved protein, before (t = 0) and after the reaction was started. MS analyses allowed us to verify that no other peptide material co-eluted with intact Ses i 2. For comparison, proteolysis was conducted under identical conditions with BSA, α-lactalbumin and ovalbumin, as indicated.

Protease inhibition properties of Ses i 2

To discriminate whether the resistance of Ses i 2 to proteolytic degradation is caused by the intrinsic stability of the secondary and tertiary structure or whether Ses i 2 resists to the action of proteases by directly inhibiting their hydrolytic activity, we decided to investigate the inhibitory properties of Ses i 2 against the proteases previously tested (see Methods).

The data shown in Figure 12A indicate that, under the experimental conditions employed, Ses i 2 does not inhibit any of the proteases assayed but thrombin. For this enzyme (200 pM), only ~5% of the initial enzymatic activity was recovered in the presence of Ses i 2 (4.6 μM) and FPR substrate (21.6 μM). The inhibitory potency of Ses i 2 for thrombin was quantified by measuring the initial velocity (v_i) of FPR hydrolysis by thrombin as a function of inhibitor concentration. From the dose-response plot (Figure 12B) a IC_{50} value of 1.60±0.05 μM was calculated. In conclusion, our results indicate that Ses i 2 inhibits human α-thrombin with high potency and selectivity. This result is even more surprising if one considers that thrombin shares with the other coagulation proteases the same catalytic machinery and similar specificity sites. In the next future, we will address the problem of defining the mechanism (i.e., competitive, non-competitive, etc) of thrombin inhibition by Ses i 2 and the regions on the inhibitor and enzyme involved in protein binding and responsible for affinity and selectivity.

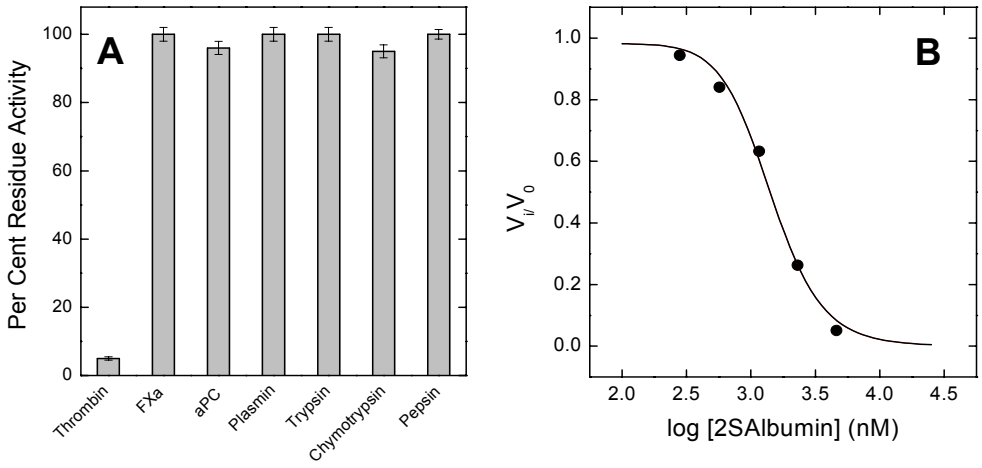

Figure 12. Protease inhibitory properties of Ses i 2 (**A**) The per cent residual activity was calculated at 25±0.2°C as the ratio of the initial velocity of substrate hydrolysis, measured in the presence and absence of a fixed concentration of Ses i 2 (see Methods). The values of residual activity are the average of three separate experiments and error bars are the standard deviations for each set of measurements. (**B**) Dose-response plot of thrombin fractional activity (v_i/v_0) as a function of Ses i 2 concentration (on a Log scale). The initial velocity of the FPR substrate (22 μM) hydrolysis by thrombin (200 pM) was determined at 25±0.2°C in 5 mM Tris-HCl buffer, pH 8.0, 0.1% PEG 8000 and 0.2 M NaCl, in the absence (v_0) and presence (v_i) of increasing inhibitor concentrations. The data points were fitted to equation 5, yielding an IC_{50} value of 1.44±0.30 μM.

Structural model of Ses i 2

For homology modelling, the template structure was identified by pairwise aligning the 18-123 sequence of the mature Ses i 2 protein (SwissProt entry code: Q9XHP1), as determined from mass spectrometry analysis (see Figure 2E), with the sequence of all other 2S albumins for which the three-dimensional structure is known: the rproBnIb napin from rapeseed (*Brassica napus*) (PDB entry code: 1SM7) (Pantoja-Uceda et al., 2004), the RicC3 allergen from castor bean (*Ricinus communis*) (1PSY) (Pantoja-Uceda et al., 2003), the methionine-rich SFA-8 protein from sunflower seeds (*Helianthus anuus*) (1S6D) (Pantoja-Uceda et al., 2004), and the Ara h 6 allergen from peanut (*Arachis hypogaea*) (1W2Q) (Lehmann et al., 2006).

Napin (Swiss-Prot entry code: Q8GT96) was chosen as the best structural template because, among all the 2S albumins selected, its sequence shows the highest amino acid identity (30.2%) and similarity (45.9%), as well as the best alignment score (91.0) with Ses i 2. Our choice was supported by the results obtained using fold-recognition programs like $123D^+$ (2http://123d.ncifcrf.gov/123D+.html) and Phyre (http://www.sbg.bio.ic.ac.uk/~phyre/index.cgi), both working by performing threading simulations of the target sequence on a selected template structure. Notably, the $123D^+$ server identified the structure of the mature napin (1PNB) (Rico et al., 1996) as the best template for Ses i 2 sequence. The same conclusion was achieved using the Phyre server, which identified the structure of the recombinant precursor of napin (1SM7) (Pantoja-Uceda et al., 2003) by far as the best template structure.

The model was built by keeping the secondary structure segments of napin (1SM7) (Pantoja-Uceda et al., 2004) fixed in Ses i 2 structure, whereas insertions/deletions in loop regions were manually introduced as detailed in the Methods. After energy minimization, the refined model was validated using the structure validation option of WHAT IF (Hooft et al., 1996), yielding a Z-score of –1.9 on all contacts, which was taken as an indication of good quality of the Ses i 2 model. The structural architecture of Ses i 2 consists of four helical segments forming a compact hydrophobic core and interconnected by five disulfide bridges. In particular, eight of the ten Cys-residues of Ses i 2 are precisely conserved in the napin structure, with cysteine spacing …C…C…/…CC…CXC…C…C… typical of the prolamin superfamily (Shewry et al., 2002; Pantoja-Uceda et al., 2002). Therefore, the topology of the resulting four disulfides in Ses i 2 (i.e, Cys21-Cys76, Cys33-Cys65, Cys66-Cys112, and Cys78-Cys120) was assigned by homology on the SS pattern determined for napin. Notably, the nonconserved Cys28 (in the LC) and Cys83 (in the HC) are spatially close (i.e., Cβ-Cβ <

5Å) in the structural model of Ses i 2. Moreover, as demonstrated by chemical methods (see above), all Cys-residues in Ses i 2 are disulfide bonded and therefore these unpaired cysteines were linked together to form the fifth disulfide of Ses i 2 (i.e., Cys 28-Cys83). The distribution of charged amino acids in Ses i 2 is highly asymmetric, with a large positively charged patch (i.e., cluster I+) spanning the equatorial region of the molecule (see Figure 13 B), and two relatively small negative patches, cluster I and cluster II. Cluster I- is formed by acidic residues from different parts of the molecule (i.e, Glu22, Glu79, and Glu119), whereas cluster II comprises three acidic residues all in helix II (i.e., Glu60, Glu64, and Asp71).

The overall topology of Ses i 2 structure consists of a globular four-helical motif (i.e., helix Ia and Ib, II, III, and IV) arranged in a right-handed superhelix with a simple "up and down" topology, quite common in 2S albumins (Pantoja-Uceda et al., 2002) and in other members of the prolamin superfamily (Shewry et al., 2002). Notably, the tertiary structure of Ses i 2 is stabilized by a compact hydrophobic core and five disulfide bridges.

The first helix is split in two (i.e., helix Ia and Ib) and in the precursor protein is linked to helix II by the flexible loop ^{44}YEESFLRSAEAN^{55}, that in the mature protein is lacking due to endogenous proteolytic processing (see Figure 2E). This in keeping with the notion that proteolysis occurs at exposed and flexible loops (Fontana et al., 1997) and is taken as a first, albeit partial, indication of the reliability of our model. Next, helix Ia is linked to helix III by the Cys21-Cys76 bond, while the disulfide Cys33-Cys65 connects helix Ib to helix II. The additional disulfide bond Cys28-Cys83, not present in other 2S albumins, latches helix I to helix III and contributes to strengthen the interaction of the LC with the HC in Ses i 2 structure. Helix III is connected to helix IV by the loop ^{89}QQEYGMEQ^{96}, corresponding to the so-called "hypervariable region" in 2S albumins, because of the high sequence variability among the family members (Monsalve et al., 1991; Pantoja-Uceda et al., 2002; Shewry et al., 2002). Two intrasubunit disulfides stabilize the HC: the Cys66-Cys112 bonds, connecting helix II to the C-terminal end of helix IV, and the Cys78-Cys120 bond, linking the N-terminal end of helix III to the extended and flexible C-terminal region of the molecule.

Sequence of mature Ses i 2

^{18}QRGCEWESRQCQMRHCMQWMRSMRGQQGQFEHFRECCNELRDVKSHCRCEALRCMMRQMQQEYGM

EQEMQQMQQMMQYLPRMCGMSYPTECRMR^{123}

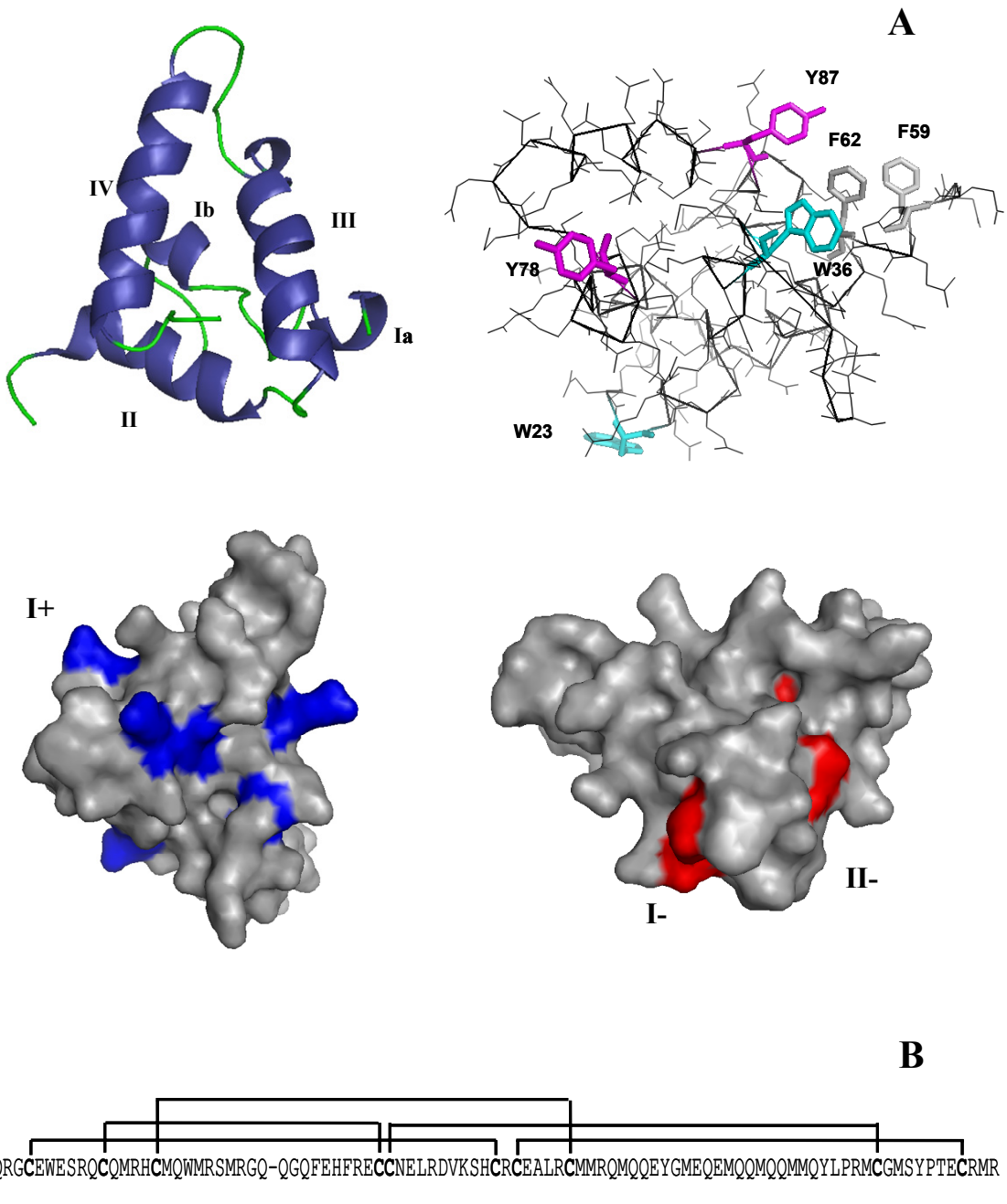

Figure 13. Homology model of Ses i 2. (A) Schematic representation of helix motif and surface positive and negative charged clusters. **(B)** Schematic representation of disulphide bond patterns.

Beyond disulfide bonds, Ses i 2 is stabilized by a compact hydrophobic core. With respect to this, six conserved hydrophobic positions (i..e, ϕ1 to ϕ6) have been previously

identified in prolamins (Pantoja-Uceda et al., 2004) and the comparative analysis of the structural model of Ses i 2 with the experimental template structure of napin (1SM7) reveals that the protein core is largely conserved in the two proteins. In particular, positions ϕ4, ϕ5, and ϕ6 of the hydrophobic core is always a Leu in both proteins; even at position ϕ2, there is a Trp-residue in both proteins; conversely, Leu15 and Ile22 at position ϕ1 and ϕ3 in napin are replaced by two Met in the structural model of Ses i 2; similarly, Ala67, Ala68, and Ala89, Val73, Ile85 and Ile88 in the core of napin are all replaced by Met in Ses i 2 structure, while Met98 in napin is conserved in the Ses i 2 core. Because of their high conformational adaptability Met side-chains could be readily accommodated in the template structure of napin, without significant steric hindrance. Notably, the indole-ring of Trp21 at position ϕ2 in the helix Ib of napin favourably interacts on one side with Ile22, through aliphatic-aromatic interaction, and on the other side with Arg45 in helix II, through cation-aromatic interaction. In the structural model of Ses i 2, this interaction is retained: the conserved Trp36 in helix Ib favourably interacts with Met37, through sulphur-aromatic interaction, and with Phe62 in helix II, through an edge-to-face aromatic-aromatic interaction. The phenyl-ring of Phe62 is also favourably stacked on to the disulfide bond Cys66-Cys112, connecting helix II and IV. The interaction of Trp36 in helix Ib with Phe62 in helix II may help to stabilize the folded structure, especially if one considers that the loop 44-55 connecting the two helices is missing in the mature Ses i 2. Strikingly, the beneficial interaction of an aromatic residue (i.e., ϕ) in helix I with another amino acid in helix I, having different chemical properties, is highly conserved in the prolamin superfamily, In 2S albumins, for instance, ϕ is Trp or Tyr and X may be an aliphatic residue, as in RicC3 (i.e., Tyr33-Leu63) (1PSY, Pantoja-Uceda et al., 2003), a basic amino acid, as in napin (i.e., Trp21-Arg45) (SM7, Pantoja-Uceda et al., 2004), or even an acidic amino acid, as in SFA-8 (i.e., Tyr27-Asp46) (1S6D, Pantoja-Uceda et al., 2004). Notably, in trypsin/α-amylase inhibitors (1B1U, 1BEA, 1BFA), ϕ and X were always Tyr and Lys, respectively.

Experimental validation of the Ses i 2 model

The model of Ses i 2 herein reported is consistent with and validated by several different spectroscopic and biochemical data.

The % helix estimated from the far-UV CD spectrum at pH 2.0 (Figure 4A) (53%) nicely agrees with that deduced from the structural model of Ses i 2 (59%), which is based on the NMR solution structure of napin solved at pH 3 (1SM7, Pantoja-Uceda et al., 2004). In

addition, the increment of the helical structure observed going from neutral to acidic pH, resembles the pH-dependent folding transition (i.e., coil → helix) observed in poly-α-glutamic acid and in acidophilic enzymes, like pepsin and xylanase, where the presence of surface acidic clusters destabilizes the native structure at neutral pH, due to electrostatic repulsion. In the structural model of Ses i 2, an acidic cluster is formed by glutamic acids from different regions of the molecule (i.e, Glu5 in helix Ia, Glu62 in helix III, and Glu102 in the C-terminal end). Furthermore, helix Ia contains two Glu, while helix II contains three Glu and one Asp. At low pH, these residues are in the neutral form and thus stabilize the folded helical structure by alleviating electrostatic repulsion. A similar increase in the helix content has been already reported for mature napin going from neutral to acidic pH [Murèn et al., 1996]. Notably, helix Ia and helix II in napin structure contain the same number of Glu and Asp as in Ses i 2. Thus it can be proposed that in both proteins helix I and II become folded by lowering the solution pH.

The appearance of a distinct Tyr contribution in the 280-nm fluorescence spectra (Figure 5C) is indicative of poor Tyr-to-Trp resonance energy transfer (RET). Low efficiency of RET usually occurs when the distance separating the energy donor (i.e., Tyr) and acceptor (i.e, Trp) in the protein structure is larger than the Förster distance (i.e., 10-12 Å, for the Tyr-Trp pair) and/or when the donor and acceptor are highly flexible as, for instance, when they are exposed to the solvent on the protein surface (Lakowicz, 1999). As expected, the three Tyr-residues in the mature Ses i 2, all in the HC, are largely solvent exposed and manly localized in loop regions, at a distance from Trp23 or Trp36 (i.e., Cβ-Cβ distances 22-27 Å) more that two-fold the Förster distance. Only Tyr78 is at 12 Å distance from Trp36. The structural model of Ses i 2 also accounts for the dramatic increase of Trp-fluorescence upon Gnd-HCl-induced denaturation. At low pH, both Trp-residues in Ses i 2 are quenched: Trp23 is likely quenched by the flanking carboxyl-groups of Glu22 and Glu24, while the emission of Trp36 may be decreased by the sulphur atom of the nearby Met37. Upon increasing [Gnd-HCl], Trp-quenching is reduced and the emission intensity increases with a sigmoidal shape, indicative that Ses i 2 denatures cooperatively as a single folding unit. At neutral pH, instead, the carboxyl-groups are in the form of carboxylates, unable to quench Trp23 (Figure 5D). In addition, both helix I and II are likely partially unfolded, due to the destabilizing effect of the carboxylates. In this situation, the two Trp-residues seem to unfold almost independently, according to the relative stability of their chemical environments. Hence, the biphasic profile reported in Figure 6A results from the overlapping of two denaturation curves, each monitoring the unfolding of a single Trp-residue. Probably, the first transition at $[Gn\text{-}HCl]_{1/2}$

~3 M corresponds to the denaturation of Trp23, with a concomitant decreasewhich is exposed to solvent in helix Ia, whereas the second transition at $[Gn\text{-}HCl]_{1/2}$ ~6.8 M tracks the unfolding of Trp36, which is more tightly packed in the hydrophobic core of Ses i 2.

Taken together, these observations provide key experimental validation for the reliability of our structural model.

CONCLUSION

In this study we have purified (20-30 mg) to homogeneity (> 98%) Ses i 2, the major allergen from sesame seeds (*S.indicum*). Ses i 2 (SwissProt code Q9XHP1) exhibited common features with other 2S albumin family such as a blocked N-teriminus (i.e., pyroglutamic acid), the absence of glycosylation and α-helical nature. Also, Ses i 2 is characterised by a Light (LC) and Heavy chain (HC) that are stabilised by disulphide bridges. Surprisingly, our data demonstrated the presence of additional two cysteine residues in the common pattern in prolamin superfamily of eight Cys (-C-X_n-C-X_n-C-X_n-CC-X_n-CXC-X_n-C-X_n-C-X_n-C-); Cys28 and Cys83 are involved in the formation of a fifth disulphide bridge. Ses i 2 has also be shown to be extremely stable to acidic conditions, thermal processing and in vitro gastrointestinal digestion. Such unusual high stability is mainly attributed to the rigidity of structure dominated by the well-conserved skeleton of cysteine residues. Stabilization of protein structure is partially attributed to hydrophobic core of nine methionines residues, (in the next chapter we will explore the effects of methionine oxidation on protein structure). These characteristics contribute to high resistance toward proteolysis of a wide range of proteases. Following in vitro gastric digestion Ses i 2 remains completely intact and then when followed by duodenal digestion retains largely intact structure with the formation of nicked species in which only two peptide bonds are cleaved at position Trp23 in LC and Tyr92 in HC. At the light of these data we have demonstrated that largely intact allergen is likely to remain in the gut lumen as it moves down the duodenum and into the jejunum/ileum to the site of the first Peyer's patches. It has been claimed that Peyer's patches are likely to be the major site of sampling for food antigens and allergens (through the activities of constituent M cells) and hence may play a key role in the development of food allergy (Chambers et al., 2004).

In conclusion, although it is not possible yet to determine exactly what makes a protein an allergen, it is evident that the stability of food allergens to low pH, sulfactants such as bile

salts and proteolytic enzymes in the gastrointestinal tract is needed in order to reach (and stimulate) the immunological system.

Chapter 2.2

Oxidation of Methionine Residues in Major Allergen Ses i 2 from Sesame Seeds: The Effect of Oxidative Damage on Protein Structure and Stability

INTRODUCTION

The oxidative damage of biomolecules has recently received a great attention because of its importance in understanding a variety of biological phenomena (aging process, cancer study, different diseases, endogenous toxins).

Reactive oxygen species (ROS) are produced in cells by a variety of enzymatic and non-enzymatic mechanisms. The spectrum of oxidants generated and diffused in extracellular matrix (ECM) may therefore differ from those formed within a cell (Rees et al., 2008). In inflammation sites, H_2O_2 and HOCl, non-radical and non-charged oxidants, are the major oxidants produced and they are highly reactive with a wide range of biological molecules. As most radical oxidants have restricted diffusion radii due to their rapid rates of reaction with biological molecules, including the side chains of amino acids, and cannot diffuse out of the cell but in physiological process these molecules, at a low levels, may diffuse outside cells in cell signalling pathway and at high levels oxidants are used to kill ingested organisms within phagocytes.

Proteins are the major target for oxidants as a results of their abundance in biological systems, and their high rate constants for reactions. Protein oxidation by radical and non-radical oxidants is highly complex, with multiple products generated from 20 common side chains and peptide backbone. In ECM protein modification is dominated by protein side-chain oxidation, with backbone damage apparently less important (Davies et al., 2008). All amino acids are susceptible to oxidation, but together with cysteine and tryptophan, methionine belongs to the most easily oxidized amino acid in proteins. It is attacked by H_2O_2, hydroxyl radicals, hypochlorite, chloramines, and peroxinitrite, all these oxidants being produced in biological system. The first stage of oxidation leads to methionine sulfoxide, a biological occurring product. Two major pathways of Met and sulfide oxidation may be

differentiated, one- and two-electron oxidation. The two electron oxidation of an organic sulphide formally yields the sufide dication (reaction 1). In water, such a dication will transform into the respective sulfoxide (reaction 2).

$$R_2S \rightarrow R_2S^{2+} + 2e^- \quad (1)$$

$$R_2S^{2+} + H_2O \rightarrow R_2S{=}O + 2H^+ \quad (2)$$

The methionine oxidation to methionine sulfoxide can be reversed by two classes of methionine sulfoxide reductase MrsA and MrsB, which react diastereospecifically with MetSO diasteroisomers displaying S- and R-configuration at sulphur atom (Brot N. and Weissebach H., 1983).

MetSO may be oxidized to the sulfone, but this reaction requires more drastic chemical attack and it is rarely been found in biological system.

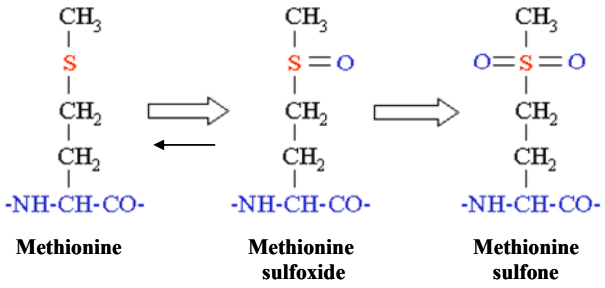

Structure of methionine and its oxidation products

Site-specific oxidation of the proteins allows to study the consequences of oxidant reaction on the protein conformation and internal dynamics. Redox processes of methionine play an important role in altering a protein stability during pathologic conditions associated with oxidative stress. Methionine and cysteine are the sulfur-containing amino acids which occur in proteins. The structural and catalytic roles of cysteine have been defined for many proteins, but this is not the case for methionine. There are as yet no enzymes for which methionine has been shown to function in the catalytic cycle. Although there are many examples from which methionine has been postulated to play an essential structural role. For example, in α_1-antiproteinase, oxidation of Met^{358} to methionine sulfoxide destroys the antiproteinase activity, presumably by alteration in complex formation with target (Jhonson and Travis, 1979). However, the thiol ether is not required for interaction since replacement of the methionine with valine gives a fully active antiproteinase (Rosenberg et al, 1994) and explain the importance of hydrophobic interaction in stabilization of protein structure. The

results of earlier studies (Levine et al., 2000) have shown that Met-residues may act as "molecular bodyguard", providing efficient scavenging of oxidant species that are produced in vivo.

Ses i 2 is the major allergen from white sesame seeds and belongs to the 2S albumin family. This food allergen represents a suitable model for understanding the structural consequences of oxidative damage in proteins occurring in several pathological states in which inflammatory processes are involved. In this work, time-dependent oxidation of Ses i 2, in 50 mM potassium phosphate, pH 5.0, with 5 mM or 50 mM of H_2O_2 at a room temperature or at 37°C, was analysed by RP-HPLC combined with mass spectrometry, yielding a mass value of 11967±0.8 Da, consistent with the oxidation of all the 15 methionines present in the mature Ses i 2 sequence. Similar results were obtained at 50 mM of H_2O_2 and gastric pH (pH 1.2), in keeping with the notion that Met-oxidation occurs via an acid-catalyzed mechanism (Shechter Y., 1986). The involvement of other amino acid types, besides Met, in the oxidation of Ses i 2 was ruled out by peptide mass fingerprint analysis on the light and heavy chain. Circular dichroism (CD) spectra confirmed a dramatic alteration of protein structure, upon Met oxidation and the stability to guanidine-HCl induced denaturation, monitored by recording the CD value at 222 nm was dramatically reduced down to 3.2 M. With the aim to elucidate the importance of Met-residues on the stability of Ses i 2 to proteolytic degradation, both genuine (Ses i 2) and the Met-oxidized species (Ses i 2-ox) were treated, under physiological conditions with proteases of the gastrointestinal tract (i.e., pepsin, trypsin and chymotrypsin), simulated gastric (SGF) and intestinal (SIF) fluids. Strikingly, whereas genuine Ses i 2 is fully resistant to all protease tested, the oxidized species is highly susceptible to proteolytic attack. These results confirmed the importance of methionine residues in the stabilization of Ses i 2 structure through hydrophobic interactions. Oxidation of unmodified Met to MetSO, indeed, is expected to convert an apolar amino acids, like Met, into a hydrophilic and partially charged residue, like MetSO. At inflammation sites, oxidation of protein allergens may represent a critical step in tissue defence, immunospecific response and allergic reactions. Alterations in this pathway in the oxidation step, followed by the proteolytic processing operated by immunocompetent cells might play a key role to induce allergic response.

MATERIALS AND METHODS

Materials

"White" sesame seeds of Ethiopian origin were kindly supplied by Chelab s.r.l. (Resana, TV, Italy). Trypsin (E.C. 3.4.21.4), chymotrypsin (E.C. 3.4.21.1) and pepsin (E.C. 3.4.23.1), S. aureus V8 protease (E.C. 3.4.21.19), thermolysin (E.C. 3.4.24.27), dithiotreitol (DTT) and hydrogen peroxide were purchased from Sigma (St. Louis, MO).

Methods

Extraction and purification of Ses i 2 from sesame seeds

To 1 g of coarsely ground sesame seeds were added 10 ml of 0.1 M Tris-HCl buffer, pH 8.0, containing 0.2 M NaCl. The mixture was gently stirred at room temperature for 24 h on a model 708 Asal (Milan, Italy) rotating stirred. Thereafter, the suspension was centrifuged at 13000 r.p.m. for 5 min and the supernatant filtered on 0.45-μm durapore filters (Millipore, Badford, MA, USA). The crude extract 1 ml (~ 8 mg) was loaded onto a (1.6 x 60 cm) column (Pharmacia Fine Chemicals), packed in-house with Sephacryl HR-100 and eluted at a flow-rate of 0.8 ml/min in 50 mM Tris-HCl buffer, pH 7.5, containing 1 M NaCl and 10% ethanol (v/v). The absorbance of the effluent was recorded at 280 nm. In a second step, the fractions (1.5-2.0 ml each) eluted from the Sephacryl column, denoted as P5 and found to correspond to the Ses i 2 allergen, were pooled, lyophilised and further purified by reversed-phase high-performace liquid chromatography (RP-HPLC) on a Grace-Vydac (The Separation Group, Hesperia, CA, USA) C18 semi-preparative column (1 x 25 cm, 5 μm, 300 Å porosity), eluted with a linear acetonitrile-0.1% TFA gradient, at a flow rate of 1.5 ml/min. The material eluted in correspondence of the major chromatographic peak was collected, lyophilised and stored at –20°C for subsequent studies.

Selective Methionine Oxidation of Ses i 2

Aliquots of purified Ses i 2 (42 μM) was dissolved in 50 mM potassium acetate pH 5.0 buffer, and stock solution of hydrogen peroxide was added to make the final concentration of H_2O_2 to 5 mM or 50 mM in the reaction mixtures. The concentration of H_2O_2 was determined by UV absorption at 240 nm (ε_{240nm}= 39.4 ±0.2 M^{-1} cm^{-1}; Nelson and Kiseow, 1972) on a double beam Model V-630 from Jasco (Tokyo, Japan) spectrophotometer. Under this

conditions, methionines are predicted to be selectively oxidized to their corresponding sulfoxide (Vogt W., 1995). The oxidations were carried out at 25 °C an at 37°C. At different time intervals, aliquots (10 μg) were taken and analysed by reversed-phase high-performance liquid chromatography (RP-HPLC) on a Grace-Vydac (The Separation Group, Hesperia, CA, USA) C18 analytic column (4.6 x 150 mm, 5 μm, 300 Å porosity), eluted with a linear acetonitrile-0.1% TFA gradient from 5 to 60% in 15 minutes at a flow rate of 0.8 ml/min. The effluent was monitored at 226 nm.

When oxidation was carried out in acidic condition, Ses i 2 (42 μM) was incubated in 10 mM sodium phosphate pH 1.2 in presence of 50 mM H_2O_2 at 37°C. Aliquots were collected at different time points and analysed by RP-HPLC onto analytical column (4.6 x 150 mm, 5 μm, 300 Å porosity), eluted with a linear acetonitrile-0.1% TFA gradient, at a flow rate of 0.8 ml/min.

Analytical SEC (size exclusion chromatography)

A equimolar mixture of Ses i 2 and Ses i 2-ox (1.5 nmol) was analysed by analytical size exclusion chromatography. The mixture was loaded on a HR10/30 Superose-12 column (1 cm x 30 cm, Amersham-Pharmacia Biotech) equilibrated in 50 mM Tris-HCl buffer, pH 7.5, containing 1 M NaCl and 10% ethanol (v/v) and eluted with the same buffer at a flow rate of 0.3 ml/min. The absorbance of effluent was monitored at 280 nm. The apparent molecular weight of Ses i 2-ox was estimated by SEC on a HR10/30 Superose-12. The column was calibrated using the low molecular mass gel filtration protein calibration kit (GE Healthcare): bovine serum albumin (67 kDa), ovalbumin (43 kDa), charbonic anidrase (29 kDa), Ribonuclease A (13.7 kDa) and aprotinina (6.5 kDa). The values of void volume (Vo) and interstitial volume (Vi) were determined by loading Dextran Blue (2 x 10^3 kDa) and dipeptide H-Tyr-Gly-OH. The distribution constant (K_D) value was calculated by the equation K_D= (Ve-Vo)/(Vi-Ve).

Reduction of Ses i 2-ox and chemical characterization of the large and small chain

An aliquot of purified Ses i 2-ox (79 μg) was subjected to reduction of disulfide bonds with the intent to separate small and large subunits of protein. The reduction reaction was carried out under denaturing condition in 0.125 M Tris-HCl buffer, pH 8.3, containing 1 mM EDTA and 6 M Gnd-HCl in the presence of 10 mM dithiothreitol (DTT) and incubation was conducted at 25°C for 90 min in the absence of oxygen. The reaction mixture was fractionated by RP-HPLC on a C18 analytical column (4.6 x 150 mm, 5 μm, 300 Å porosity) eluted with a

linear acetonitrile-0.1% TFA gradient from 5 to 20% in 10 minutes and from 20 to 45% in 30 minutes, at a flow rate of 0.8 ml/min. The absorbance of the effluent was recorded at 226 nm. Two peaks was observed and eluted at about 24 and 32 minutes, peaks were denoted as LCox and HCox. These fractions was collected, lyophilized and solubilised in 10 µl of H2O-acetonitrile solution (1:1 v/v), containing 1% formic acid, and analysed by mass spectrometry on a Mariner Electro Spray Ionization-Time of Flight (ESI-TOF) instrument (Prespective Biosystem, Stafford, TX). Spray tip potential was set at 3.0 kV, the nozzle potential and temperature at 200 Volts and temperature were set at 140°C, respectively.

Peptide mass fingerprinting of HCox and LCox

Aliquots of purified LCox or HCox (10 µg or 30 µg) were dissolved in 300 µl of 50 mM Tris-HCl, pH 7.8, containing 10 mM $CaCl_2$. Primarily, heavy chain was proteolysed in 50 mM ammonium acetate pH 4.0 in presence of Glu-C endopeptidase V8 from *S.aureus* at enzyme/substrate ratio of 1:50 (w/w) for 24 h at 25°C. Subsequently, with the intent to eliminate overlapped peptides, HCox was solubilised in 300 µl of 50 mM Tris-HCl, pH 7.8, containing 10 mM $CaCl_2$ and it was digested in presence of TPCK (tosylphenylalanylchloromethane)-treated bovine trypsin (Sigma). Enzyme was added to final enzyme/protein ratio of 1:50 w/w. Reaction mixture was incubated at 25°C overnight, and digestion was stopped by adding 50 µl of 20% aqueous formic acid. LCox was digested in the presence of chymotrypsin in 50 mM Tris-HCl, pH 7.8, containing 10 mM $CaCl_2$ with an enzyme/substrate ratio of 1:50 (w/w). Reaction mixture was incubated at 37°C for 2 h, and digestion was stopped by adding 50 µl of 20% aqueous formic acid. Proteolysis were fractionated by RP-HPLC on a C18 analytical column eluted at flow rate of 0.8 ml/min with linear acetonitrile-0.1% TFA gradient from 5 to 20 in 10 min and from 20 to 60 in 35 min. The absorbance of effluent was recorded at 226 nm for HCox digestion and at 214 nm for LCox. Peptide material eluted in correspondence of chromatographic peaks were collected, lyophilised, and dissolved in 1%-aqueous formic acid for subsequent mass spectrometry analysis. Peptide profiles were searched (on the basis of mass) against the NCBI nonredundant protein database using the Mascot program from Matrix Science (http://www.matrixscience.com/). The search parameters were as follows: (1) peptide masses were stated to be monoisotopic; (2) methionine residues were assumed to be oxidized.

UV Absorption

All measurements were recorded at 25°C in 10 mM sodium phosphate buffer (pH 2.0 or pH 7.0). The protein concentration was determined by UV absorption at 280 nm on a double beam Model V-630 from Jasco (Tokyo, Japan) spectrophotometer. Extinction molar coefficient at 280 nm for Ses i 2 was calculated according to Gill and Von Hippel (1989) and taken as 15820 M^{-1} cm^{-1} or 1.34 mg^{-1} cm^2 and 1.32 mg^{-1} cm^2 for Ses i 2 and Ses i 2-ox, respectively. Second-derivative ultraviolet absorption spectra of Ses i 2, Ses i 2-ox and subunits (100 μg) were recorded in 350 μl of buffer at 25 °C.

Circular Dichroism (CD)

CD spectra were recorded on a Jasco model J-810 spectopolarimeter equipped with a thermostatically controlled cell holder, connected to a model RTE-111 (NesLab) water-circulating bath. CD spectra in the Far-UV region were recorded in a 1-mm path-length quartz cell, at a scan speed of 10 nm/min, using a response time of 16 s. The final spectra resulted from the average of four accumulations, after baseline subtraction. Near-UV spectra were recorded in a 1-cm path-length quartz cell, at a scan speed of 10 nm/min, using a response time of 16 s. The final spectra resulted from average of ten accumulations, after baseline subtraction. The CD signal was expressed as the mean residue ellipticity, calculate with the formula:

$$[\theta] = \theta_{obs} \cdot MRW/(10 \times l \times c)$$

where θ_{obs} is the observed ellipticity in degrees, MRW is the mean residues molecular mass of Ses i 2-ox taken as 127.3 Da, l is the optical path-length in cm and c is the protein concentration in g/ml. Otherwise, only the baseline-subtracted spectra were reported.

Far-UV CD spectra were analysed in order to estimate the percentage of protein secondary structure using equation:

$$\%_{helix} = 100 / \{1+[(\theta_{222nm,obs} - \theta_{222nm,H})/(\theta_{222nm,C} - \theta_{222nm,obs})]\} \quad (1)$$

where $\theta_{222nm,obs}$ is the observed mean residue ellipticity at 222 nm and $\theta_{222nm,H}$ and $\theta_{222nm,C}$ are the mean residue ellipticity values for the 100% helical and coil conformation, respectively.

For $\theta_{222nm,H}$ and $\theta_{222nm,C}$ at 25°C were taken as -33500 and -485 deg·cm^2· dmol^{-1}, respectively, according to (Scholtz et al., 1991).

Fluorescence

Fluorescence emission spectra were recorded at 25°C on a Jasco spectrofluorimeter Model FP-6500, exciting the samples (0.6 μM) in 10 mM sodium phosphate pH 2.0 or pH 7.0 at 280 nm or 295 nm and recording the emission fluorescence in wavelength range 285-500 nm or 300-500 nm, respectively. The emission spectra under denaturing conditions were taken in presence of 8M Gnd-HCl in 10 mM sodium phosphate buffer pH 2.0 after 1 h of incubation at 25°C.

Stability Studies

Urea-mediated and Gnd-HCl denaturation curves of Ses i 2-ox was carried out at 25°C by measuring the CD signal at 222 nm. Solution at different concentrations of urea or Gnd-HCl were prepared by diluting with buffer a 10 M urea or 8 M Gnd-HCl stock solution dissolved in 20 mM sodium phosphate pH 2.0. Samples (50 μl) of Ses i 2-ox (64 μM) were added to 200 μl of denaturant solution at the appropriate concentration and incubated at room temperature for 1 h prior to CD measurements. The CD signal was recorded at function of [denaturant].

Urea-mediated unfolding curves of Ses i 2-ox was carried out at 25°C by measuring the fluorescence intensity at the λ_{max}. Solution at different concentrations of urea were prepared by diluting with buffer a 10 M urea stock solution dissolved in 20 mM sodium phosphate pH 2.0. Samples (200 μl) of Ses i 2-ox (3 μM) were added to 1800 μl of denaturant solution at the appropriate concentration and incubated at room temperature for 1 h prior to measurements. After incubation protein samples (2 ml, 0.3 μM) were excited at 280 nm, using an excitation/emission slit of 5-10 nm. The reversibility of protein unfolding process was at least 96%, as checked by diluting samples of the unfolded protein in the presence 9 M urea to 1.8 M urea and measuring the recovery of the fluorescence intensity at λ_{max}.

Limited proteolysis

Digestive proteases (trypsin, chymotrypsin and pepsin). Purified Ses i 2-ox (100 μg) were dissolved in 260 μl of *Simulated Gastric Fluid* (SGF), containing 50 mM HCl, 30 mM NaCl and 0.56 μM bovine pepsin (enzyme:protein ratio of 1:20 w/w). The reaction mixture

was incubated at 37°C and at different time intervals aliquots were taken and the proteolysis was stopped by adding 20 µl of 1M $NaHCO_3$.

Purified Ses i 2-ox (100 µg) were dissolved in 260 µl of 50 mM Tris-HCl, pH 7.8, containing 10 mM $CaCl_2$. To this solution TPLK (tosylphenylalanylchloromethane)-treated bovine trypsin (Sigma) was added to final concentration of 0.4 µM (enzyme:protein ratio of 1:40 w/w). The reaction mixture was incubated at 37°C, and stopped by adding 50 µl of 20% aqueous formic acid.

Purified Ses i 2-ox (100 µg) were dissolved in 260 µl of 50 mM Tris-HCl, pH 7.8, containing 10 mM $CaCl_2$. To this solution TLCK (Nα-Tosyl-Lys-chloromethylketone)-treated bovine chymotrypsin (Sigma) was added to final concentration of 1.5 µM (enzyme:protein ratio of 1:10 w/w). The reaction mixture was incubated at 37°C, and stopped by adding 50 µl of 20% aqueous formic acid.

Bacterial proteases. Proteolysis with thermolysin from *B. thermoproteolyticus* was conducted for 180 min at 70 °C in 50 mM Tris-HCl buffer, pH 7.8, containing 5 mM $CaCl_2$ and 10µM $ZnCl_2$, at a substrate:protease ratio of 100:1 (w/w). Aliquots were analysed by reversed-phase high-performance liquid chromatography (RP-HPLC) on a Grace-Vydac (The Separation Group, Hesperia, CA, USA) C18 analytic column (4.6 x 150 mm, 5 µm, 300 Å porosity), eluted with a linear acetonitrile-0.1% TFA gradient from 5 to 60% in 15 minutes at a flow rate of 0.8 ml/min. The effluent was monitored at 226 nm. The percentage of intact protein was determined by integrating the area under the HPLC peak of the protein.

RESULTS AND DISCUSSION

Purification of Ses i 2 from white sesame seed

In the previous chapter has been described method for obtaining large quantities of pure Ses i 2 and this procedure was optimized. The major allergen from sesame seed Ses i 2 has been extensively characterised by chemical and spectroscopic techniques. Briefly, protein extraction from coarsely ground sesame seeds with Tris-HCl buffer, pH 8.0 (10% w/v), resulted in a crude extract with a total proteins content of about 8 mg/ml. Ses i 2 was purified in two steps, including gel-filtration chromatography on a Sephacryl HR 100 column and semi-preparative RP-HPLC (Figure 1A). Mature form of the protein allergen Ses i 2 is formed by two subunits: a light chain (LC), comprising residues 18-43, and a heavy chain (LC), comprising residues 56-123, held together by three S-S bonds and with the N-terminal Gln18 and Gln56 in the Pyr-Glu form. The mature Ses i 2 sequence accounts for about 63% of the

full-length protein chain (i.e, 148 amino acids), encoded by the corresponding sesame DNA sequence (accession no. AF091841) (Tai et al. 1999). Strikingly, Ses i 2 sequence is particularly abundant in Met-resiudes (~16%). Notably, the abundance of Cys (10.6%), Arg (13.8%) and Gln (17%) in the mature Ses i 2 (containing 94 amino acids) is much higher than that normally observed in natural proteins. The identity of purified protein was confirmed by mass spectrometry yielding a mass value of 11726. 4±0.7 a.m.u (Figure 1 B).

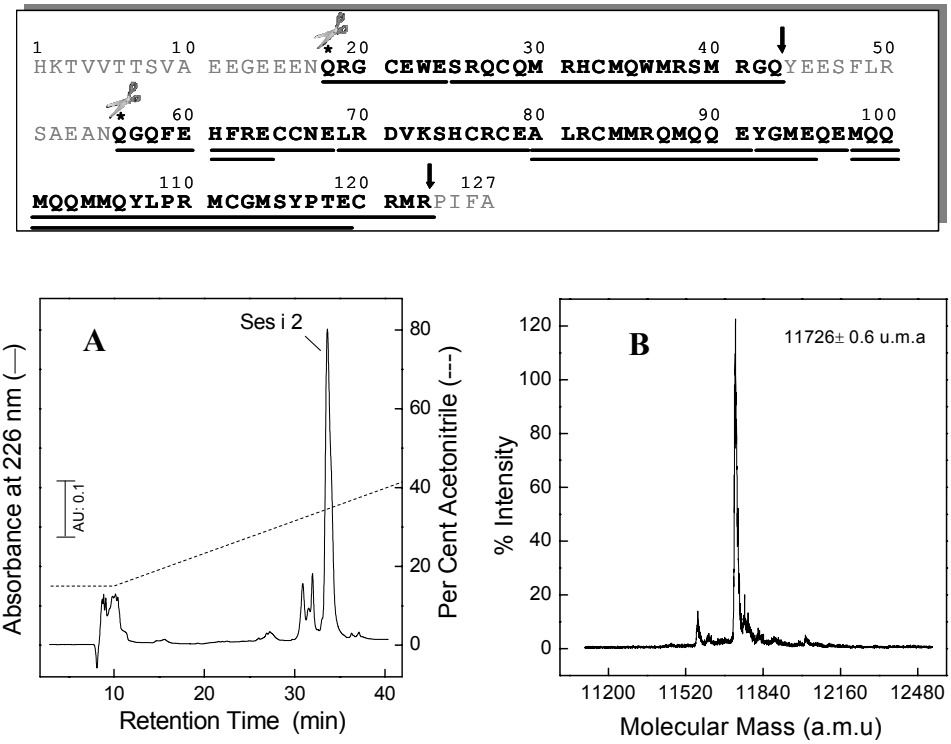

Figure 1 Purification of Ses i 2(A). Deconvoluted ESI-TOF mass spectrum of the RP-HPLC purified Ses i 2 (B).

Selective Oxidation of Methionine Residues in Ses i 2

The thioether groups in methionine side chains in proteins are weak nucleophiles, and, like other hydrophobic residues, usually have little access to aqueous environment. In contrast with other nucleophilic residues in proteins, they resist protonation from pH 1 to 14 and can therefore be selectively modified under acidic conditions. Hydrogen peroxide, under suitable, relatively mild conditions, might be modify several functional groups in proteins, such as thioethers, indoles, sulphydryls, disulfides, imidazoles, and phenols. Under acidic conditions the primary reaction is oxidation of methionines, while under neutral and slightly alkaline environment tryptophan and other functional groups are also modified (Shechter at al., 1975).

The quantitative and selective oxidation of all fifteen methionine residues in the Ses i 2 to sulfoxides (Ses i 2-ox) can be accomplished *in vitro* using H_2O_2, the main non-radical and non-charged oxidant produced in the inflammation site (Halliwell et al., 2000). In view of the oxidative sensitivity of methionine and their important structural role, our strategy was to use

oxidizing conditions that are as specific as possible for methionine, in order to determine the relationship between specific sites of oxidative modification in the primary sequence and conformational alteration in the protein. To assess whether H_2O_2 modifies Ses i 2 *in vitro*, aliquots of purified protein (42 μM) in 50 mM potassium phosphate, pH 5.0, were exposed to 5 mM or to 50 mM of H_2O_2 at a room temperature or at 37°C. Aliquots of reaction mixture were collected at different time intervals and analysed by RP-HPLC combined with mass spectrometry (Figure 2). Hydrogen peroxide induces a concentration- and temperature-dependent shift in the mobility of Ses i 2 in reverse phase chromatography. The retention time of the native protein (N) peak prior to the oxidation and peak after oxidation (O) are indicated in Figure 2 with continue and dot line, respectively. Chromatographic profiles of Ses i 2, in the presence of 5 mM of H_2O_2 at 25°C, show a single peak that after 1h-incubation presents an enlargement correlated to an initial alteration of hydrophilic-hydrophobic balance of the protein. After 24 h-incubation chromatogram plot shows an ensemble of unresolved peaks as consequence of the formation of multiple oxidized species of Ses i 2. In these conditions, Ses i 2 undergoes dramatic alterations that induced the formation of heterogeneous populations corresponding to different oxidized intermediates. The mixture of intermediates is eluted at shorter retention time compared to non-oxidized protein (Figure 2A) and this observation suggests that the retention time of Ses i 2 oxiforms is primarily determined by the change in the polarity of the protein. Eluted materials were analysed by mass spectrometry and data indicate the presence of multiple species with a mass values of 11742.6 Da (Δm= + 16 a.m.u) and 11788.1 Da (Δm= + 61.5 a.m.u). The methionine oxidation to methionine sulfoxide involves an increase of mass of + 16 Da and our results are in agreement with the addition of one or four oxygen atoms, respectively.

Also, Ses i 2 oxidation was carried out in the presence of 5 mM of hydrogen peroxide at 37°C and after 120 min-incubation the chromatographic profile is dramatically altered and eluted materials were analysed by mass spectrometry that gave mass values of 11803 Da and 11935 Da. These mass values are due to oxidation of five and thirteen methionines, respectively (Figure 2B).

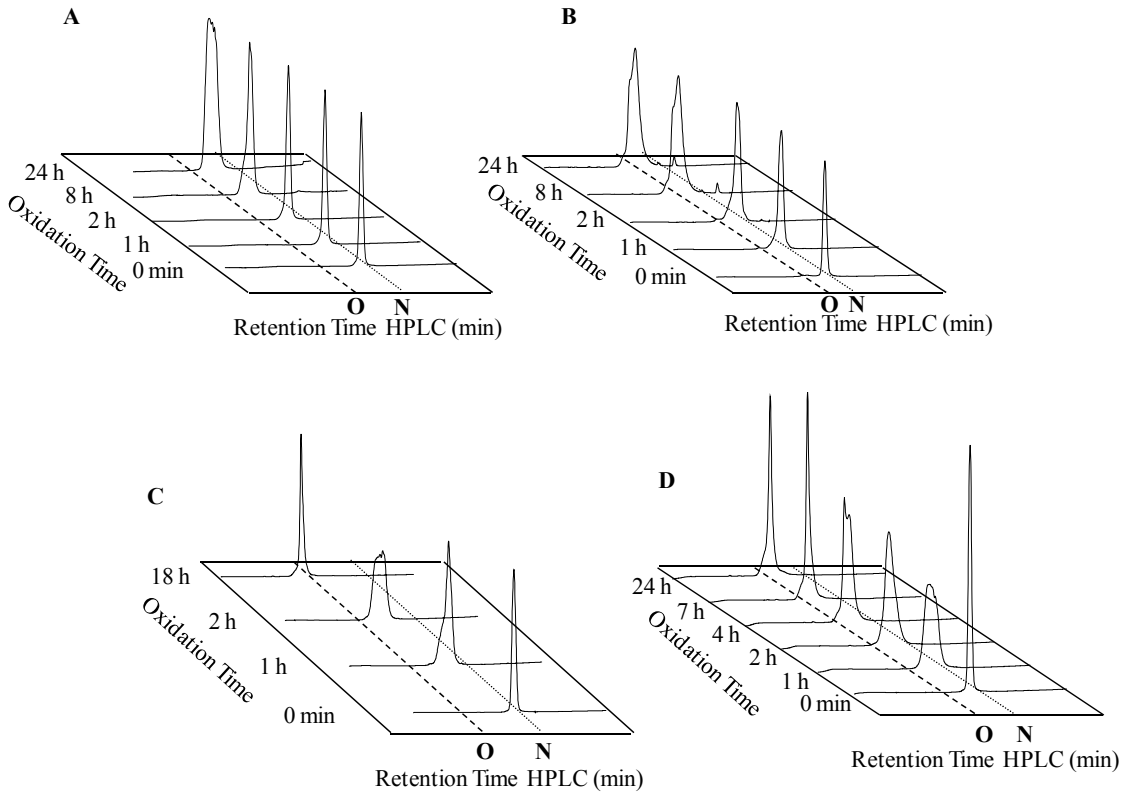

Figure 2. Reverse-phase HPLC analysis of the Ses i 2 oxidation in potassium phosphate, pH 5.0. RP-HPLC of Ses i 2 (40 μM) in potassium phosphate, pH 5.0, in presence of 5 mM H_2O_2 at 25°C **(A)** and at 37°C **(B)**, in presence of 50 mM H_2O_2 at 25°C **(C)** and at 37°C **(D)**. An aliquot (10 μg) was loaded in onto Vydac C-18 column (4.6 x 250 mm, 5 μm) and elution was performed at flow rate of 0.8 ml/min with a linear 0.1% (v/v)-TFA-acetonitrile gradient (---).

In addition, oxidation experiments were conduced in the presence of 50 mM H_2O_2 at both temperature of 25°C and 37°C. Already, at 120 min at 25°C, chromatographic plot shifts into an asymmetric unresolved peak in which the major species shows a molecular mass about of 11836.9 Da (Δm= + 110.3 a.m.u) corresponding to the introduction of seven oxygen atoms. As shown in Figure 2C and 2D, after 7 h at 37°C or 18 h at 25°C, a single symmetric peak indicates the formation of a species with a minor retention time compared to native protein (dash line). Eluted material in this single peak was analysed by mass spectrometry yielding a mass value of 11968.3±0.8 a.m.u. The oxidized form differs from the native protein (11726.4±0.7 a.m.u) about of 241.9 a.m.u, this data is in agreement with the complete oxidation of fifteen methionine in Ses i 2.

Similar results were obtained at 50 mM of H_2O_2 at pH 1.2, actually in these conditions after 240 min of incubation at 37° in the chromatographic profile is possible to identify a single sharp peak characterised by the same retention time compared to oxidized form (Figure 3A). Our observations are confirmed by mass analysis that showed the complete oxidation of

Ses i 2 (Figure 3B). These results are in keeping with the notion that Met-oxidation occurs via an acid-catalyzed mechanism (Shechter et al, 1986).

Several mechanisms was proposed to explain the Met/hydrogen peroxide oxidation, a clean overall two-electron oxidation process (oxygen transfer). Recent reports (Chu and Trout, 2004 and Chu et al., 2004) gave an overview on the earlier proposed mechanisms and introduce new details on the participation of water. Initially, the mechanism was considered to be an S_N2-type reaction with heterolytic O–O bond scission of the peroxide. Later a general acid dependent 1,2-H-shift to yield an intermediary water oxide (H_2O-O) was proposed to control the oxidation. However, calculations showed that such reaction mechanism should have activation barriers significantly higher than those experimentally determined. Therefore, the mechanism was modified such to include not only general acid but also protonated solvent. New calculations show now that coordination of hydrogen peroxide with two to three molecules of water through hydrogen bonding can stabilize the charge separation in the transition state sufficiently. Transfer of the hydrogen atom to the distal oxygen of hydrogen peroxide occurs after the system has passed the transition state (see conclusion).

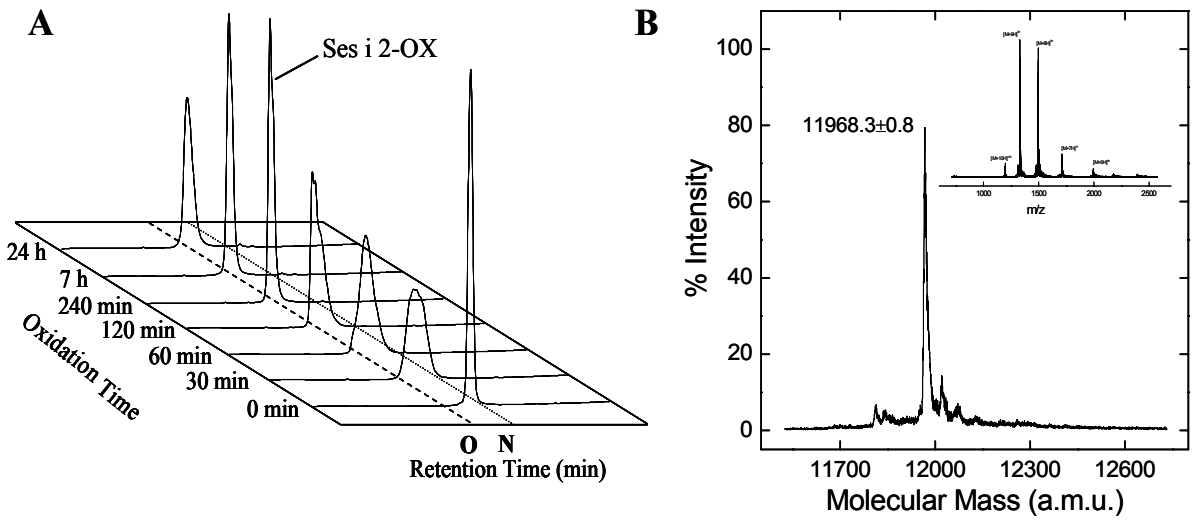

Figure 3. RP-HPLC analysis of the Ses i 2 oxidation in SGF at pH 1.2 in the presence of 50 mM H_2O_2(A). An aliquot (10 ug) was loaded in onto Vydac C-18 column (4.6 x 250 mm, 5 µm) and elution was performed at flow rate of 0.8 ml/min with a linear 0.1% (v/v)-TFA-acetonitrile gradient (---). **Deconvoluted ESI-mass spectra of Ses i 2-ox (B).**

Peptide mass finger-printing

The involvement of other amino acid types, besides Met, in the oxidation of Ses i 2 was ruled out by peptide mass fingerprint analysis and second-derivative UV absobtion spectra on the light and heavy chain.

Ses i 2-ox was subjected to reduction using DTT as reducing agent in the denaturant conditions at pH 8.35. After 90 min of incubation at 25°C the reduction mixture was analysed by RP-HPLC and two main peaks were isolated (Figure 4A). The peaks are identified in homologous regions of the small ^{18}Glu–^{43}Glu and the large subunit ^{56}Glu–^{123}Arg. Molecular weight of two subunits are: 3377.7 ± 0.5 u.m.a (Figure 4B) and 8601.2 ± 1 u.m.a (Figure 4C) for LCox and HCox, respectively (Table 1).

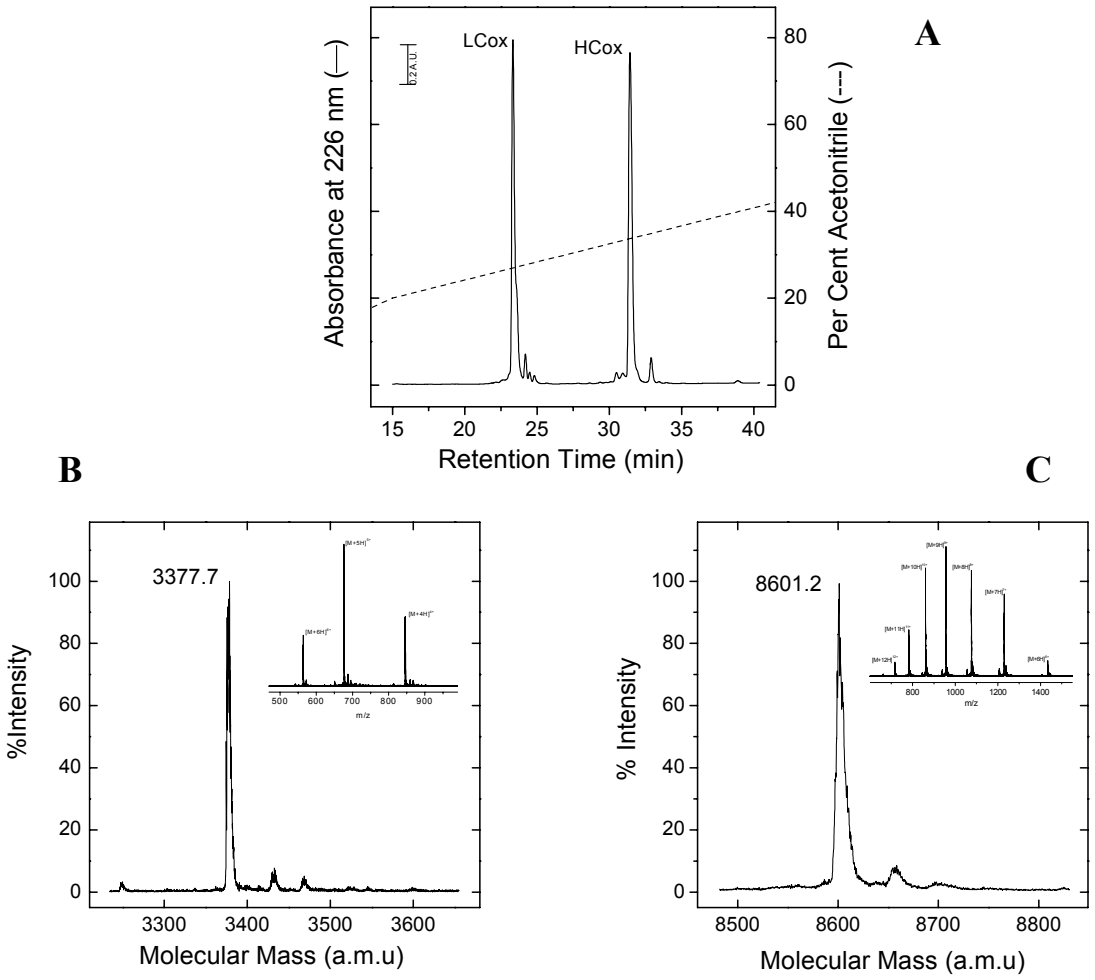

Figure 4. RP-HPLC analysis of the disulfide reduction of Ses i 2-ox. The reaction products, denoted as LCox and HCox, were separated on a C18 column and analysed by ESI-TOF mass spectrometry, which gave mass values of 3377.7±0.4 (B) and 8601.2±0.3 a.m.u. (C), respectively.

Table 1. Mass data of LCox and HCox

	Theoretical Mass(a.m.u)	Experimental Mass (a.m.u)	Δm (a.m.u)	Oxidative Modification
Light Chain	3312. 5±0.5	3377.7±0.5	65.2	4 MetSO
Heavy Chain	8424.7±0.3	8601.2±0.3	176.5	11 MetSO

Altogether these data indicate that the hydrogen peroxide selectively induces an increment about of + 63.7 u.m.a. assigned to the formation of four MetSO derivatives in LCox, while in HCox the mass increment about of +177 u.m.a is in agreement with the formation of eleven MetSO (Table 1).

The chemical identity of oxidized species and the involvement of other amino acids, besides Met, in the oxidation of Ses i 2 were elucidated by peptide mass finger-print of LCox and HCox. The two subunits were subjected to enzymatic fragmentations and the experiments were conducted using a limited proteolysis approach (Fontana et al., 1997). Proteolysis were carried out in presence of chymotrypsin, trypsin or V8 (E/S ratio of 1:50 w/w) at pH 7.8 or pH 4.0 (i.e., V8 digestion) (Figure 5-6). After incubation at 37°C LCox and HCox were rapidly cleaved at several peptide bonds along the polypeptide chains. Peptides were analysed by mass spectrometry on a Mariner Electro Spray Ionization-Time of Flight (ESI-TOF) instrument (Prespective Biosystem, Stafford, TX). Data were elaborated by MASCOT program and we obtained the integral sequence of oxidized light and heavy chain. Data (Table 2, 3 and 4) indicate that the oxidation of Met residues in the HCox (11 Met) and LCox (4 Met) is selectively induced by 50 mM H_2O_2. Notably, three main peptides are produced by the proteolysis of LCox (Figure 5): the N-terminal fragment ^{18}QRGCEW^{23} is characterized by cyclization of ^{18}Q in pyroglutamic acid (-17 a.m.u), the fragment ^{24}ESRQCQMRHCMQW^{36} presents a mass increment of + 32 Da induced by the formation of two MetSO. Finally, mass data demonstrate that Met37 is in oxidized form (MetSO) in the fragment ^{29}MRHCMQWM^{37}. To assess whether Met40 is in the oxidized form, LC was subjected to proteolysis in the presence of trypsin.

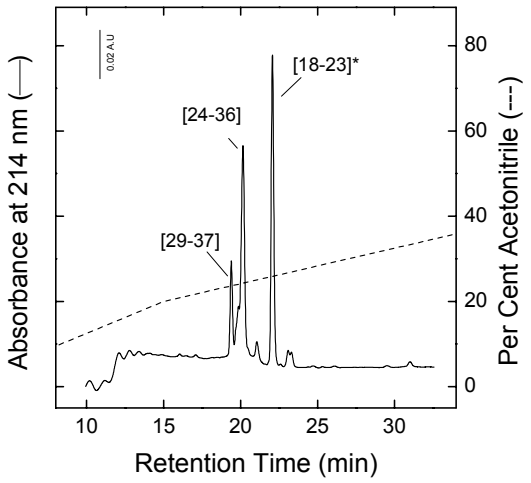

Figure 5. LCox proteolysis with the chymotrypsin. RP-HPLC analyses of the proteolysis reaction of purified LCox in the presence of chymotrypsin. The numbers next to the chromatographic peaks refer to the peptide segments of LCox, as identified by ESI-TOF mass spectrometry. (*) indicates that Q18 is in the form of Pyr-Glu.

Table 2. Chymotryptic peptide profile of LCox.

Fragment	Theoretical Mass (a.m.u)	Experimental Mass (a.m.u.)	Δm (a.m.u)	Modification
[29-37]	1136.5	1168.5	+32	2 MetSO
[24-36]	1721.7	1753.7	+32	2 MetSO
[18-23]*	777.3	761.3	-17	Pyroglutamic acid

HCox was subjected to proteolysis in the presence of trypsin and protease V8 from *S.aureus* with the intent to isolate all oxidized MetSO. Several fragments were obtained by enzymatic digestion (without overlapping in presence of trypsin). Molecular masses (Table 3) are in agreement with the oxidation of eleven methionine residues, in particular (Figure 6A): peptide ^{56}QGQFEHFRE^{64} represents the N-terminal of heavy subunits characterized by pyroglutamic acid (-17 a.m.u); fragment ^{87}QMQQEYGMEQEMQQMQQMMQYLPR^{110} with a mass of about 3191 Da that corresponds to six methionine in oxidized form with a increment of molecular weight about of + 97 u.m.a. Finally, peptide ^{111}MCGMSYPTECR^{121} has a molecular weight equal to 1308.5 a.m.u., this value is in agreement with the oxidation of Met111 and Met114. With the intent to discover the complete oxidation of the HCox, heavy subunit was subjected to proteolysis with protease Glu-C for 18 h at room temperature and the reaction mixture was analysed by RP-HPLC.

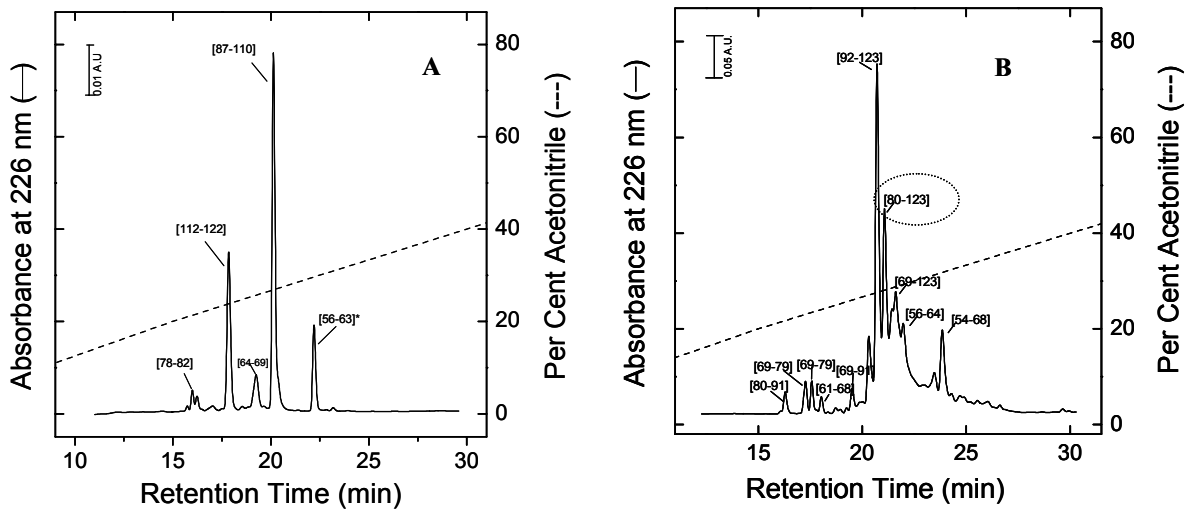

Figure 6. HCox proteolysis with the trypsin (A) and Glu-C (B). RP-HPLC analyses of the proteolysis reaction of purified HCox proteolysis. The numbers next to the chromatographic peaks refer to the peptide segments of LCox, as identified by ESI-TOF mass spectrometry. (*) indicates that Q18 is in the form of Pyr-Glu.

Table 3. Tryptic peptide profile of HCox.

Fragment	Theoretical Mass (a.m.u)	Experimental Mass (a.m.u.)	Δm (a.m.u)	Modification
[56-63]*	1048.5	1031.5	-17	Pyroglutamic acid
[64-69]	864.3	864.3		
[78-82]	590.8	591.3		
[87-110]	3094.3	3191.3	+97	6 MetSO
[112-122]	1276.5	1308.5	+32	2 MetSO

Table 4. Peptide profile of HCox digested with V8.

Fragment	Theoretical Mass (a.m.u)	Experimental Mass (a.m.u.)	Δm (a.m.u)	Modification
[69-91]	1524.7	1571.7	+47	3 MetSO
[80-91]	2852.3	2899.4	+47	3 MetSO
[92-123]	3997.7	4125.6	+127.9	8 MetSO
[80-123]	5504.5	5681.5	+177	11 MetSO
[69-123]	6832.1	7007.7	+175	11 MetSO

Chromatographic profile (Figure 6B) shows a dramatic fragmentation of HCox and the mass data confirm the presence of overlapping peptides in the proteolysis. However, the experiment contributed to improve the mass data by identification of the fragment ^{80}ALRCMMRQMQQEYGMEQEMQQMQQMMQYLPRMCGMSYPTECRMR^{123}. This peptide presents a mass of 5681.5 a.m.u rather than to a theoretical value of 5504.5 a.m.u. and this mass increment is due to the oxidation of eleven methionine residues (Table 4).

Overall, these information suggest that methionine residues are mainly involved in oxidative damage induced by hydrogen peroxide.

Second-derivative absorption

With the aim to definitely rule out the involvement of aromatic residues was registered the second derivative UV spectrum of Ses i 2, Ses i 2-ox and subunits. Second derivative absorption spectroscopy of proteins can be used as a finger-printing method for a given protein structure in order to compare aromatic said chain topology. The first derivate ($dA/d\lambda$) is the rate of change of absorbancy with wavelength; the second derivative ($d^2A/d\lambda^2$) is the velocity of that change (Levine & Federici, 1982). This technique is utilized to resolve the complex protein absorption spectrum into individual contributions of the three aromatic residues. In the second derivative spectrum ($d^2A/d\lambda^2$), the absorbance arising from these residues is resolved as minima in the spectral regions 245–270 nm (Phe), 265–285 (Tyr), and 265–295 nm (Trp), and thus spectral overlap is significantly reduced. Also, second-derivative spectroscopy is employed for detecting conformational changes involving in microenvironments of aromatic amino acids (Ragone et al, 1984). Therefore, the second derivative spectra was used to detected the possible chemical alterations to the aromatic side chains. The profiles of the second derivative absorption spectra of Ses i 2 and Ses i 2-ox (Figure 7A) strongly indicate that the aromatic side chains are not damaged in the oxidative reaction. The spectral region between 280 nm-300 nm shows two maxima around 287 nm and 295 nm and two minima at 283 nm and 290 nm that is the characteristic profile of tryptophan/tyrosine residues. Actually, second-derivative spectrum of Ses i 2-ox shows a weak blue shift compared to the un-oxidized protein. This behaviour is in agreement with the dependence of wavelength position of the near-UV bands of the aromatic amino acids on the polarity of their microenvironments. Also, Ses i 2-ox second derivative spectrum shows an increment of the intensity of minima at 283 nm and 290 nm. These data suggest an exposure of Tyr residues to solvent and these observations reflected that the oxidative damage might induce modifications in the protein tertiary structure. However, the spectrum of native protein shows the same profile and shape of Ses i 2-ox spectra and this is due to exposure of aromatic amino acids to a polar environment in agreement with structural model (see Figure 12 in previous chapter). Hence, the superimposability of the second derivative absorption profile for Ses i 2-ox and Ses i 2 (Figure 7A) strongly indicates that the aromatic amino acid side chains are not modified by oxidative damage and are located in similar environment, but the high surface exposure of Trp and Tyr residues precluded the speculation about tertiary structure alteration. Second derivative spectra of HCox and LCox (Figure 7B) show a single contribution of Tyr and Trp residues in UV absorption, respectively.

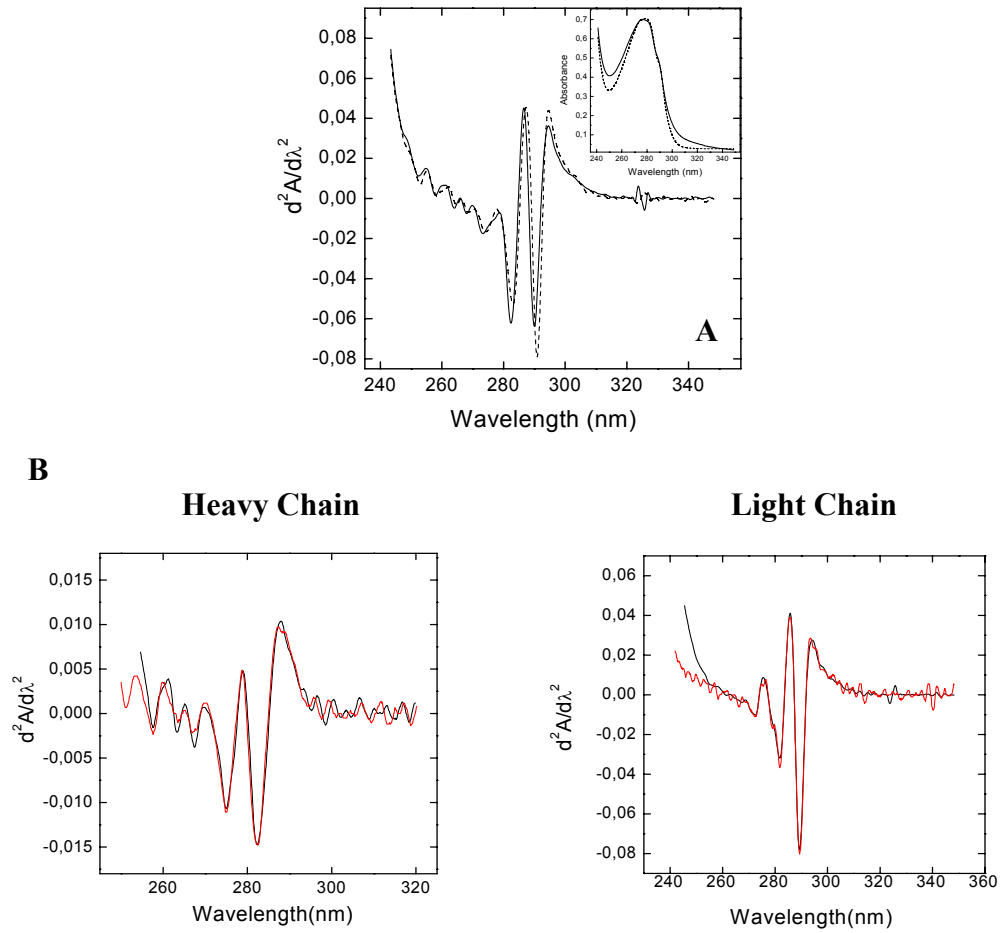

Figure 7. Second-derivative UV spectra of Ses i 2 (----) and Ses i 2-ox (—) (A). Measurements were taken at protein concentration of 10 μM in 10 mM sodium phosphate pH 2.0. Second-derivative UV spectra of HC and LC of Ses i 2 (—) and Ses i 2-ox (—) (B).

Analytical SEC and RP-HPLC of equimolar mixture of Ses i 2 and Ses i 2-ox

Size exclusion chromatography is one of the most powerful techniques for determining the molecular weight and the hydrodynamic volume of proteins, but this analysis is often characterised by a discrepancy in mass determination (Fazeli et al., 2004).

Ses i 2 and Ses i 2-ox presenting similar molecular masses, and thus the change observed in the retention time might be induced by alteration in the global structure of the oxidized protein. In order to assess the extent of changes in structure occurring in the oxidation Ses i 2 and Ses i 2 were solubilised in buffer pH 7.5 with the intent to obtain an equimolar mixture of both protein. This solution was loaded onto a analytical column Superose-12 previously calibrated with a low-molecular-mass kit. SEC profile shows a dramatic alteration in the elution time of Ses i 2-ox (Figure 8B), in particular un-oxidized protein is eluted with a retention time similar to the apoprotinine (Inset Figure 8B) and the apparent molecular weight of Ses i 2 is estimated about of 5000 Da. Instead, the retention time of Ses i 2-ox is in

agreement with the expected value and the apparent molecular weight for the oxidized protein is about 16000 Da.

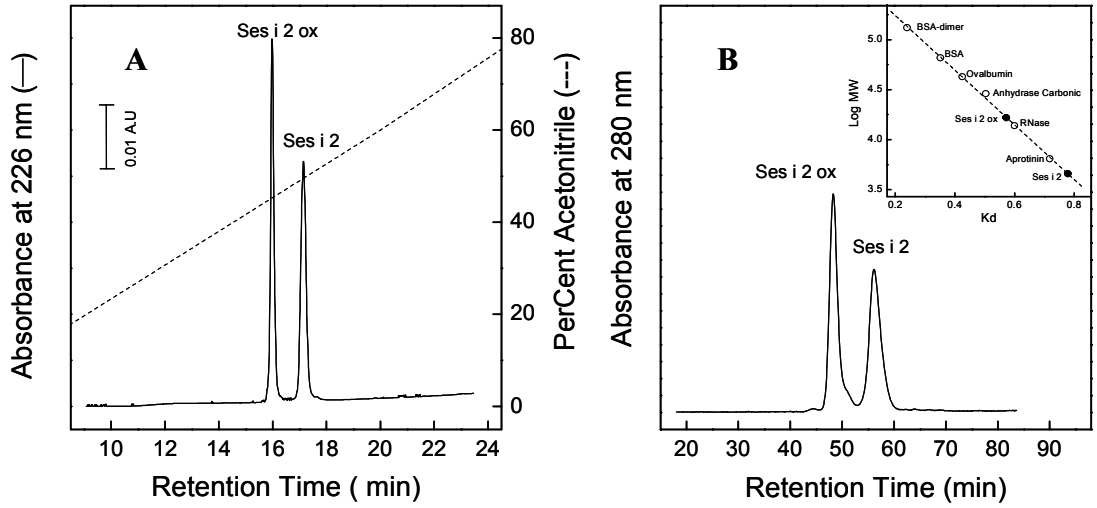

Figure 8. RP-HPLC analysis of the equimolar mixture of Ses i 2 and Ses i 2-ox (A). Sample was loaded onto Vydac C-18 column (4.6 x 250 mm, 5 μm) and elution was performed at flow rate of 0.8 ml/min with a linear 0.1% (v/v)-TFA-acetonitrile gradient (---). **Size exclusion chromatography (SEC) of the equimolar mixture of Ses i 2 and Ses i 2-ox (B).** Chromatographic analysis was carried out on a Superose-12 column, eluted at the flow rate of 0.3 ml/min in 50 mM Tris-HCl, pH 7.5, containing 1M NaCl and 10% ethanol (v/v). Absorbance of effluent was monitored at 280 nm. (Inset) SEC calibration curve. The column was calibrated using the low molecular mass gel filtration protein calibration kit.

Although the elution was performed in presence of 1M NaCl and 10% ethanol with the aim to minimized nonspecific interactions on the stationary phase, the discrepancy in the elution time is due to unspecific interactions among Ses i 2 and stationary phase of column, in this phenomena the hydrophobic clusters on the surface of Ses i 2 probably play a key role. The decrease in surface hydrophobicity (Figure 9) as a consequence of the oxidation characterised by introduction of an oxygen atom in side chain of Met residues and this alteration diminishes the hydrophobic interaction with the stationary phase. Thus, the increment of hydrodynamic radius of oxidized protein as result of oxidative damage induces a minimum effect on retention time of Ses i 2-ox in SEC analysis.

RP-HPLC analysis of the equimolar mixture of Ses i 2 and Ses i 2-ox demonstrates high hydrophilic character of Ses i 2-ox that is due to introduction of oxygen atom in protein structure (Figure 8A) (Chao et al, 1997).

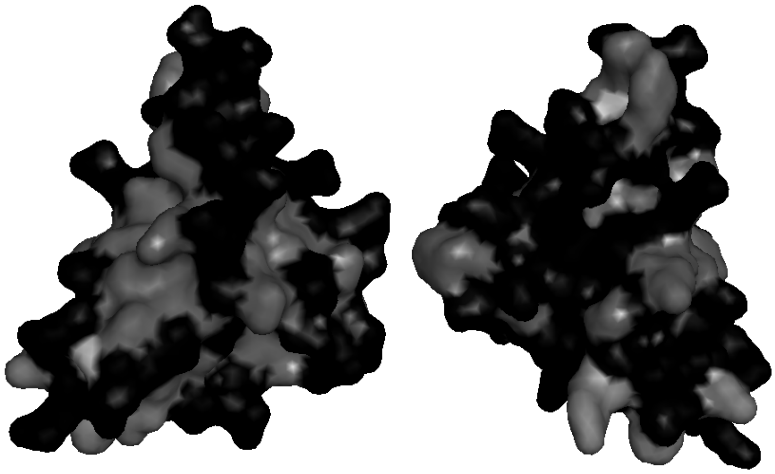

Figure 9. Schematic representation of Ses i 2 model surface hydrophobic patches (grey).

Conformational Characterization

Far- and Near-UV CD. The effects of oxidative modification on the secondary structure of Ses i 2 were assessed by CD spectroscopy to estimate the apparent α-helical content of native and modified 2S albumin. The far-UV CD spectra of native protein (Ses i 2) and oxidized protein (Ses i 2-ox) were recorded at pH 2.0, pH 7.0 and in the presence of 8M Gnd-HCl.

In the previous chapter far-UV CD spectra of native protein at different pH were extensively discussed and, the main characteristic that has been observed is the high content of alpha-helix structure.

As illustrated in Figure 10, far-UV-CD spectra of oxidized protein under neutral and acidic conditions (10 mM phosphate buffer pH 7.0 or pH 2.0) are characterized by two minima at 222 nm and 202 nm. In Ses i 2-ox minimum at 222 nm is characteristic of α-helix structure, whereas the 202 nm band may be attributed to the contribution of random coil. Both the shape of the CD spectra and the ellipticity values at pH 2.0 and 7.0 is very similar, conversely (see Figure 5A in previous chapter) Ses i 2 presents high content of alpha-helix structure and the intensity of spectra shows a strong dependence to pH.

These observations suggest that the methionine oxidation involves a significant increase in structural disorder of protein. Spectrum of oxidized protein presents a weak minimum at 222 nm attributed to alpha-helix, these findings are confirmed by spectrum in the presence of 8 M Gnd-HCl that displays a noticeable increase in the ellipticity (Figure 10A △). The difference spectrum, obtained by substracting the CD spectrum of Ses i 2-ox in the presence of 8 M Gnd-HCl from that of Ses i 2-ox, shows negative ellipticity at 250-200 nm and a

minimum at approximately 222 nm and this value confirms the presence of α-helix structure (Inset Figura 10A). The spectrum in 8 M Gnd-HCl presents a positive ellipticity probably correlated with the mixture of Ses i 2-ox species resulting from both (R)- and (S)- methionine sulfoxides; the ratio of two isomers has been shown to vary between different oxidants, and also between different Met residues in proteins (Davies at al, 2005). Current evidences suggest that the protein structure is the most important controlling factor in determining which stereoisomer predominates at any particular Met residues within a protein (Sharov et al, 2000). The oxidation of methionine induces a drastic alteration in the secondary structure of Ses i 2, however Ses i 2-ox retains alpha-helical moieties that might be stabilized by disulphide bridges. Analysis of far-UV CD spectra allowed us to estimate the percentage of helical content of Ses i 2-ox and Ses i 2 under different conditions (Table 5). Estimation of the secondary structure of native protein content was carried out with equation (1) (Schlotz et al., 1991) and data suggest that going from pH 7.0 to pH 2.0, there is a significant increase in the helix content, from 39 to 53%. Structural model of Ses i 2 has demonstrated that the presence of surface acidic clusters destabilizes the native structure at neutral pH, due to electrostatic repulsion (Glu residues). At low pH, these residues are in the neutral form and thus stabilizes the folded helical structure by alleviating electrostatic repulsion (see figure 13 in previous chapter).

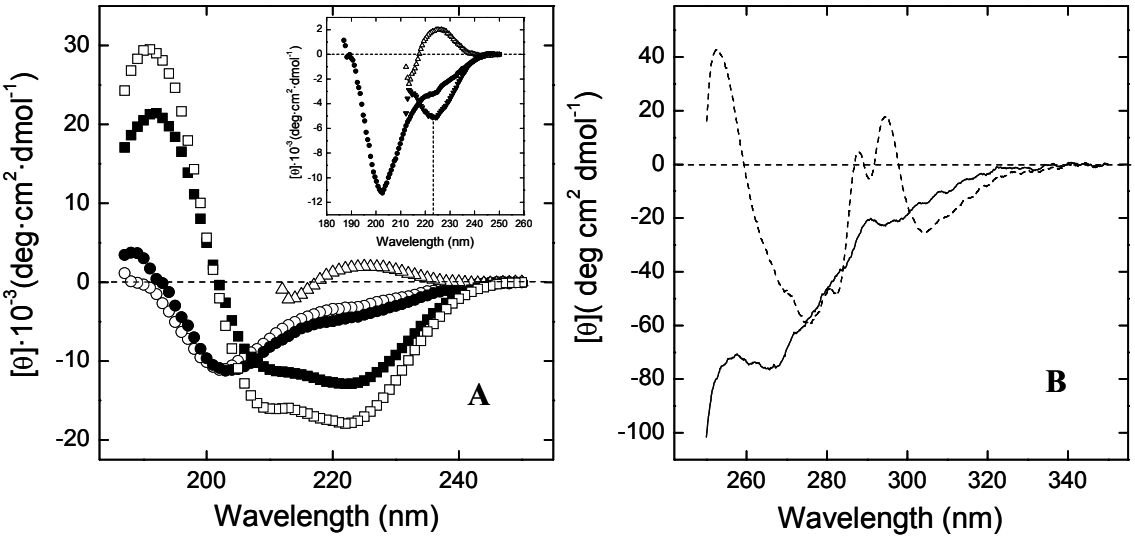

Figure 10. Far-UV CD spectra (A) of Ses i 2 at pH 7.0 (■), pH 2.0 (□) and Ses i 2-ox at pH 7.0 (●), pH 2.0 (○)and in the presence of 8M Gnd-HCl at pH 2.0 (△). Measurements were recorded at a protein concentration of 0.1 mg/ml and all spectra were taken at 25°C in 10 mM sodium phosphate at pH 2.0 or pH 7.0. **Near-UV CD spectra of Ses i 2 (----) and Ses i 2-ox (—) (B).**Measurements were recorded at a protein concentration of 0.4 mg/ml and spectra were taken at 25°C in 10 mM sodium phosphate at pH 2.0.

Table 5. Structural parameters for Ses i 2 and Ses i 2-ox. The percentage of α-helix content was calculated from far-UV CD spectra.

% α-helix $\%_{helix} = 100 / \{1+[(\theta_{222nm,obs} - \theta_{222nm,H})/(\theta_{222nm,C} - \theta_{222nm,obs})]\}$ [a]		
pH	**Ses i 2**	**Ses i 2-ox**
2.0	53	8
7.0	39	12

[a] $\theta_{222nm,obs}$ is the observed mean residue ellipticity at 222 nm and $\theta_{222nm,H}$ and $\theta_{222nm,C}$ at 25°C were taken as -33500 and -485 deg·cm^2· dmol^{-1}, respectively.

Profile and intensity of far-UV CD spectra of Ses i 2-ox are in agreement with the lower content of alpha-helix that is probably due to the decrease of hydrophobic interactions. In Ses i 2-ox the percentage of alpha-helix is about 8% at pH 2.0 and 12% at pH 7.0, these values are in agreement with the loss of secondary structure as consequence of oxidation.

The near-UV CD spectra of Ses i 2 and Ses i 2-ox at pH 2.0 are shown in Figure 10B. Near-UV CD is often taken as a fingerprint of aromatic-side chain an disulfide bond topology in proteins, since both the shape and intensity of dichroic bands strongly depend on the exact type and orientation of interacting groups in the asymmetric protein environment and, usually, higher conformational flexibility lowers signal intensity. In the near-UV (240-350 nm) signals in the region from 250-270 nm are attributable to phenylalanine residues, signals from 270-290 nm are characteristic of tyrosine residue, and those from 280-300 nm are attributable to tryptophan (Strickland, 1974). Native protein spectrum presents a extensive fine structure between 280 nm and 300 nm, assigned to the contribution of Trp-residues, whereas the bands in the region from 260 nm and 280 nm are attributed to Tyr- and Phe-residues. Moreover, in the spectrum is possible to observe a strong contribution of the disulphide bridges with a positive band at 250 nm. Near-UV CD spectrum of Ses i 2-ox is characterised by a dramatic alteration in the shape and intensity, suggesting that the oxidation of methionine residues induces a more flexible environment nearby aromatic residues. However, spectrum of Ses i 2-ox presents a weak signal at 290 nm and, this band is attributed to a Trp residues positioned in a semi-rigid microenvironment. Moreover, in the region from 290 to 240 nm spectrum shows a strong negative trend correlated with changes in the microenvironment where Tyr and Phe residues are located or this profile may be induce by a change in the chirality of disulphide bridges.

This data suggest that the oxidation of Met residues in Ses i 2 is a dramatic event in which protein loses a high percentage of secondary and tertiary structure. Our results, also, showed that Ses i 2-ox retains a minimal degree of ordered structure and these moieties are partially stabilized by disulphide.

Fluorescence Emission. The fluorescence spectra of Ses i 2 and Ses i 2-ox were taken at pH 2.0, pH 7.0 and in presence of 8 M Gnd-HCl. The properties of the chemical environment in which Trp-residues are embedded was investigated by fluorescence spectroscopy after excitation at 280 and 295 nm. Spectra registered in native condition show a maximum of emission at 346 nm and 344 nm for non-oxidized and oxidized protein (Figure 11A), respectively. The values of λ_{max} indicate that two tryptophan residues Trp23 and Trp36 are significantly exposed to solvent (Lakowicz, 1999). Moreover, the emission spectrum measured by excitation at 295 nm shows a maximum at approximately 350 nm, which is taken as an indication that the two Trp residues are exposed to polar environment in both conditions. In 280 nm-spectra, tyrosine fluorescence appears as a shoulder at 303 nm, indicating that in proteins (i.e., Ses i 2 and Ses i 2-ox) there is an inefficient Tyr-to-Trp resonance energy transfer (RET) between the three Tyr and two Trp residues. The intensity of the 295-nm spectrum of Ses i 2-ox is about two-fold lower than that recorded after excitation at 280 nm. In previous chapter we have demonstrated that the fluorescence emission of Ses i 2 is dependent on pH and, in particular it is a consequence of ionization state of Glu and Asp residues. Measurements conducted on model compounds demonstrate that, on going from neutral to acidic pH, the Trp quantum yield is reduced by about 10% while λ_{max} remains constant. In Ses i 2-ox spectra the reduction of Trp emission is marginally caused by acid quenching and, the phenomena is correlated to a near-neighbour effect for which protonation of a specific chemical group quenches the fluorescence of some Trp-residue nearby in the protein. Moreover, spectra of Ses i 2-ox was recorded at different pH with the intent to observe changes in the fluorescence intensity at acidic or neutral pH (Figure 11B). At pH 2.0 signal intensity observed in Ses i 2-ox spectra is higher than signal registered for Ses i 2 and this might be correlated to the decrease of quenching effect to Trp as consequences to the disordered structure generated by the oxidative damage. At pH 7.0, the intensity of emission spectrum of oxidized protein is about 17% higher than recorded at pH 2.0 in close agreement with the behaviour previously observed in native protein. The quenching effect as a decrease in fluorescence emission in function to the pH is in agreement with the presence of clusters of tertiary structure in oxidized protein. In the presence of 8M Gnd-HCl spectra (Figure 11A) of

oxidized protein is characterised by an increase of fluorescence intensity (i.e., about 23%) and, this increment is due to a unfolding process as a demonstration of the presence of partially fold moieties in protein.

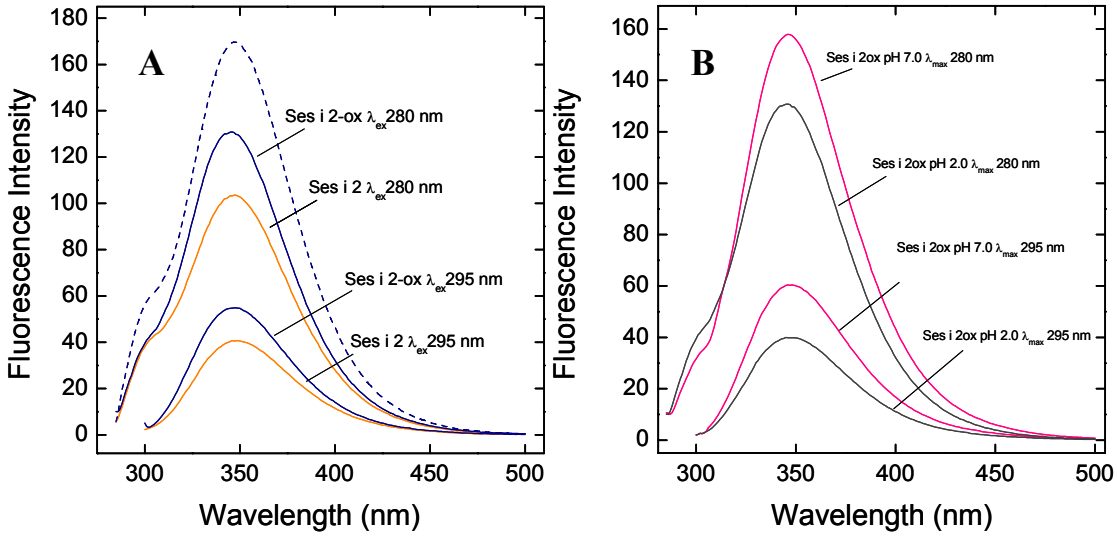

Figure 11. Fluorescence spectra of of Ses i 2 and Ses i 2-ox. All spectra were recorded at protein concentration of 0.6 μM in 10 mM sodium phosphate pH 2.0 or pH 7.0. The emission spectra of proteins were also measured in the presence of 8M Gnd-HCl (----). All measurements were taken at 25°C.

Stability studies

For characterise the conformational stability properties of Ses i 2-ox, the oxidised protein was subjected to urea and guanidinum unfolding process at pH 2.0. As shown in Figure 12A, the profiles of $[\theta]_{222\ nm}/[\theta]_0$ *versus* denaturant concentration of urea or Gnd-HCl are essentially identical. The unfolding process is less cooperative and it is possible to observe the absence of pre-transition region in unfolding curve. Ses i 2-ox exhibits a slight variation of signal in the presence of both denaturing agents as a indication that protein is poorly stabilized by hydrophobic and electrostatic interactions. In the presence of urea or Gnd-HCl Ses i 2-ox unfolds in identical manner, this behaviour is a strong indication that Ses i 2-ox is stabilised by disulphide bridges. Unfolding data was fitted using sigmoidal equation and simulation of unfolding curve (Inset Figure 12A) demonstrates that each point of unfolding is located on transition or post- transition region of denaturation curve and the value of $[D]_{1/2}$ is about of 3-3,2 mol/L.

Also, unfolding process was monitored at 25°C following the increase of fluorescence at λ_{max} after increasing the urea concentration with the intent to observe different behaviour of tertiary structure. In Figure 12B is reported the unfolding curve of Ses i 2-ox (Ses i 2 Inset).

In previous chapter unfolding data of Ses i 2 in the presence of urea were fitted and the value of $[denaturation]_{1/2}$ is about 8.8 ± 0.05 M, this value is in agreement with the high stability of native protein, also demonstrated in the presence of Gnd-HCl (i.e, 6.3±0.05 at pH 7.0). Unfolding curve of Ses i 2-ox is less cooperative and the unfolding profile is similar to the pre-transition region of unfolding curve of Ses i 2.

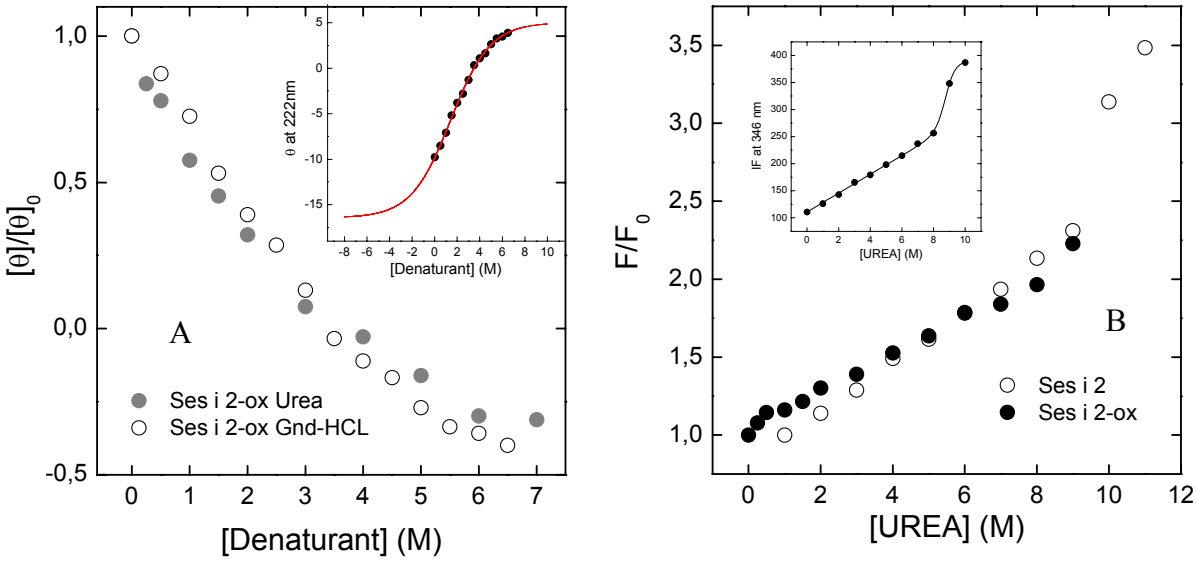

Figure 12. Conformational stability of Ses i 2-ox at pH 2.0. Urea-induced unfolding (●) and guanidinum-unfolding (○) of Ses i 2-ox was monitored by far-UV CD spectroscopy. CD measurements were taken at protein concentration of 12 μM and all spectra were recorded at 25°C. The results were reported as $[\theta]/[\theta]_0$, where $[\theta]_0$ is the ellipticity values of Ses i 2-ox without urea or Gnd-HCl **(A)**. Simulation of urea unfolding curve **(Inset)** Urea-induced unfolding (○) of Ses i 2-ox and Ses i 2 **(●)** was monitored by fluorescence spectroscopy. The emission measurements were taken at protein concentration of 0.3 μM and all spectra were recorded at 25°C. The results were reported as F/F_0, where F_0 is the fluorescence values of Ses i 2-ox or Ses i 2 without urea **(B)**.

In the previous chapter, the structural model of Ses i 2 reveals the presence of a large hydrophobic core that stabilizes the protein in its folded structure. The presence of nine methionines (Figure 13) in the protein core may potentially destabilize the native state, because of the high conformational entropy of the long side-chain. At the same time, the high conformational adaptability and (more importantly) the hydrophobic character of Met-residues (Fauchere and Pliska, 1987) are expected to significantly stabilize the folded structure. Unfolding data of Ses i 2-ox confirms the main role played by Met residues in stabilization of 2S albumin fold. Finally, the extraordinary stability of Ses i 2 cannot only attributed to five disulphide bridges, but it is a consequence of hydrophobic interactions in which Met-residues are fundamental.

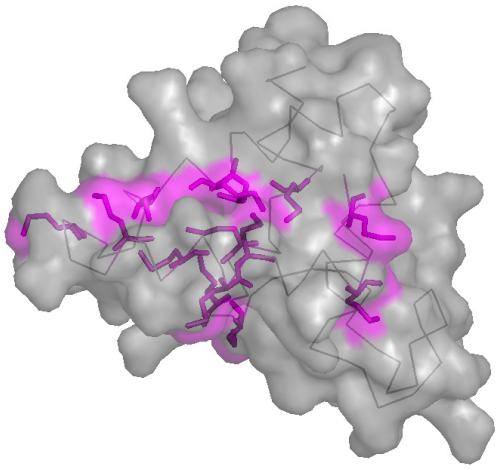

Figure 13. Schematic representation of Met hydrophobic core of Ses i 2.

Limited Proteolysis

Proteolytic enzymes can be effectively used as a probes of protein conformation and dynamics (Fontana et al., 1997). The rationale of this approach resides in the fact that the key parameter dictating proteolysis events is the mobility of the polypeptide chain substrate at the site of proteolysis. Consequently, partly or fully unfolded proteins are rather resistant to deigestion (Picotti and Zambonin, 2004). In the present study, the susceptibility of Ses i 2-ox to digestive and bacterial proteases was evaluated in pseudo-physiological or in other appropriate buffer (see Materials and Methods). For comparative purposes, proteolysis experiments were also conducted, under identical experimental conditions, on alpha-lactalbumin, ovalbumin and BSA (see previous chapter). Proteolytic digests were analysed by RP-HPLC. Results illustrated in Figure 14A clearly indicate that after only 15 min at 37 °C in SGF or SIF, Ses i 2-ox is cleaved by intestinal proteases, while in presence of pepsin, the most important enzyme in stomach, the oxidized protein demonstrated a slight resistance. However, after 60 min of incubation in presence of pepsin the percentage of intact protein is only about 10%. In previous chapter the proteolysis of Ses i 2 has been deeply investigated and the native protein is fully resistant to digestion of pepsin and trypsin, while it is partially digested in the presence of chymotrypsin after 240 min of incubation. The partial peptic digestion of Ses i 2-ox might be correlated to presence of structure in which the cleavage sites are buried from the enzyme action.

Figure 14B shows proteolysis of Ses i 2-ox in the presence of thermolysin in which oxidized protein is dramatically digested.

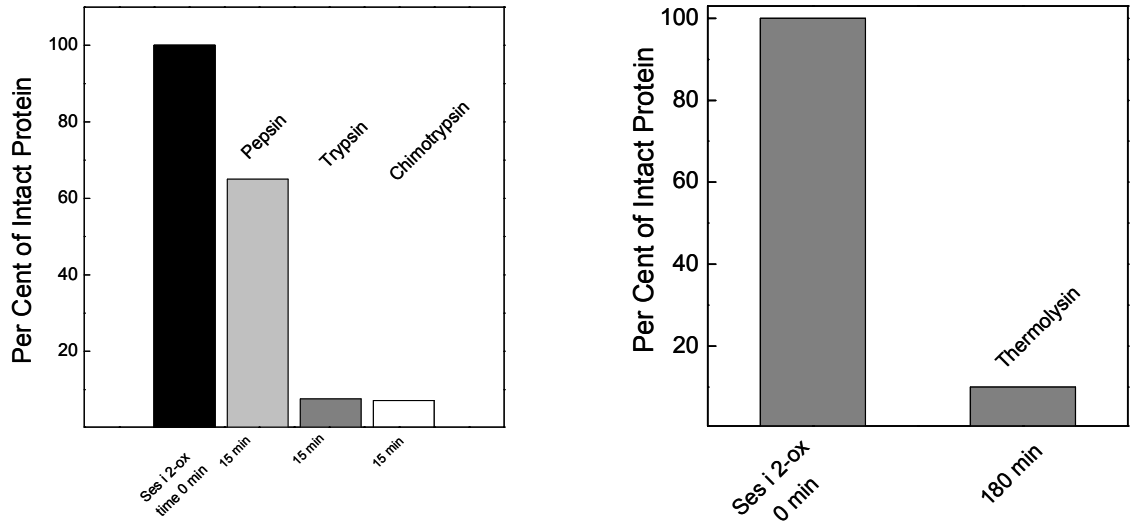

Figure 14. Enzymatic digestion of Ses i 2-ox. Proteolysis with pepsin was conduced in SGF and with the trypsin and chymotrypsin in SIF at 37°C (A). Proteolysis with the thermolysin was conduced at 70 °C in 50 mM Tris-HCl buffer, pH 7.8, containing 5 mM $CaCl_2$ and 10μM $ZnCl_2$ (B).The percent recovery of intact protein was determined as described under Material and Methods.

CONCLUSION

Oxidation is one of the most common chemical degradation pathways, often resulting in structural changes and bioactivity losses (Kim et al., 2001).

In this study we have selectively oxidized 15 Met residues in Ses i 2, 2S albumin from sesame seed, inducing the formation of MetSO. Overall our results demonstrated that Met residues in Ses i 2 are not equally exposed to oxidized agent and then we have observed the formation of intermediates during the oxidative reaction. Obviously, the rate constant of oxidation of single Met residues is related to structure and conformation of Ses i 2, with a strong correlation among temperature and the hydrogen peroxide/Met ratio. These data are in close agreement with a recent works in which at ambient temperature and at physiological temperature, the oxidation rate constants of different methionine residues in a given protein, such as G-CSF (Chu et al., 2004) and human a1-antitrypsin (Griffiths et al., 2002), can differ by an order(s) of magnitude. Chu and co-workers (Chu et al., 2004; Chu and Trout, 2004) explained this observation with the introduction of a new mechanism for methionine oxidation in proteins by hydrogen peroxide. In this mechanism, water molecules play an

important role in stabilizing the transition state. They also found that solvent accessible area is not sufficient to distinguish the disparate oxidation rate constants among methionine residues, as previously thought. Instead, they proposed a new structural quantity, ensemble-average two-shell water coordination number, derived from to correlate well with oxidation rate constants. Next questions in protein oxidation mechanism are how local variations in amino acids near a given methionine site affect oxidation in the absence of structural effects. Pan and co-workers (Pan et al., 2006) observed that in rhG-CSF the oxidation rate constants vary by more 2 orders of magnitude among different methionine residues. They shown that oxidation of methionine residue in protein depends mainly to the relation temperature-conformation and on the basis of these observation three models for the relationship between protein structure and oxidation kinetics have been proposed. In the oxidant-bound intermediate model the oxidation proceeds through an intermediate state which is a complex formed by binding of oxidant and protein after the oxidant molecules becomes close to the sulphur site. Alternatively, the non-oxidant-bound intermediate model depicts the oxidation of sequestered methionine residues in a protein with a complex structure requiring the local structural changes. In the "effective oxidant concentration" model, the oxidant concentration in near the methionine site is not equal to its bulk concentration but rather an effective concentration.

Probably, and this hypothesis is partially confirmed in the next chapter, Ses i 2 presents on protein surface a cluster of methionine residues exposed or partially exposed to solvent, and this cluster is primarily oxidized by hydrogen peroxide. This first oxidation induces an alteration in the protein structure that permits the subsequent oxidative damage in the core of the protein.

Data in this study show that methionine oxidation of Ses i 2 has a significant effect on its structural properties and conformational stability. The far-UV and near-UV CD spectra indicate that a strong alteration of secondary and tertiary structure is a consequence of the oxidation process. In the profiles of dichroic spectra is possible to observe the presence of partial fold and fluorescence emission spectra are in agreement with this observation. Structural and conformational alterations are correlated with a decrease in the stability against chemical denaturant or proteolysis. Methionine carries a hydrophobic side chain containing a sulfur atom. The larger thioether function, indeed, makes the side-chain of Met much more flexible than that of other aliphatic amino acids of comparable size and hydrophobicity (e.g., Ile, Nle, Leu), and the highly polarizable nature of sulfur makes methionine well suited at protein-ligand interfaces, where dispersion forces are important for binding. The conversion of Met to MetSO only slightly increases the side-chain volume (i.e., 6-8 $Å^3$), while

completely abrogating the nucleophilic properties of Met. Notably, oxidation of the sulfur atom converts a hydrophobic amino acid like Met into a polar and partially charged amino acid like MetSO. Besides increasing side-chain polarity, the presence of an oxygen atom on the Met-SO leads to the generation of an asymmetric center and is also expected to restrict the number of side-chain rotamers and alter the local backbone conformational propensities of the polypeptide chain. Overall, our result demonstrate that hydrophobic interactions play a key role in stabilization of Ses i 2.

At inflammation sites, oxidation of protein allergens may represent a critical step in tissue defence, immunospecific response and allergic reactions. Alterations in this pathway in the oxidation step, followed by the proteolytic processing operated by immunocompetent cells might play a key role in inducing allergic response.

3.RESULTS

Cellular Uptake and Role of Oxidative damage in Antigenicity of Ses i 2

Chapter 3.1

Derivatization of Ses i 2 to Track the Uptake in Human Caco-2 Cell Line

INTRODUCTION

The gastrointestinal tract (GI) encounters a wide variety of antigens daily. To maintain homeostasis in the body, the intestinal epithelium works with the gut-associate lymphoid tissue to regulate gut mucosal immune responses. The intestinal epithelium is not just a passive physical barrier serving to exclude the entry of antigens. Proteins derived from dietary sources are able to cross the intestinal epithelium to allow the gastrointestinal tract to fulfil its primary role in nutrient absorption. However, digestion is not an absolute prerequisite for antigen uptake by the intestinal epithelium. A small percentage of dietary proteins can escape digestion in the lumen and enter the systemic circulation. In fact, limited intact antigen entry through the intestinal epithelium might allow the interaction between antigens and immunocompetent cells of the mucosa to elicit antigen specific mucosal immune responses (Gardner M.L., 1988). A clear example of that is given by food allergens. In gut enterocytes plasma membrane represents an impermeable barrier for most macromolecules. Specific transport mechanisms have been evolved in the intestine to facilitate the uptake of various nutrients, including small peptides and macromolecules. For proteins and peptides, four types of uptake mechanism have been recognized. They include 1) highly specific, receptor-mediated endocytosis (RME), 2) adsorptive mediated endocytosis (AME) after binding of molecules to cell surface anionic sites, 3) nonspecific fluid-phase endocytosis of substance dissolved in the extracellular fluid, and 4) carrier-mediated transport for small peptides (Gardner M.L., 1994; Pardridge and Boado, 1991, Say et al., 1998).

With the intent to elucidate the pathway involves in the allergen cell uptake, we have derivatized Ses i 2 with fluoresceine isothiocyante. The technique of fluorescein labeling of antibodies or the detection of antigenic material, histochemical staining, and quantitative antigen-antobody reactions has been used increasingly since Coons and co-workers (Coons et al.,1942) introduced fluorescein isocyante as a labeling agent. Riggs (Riggs J.L.,1957) later substituted the more easily prepared and relatively more stable fluorescein isothiocyanate

(FITC). Fluorescein is the most widely used fluorophore in the biosciences used to attach a fluorescent label to proteins via the amine group; the isothiocyante group reacts with amino terminal and primary amines in protein. FITC has a molecular weight of 389 Da, and excitation and emission wavelengths of 494 nm and 520 nm, respectively, therefore emitting green visible light. This compound is commercially available as isomer I or isomer II, or as a mixture of the two. Isomer I has the thiocyante group on the 4 carbon of the benzene ring, whereas isomer II has the thiocyante on the carbon 5; two isomer are indistinguishable spectrally, either by wavelength or intensity. Popularity of FITC derives from a high extinction coefficient and high quantum yield and from the availability of a variety of chemistries that can be used to conjugate it to functional biomolecules. It is used as a general reporter group in bioassays, as a fluorophore for flow cytometry and fluorescence microscopy and as a donor or acceptor in fluorescence resonance energy transfer studies. The existence of multiple prototropic forms of the molecule also permits its use as a pH probe over a broad pH range. Fluorescein in aqueous solution occurs in cationic, neutral, anionic and dianionic forms making its absorption and fluorescence properties strongly pH dependent. The dianion and monoanion forms of fluorescein are the dominant ground-state species observed under conditions commonly employed in biological studies (Figure 1). However, the dianion dominates the fluorescence emission due to its larger extinction coefficient and quantum yield**.**

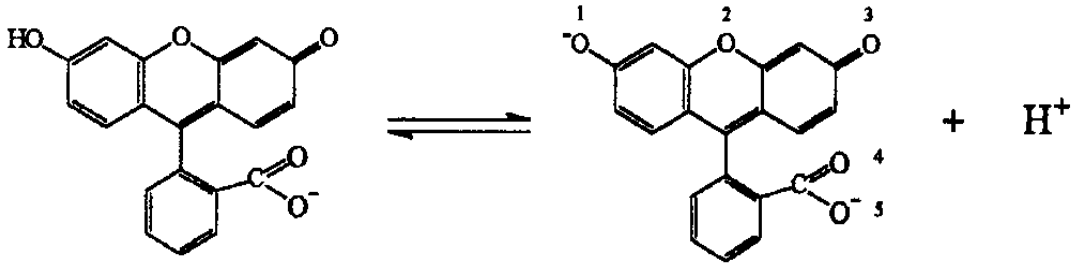

Figure 1. The monoanion and dianion froms of fluorescein. The pKa for the indicated transition is 6.3 in water.

In this work we have derivatized Ses i 2, 2S albumin from sesame seed, with fluorescein isothiocyante with the intent to obtain a fluorescent derivative for cellular uptake studies in Caco-2 cell line. Caco-2, a human colon carcinoma cell line, forms a highly polarized membrane when grown to confluence on plastic dishes and exhibits structural and functional

differentiation patterns characteristic of mature enterocytes (Pinto et al, 1983). Caco-2 cells have been used as an in vitro model in various studies, including characterization of the intracellular sorting or cytosis of proteins (Hyman et al., 1990), because of their close morphological and functional similarity to intestinal epithelium. We have used this system in studies of the Ses i 2 transport mechanisms with the aim to elucidate a possible transport through gut epithelium. This pathway may be crucial in the contact among Ses i 2 allergen and GALT gut associated lymphoid tissue.

The results have been obtained during my stage in the laboratory of Prof. Ignazio Castagliuolo at the Department of Histology, Microbiology and Medical Biotechnologies (University of Padua) in collaboration with Dr. Paola Brun.

MATERIALS AND METHODS

Materials

"White" sesame seeds of Ethiopian origin were kindly supplied by Chelab s.r.l. (Resana, TV, Italy). Fluorescein isothiocyante isomer I was purchased from Sigma (F4274 St. Louis, MO). All salts used were purchased at microselect grade from Sigma. The medium used throughout was DMEM supplemented 2 mM L-glutamine, 1% nonessential amino acids, 1% pyruvate, 50 ug/ml kanamicina, GM-CSF and IL-4 (Gibco, Grand Island, NY) and 10% fetal calf serum (FCS; Gibco, Grand Island, NY).

Methods

Extraction and purification of Ses i 2 from sesame seeds

To 1 g of coarsely ground sesame seeds were added 10 ml of 0.1 M Tris-HCl buffer, pH 8.0, containing 0.2 M NaCl. The mixture was gently stirred at room temperature for 24 h on a model 708 Asal (Milan, Italy) rotating stirred. Thereafter, the suspension was centrifuged at 13000 r.p.m. for 5 min and the supernatant filtered on 0.45-μm durapore filters (Millipore, Badford, MA, USA). The crude extract 1 ml (~ 8 mg) was loaded onto a (1.6 x 60 cm) column (Pharmacia Fine Chemicals), packed in-house with Sephacryl HR-100 and eluted at a flow-rate of 0.8 ml/min in 50 mM Tris-HCl buffer, pH 7.5, containing 1 M NaCl and 10% ethanol (v/v). The absorbance of the effluent was recorded at 280 nm. In a second step, the fractions (1.5-2.0 ml each) eluted from the Sephacryl column, denoted as P5 and found to

correspond to the Ses i 2 allergen, were pooled, lyophilised and further purified by reversed-phase high-performace liquid chromatography (RP-HPLC) on a Grace-Vydac (The Separation Group, Hesperia, CA, USA) C18 semi-preparative column (1 x 25 cm, 5 μm, 300 Å porosity), eluted with a linear acetonitrile-0.1% TFA gradient, at a flow rate of 1.5 ml/min. The material eluted in correspondence of the major chromatographic peak was collected, lyophilised and stored at –20°C for subsequent studies.

Oxidation of Ses i 2 in gastric environment

Aliquots of purified protein (100 μg) were solubilised in 300 μl of SGF (i.e., simulated gastric fluid) at pH 1.2. One solution was gently stirred at room temperature, while other aliquot was incubated at 37°C, and at different time intervals aliquots (10 μg)were taken from 1 h to 24 h. Samples were analysed by RP-HPLC on a Grace-Vydac (The Separation Group, Hesperia, CA, USA) C18 analytic column (4.6 x 150 mm, 5 μm, 300 Å porosity), eluted with a linear acetonitrile-0.1% TFA gradient from 5 to 60% in 15 minutes at a flow rate of 0.8 ml/min. Eluted materials were analysed by mass spectrometry with the intent to individuate a oxidative damage.

In vitro digestion of Ses i 2

Purified Ses i 2 was digested in vitro in simulated gastric fluid in presence of pepsin followed by digestion in presence of pancreatin (Sigma). An aliquot of purified Ses i 2 (80 μg) was suspended in 200 μl of 0.03 M NaCl, the pH was then adjusted at pH 1.3 with HCl. To SGF solution was added pepsin solution with the intent to obtain the final E/S ratio about of 1:20 (w/w). SGF was incubated at 37°C for 2 h. For the intestinal digestion step, the pH was raised to 6.0 with 1M $NaHCO_3$ dropwise, and 16 μl of pancteratin-bile salts mixture (4 mg of panceratin and 12 mg bile extract in 20 ml of 100 mM $NaHCO_3$) was added. The pH was adjusted to pH 7.5 with 1 M NaOH. Intestinal digestion of Ses i 2 was carried out at 37°C and aliquots of digestion mixture were collected at time intervals.

Samples were analysed by RP-HPLC on a Grace-Vydac (The Separation Group, Hesperia, CA, USA) C18 analytic column (4.6 x 150 mm, 5 μm, 300 Å porosity), eluted with a linear acetonitrile-0.1% TFA gradient from 5 to 20% in 10 minutes and from 20% to 60% in 30 min at a flow rate of 0.8 ml/min.

FITC derivatization of Ses i 2. FITC isomer I dissolved in DMSO was added to protein solution in 100 mM sodium carbonate buffer, pH 9.0. Mixture was gently stirred in the dark at

25°C and after 1 h, 3 h or 24 h samples were collected and partially desalted by G-10 Sephadex column. Materials eluted by gel filtration column were analysed by RP-HPLC onto a Grace-Vydac (The Separation Group, Hesperia, CA, USA) C4 pre-column, eluted with a linear acetonitrile-0.078% TFA gradient from 5 to 60% in 15 minutes at a flow rate of 0.8 ml/min. Same protocol was used in presence of 5 M or 4 M Urea. Materials eluted were analysed by mass spectrometry. In the Table 1 were summarized multiple conditions tested.

Table 1.

Ses i 2 concentration (μM)	FITC concentration (μM)	Ratio 2S/FITC (mol/mol)	Urea (M)	Incubation Time (h)
25	500	1:20	-	1, 2, 3
25	2500	1:100	-	1, 3
25	2500	1:100	5	1, 3, 24
25	2500	1:100	4	3, 12
25.5	5100	1:200	4	3,12
25.5	5100	1:200	3	3

Chemical characterization of Ses i 2-[F]

RP-HPLC analysis. Equimolar mixture of Ses i 2 and Ses i 2-[F] was analysed by RP-HPLC on a Grace-Vydac (The Separation Group, Hesperia, CA, USA) C18 analytic column (4.6 x 150 mm, 5 μm, 300 Å porosity), eluted with a linear acetonitrile-0.078% TFA gradient from 5 to 60% in 25 minutes at a flow rate of 0.8 ml/min.

UV-absorption. Ses i 2-[F] was mainly characterised by UV-absorption spectra to determine integrity of FITC conjugate. Spectra were measured on a double beam Model V-630 from Jasco (Tokyo, Japan) spectrophotometer. Aliquot of purified Ses i 2-[F] was solubilised in 5 mM borate-citrate-phosphate at pH 2.0 and by addition of 1 M NaOH the pH buffer was increased to 3.5, 5.5 and 8.0, and UV-spectra were recorded.

Fluorescence. Fluorescence emission spectra were recorded at 25°C on a Jasco spectrofluorimeter Model FP-6500, exciting the sample (1 μM) in 10 mM sodium phosphate pH 7.4 at 495 nm and recording the emission fluorescence in wavelength range 497-700 nm.

Heparin Affinity chromatography.

The interaction among Ses i 2 and heparin was assessed qualitatively by affinity chromatography. A 1.0 ml HiTrap Heparin HP Sepharose column (Amersham Pharmacia Biotech, Piscataway, NJ) was equilibrated with 10 mM sodium phosphate, pH 7.4, in the presence and absence of 150 mM NaCl. Also, the binding studies were carried out in acid condition where HiTrap column was eluted in 10 mM sodium acetate, pH 5.0, in the presence and absence of 150 mM NaCl. Protein (100 μg) was loaded onto the column and eluted with linear gradient of NaCl (0-1M) in the same buffer. Protein elution was monitored by absorbance at 280 nm.

Fluorescence microscopy

Human intestinal Caco-2 cell line were seeded onto 20-mm glass-bottomed slides (Menzel-Glaser, Menzel GmbH, Saarbruckener, Braunschwerg) in 12-well culture plate ($2x10^5$ cells/well) in a humidified 37°C/5% CO_2 incubator for 48 h at 37°C in DMEM (Gibco) supplemented with 10% FBS and 1% penicillin-streptomycin antibiotic solution. Cellular monolayers were then incubated at 37°C for 1 h or 5 h with fresh DMEM without FBS (300 μl) containing 8.5 μM of Ses i 2-[F]. With the intent to elucidate the process on the basis of Ses i 2 cellular uptake Caco-2 cells were pretreated with different endocytic inhibitors (5 μM cytochalasin D, 10 μM nocodazole, nystatine 1 μg/ml and 100 μM EIPA) for 30 min in serum-free DMEM, and then Ses i 2-[F] in fresh serum-free medium containing the same inhibitors were added and cells were incubated 1 h at 37°C. After incubation, cells were washed three time with TBS and fixed with 5% w/v PFA for 10 min. After fixation, cells were washed and glass-bottomed slides were mounted with a 70% v/v glycerol solution onto cover-slides. Green fluorescent images were recorded by the TCS SP2 confocal microscope system (Leica, Wetzlar, Germany). For the Ses i 2-[F] instrument was selected excitation at 488 nm and emission at 500-530 nm. Images was collected and analysed using LCS 2.61 software.

RESULTS AND DISCUSSION

Oxidation of Ses i 2 in gastric environment

In stomach lumen paretial cells, also called oxyntic cells, produced high quantity of acid solution with a pH of 1 to 2, consisting mainly of hydrochloric acid (HCl) and large quantities of potassium chloride and sodium chloride. With the aim to investigate the possible oxidation of Ses i 2 in the gastric environment with the consequent formation of Ses i 2-ox in stomach environment, we have carried out the incubation of Ses i 2 in SGF buffer. In both cases, (Figure 1), chromatographic profiles show a single-symmetric peak and changes in the retention time were not observed. In these conditions our results suggest that Ses i 2 is not subjected to oxidation. With the intent to confirm previous results, eluted materials were analysed by mass spectrometry, and deconvoluted mass to charge spectra show a mass value of Ses i 2 of 11727.2 ± 0.6 Da.

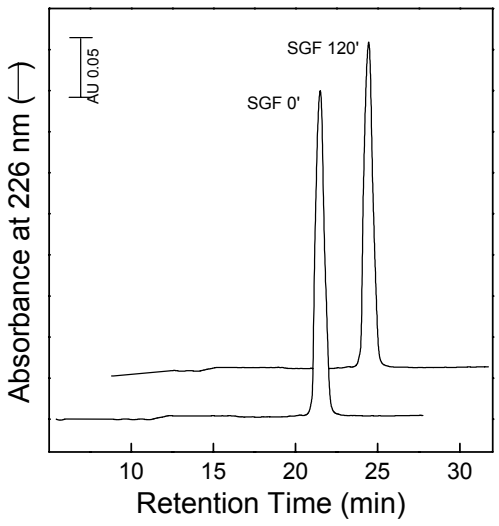

Figure 1. RP-HPLC analysis of the Ses i 2 oxidation in SGF at pH 1.2. An aliquot (10 ug) was loaded in onto Vydac C-18 column (4.6 x 250 mm, 5 μm) and elution was performed at flow rate of 0.8 ml/min with a linear 0.1% (v/v)-TFA-acetonitrile gradient.

This experiment allowed us to confirm that in gastric environment the oxidative damage is abrogated and therefore non-oxidized Ses i 2 is the main form of allergen in the gut.

In vitro digestion of Ses i 2

2S albumin allergens from different species have been reported to be highly resistant to in vitro digestion (Moreno et al., 2005; Astwood et al., 1996 and Murtagh et al., 2003). In

good agreement with these findings, our results demonstrated the extraordinary resistance to proteolysis in gastrointestinal environment (see previous chapter). At 90 min-incubation in presence of pancreatin-bile salts mixture Ses i 2 presents partial cleavage demonstrated by the chromatographic plot in which are two minor chromatographic peaks have been identified such as nicked forms of Ses i 2 (see previous chapter). Our pancretin-digestive model is validated by digestion of minor allergen alpha-lactalbumin (Figure 2B).

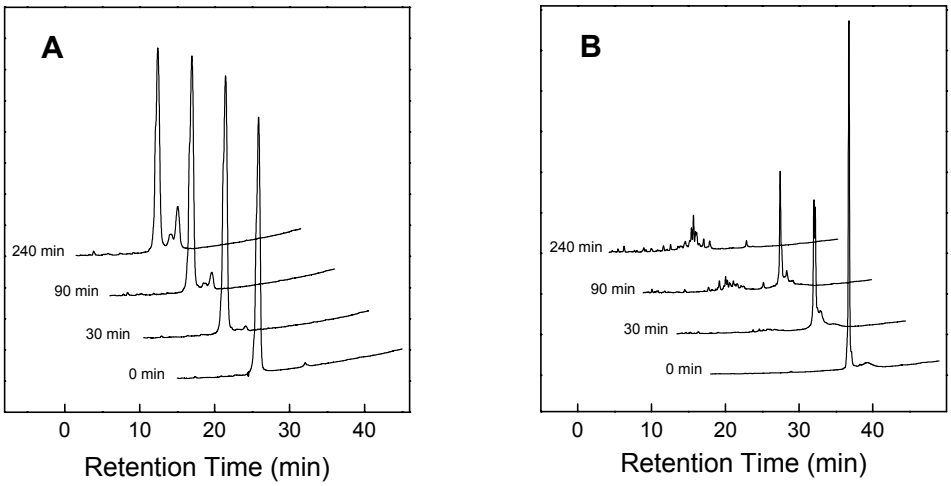

Figure 2. RP-HPLC analysis of Ses i 2 (A) and alpha-lactalbumin (B) proteolysis in presence of pancreatin bile salts mixture. An aliquot (10 ug) was loaded in onto Vydac C-18 column (4.6 x 250 mm, 5 μm) and elution was performed at flow rate of 0.8 ml/min with a linear 0.1% (v/v)-TFA-acetonitrile gradient.

These results, obtained with a porcine mixture of intestinal fluid added with bile salt mixture, confirm the high resistance to proteolysis of major allergen from sesame seed. These findings suggest that Ses i 2 might be absorbed in intact form in intestinal epithelial barrier.

Derivatization with fluorescein isothiocyanate (FITC)

Ses i 2 derivatization with fluorescent label as FITC was conducted using many different conditions with the intent to maximise the reaction yield. The conjugation reaction may be described as an electrophilic attack of a positively charged isothiocyanate group on the protein at the amino group of highest electron availability (Klugerman M.R., 1966). Ses i 2 presents a single Lys residue in position 73 and both N-terminal of two subunits are blocked by formation of pyroglutamic acid. Our mass data are in close agreement with these features,

in fact derivatization of Ses i 2 permits the formation of single FITC derivative in position 73 (Figure 3).

Generally, the protein is labeled using a carbonate buffer at pH 9.0, in this condition amino group in side chain of Lys (ε-amine) is deprotonated (pKa of ε-amine is about 10.4).

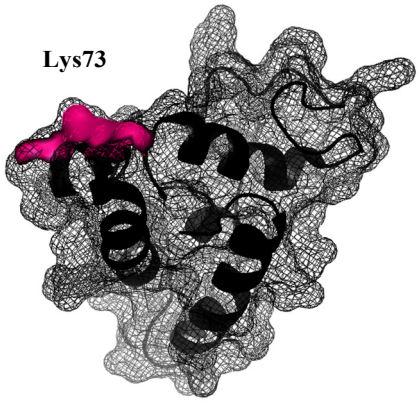

Figure 3. Schematic representation of Ses i 2 and Lys73.

Initially, Ses i 2 was solubilised at concentration of 25 μM in 0.2 M carbonate buffer pH 9.0 and the FITC mixture in DMSO was added to this solution at final concentration of 500 μM. Mixture was incubated in the dark at 25°C and samples was collected at time intervals (1 h, 2 h, 3 h and 24 h). Aliquots were desalted onto G-10 Sephadex column then analysed by RP-HPLC and mass spectrometry. After 3 h-incubation RP-HPLC profile (Figure 4A) presents three peaks that analysed by mass spectrometry giving a mass value in agreement with the molecular weight of 2s albumin (P1), Ses i 2-[F] (P2) and FITC (P3) (11726.7 ± 0.6 Da, 12115.5 ± 0.3 Da and 389.4 ± 0.2 Da, respectively). Changes in the chromatographic plot are not detected after 24 h of incubation at 25°C. These results confirm the low yield of derivatization in these experimental conditions, probably data are due to the localization of Lys73 in which ε-amine may be partially exposed to solvent. With the intent to increase yielding of conjugation in aqueous buffer the 2s/FITC ratio was increased to 1:100 (mol/mol) at 37°C, and in these conditions obtained data show a weak rise in the derivatization of Ses i 2 (data not shown). In aqueous solution FITC is degraded to form a less fluorescent aminofluorescein derivative, a study of Felton and McMillion (Felton and McMillion, 1963) has demonstrated that the reaction of FITC with aminofluorescein to form the thiourea derivative competes with the Lys-derivatization, and in this way FITC is subtracted to reaction environment. With the aim to induce a strong increment in protein FITC conjugation, Ses i 2 was solubilised in 0.2 M sodium carbonate, pH 9.0, containing 5 M urea (Figure 4B). Urea is a chaotropic agent that promotes unfolding by both indirect and direct mechanisms.

Direct urea interactions consisted of hydrogen bonding to the polar moieties of the protein, particularly peptide groups, leading to screening of intramolecular hydrogen bonds. Solvation of the hydrophobic core proceeded via the influx of water molecules, then urea. Urea also promoted protein unfolding in an indirect manner by altering water structure and dynamics, as also occurs on the introduction of nonpolar groups to water, thereby diminishing the hydrophobic effect and facilitating the exposure of the hydrophobic core residues (Bennion and Daggett, 2003). In the Ses i 2 derivatization, urea has two main functions such as render more flexible protein structure and then serves as organic co-solvent. In the presence of 5 M urea at ratio 1:100 (mol/mol) 2S/FITC, the conjugation yield is higher than the data collected in aqueous solution, however the percentage of Ses i 2-[F] is about 15% of total protein concentration (Figure 4B). A possible explanation of this result is correlated to the urea structure that presents two primary amines. At light of these considerations Ses i 2 was incubated in the presence of 4 M urea, pH 9.0 at molar ratio 1:100 and 1:200 2S/FITC, surprisingly maximum yield of derivatization (about 30%) is obtained in the presence of 4 M urea after 3 h of incubation at molar ratio 1:200 Ses i 2/FITC. Mixture was desalted onto Sephadex G-10 column (Figure 4C), then eluted material was analysed by RP-HPLC (Figure 4D). Our results confirm that urea has a dramatic influence in the Ses i 2 conjugation, probably this function is due to co-solvent character of this chaotropic agent.

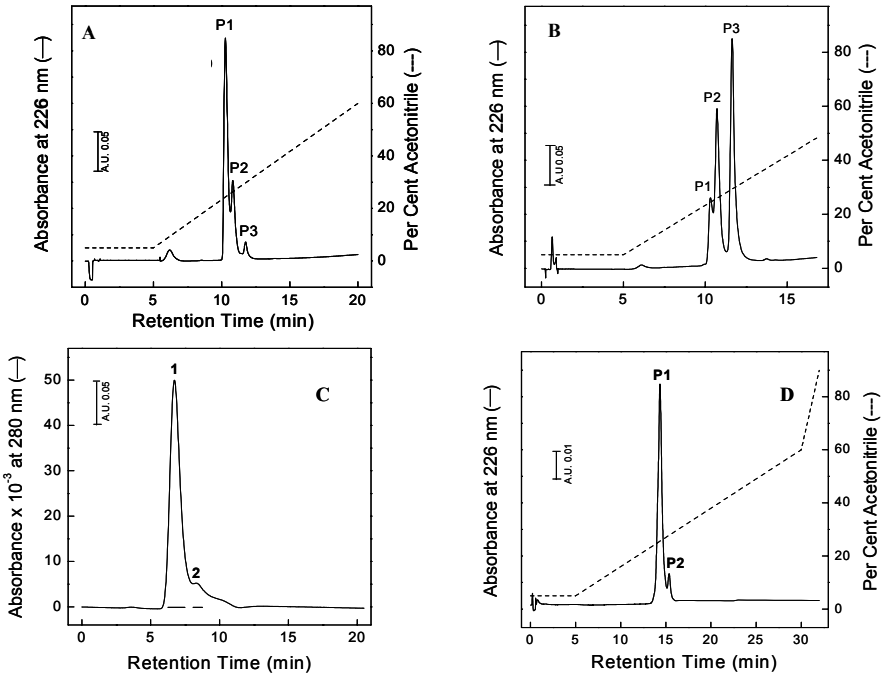

Figure 4. RP-HPLC analysis Ses i 2 derivatization. (A) Ses i 2/FITC ratio 1:20 (mol/mol). (B) Ses i 2/FITC ratio 1:100 (mol/mol) 5 M urea. An aliquot (10 ug) was loaded in onto Vydac C-18 column (4.6 x 250 mm, 5 μm) and elution was performed at flow rate of 0.8 ml/min with a linear 0.1% (v/v)-TFA-acetonitrile gradient (----).**(C) SEC of Ses i 2-FITC reaction mixture ratio 2S/FITC 1:200 (mol/mol) 4M urea. (D) RP-HPLC analysis of material eluted in 1 by SEC.**

Chemical characterisation of Ses i 2-[F]

Ses i 2 FITC derivative has a mass value of 12115 ± 0.6 Da (Figure 5A), this data is in close agreement with the conjugation among FITC dye and Lys73 in Ses i 2. Mass data is not a prove to the integrity of conjugate dye, with the intent to confirm the existence of the unmodified carboxyl group in position 2 of FITC dye, the UV absorption spectra of Ses i 2-[F] were recorded in the pH range 2-8 in borate/citrate/phosphate buffer. The spectroscopic properties of FITC are due to enol-keto tautomerism involving the carboxyl group and one of the two phenolic groups (Weber et al., 1998). Ses i 2-[F] shows high pH dependence of the UV absorption spectra, this feature is due the different protolytic forms of the dye (Figure 5B). Spectra are in agreement with the presence of four protolytic forms, which have been identified as the cation, neutral species, anion and dianion. The dianion has its main absorption peak at 490 nm (76 900 M^{-1} cm^{-1}), with a shoulder around 475 nm. It has very weak absorption in the region 350-440 nm, and distinct absorption peaks in the UV region at 322 nm (9500 $M^{-1}cm^{-1}$), 283 (14 400 $M^{-1}cm^{-1}$) and 239 (43 000 $M^{-1}cm^{-1}$) nm. The anion has somewhat weaker absorption in the visible region with peaks at 472 nm and 453 nm of roughly the same molar absorptivity (29 000 $M^{-1}cm^{-1}$). It absorbs weakly in the near UV region, and has peaks at 310 nm (7000 $M^{-1}cm^{-1}$) and 273 (17000 $M^{-1}cm^{-1}$) nm. The neutral species has by far lowest absorption in the visible region, with a maximum at 434 nm (11 000 $M^{-1}cm^{-1}$) and a side maximum at 475 nm (3600 $M^{-1}cm^{-1}$). Its absorption below 400 nm is very small (Sjöback et al, 1995). All forms have rather high molar absorptivities being $\varepsilon_{437}^{FH_3^1}$ = 53 000, $\varepsilon_{434}^{FH_2}$ = 11 000, $\varepsilon_{453}^{FH^-}$ = 29 000 (ε_{472}^{FH} = 29 000) and ε_{490}^{F2} = 76 900 M^{-1} cm^{-1} for the cation, neutral form, anion and dianion, respectively. The protolytic constants relating the chemical activities (which at low ionic strength equal concentrations) of the cation, neutral form, anion and dianion are pK_1 = 2.08, pK_2 = 4.31, and pK_3 = 6.43 (Sjöback et al, 1995). In an acidic solution , the carboxyl group forms a cyclic “lactoid” ring that prevents the tautomeric shift and thus inhibits fluorescence. This ring is disrupted in alkaline solutions, with the result that resonance is enhanced and fluorescence intensified. In figure 5B are reported UV-vis spectra of Ses i 2-[F] at pH 2.0, pH 3.5, pH 5.5 and pH 8.0, in which are evident the usual profile of cation, neutral, anion and dianion forms of FITC. These data are a prove of integrity of carboxyl group in position 2 of FITC. Ses i 2-[F] spectrum at pH 8.0 shows maximal absopitivity at 492 nm typical of FITC-protein conjugate. Since the confocal images were acquired at physiological pH the emission spectrum as well as UV spectra of FITC changed at function of pH. The dianion has the most intense fluorescence with a quantum yield of 0.93 but also the anion shows considerable fluorescence with a quantum

yield of 0.37 (Sjöback et al, 1995). The neutral and cationic species are upon excitation converted into the anion and fluoresce with quantum yields of about 0.30 and 0.18, respectively (Klonisl et al., 1998). With the aim to observe the features of emission spectrum of Ses i 2-[F] at neutral pH, fluorescence spectra of Ses i 2-[F] was recorded at pH 7.4, sample was exited at 495 nm and fluorescence spectrum shows a λ_{max}= 518 nm, in strong relation with fluorescence properties of monoanion and dianion forms of FITC (Figure 5C).

Finally, an equimolar mixture of Ses i 2 and Ses i 2-[F] was analysed by RP-HPLC on C18 analytical column. Chromatographic profile shows a increase of the retention time of Ses i 2-[F], this observation is in close agreement with the introduction in the protein structure of a hydrophobic group by a stable thiocarbamido bond (Figure 5D).

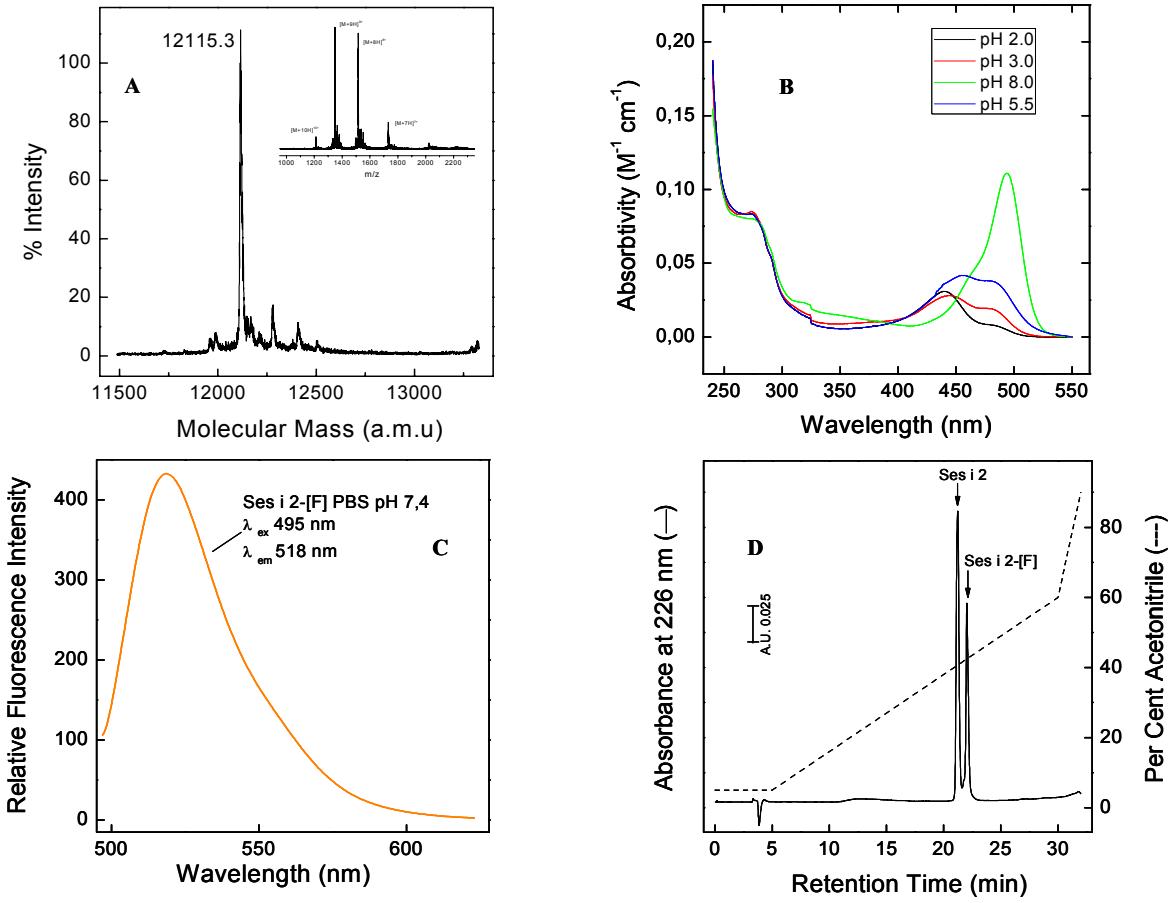

Figure 5. Deconvolute and m/z ESI-TOF mass spectra of Ses i 2-[F] (A). Uv/Vis spectra of Ses i 2-[F] from pH 2.0 to pH 8.0 (B). Fluorescence emission spectra of Ses i 2-[F] at pH 7.4 (C). RP-HPLC analysis of equimolar mixture of Ses i 2/Ses i 2-[F] (D).

Heparin Affinity chromatography

Previously, Ses i 2 has demonstrate an uncommon stability to the digestive protease as pepsin, chymotrypsin and trypsin in the gastointestinal environment, therefore in gut is possible that Ses i 2 can be absorbed in intact form through cellular uptake. The first barrier to efficient and controlled intracellular delivery is the plasma membrane which prevents direct translocation of macromolecules. It is therefore highly remarkable that some proteins and peptides possess the ability to cross this border and reach the cytoplasm. Initially, the import of these cell-penetrating peptides alike, is considered to occur by direct permeation of the plasma membrane (Prochiantz A., 2000). More recently, it is shown that endocytosis plays a major role in the import of macromolecule into the a cell (Schmidt et al, 2009).In these pathway non specific receptor has been implicated in process, and in some cases, the initial association with the plasma membrane is attributed to multivalent interactions with cell surface heparan sulfate proteoglycans. The attachment of protein to cell surface is mainly governed by electrostatic interactions between proteoglycans with basic amino acids mediated by the negatively charged sulfate and carboxyl groups of the GAG side chains. Cell surface heparan sulfate proteoglycans (HSPGs) are composed of a protein core with covalently attached HS chains generated through a process initiated by polymerization of glucuronic acid and *N*-acetylglucosamine units in alternating sequence (Esko et al., 2001). This backbone undergoes a series of modifications that give a large number of distinct HS species that appear to be cell/tissue-specific. Numerous methods are available for analyzing proteoglycans (GAG)-protein interactions, and a common method involves affinity fractionation of proteins on Sepharose columns containing covalently linked GAG chains, usually heparin. The bound proteins are eluted with different concentrations of NaCl, and the concentration required for elution is generally proportional to the K_d. High affinity interactions require at least 1 M NaCl to displace bound ligand. Proteins with medium-low affinity (10^{-4}–10^{-6} M) either do not bind under normal conditions (0.15 M NaCl) or require 0.3–0.5 M NaCl to elute. This method is based on the assumption that GAG-protein interaction is entirely ionic, which may not be entirely correct. Ses i 2 shows a extraordinary high percentage (~14%) of Arg residues and with the intent to study the possible interaction toward HSPGs, Ses i 2 was loaded onto HiTrap heparin sepharose column at different salt concentrations and pH conditions. Ses i 2 in the presence of 150 mM NaCl is immediately eluted, whereas in the absence of physiologic concentration of NaCl Ses i 2 is eluted at about 290 mM NaCl (Table 1). These results demonstrated that Ses i 2 engages a weak interaction with heparin. In the site of allergic response the mast cells and neutrophile degranulation might induce a inflammatory state

associated with a decrease of pH (Vetter et al., 2006), to assess whether at pH 5.0 protein-heparin interaction is favourited an aliquot of Ses i 2 was loaded onto HiTrap heparin and eluted in 10 mM sodium acetate, pH 5.0, with a linear gradient of NaCl. Interestingly, in the binding studies at pH 5.0, were used to mimic the inflammation tissue, Ses i 2 has different behaviour than at pH 7.4 demonstrating a medium-high affinity to heparin. At acidic pH, the presence of 150 mM NaCl in the buffer prior to generate linear salt gradient does not influence the Ses i 2-heparin interaction. In both cases Ses i 2 is eluted at about 600 mM NaCl.

Table 1 Binding Heparin HiTrap Heparin Sepharose

	[NaCl]	**Conductivity (mS/cm)**
Ses i 2 10 mM sodium phosphate pH 7.4	297 mM	26.5
Ses i 2 10 mM sodium acetate pH 5.0	600 mM	65
Ses i 2 10 mM sodium acetate pH 5.0 150 mM NaCl	550 mM	65.8

Ses i 2 is characterised by the presence of positive and negative charged clusters. The distribution of charged amino acids in Ses i 2 is highly asymmetric, with a large positively charged patch spanning the equatorial region of the molecule (see Figure 13 in previous chapter), and two relatively small negative patches, cluster I and cluster II. Cluster I- is formed by acidic residues from different parts of the molecule (i.e, Glu22, Glu79, and Glu119), whereas cluster II- comprises three acidic residues all in helix II (i.e., Glu60, Glu64, and Asp71). At pH 5.0, negative charges on surface are partially quenched allowing interaction with heparin, these observations strongly suggest that the presence of negative charges is deleterious for functional binding among Ses i 2 and heparin/HSPG, while positive charges facilitate this interaction. Since R has the highest pKa (12.48) and therefore the strongest interaction, accordingly, due to their lower pKa values (10.79 and 6.04, respectively), K and H seem to play a less important role compared to that of R. These considerations allow to assert that Ses i 2-heparin interaction is strongly dependent on protein structure. In 1991 Alan Cardin and Herschel Weintraub proposed that typical heparin-binding sites had the sequence XBBXBX or XBBBXXBX, where B is lysine or arginine and X is any other amino acid. Ses i 2 does not present these motives in its sequence, however it should be

obvious that only some of the basic residues in these sequences could participate in GAG binding, the actual number being determined by whether the peptide sequence exists as an α-helix or a β-sheet. It is likely that binding involves multiple protein segments that juxtapose positively charged residues into a three-dimensional turn-rich recognition site the basic residues to occur every third or fourth position along the helix in order to align with an oligosaccharide. Ses i 2 is not a typical heparin-binding protein and our data demonstrate low affinity in binding studies to support this consideration. However, Ses i 2, at acidic pH, typical of inflamed tissues, shows a medium-high affinity to heparin, thus this interaction can modulate the cellular uptake in gut system of atopic patient. Finally, this behaviour indicate a strong influence of "surface charged" amino acid as well as protein structure in protein-GAG interaction.

Fluorescence microscopy

Ses i 2 presents a high stability to digestive enzymes, this characteristic may be play a pivotal role in allergic response. The epithelial barrier of the gut represents a unique environment that is exposed throughout the life to a limitless variety of antigens and its main task is to provide an efficient barrier against pathogens and macromolecules. This is mainly achieved by columnar epithelial cells joined by tight junction that allow passage of water and ions but provide a mechanical barrier to the vast majority of macromolecules (Chambers et al., 2004). Small quantities of intact proteins may be absorbed, normal absorption probably occurs predominantly by transecellular endocytosis with some possible contribution by a route between cells; increased net entry of protein to the lamina propria may reflect (a) increased paracellular passage (intercellular), (b) increased transcellular passage, and/or (c) decreased lysosomal proteolysis (Gardner M.L.,1994).

Cellular uptake of Ses i 2-[F] was studied in fixed Caco-2 by fluorescence microscopy. Caco-2, a human colon carcinoma cell line, forms a highly polarized membrane when grown to confluence on plastic dishes and exhibits structural and functional differentiation patterns characteristic of mature enterocytes (Pinto et al., 1983). Caco-2 cells have been used as an in vitro model in various studies, including characterization of the intracellular sorting or cytosis of proteins (Matter et al., 1990), because of their close morphological and functional similarity to intestinal epithelium. We have also used this system in studies of the carrier-mediated transport mechanism (Ogihara T. et al., 1994).

Images of time dependent internalization into Caco-2 cells of Ses i 2 labeled with the fluorescent probe FITC were selected after 1 h or 5 h of incubation. As shown in Figure 7A at

1 h-incubation, significant fluorescence appeared within the cells, excluding the nuclei, and the granular staining indicated the sequestration of Ses i 2-[F] within endocytotic vesicle. After 5 h of incubation (Figure 7B), distribution of peptide is diffuse on cytoplasm of cells, simultaneously, the cell population become very heterogeneous with respect to protein uptake. Some cells are fluorescent to the point of detection range. As shown in Figure 7 other cells are characterised by a moderate uptake, and finally, some cells exhibited only weak intracellular fluorescence. This heterogeneity in the level of the cell population is reflected by a heterogeneity in the distribution of fluorescence on subcellular level. Duchardt and co-workers (Duchardt et al., 2007) reported a correlation between protein concentration and the increasing number of cells exhibited a clear enrichment of protein in the cytoplasm, with little vesicular fluorescence. However, recent reports shed doubt on these data (Kosuge et al., 2008), and attributing the diffuse localization in cytoplasm of labelled protein to an artifacts. These behaviour is a consequence of fixation on the microscopic observation of the internalized proteins.

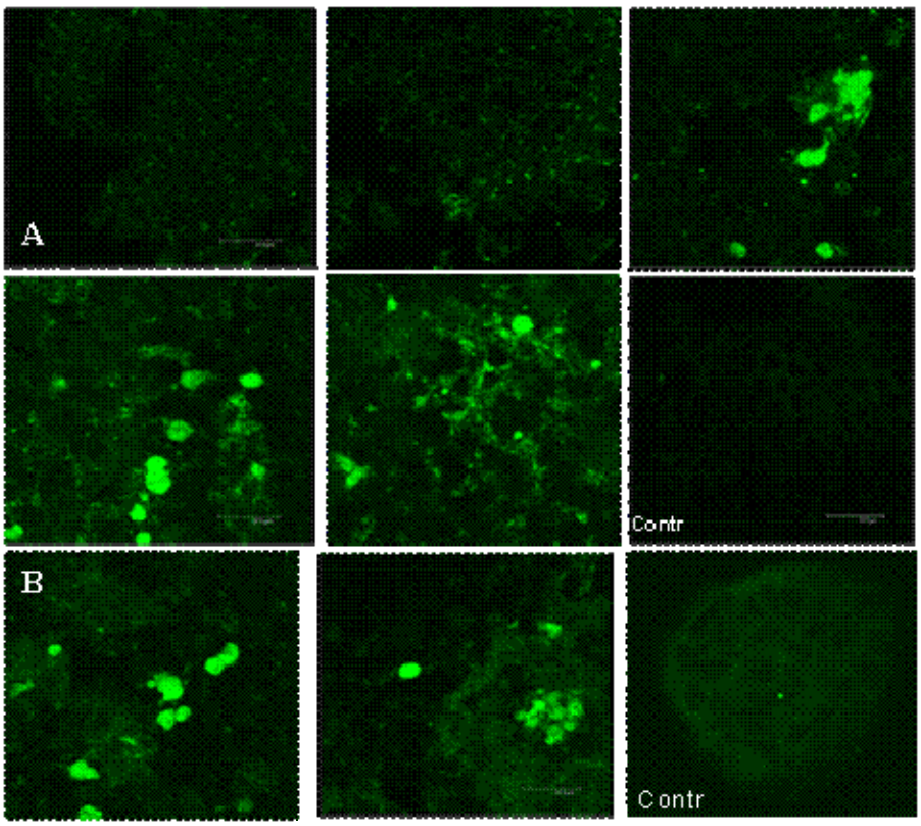

Figure 7. Analysis of the cellular uptake of Ses i 2-[F]. Confocal microscopy of Caco-2 cells treated with 8.5 μM labelled protein at 1 h of incubation **(A)** or at 5 h of incubation **(B)**.

Since little is known about the effect of IgG immune complexes on antigen uptake by the intestinal epithelial cells in humans (So et al., 2000), we studied the effect of complexes Ses i 2-[F] with IgG anti-Ses i 2 on uptake by Caco-2. Ses i 2-[F] was incubated for 15 min at 37°C with serum of mice immunized with Ses i 2, and after incubation protein/serum solution was diluted in culture medium. After 1h of incubation, not significant fluorescence appeared within the cells as a consequence of abolishing of cellular uptake (Figure 8). Insoluble and soluble immune complexes are poorly endocytosed and this observation is not in agreement with the behaviour of monocytes (professional APC) which are capable of taking up insoluble immune complexes (So et al., 2000). Several differences were noted between monocytes and intestinal epithelial cells (So et al., 2000); opsonisation promotes antigen uptake in monocytes, in contrast, insoluble IgG immune complexes impede antigen uptake by Caco-2 cell line, while soluble Ses i 2 is taken up. These data suggest that insoluble immune complexes formed in the lumen are excluded from uptake by the intestinal epithelium and only soluble antigens can be sampled by intestinal epithelial cells. Data suggest that antigen uptake in Caco-2 cell line is a stable process, although the physical form (soluble vs insoluble) of the antigen appears to play a central role (Figure 8).

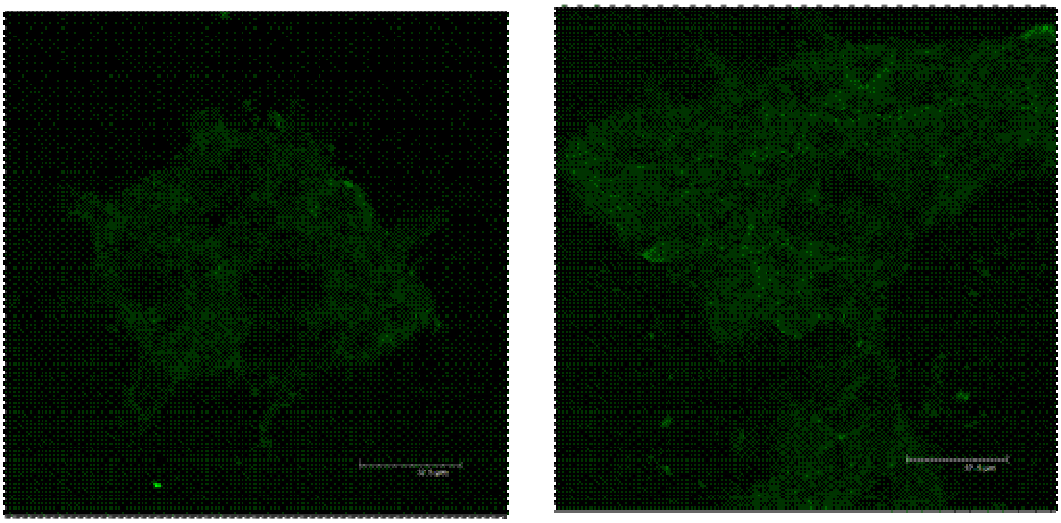

Figure 8. Analysis of the cellular uptake of Ses i 2-[F] incubated with serum of mice immunized with Ses i 2.

Results suggest that a non-specific fluid-phase endocytosis by Caco-2 is the main process involved in Ses i 2 uptake. And this pathway appears to be a slow and stable process. These findings demonstrate that the uptake of soluble protein via fluid-phase endocytosis by Caco-2 is tightly regulated, and Caco-2 cells show nonphagocytic processing and only take up soluble antigens by fluid-phase endocytosis. Endocytosis is a complex mechanism that involves

different pathways and a large network of protein-protein and protein-lipid interactions. The firs and the best characterised pathway is clathrin-dependent endocytosis., which starts on the plasma membrane with the formation of clahtrin-coated invaginations that pinch off to make up clathrin-coated vesicle. Less defined are the non-classical, clathrin-independent pathways, among which is caveolae-mediated endocytosis. Caveolae are flask-shaped, small invaginations in the plasma membrane that constitute a subclass of detergent-resistant membrane domains enriched in cholesterol and sphingolipids that are called lipid rafts, whereas proteins internalized by the clathrin pathway are excluded from caveolae process (Fittipaldi et al, 2003). With the intent to elucidate the internalization mechanism by which Ses i 2 is taken by intestinal lumen Caco-2 monolayers were incubated in the presence of endocytotic inhibitors such as nystatin, citochalasin D (Cyt. D), nocodazole and ethylisopropylamiloride (EIPA) (Swanson and Watts, 1995).

In the presence of nystatin, confocal images (Figure 9A) are not characterised by a decrease in cellular uptake of fluoresceinated Ses i 2. Nystatin induces the distruption of lipid rafts microdomains (caveolin dependent endocytic process) by sequestration of cholesterol. Incubation of Caco-2 cells in the presence of nocodazole, microtubule depolymerizing agent, shows a slight decrease in cellular uptake (Figure 9B). Data suggest that caveolae process is not involved in Ses i 2 uptake, this consideration is in close agreement with the notion that the velocity at which caveolae endocytosis proceeds is remarkably slower than that of clahtrin-dependent uptake. In the presence of citochalasin D (Cyt D), which is known to induce depolymerisation of F-actin, the clathrin-mediated endocytosis is hardly inhibited, while lipid rafts and macropinocytosis is weakly inhibited. Confocal images (Figure 9C) show a high degree of fluorescence in cell, but confocal analysis revealed modifications in a cell morphology induced by Cys D. (Nakase at al., 2004). Images suggest that the clahtrin-mediated endocytosis may not play a central role in Ses i 2 uptake. A third endocytic process is macropinocytosis a fluid-phase endocytosis in which macropinosomes are development from cell surface ruffles that close back against the plasma membrane to form a intracellular vesicle, and are heterogeneous in size, sometimes as large as 5 μm diameter. This process is distinguish from endocytotic processes involving smaller, chalthrin-coated or uncoated vesicles. Membrane ruffling and macropinocytosis can be inhibited by amiloride and its more potent analogues, such as dimethyl amiloride (Gekle et al., 1999), which inhibit the Na^+/H^+ exchange protein in the plasma membrane, and these agents modulate cytoplasmic pH, which also inhibits clathrin-mediated endocytic activity. However, as reported in several articles clathrin-mediated uptake of proteins such as EGF continues under conditions where

macropinocytosis is inhibited suggesting that ruffling and macropinocytosis may be acutely sensitive to cytosolic acidification (Swanson and Watt, 1995). Caco-2 cells were incubated for 1 h at 37 °C in presence of EIPA strong and specific inhibitor of maropinocytosis.

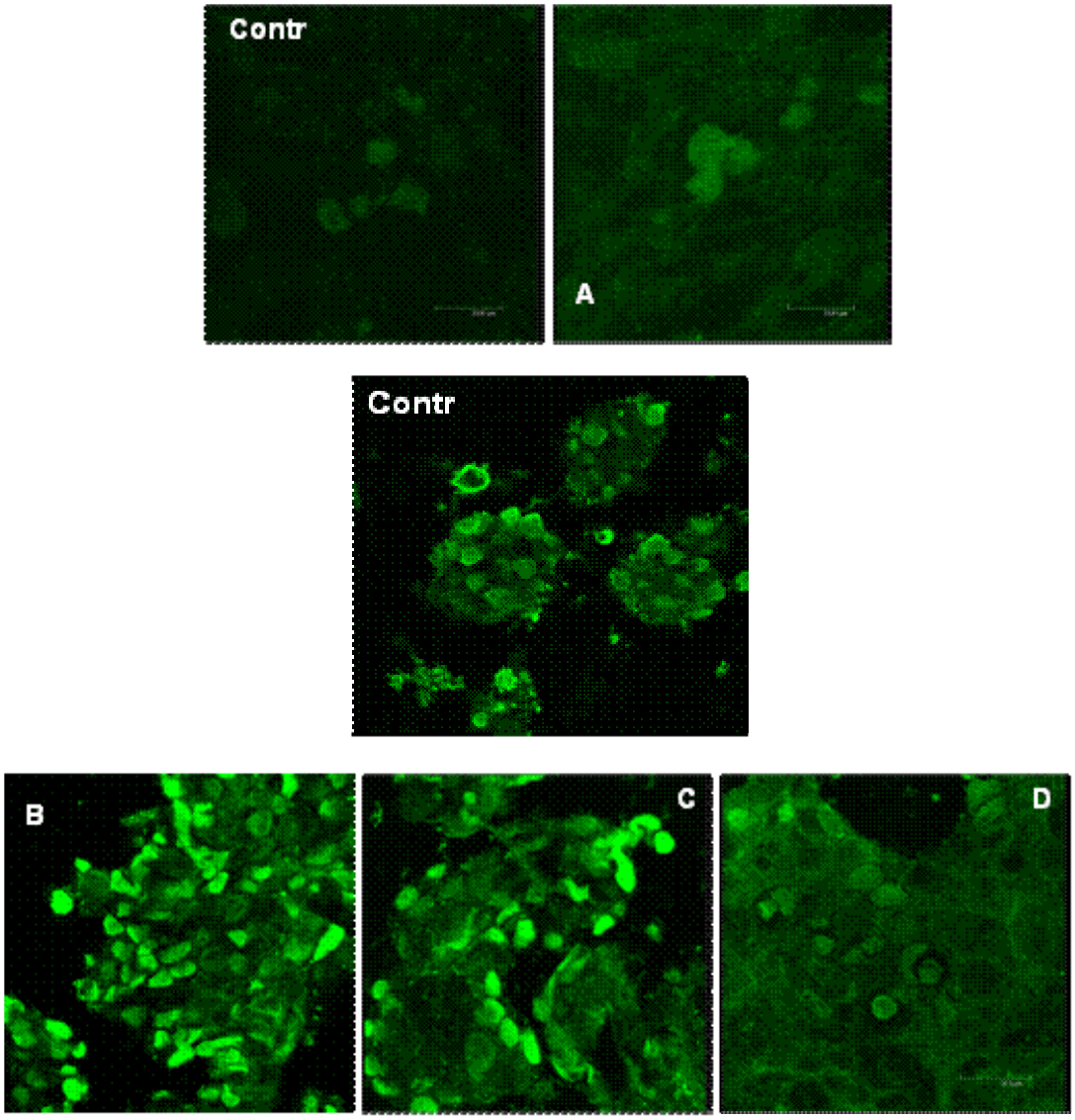

Figure 9. Analysis of the cellular uptake of Ses i 2-[F] incubated with nystatine (A) at 5 h incubation. Analysis of the cellular uptake of Ses i 2-[F] incubated with nocodazole (B), cytochalasin D (C), EIPA (D) at 1h of incubation.

As shown in Figure 9D EIPA induces a inhibition of Ses i 2-[F] uptake in agreement with the hypothesis that macropinocystosis is involved in the Ses i 2 internalization.

CONCLUSION

Our results confirm that oxidized Ses i 2 is not produced in gastric environment and allergen moves to intestinal epithelial monolayer in a non-oxidized form. Thus, to study the internalization mechanism of Ses i 2, protein was labeled with fluorescein isothicyante (FITC). Briefly, purified Ses i 2 was subjected to derivatization with common and widely used dye as FITC with the aim to obtain Ses i 2-[F] conjugate. Conjugation was conducted at different molar excess of FITC and in the presence of different buffer. Our results show a strong dependence of the derivatization yield to urea concentration, probably this chaotropic agent has dual effect as a co-solvent, also, urea may induce more flexibility in the protein structure. In presence of 200-fold molar excess of FITC at 4 M urea the conjugation yield is about 30% to initial protein concentration. Ses i 2-[F] was characterised to prove the integrity of carboxyl group in position 2 of FITC, UV-vis absorption spectra of FITC-protein conjugate are pH dependent as a consequence of different protolytic forms of FITC. UV-vis spectra of Ses i 2-[F] in the pH range 2-8 confirmed the integrity of 2S derivative. Ses i 2-[F] was used to confocal studies with the intent to identify cellular uptake mechanism in which Ses i 2 is involved in intestinal epithelium. Previously, heparin binding studies were conducted to elucidate the possible involvement of HSPG in the endocytosis mechanism, Ses i 2 is not typical heparin binding protein, but it presents a high number of arginine resiudes in amino acid sequence. Ses i 2, at pH 7.4, shows mild heparin affinity in absence of ionic strength in agreement with a non-specific interactions. At pH 5.0 Ses i 2 demonstrates a medium affinity and this result is important considering acidic pH present in inflammation site of allergic response. Caco-2 cell line is a specific model of the intestinal monolayer epithelium to conduce in vitro study of the endocytic mechanisms involved in Ses i 2 uptake in lumen of gut. Confocal images, in the presence or in the absence of endocytosis inhibitors, and heparin binding studies reveal a probably involvement of macropinocytosis in allergen uptake. Finally, is necessary to consider the presence of M cell in Peyer's patches of gut, this cells are significantly different from columnar ephitelial cells with a unique function to permit direct access of lumina antigens to subepithelial lymphocytes. These cells might be contribute to direct traslocation of Ses i 2 in lamina propria.

Chapter 3.2

Oxidative Damage and Modulation of Dendritic Cells Stimulatory Activity

INTRODUCTION

Specific plant protein families are involved in many cases of allergy to food products. Toward this small and specific group of proteins, there appears to be a breakdown in tolerance that is manifested by an immune response that causes a direct hypersensitivity reaction. In this context, the cross-linking of mast cell-bound IgE Ab response by specific proteins (allergens) represents the initial signal for release of inflammatory mediators (i.e., immediate response). Although several steps on this cascade of events are well described, the initial stages leading to the recognition of foreign proteins and the introduction of an IgE Ab response, also called the sensitization phase (this phase is asymptomatic), are less clear. This process depends upon the interaction of several cellular components of the immune system with their soluble products, the cytokines. A third phase of allergic response is the late-phase reaction begins to develop 4–6 h after the initial type I reaction and persists for 1–2 days. This phase is characterized by infiltration of neutrophils, eosinophils, macrophages, lymphocytes, and basophils.

The central event in the generation of both humoral and cell mediated immune responses is the activation and clonal expansion of Th cells. The imbalance between allergen-specific pro-inflammatory Th1 and pro-allergenic T-cell responses Th2 on one hand and regulatory or suppressive T-cell responses on the other may best explain the development of unwanted immune responses against food allergens, which lead to IgE production and inflammation (Beier et al, 2007). T_H cell activation is initiated by interaction of the TCR-CD3 complex with a processed antigenic peptide bound to a class II MHC molecule on the surface of an antigen-presenting cell. Only professional antigen-presenting cells (APCs) are able to present antigen together with class II MHC molecules and deliver the co-stimulatory signal necessary for complete T-cell activation that leads to proliferation and differentiation. The most important APCs are dendritic cells (DC), these cell in the periphery capture and processing antigens, express co-stimulatory molecules, migrate to lymphoid organs and secrete cytokines to

initiate immune responses. In this mechanism the first step is the pathway responsible for generating antigenic peptides from endocytosed proteins, and this remain poorly understood. Internalized antigen is degraded into oligopeptides of about 13–18 residues, and it takes 1–3 h to transverse the endocytic pathway and appear at the cell surface in the form of peptide–class II MHC complexes. The simplest model for antigen processing would suggest that selected endopeptidases cleave endocytosed proteins at specific position, generating sets of short peptides that compete for binding to class II MHC based on relative affinities. Most native proteins are highly resistant to proteolysis and must first be denatured or partially unfolded to become suitable substrates for endopeptidases. Many studies have been suggested the central role of unfolding of the native proteins in major histocompatibility complex class II-restricted antigen presentation pathway (Carrasco-Marin at al., 1998; Jensen P.E., 1995). Thus, antigen unfolding might be done before the endocytic proteolysis and in this contest reactive oxygen species play a pivotal role. Oxidation of protein allows protein unfolding and enhance both susceptibility to proteolysis and exposure of immunogenic epitopes to specific T cells (Davies at al., 1990 and Stadtman et al., 1990). Antigen processing pathways involves several process that are mainly divided in oxygen-dependent mechanisms (i.e., HOCl-MPO system, hydrogen peroxide, superoxide and peroxynitrite) and oxygen independent mechanisms (i.e., proteases). Oxidation of allergens may represent a critical step in immunospecific response, a probable condition in atopic patients is the alteration of oxidative mechanisms involved in unfolding of antigens. As a consequence of this alteration allergen may be proteolysed in an erroneous way or not digested by proteases, thus this step might play a key role to induce a Th1 or Th2 response. In this chapter, we studied the oxidative mechanisms (MPO system) involved in unfolding pathway of allergen as well as the different susceptibility to proteolytic degradation of Ses i 2 and Ses i 2-ox in presence of extracellular matrix or lysosomal enzymes. Finally, we investigated the effects of both genuine and oxidized 2S albumin on the activation of dendritic cells, which are sentinels and key regulators of the immune response. DCs cells can bias the immune response toward a Th1 or Th2 phenotype through co-stimulatory molecule interaction and release of cytokines. We therefore examined the ability of Ses i 2 and Ses i 2-ox to induce cytokine production and surface co-stimulatory molecule by DCs.

The results have been obtained during my stage in the laboratory of Prof. Ignazio Castagliuolo at the Department of Histology, Microbiology and Medical Biotechnologies (University of Padua) in collaboration with Dr. Paola Brun.

MATERIALS AND METHODS

Materials

"White" sesame seeds of Ethiopian origin were kindly supplied by Chelab s.r.l. (Resana, TV, Italy). MPO (E.C. 3.4.21.4)**,** Cathepsin G *from human neutrophil leucocytes* (E.C. 3.4.21.20) Cathepsin D (E.C. 3.4.23.5) *from human neutrophil leucocytes*, Elastase *from human neutrophil leucocytes* (E.C. 3.4.21.36) and Proteinase 3 *from human leukocyte* (E.C. 3.4.21.76) are purchased from Calbiochem (Beeston Nottingham, UK). Cathepsin B1 *from human liver* (E.C. 3.4.21.1), hydrogen peroxide and hypochlorous acid solution are from Sigma (St. Louis, MO).

The medium used throughout was RPMI 1640 or DMEM supplemented 2 mM L-glutamine, 1% nonessential amino acids, 1% pyruvate, 50 ug/ml kanamicina (Gibco, Grand Island, NY) GM-CSF, IL-4 and 10% fetal calf serum (FCS; Gibco, Grand Island, NY).

Methods

Oxidation of Ses i 2 in presence of MPO-H_2O_2-Cl^- system (MOPS)

When Ses i 2 was oxidized by MOPS, myeloperoxidase at a concentration of 50 nM was added to the Ses i 2 solution (20 μM) and the reaction of the MPO-H_2O_2 system was started by the addition of hydrogen peroxide. The oxidation reactions were conducted in presence of different concentration of H_2O_2: 100 μM, 200 μM and 400 μM. H2O2 was diluted with reaction buffer from stock immediately before use. The of diluted H2O2 was measured at 240 nm and the concentration of hydrogen peroxide was calculated using an absorption coefficient of 39.4 M^{-1} cm^{-1} (Nelson and Kieswo, 1972). Incubation were done in 10 mM sodium phosphate, pH 7.4, containing 150 mM NaCl at 37°C and at different time intervals (2 min, 5 min, 15 min, 30 min and 120 min) aliquots were taken (10 μg) and MPO activity was stopped by adding 1 mM sodium azide. Also, kinetics were conducted further prolonged incubation time at 4 h and 24 h at 37 °C. Aliquots were analysed by reversed-phase high-performance liquid chromatography (RP-HPLC) on a Grace-Vydac (The Separation Group, Hesperia, CA, USA) C18 analytic column (4.6 x 150 mm, 5 μm, 300 Å porosity), eluted with a linear acetonitrile-0.1% TFA gradient from 5 to 60% in 15 minutes at a flow rate of 0.8 ml/min.

Reactions were carried out in same conditions using only H_2O_2 in absence of MPO, with the intent to attribute the oxidative modification to HOCl produced by MPOS. When reagent

HOCl was used to oxidized Ses i 2, it was added at 3:1, 10:1, 20:1 stoichiometric ratios with respect to 20 μM Ses i 2. HOCl stock solution was standardized by measuring the absorbance at 235 nm [ε_{235} nm (HOCl) = 100 $M^{-1}cm^{-1}$] and at 292 nm [ε_{292} nm (ClO^-) = 350 $M^{-1}cm^{-1}$] (Witting et al., 2005). HOCl solution were prepared immediately before use by diluting the concentrated stock solution in to phosphate buffer saline. Aliquots were analysed by reversed-phase high-performance liquid chromatography (RP-HPLC) on a Grace-Vydac (The Separation Group, Hesperia, CA, USA) C18 analytic column (4.6 x 150 mm, 5 μm, 300 Å porosity), eluted with a linear acetonitrile-0.1% TFA gradient from 5 to 60% in 15 minutes at a flow rate of 0.8 ml/min.

With the intent to identify the oxidative intermediates of Ses i 2 were formed at short times of incubation with MPOS, genuine protein was incubated in the presence of 0.05 μM MPO at final concentration of 20 μM. Reaction was started when H_2O_2 was added to final value of 100 μM. Mixture was incubate at 37°C for 3 h and subsequently material was analysed onto on a Grace-Vydac (The Separation Group, Hesperia, CA, USA) C18 analytic column (4.6 x 150 mm, 5 μm, 300 Å porosity), eluted with a linear acetonitrile-0.1% TFA gradient from 5 to 60% in 15 minutes at a flow rate of 0.8 ml/min. The absorbance of the effluent was recorded at 214 nm. Eluted materials were collected and analysed by mass spectrometry and then aliquots of oxidized materials were reduced in the presence of 10 mM DTT with the intent to divide oxiforms of LC and HC. The reduced mixture was analysed by RP-HPLC and eluted materials in correspondence of the major chromatographic peaks were collected, lyophilized and analyzed by high-resolution mass spectrometry on a Mariner ESI-TOF instrument, which yielded mass values in agreement with the theoretical mass of two oxidized intermediates of LC and HC. Oxidative products were subjected to proteolysis: LC-ox intermediate was digested in the presence of pepsin (0.14 μM) in 10 mM glycine-HCl, pH 2.5 and HC-ox intermediate was digested with chymotrypsin (0.2 μM) in 50 mM Tris-HCl, pH 8.0, containing 5 mM $CaCl_2$. Fragments were identified by liquid chromatography coupled to mass spectrometry (LC-MS), using a micro pump 200 HPLC system from Perkin-Elmer (Norwalk, CT) connected to a Mariner eletrospray-ionization time of flight (ESI-TOF) mass spectrometer from PerSeptive Biosystems (Stafford, TX). Specifically, 50 μl of digested solutions in glycine or 50 mM Tris-HCl, pH 8.0, containing 5 mM $CaCl_2$ were loaded onto a C18 Grace-Vydac microbore column (1 x 50 mm, 5μm granulometry), equilibrated for 20 min at a flow-rate of 20 μl/min with H_2O:CH_3CN (95:5), containing 1% HCOOH. Salts and polar reagents were not retained on the column and thus eluted in the void volume, whereas fragment species were eluted at higher CH_3CN concentration as a single peak in total ion

current mode in the mass spectrometer Spray-tip potential was set at 3.0 kVolts, while the nozzle potential was set at 200 Volts and temperature at 140.0 °C.

Proteolytic processing of Ses i 2 and Ses i 2-ox

Extracellular matrix proteinase. Aliquots of purified genuine proteins and Ses i 2-ox (50 μg) were dissolved in 10 mM sodium phosphate, pH 7.4, containing 150 mM NaCl. In the proteolysis solution the protein concentration was about 32 μM. Elastase was added until to an final concentration of 0.27 μM (enzyme:substrate ratio 1:100 w/w). The reaction mixtures were incubated at 37°C and at different time intervals aliquots were taken and digestion were stopped by adding 10 μl of 1% formic acid. When cathepsin G was used to proteolysed Ses i 2 and Ses i 2-ox (32 μM), it was added to a final concentration of 0.28 μM (enzyme:susbtrate ratio 1:100 w/w). Reaction were conducted 10 mM sodium phosphate, pH 7.4, containing 150 mM NaCl and incubated at 37°C. At different time intervals aliquots were taken and before analysis reaction was stopped by adding 10 μl of 1% formic acid. Also, aliquots of purified genuine proteins and Ses i 2-ox (50 μg) were dissolved in 10 mM sodium phosphate, pH 7.4, containing 150 mM NaCl and the protein concentration was about 32 μM. In these solutions were added proteinase 3 until to an final concentration of 0.24 μM (enzyme:substrate ratio 1:100 w/w). The reaction mixtures were incubated at 37°C and at different time intervals aliquots were taken and stopped by adding 10 μl of 1% formic acid.

Aliquots were analysed by reversed-phase high-performance liquid chromatography (RP-HPLC) on a Grace-Vydac (The Separation Group, Hesperia, CA, USA) C18 analytic column (4.6 x 150 mm, 5 μm, 300 Å porosity), eluted with a linear acetonitrile-0.1% TFA gradient from 5 to 60% in 15 minutes at a flow rate of 0.8 ml/min. The effluent was monitored at 226 nm. The percentage of intact protein was determined by integrating the area under the HPLC peak of the protein. For comparison, the enzymatic digestions and analyses were also conducted on alpha-lactalbumin, BSA (i.e., minor allergen) and ovalbumin (i.e., major allergen).

Lysosomal proteases (Cathepsin D and Cathepsin B1)

Aliquots of purified genuine proteins and Ses i 2-ox (50 μg) were dissolved in 0.2 mM sodium acetate pH 5.2 with the intent to obtained a final protein concentration about of 32 μM. Cathepsin D (0.5 μg) was added until to an final concentration of 0.1 μM (enzyme:substrate ratio 1:100 w/w). The reaction mixtures were incubated at 37°C and at

different time intervals aliquots were taken and stopped by adding 1 µl of solution of pepstatin A (1mg/ml). When cathepsin B was used to proteolysed Ses i 2 (32 µM), it was added to a final concentration of 0.14 µM (enzyme:susbtrate ratio 1:100 w/w). Reaction was conducted in buffer 0.25 M sodium acetate, pH 5.5, 0.150 M NaCl, containing 1 mM EDTA and 2 mM DTT. Cathepsin B is cysteine proteinases, the proteolysis was conduced in the presence of DTT with the aim to exclude the formation of dimeric inactivate form of enzyme. Therefore, Ses i 2 was incubated in proteolysis buffer in the absence of enzyme with the intent to observe the behaviour of the genuine protein in the presence of 2 mM DTT. Aliquots were taken at different time intervals and analysed by reversed-phase high-performance liquid chromatography (RP-HPLC) on a Grace-Vydac (The Separation Group, Hesperia, CA, USA) C18 analytic column (4.6 x 150 mm, 5 µm, 300 Å porosity), eluted with a linear acetonitrile-0.1% TFA gradient from 5 to 60% in 15 minutes at a flow rate of 0.8 ml/min. The effluent was monitored at 226 nm. The percentage of intact protein was determined by integrating the area under the HPLC peak of the protein. For comparison, the enzymatic digestions and analyses were also conducted on alpha-lactalbumin, BSA (i.e., minor allergen) and ovalbumin (i.e., major allergen).

Proteolysis of Ses i 2-ox in the presence of mixture of extracellular matrix enzymes (cathepsin G, elastase and proteinase 3). Aliquots of purified Ses i 2-ox (100 µg) were dissolved in 10 mM sodium phosphate, pH 7.4, containing 150 mM NaCl and final concentration of protein was about 32 µM. In this solutions were added aliquots of elastase (1 µg), proteinase 3 (1 µg) and cathepsin G (1 µg) until to an enzyme:substrate ratio 1:100 w/w. The reaction mixtures were incubated at 37°C and at different time intervals aliquots were taken and stopped by adding 10 µl of 1% formic acid. Aliquots were analysed by reversed-phase high-performance liquid chromatography (RP-HPLC) on a Grace-Vydac (The Separation Group, Hesperia, CA, USA) C18 analytic column (4.6 x 150 mm, 5 µm, 300 Å porosity), eluted with a linear acetonitrile-0.1% TFA gradient from 5 to 60% in 15 minutes at a flow rate of 0.8 ml/min. The effluent was monitored at 226 nm. The percentage of intact protein was determined by integrating the area under the HPLC peak of the protein.

DC preparation and culture

Human DCs were obtained from freshly collected buffy-coat preparations of whole human blood. Mononuclear cells were separated by Ficoll-Paque^{TM} PLUS gradient (GE Healthcare, Sweden) and seeded into 6-well tissue-culture plate at density of $3x10^6$ cells per

ml and incubated for two hours at 37°C, 5% CO_2. The non-adherent cells (mainly lymphocytes) were removed and adherent mononuclear cells were differentiated in DCs by incubation in RPMI-1640 supplemented with 10% v/v inactivated fetal bovine serum (FBS), 2 mM L-glutamine, 1% v/v non essential amino acids, 1% v/v pyruvate, 100 U/ml streptomycin and penicillin (all provided from Gibco, Milan), 20 ng/ml of recombinant human GM-CSF and 30 ng/ml of recombinant human IL-4 (ImmunoTools, Friesoythe, Germany). Cells were cultured in a humidified 37°C/5% CO2 incubator for 10 days and medium was replaced every other day. Non-adherent or loosely adherent cells were recovered by centrifugation (10 min at 5000 r.p.m) and complete RPMI-1640 containing freshly supplemented IL-4 and GM-CSF was added to the pellet. After 6-7 days, the loosely adherent or non-adherent cells should display typical dendritic cell morphology. Cellular differentiation was confirmed by FACS analysis using CD1a as typical surface marker of immature human DCs. Populations of immature DCs were split in half on day 7 and cultured ("differentiation culture") in 24-well plates or in 96-well plates. In particular, DCs were washed with RPMI 1640 and plated at 1 X 10^6 cells/well in the presence of free serum culture medium in 96-well plates for ELISA analysis or in 24-well plates for FACS analysis. Seeded DC cells were incubated with 10 μg of Ses i 2 or Ses i 2-ox for 12 h or 24 h. In these experiments mature dendritic cells were generated from immature monocyte derived dendritic cells by adding 20 ng/ml of LPS to the culture and incubating for 1 day before protein stimulation.

Cytokine detection ELISA. Cytokine production was measured in the supernatants of DCs cells by ELISA using matched paired antibodies specific for IL-12p70 (eBioscience, San Diego, CA), IL-4 and IL-10 (ImmunoTools). ELISAs were performed according to the manufacturer's instructions.

FACS analysis. FACS analysis

Quantification of co-stimulatory molecules on surface of DCs was performed using flow cytometry analysis. Briefly, cells (1 x 10^6) were plated in 24-well plates and incubated with 10 μg/ml of Ses i 2 or Ses i 2-ox for 12 h or 24 h at 37°C. Cells were removed by gentle pipetting and centrifuged at 1800 r.p.m. for 8 min at 4°C. Cells were divided in vials and washed with PBS containing 0.5% BSA. After centrifugation pellets were re-suspended and incubated with human monoclonal antibodies specific for CD1-PE conjugated monoclonal antibody (ImmunoTools) and with CD80 FITC-conjugated, HLA FITC-conjugated or CD86 un-conjugated human monoclonal antibody for 30 min at 4°C in the dark. With the intent to

eliminate antibodies, cells were washed twice using PBS-BSA solution and centrifuged 1280 r.p.m for 8 min. In addiction, cells incubated with hAb anti-CD86 were stained with anti-mouse FITC-conjugate IgG (Chemicon International, Milan) for 30 min at 5°C in the dark. Samples were washed again, after incubation. Stained cells were resuspended in 200 μl of PBS-0.5% BSA and analysed by BD FACs Calibur (BD Biosciences, San Jose, CA) using an air-cooled argon ion laser (488-nm exitaction). At least 50,000 events were collected on gated $CD1^+$ cells. Data were analysed using the CellQuest software (Becton Dickinson, San Jose, CA).

Culture medium, after centrifugation are collected and analysed by RP-HPLC on a C18 analytical column (4.6 x 150 mm, 5 μm, 300 Å porosity) eluted with a linear acetonitrile-0.1% TFA gradient from 5 to 60% in 25 minutes, at a flow rate of 0.8 ml/min.

Mice sensitization protocol and ELISA

During the experiments, mice were kept in pathogen-free animal facilities at a controlled temperature and humidity, under 12-h light:12-h dark cycle, and with food and water ad libitum. All animals were acclimated for at least 1 week before the experiments began. In brief, active sensitization was performed with adjuvant by giving one i.m. injections of 30 μg of Ses i 2 or Ses i 2-ox and two i.m. injections of 50 μg of genuine or oxidized proteins (one injection per week). Two weeks after last injection, mice were killed, blood was taken, and the serum was collected and stored at -20°C. Ses i 2 and Ses i 2-ox specific IgG levels were detected by ELISA method on a ELISA high affinity 96-well plates (Corning, New York, Costar, Acton, MA) or hydrophilic 96-well plates (Falcon, Becton-Dickinson, NJ, USA) coated with Ses i 2 or Ses i 2-ox (100 μl; 10 μg/ml). Briefly, 96-well plates were coated overnight with 10 μg/ml protein solutions diluted in sodium carbonate pH 9.4, at 4°C. The plates were washed and blocked with PBS containing 2%-BSA (Sigma) for 2 h at room temperature. After washing, serial dilutions of mice serum (1:100; 1:10,000) were plated at r.t. for 2 h, and after plates were incubated at r.t. for 1 h with biotinylated anti-IgG antibody (Southern Biotechnology Associates, Birmingham, AL) followed by a 30 min incubation with peroxidase-conijugated streptavidin. Reactions were developed with TNB substrate and plates were read at 450 nm in a microplate ELISA reader. All samples were analysed for a minimum of two times.

RESULTS AND DISCUSSION

Oxidation of Ses i 2 in the presence of MPO-H_2O_2-Cl^- system (MOPS)

Recently, Cardoso and co-workers (Cardoso et al., 2009) observed in mice sensitized and challenged with peanut seed, the develop of intestinal inflammation, characterised by epithelial exulceration, edema, and leukocyte infiltrate in lamina propria, along with disruption of small gut architecture. In inflammation site, up to 80% of H_2O_2 generated by neutrophil cells is utilized to form a range of reactive oxygen species, with HOCl generated at rates between 20 and 400 μM/h accounting for 40-50% of H_2O_2 consumed in the presence of physiologic chloride anion (Winterbourn C.C. et al., 2000). Chloride (Cl^-) is a major intracellular anion of living organisms owing to its role in regulating electrogenic cation transport across intracellular and plasma membranes, membrane potential, cell volume, and intracellular pH (Estévez and Jentsch, 2002). The intracellular concentration of Cl^- ranges from 1 to 60 mM, whereas the extracellular concentration is 140 mM (± 10 mM). Myeloperoxidase is a major constituent of the azurophilic cytoplasmic granules of neutrophil and it is a classical heme peroxidise that uses hydrogen peroxide to oxidize chloride to a potent oxidant, hypochlorous acid (HOCl). The pKa of hypochlorous acid is 7.59, thus at physiological pH values, it exists in equilibrium with the anion ^-OCl. This mixture will be referred to as HOCl throughout this chapter. To assess whether MPO-H_2O_2-Cl^- modifies Ses i 2 *in vitro*, aliquot of purified protein (20 μM) in 10 mM sodium phosphate, pH 7.4,containing 150 mM NaCl was incubated in the presence of 50 nM MPO at various concentrations of H_2O_2 (i.e., 0.1 mM, 0.2 mM and 0.4 mM) at 37°C. Concentrations of H_2O_2 are used to mimic different conditions in the inflammation site in which the quantity of ROS is correlated to the number of activated neutrophil (Tsan M. and Chen J., 1980). Aliquots of reaction mixture were collected at different time intervals and analysed by RP-HPLC combined with mass spectrometry (Figure 1).

At 2 min of incubation in the presence of 100 μM of H_2O_2, genuine protein (Ses i 2) presents a dramatic shift in the chromatographic mobility as a consequence of oxidative damage on protein structure. Materials analysed by mass spectrometry show signals that correspond at approximately molecular weight of 11806 Da and 11824 Da. Respectively, the mass increments are about + 80 a.m.u and + 98 a.m.u, and these values could be correspond to oxidized intermediates characterised by the presence of 5 or 6 MetSO. The prolongation of incubation time does not induce any modification in chromatographic plot and mass data, this behaviour is probably due to the exhaustion of MPOS activity.

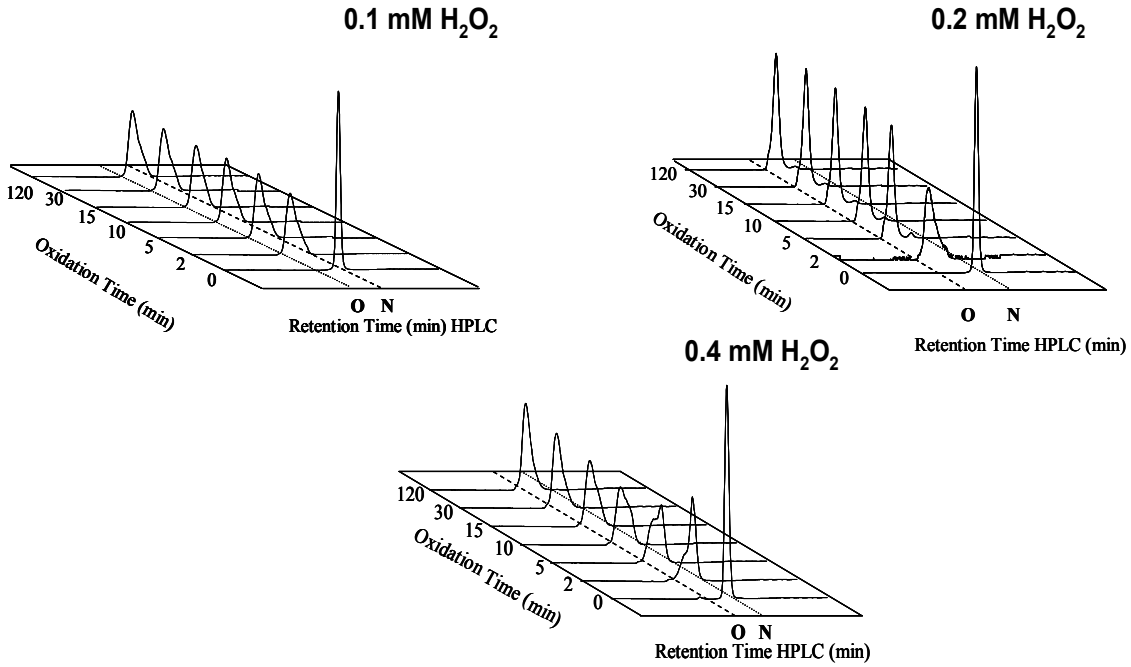

Figure 1. Reverse-phase HPLC analysis of the Ses i 2 oxidation in the presence of MPOS. RP-HPLC of Ses i 2 (20 μM) in the presence of 50 nM MPO in PBS, pH 7.4. The oxidation reactions were conduced with 0.1 mM H_2O_2, 0.2 mM $H_2O_2$and 0.4 mM H_2O_2 at 37°C. An aliquot (10 μg) was loaded in onto Vydac C-18 column (4.6 x 250 mm, 5 μm) and elution was performed at flow rate of 0.8 ml/min with a linear 0.1% (v/v)-TFA-acetonitrile gradient.

At 200 μM of hydrogen peroxide the oxidation is complicated by the presence of a multitude of species (Table 1). The oxidative reaction shows a rapid kinetic that resulted mainly to a oxidized intermediate with a molecular weight of 11884 Da, and this mass value is in agreement with a oxidation of ten Met residues in Ses i 2.

Table 1. Mass data Ses i 2 oxidation in presence of MPOS-0.2 mM H_2O_2

Incubation Time (min)	Mass (Da)	Δm (Da)	MetSO
0 min	11726.8	-------	0
2 min	11822.3; 11806.17;11850.5	96.3	6
5 min	11862.3; 11850.5;11879.4	136.3	8-9
10 min	11868.4; 11850.71;11905.4	142.4	9
15 min	11854.2 ; 11868.58; 11906.33; 11934.16	125	8
30 min	11868.5; 11854.4;11934.41	142.4	9
120 min	11884.5; 11862.5;11934.5	158.5	10

The main intermediate is indicated by underlining.

Unexpectedly, in the presence of 400 μM of H_2O_2 reaction shows a lower rate of oxidation, in fact, after 2 min the main peak is characterised by a shoulder with a mass value about of 11743 Da corresponding to one MetSO. At 120 min of incubation the major species has a mass value of 11824 Da and this data is in agreement with a maximal oxidation of six methionine residues (Table 2).

Table 2. Mass data Ses i 2 oxidation in presence of MPOS-0.2 mM H_2O_2

Incubation Time (min)	Mass (Da)	ΔPM (Da)	MetSO
0 min	11726.8	-------	0
2 min	11742.6; 11776.5	15.8 50.5	1 3
5 min	11768.8; 11806.2	42.7 80.1	~3 5
10 min	11774.4;	48.3	3
15 min	11824.4; 11807.03;11838.5	98.3	6
30 min	11824.4; 11838.5;11852	98.3	6
120 min	11824.4; 11838.5;11852	98.3	6

The main intermediate is indicated by underlining.

MPOS induces a slow oxidation of Ses i 2 in the presence of higher concentration of hydrogen peroxide, and this behaviour is closely related to the catalytic cycle of MPO. The reaction of myeloperoxidase with H_2O_2 initially results in the formation of compound I, which oxidized Cl^- to HOCl and is reduced directly to the native enzyme. During turnover, some compound I is also converted to compound II and rapid-scan studies show that at least a 20-fold excess of H_2O_2 is required to obtain a good spectrum of relatively pure compound I; a further increase in H_2O_2 concentration causes compound I to be reduced to compound II, which is a very stable intermediate. Compound I formation is reversible, with an apparent second order forward rate constant of (1.8 ± 0.1) X 10^7 $M^{-1}s^{-1}$ and a reverse rate constant of 58 ± 4 s^{-1}, giving a constant of 3.2 μM for the dissociation of compound I to native enzyme and H_2O_2. This reversibility is one factor that can explain the large excess of H_2O_2 required to form compound I. The apparent second-order rate constant for compound II formation from compound I and H_2O_2 is (8.2 ± 0.2) X 10^4 $M^{-1}s^{-1}$ (Marquez et al., 1994). A smaller excess of H_2O_2 led to incomplete formation of compound I, whereas a larger excess led to the fast

formation of compound II, inactive form of enzyme, in fact, of the oxidized intermediates of MPO compound I is the only species that takes part in both peroxidatic cycle and the chlorinating reaction. Marquez and co-workers (Marquez et al., 1994) reported that the reduction of compound I to compound II is depend not only upon hydrogen peroxide but also upon superoxide generate from the oxidation of H_2O_2. Our results are in agreement with the observation which the ratio of $[H_2O_2]$/[MPO] is increased, more complete formation of compound I is observed; also, the decay of compound I to compound II becomes faster. (Hydrogen peroxide directly and rapidly reduced compound I. Superoxide, on the other hand, once generated from oxidation of H_2O_2, can rapidly bind compound I and then slowly convert compound I to compound II, causing a slower reaction).

Also, the depletion of H_2O_2 by autoreduction ($2\ H_2O_2 \rightarrow 2\ H_2O + O_2$) probably becomes important (Galijasevic et al., 2009).

The long time oxidation reaction (4 h and 24 h) was conduced at the same conditions used in the previous experiments. Surprisingly, RP-HPLC profiles (Figura 2A) show a dramatic shift of Ses i 2 peak to a minor retention time. At 4h-incubation, in the presence of 100 μM hydrogen peroxide, oxidation leads to formation of a main species with a mass value of 11854.7 Da (Δm = + 128.7 a.m.u) corresponding to an oxidized intermediate of Ses i 2 with eight MetSO, and this data is retained at 24 h-incubation. In the presence of 200 μM of hydrogen peroxide at 4 h of incubation, chromatographic profile presents a major peak with a evident shoulder characterised by molecular mass of 11967.7 Da, corresponding to Ses i 2-ox, while main peak corresponds to an ensemble of intermediates. In the deconvoluted mass spectrum is evident the presence of other minor species with a mass value about of 11806.8 Da and 11824.3 Da, in which five Met and six Met are oxidized, respectively. These values suggest an oxidation of a cluster of five-six methionine with a subsequent oxidation of other two Met residues in the early stage of oxidative process. Already at 4h of incubation with 0.4 mM H_2O_2 Ses i 2-ox is the only species in reaction mixture. These results confirmed the particular kinetic of MPO, in fact, in the presence of low concentration of oxidant (i.e., 100 μM) MPO forms compound I that is able to oxidize Ses i 2 by production of HOCl, in this condition the formation of compound I leads the consumption of oxidant. Thus, the concentration of hydrogen peroxide is not sufficient to induce the formation of high quantity of compound II. At 200 μM H_2O_2 compound I is partially reduced to compound II, ($t_{1/2}$ is about from 12 min, but the presence of this intermediate is evident after 64 min in absence of Cl^-; Marquez et al., 1994), inactive form of enzyme. At 400 μM compound I is quantitatively shifted to compound II and this compound is not able to induce the oxidation of Ses i 2. At 4

h-incubation, compound II is completely converted to native enzyme and Ses i 2 is oxidised as consequence of the production of HOCl by restored MPO.

At 24 h-incubation in the presence of 0.4 mM H_2O_2 the chromatographic profile (Figure 2B) shows single symmetric peak that it has been identified as Ses i 2-ox, this result is in agreement with the complete consumption of hydrogen peroxide in the oxidative reaction. HOCl is a potent oxidant which is able to oxidize Trp, Tyr and Phe, and these amino acids become more exposed as a consequence of the oxidation of Met in Ses i 2. The absence of other intermediates in mass data, in which the major degree of oxidation is registered after 24 h of incubation, is a strong indication that the total consumption of HOCl is due to oxidation of Met residues.

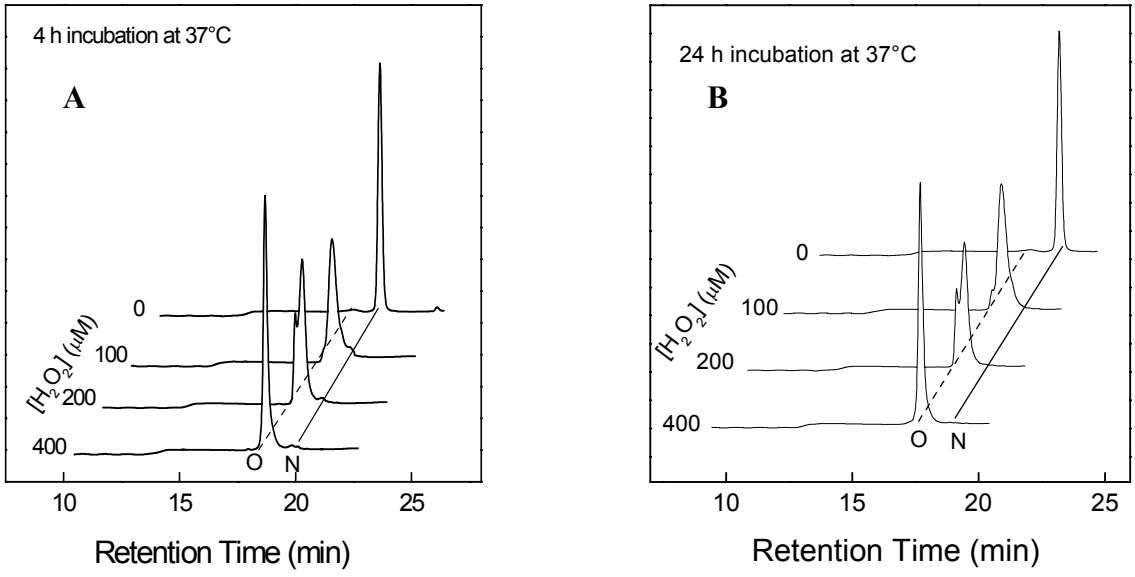

Figure 2. Reverse-phase HPLC analysis of the Ses i 2 oxidation in the presence of MPOS at 4 h or 24 h of incubation. RP-HPLC of Ses i 2 (20 μM) in presence of 50 nM MPO in PBS, pH 7.4. The oxidation reactions were conduced in presence of 0.1 mM H_2O_2, 0.2 mM $H_2O_2$and 0.4 mM H_2O_2 at 37°C. An aliquot (10 μg) was loaded in onto Vydac C-18 column (4.6 x 250 mm, 5 μm) and elution was performed at flow rate of 0.8 ml/min with a linear 0.1% (v/v)-TFA-acetonitrile gradient.

Also, oxidation of Ses i 2 was conducted in the absence of MPO and with H_2O_2 as oxidant at the same concentration used in MPOS experiments. The data reflect that oxidation of Ses i 2 is due to production of HOCl, indeed hydrogen peroxide oxidizes at 120 min of incubation only one or two Met residues, while in the presence of MPO in the oxidative damage are involved six or nine Met (Figure 3).

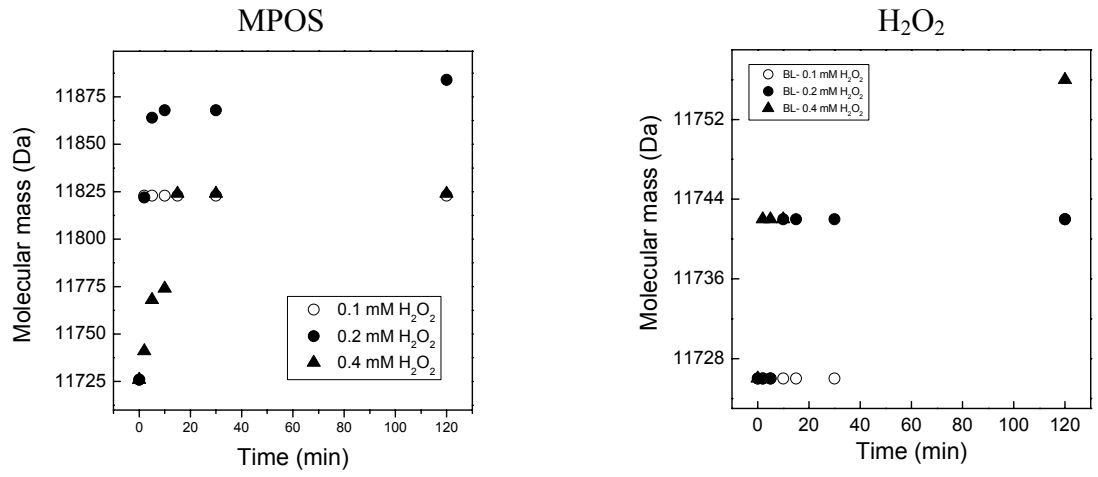

Figure 3. Mass increment induced by MPOS or H_2O_2. Reactions were conduced in the presence of MPO with 0.1 (○), 0.2 (●) e 0.4 mM (▲) H_2O_2 (MPOS) or with 0.1 (○), 0.2 (●) and 0.4 mM (▲) H_2O_2.

Finally, is evident that the myeloperoxidase induces the formation of Ses i 2-ox mainly in the presence of 400 μM of H_2O_2 at 4 h of incubation. In this process hydrogen peroxide is completely converted in HOCl (Hawkins et al., 2003).

With the intent to elucidate the role of HOCl in the oxidation of Ses i 2 we have conduced the oxidative reactions in the presence of HOCl at the concentration hypothetically formed by MPO activity (Figure 4). In these studies the degree of oxidation of Ses i 2 is quite different, in fact, with about 60 μM HOCl oxidative damage is not evident (Figure 4A). Also, in presence of higher concentrations of HOCl chromatographic profiles are altered and the mass data confirm a dramatic alteration at 200 μM of HOCl (Figure 4B) with a rapid formation of Ses i 2-ox. At 400 μM of HOCl (Figure 4C), Ses i 2 is immediately converted in Ses i 2-ox, in addition, the mass data show species with features occurring at high degree of oxidation, in which are involved other amino acids as Trp, Tyr, His and Lys. These data suggest that at low molar excesses of HOCl the majority of the HOCl is consumed by Met (> 98%). With a larger excesses of HOCl the proportion of HOCl consumed by the Met residues reduces, with the remainder of the HOCl increasingly consumed by cystine, the His and Lys residues are followed by Trp and Tyr (Pattison and Davies, 2001).

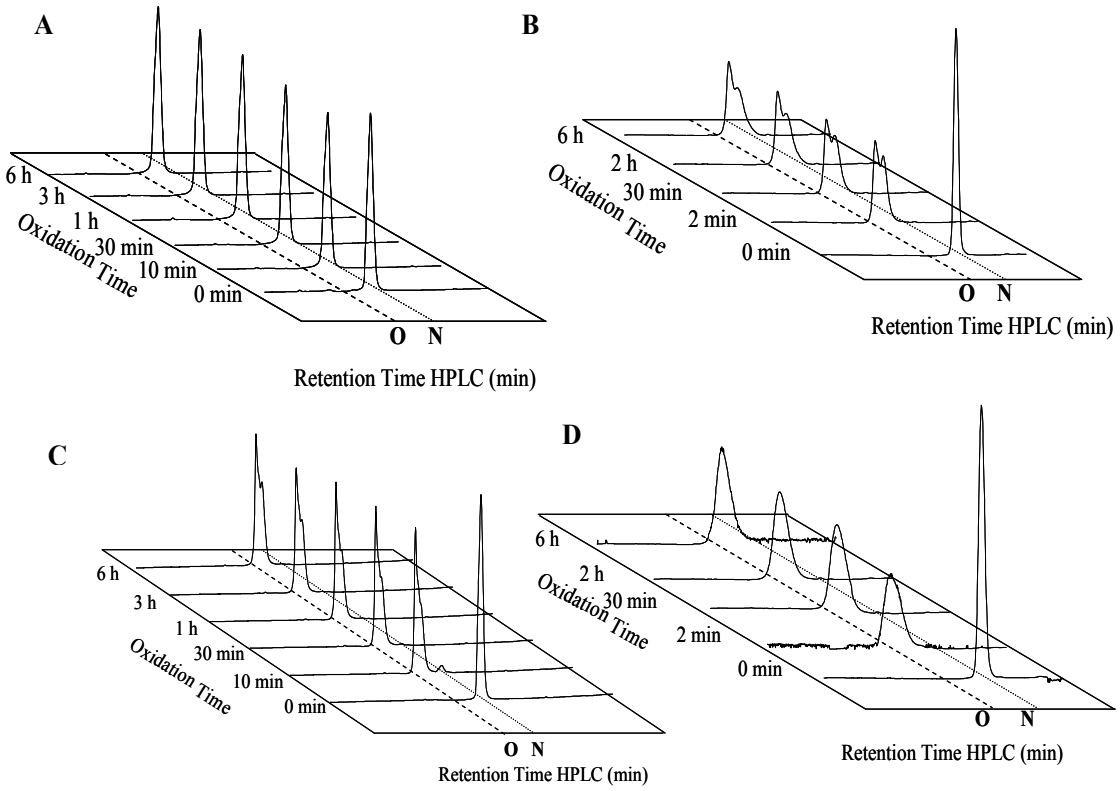

Figure 4. Reverse-phase HPLC analysis of the Ses i 2 oxidation in the presence of HOCl. RP-HPLC of Ses i 2 (20 μM) in PBS, pH 7.4, reactions were conduced in presence of 60 μM **(A)**, 200 μM **(B)**, 300 μM **(C)** and 400 μM **(D)** at 37°C. An aliquot (10 μg) was loaded in onto Vydac C-18 column (4.6 x 250 mm, 5 μm) and elution was performed at flow rate of 0.8 ml/min with a linear 0.1% (v/v)-TFA-acetonitrile gradient.

Finally, Ses i 2 ox was incubated in the presence of MPOS activated by addition of 100 μM H_2O_2 with the intent to isolate and characterise the oxidized intermediates. Primarily, the oxidation mixture was analysed by RP-HPLC and mass spectrometry that yielding mass values of three intermediates: 11826 Da, 11806 Da and 11792 Da. Respectively, these data correspond to species with 6 MetSO, 5 MetSO and 4 MetSO. After reduction LC-ox and HC-ox of different intermediates were isolated by RP-HPLC and MS analysis confirm the presence of different species characterised by molecular weights of 3344.1 ± 0.4 Da and 3328.5 ± 0.4 that correspond to LC with one MetSO and two MetSO, respectively. Other species are characterised by mass values of 8488.5 ± 0.7 Da and 8472 ± 0.3 that correspond to HC with four MetSO and three MetSO, respectively. These species were subjected to

proteolysis and analysed by LC-MS with the intent to identify MetSO. LC-MS data are reported in Table 3.

Overall, MPOS induces the formation of a mixture of intermediates of Ses i 2 with a cluster of 5-6 methionine involved in the early stage of oxidation. Two of these methionine are located in LC-ox, unfortunately we have isolated only a species with one MetSO in fragment ^{36}WMRSMRGQ^{43}. In the HC, Met residues involved in early stage of oxidation are Met84, Met85, moreover fragment ^{83}CMMRQMQQEYGMEQEMQQMQQM^{104} has been identified in which other two MetSO are present.

The oxidation of these Met residues probably induces the destabilization of protein structure that is not stable to the subsequent oxidative damage with a formation of Ses i 2-ox.

Our results are in agreement with structural homology model of Ses i 2 (see chapter 2.1 for details). As shown in figure 5, the Met84 and Met85 in HC are fully exposed on protein surface, moreover the structural model permits to identify the other HC sites of primary oxidation, in particular, Met94 and Met98 are highly exposed to solvent. Our data show the presence of two MetSO in the LC-ox intermediate, fragment ^{36}WMRSMRGQ^{43} presents one MetSO and our model permits to indicate that Met40 and Met37 are fully exposed on protein surface (Figure 5).

Table.3 LC-ox and HC-ox intermediate characterization

Theoretical mass (a.m.u.)	Experimental mass (a.m.u.)	Identity	Δm a.m.u.
[a] 1050.4	1066.5	WMRSMRGQ	+15.9 (+16.0)
[a] 990.4	990.5	MRHCMQW	
[b]2828.3	2891. 5	CMMRQMQQEYGME QEMQQMQQM	+ 63.2 (16 × 4)
[b]1594.6	1626.1	SHCRCEALRCMMR	+ 31.4 (16 × 2)
[b]1774.7	1774.54	LPRMGCMSYPTECRM	
[b]891.3875	874.42	QGQFEHF	- 17

a fragments LCox; b fragments HC-ox

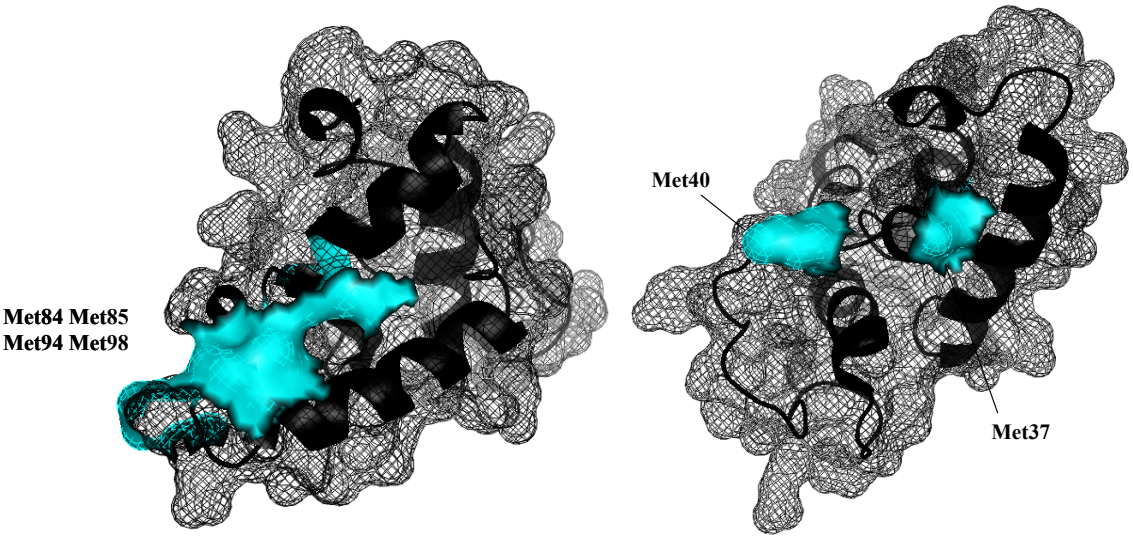

Figure 5. Schematic representation of Met clusters on the protein surface.

Proteolytic processing of Ses i 2 and Ses i 2-ox

Inflammatory cells in *lamina propria* such as macrophages and neutrophils play a major role in the tissue damage during immune response. Under conditions of tissue injury (i.e., hypersensitivity reaction), the activation of neutrophils leads to the release in extracellular matrix of multiple products, including reactive oxygen species, cationic peptides, eicosanoids, and in azurophil (also known as primary) granules released MPO and a family of structurally related serine proteases such as elastase, cathepsin G and proteinase 3. In addition to their microbicidal activities, neutrophil serine proteases have an important role in non-infectious, inflammatory processes. Cathepsin G, proteinase 3 and neutrophil elastase have a high degree of homology mast-cell chymase and tryptase (Pham C.T., 2006), these enzymes are stored in azurophil granules and once released they are potentially fully active in a neutral environment. Genuine protein (Ses i 2) and oxidized protein (Ses i 2-ox) were subjected to proteolysis in the presence of different neutrophil serine proteases at the enzyme/substrate ratio of 1:100 (w/w) in phosphate buffer saline, pH 7.4, containing 150 mM NaCl. Proteolysis were loaded onto RP-HPLC analytical column, and materials eluted were subjected to mass analysis. Minor (i.e., alpha-lactalbumin-α-Lact) and major allergens (i.e., ovalbumin-OVA) were used as a model, and they are proteolysed at the same conditions of Ses i 2 and Ses i 2-ox. Histogram (Figure 6A) shows the extraordinary resistance to proteolysis of Ses i 2, after 3 h-incubation, while model proteins are dramatically proteolysed. In particular, major allergen ovalbumin is fully digested by elastase, whereas alpha-lactalbumin retains about 60% of

intact structure. Both proteins present an increase of stability to proteolysis in presence of proteinase 3 and cathepsin G. Results at 24 h-incubation show that Ses i 2 is fully resistant to proteolysis, while ovalbumin and alpha-lactabumin are completely digested. These results confirm the surprising stability toward enzymes of Ses i 2.

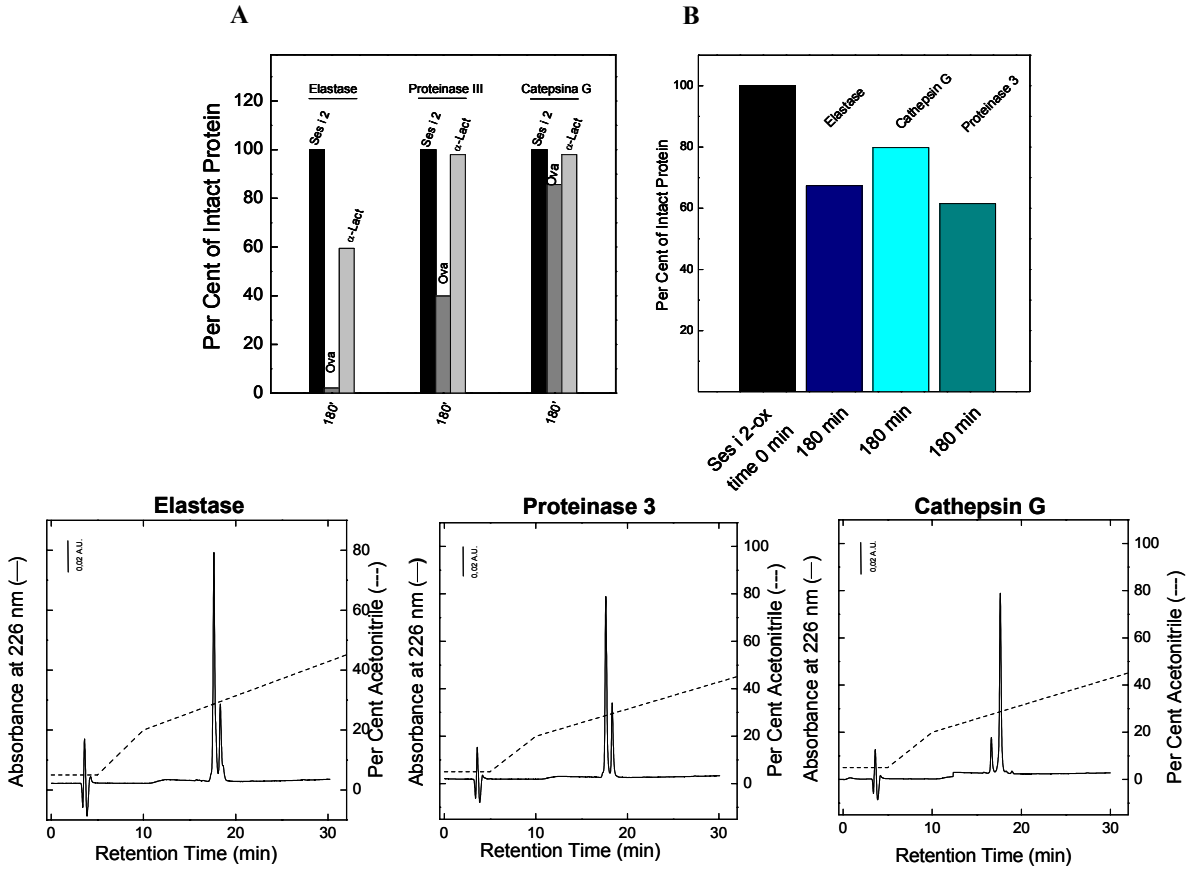

Figure 6. Enzymatic digestion of Ses i 2 and model allergen as ovalbumin (OVA) and alpha-lactalbumin (α-Lact) in the presence of elastase, proteinase 3 and cathepsin G (A). Proteolysis was conduced in 10 mM sodium phosphate, pH 7.4, containing 150 mM NaCl at 37°C. **Enzymatic digestion of Ses i 2-ox in the presence of elastase, proteinase 3 and cathepsin G (B)** Proteolysis was conduced in 10 mM sodium phosphate, pH 7.4, containing 150 mM NaCl at 37°C. The percent recovery of intact protein was determined as described under Material and Methods. **Reverse-phase HPLC analysis of the enzymatic digestion of Ses i 2-ox at 180 of incubation in the presence of HNE, P3 or CG (C).** An aliquot (10 μg) was loaded in onto Vydac C-18 column (4.6 x 250 mm, 5 μm) and elution was performed at flow rate of 0.8 ml/min with a linear 0.1% (v/v)-TFA-acetonitrile gradient.

As shown in Figure 6B after 180 min of incubation, oxidized protein is not fully resistant to proteolysis, in particular in presence of chathepsin G Ses i 2-ox retains about 80% of intact form, while in the presence of elastase or proteinase 3 intact form represents about 60%. Ses i 2-ox incubated with elastase or proteinase 3 (Figure 6C) shows a identical chromatographic profile; the main peak corresponds to a mass value of 11968.2 ± 0.6 Da, while minor peak has

a molecular weight about of 11987.2 ± 0.4 Da. These results are in close agreement with mass of Ses i 2-ox and molecular weight of a nicked species where a single peptide bond is cleaved by enzyme activity, respectively. Proteinase 3 and elastase have a similar site of cleavage (i.e., Ala-X and Val-X), thus in the Ses i 2-ox the probable amino acids involved in proteolysis are Ala80 or Val72. In presence of cathepsin G, RP-HPLC profile shows a minor peak with molecular mass of about 11110 ± 0.4 Da, this value is due to cleavage at flexible N-terminal of light chain and heavy chain.

Results confirmed extraordinary stability to proteolysis of Ses i 2, while Ses i 2-ox is not resistant to proteolysis, and when enzyme digestion is prolonged to 24 h Ses i 2-ox is fully proteolyzed in close agreement with loss in structure and stability of oxidized protein.

With the intent to mimic the extracellular matrix environment, Ses i 2-ox was subjected to proteolysis in the presence of mixture of neutrophil serine protease and in agreement with the previous results Ses i 2-ox is dramatically digested. In Figure 7, is reported the percentage of intact protein after 1 h-incubation, results show that about of 30% of Ses i 2-ox is proteolyzed, while at 24 h Ses i 2-ox is fully digested. Probably, nicked species formed in the presence of elastase or proteinase 3 are not resistant to chatepsin G, and vice versa species produced in presence of CG are not resistant to proteolytic attack by the HNE and P3.

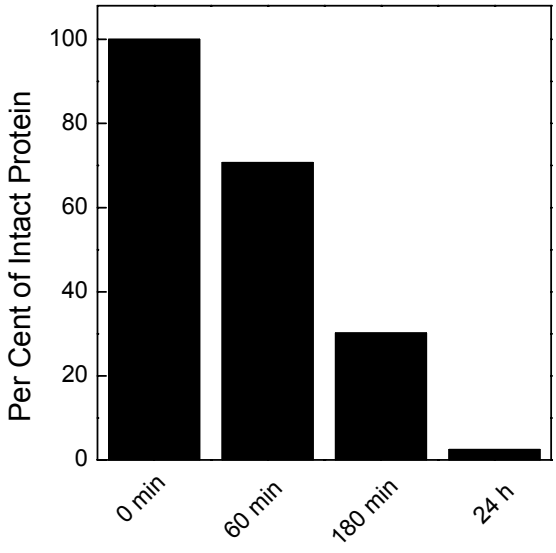

Figure 7. Enzymatic digestion of Ses i 2-ox in the presence of mixture of PMN serine proteases such as elastase, proteinase 3 and cathepsin G . Proteolysis was conduced in 10 mM sodium phosphate, pH 7.4, containing 150 mM NaCl at 37°C. The percent recovery of intact protein was determined as described under Material and Methods.

Lysosomal proteases (Cathepsin D and Cathepsin B1).

Exogenous antigens are processed by lysosomal proteases within antigen-presenting cells (APC) to create antigenic peptides and then presented by major histocompatibility complex (MHC) class II molecules prior to the activation of $CD4^+$ T cells. Enzymes such as aspartate proteases (e.g. cathepsin D and E) and cysteine proteases (e.g. cathepsin B, L and S) are proposed to be involved in this process. Zhang and co-workers (Zhang et al., 2000) suggested the pivotal role of lysosomal cathepsins in antigen processing, and they have demonstrated functional differences between these proteases in antigen processing and in inducing immune response (Chapman A.H,1998; Delammare et al., 2005).

Aliquots of purified genuine proteins and Ses i 2-ox (50 μg) were dissolved in 0.2 mM sodium acetate pH 5.2, and in these solutions were added cathepsin D or cathepsin B. The reaction mixtures were incubated at 37°C and at different time intervals aliquots were taken and analysed by RP-HPLC. Histogram (Figure 8) shows the percentage of intact protein after 180 min of incubation in presence of lysosomal proteases. In the figure 8A are reported the percentages of intact protein about two model allergen ovalbumin and alpha-lactalbumin. Results demonstrated high resistance to proteolysis of Ses i 2 and ovalbumin that are classified as major allergens, while alpha-lactalbumin a minor allergen retains about 40% of intact structure in presence of cathepsin D. In the presence of cathepsin B, Ses i 2 shows high degree of proteolysis, while after 180 min of incubation minor allergen is fully digested. Cathepsin B is a cysteine protease with in the catalytic site a free cysteine, enzyme is active in SH form, thus this residue might be involved in formation of disulphide bridge that stabilized a dimeric inactive form of enzyme. With the intent to abrogate the formation of inactive dimer of Cat.B buffer is added of 1 mM DTT, strong reducing agent. Ses i 2 in the presence of this low concentration of DTT is slowly reduced in light and heavy chain, this hypothesis is confirmed by RP-HPLC analysis of Ses i 2 incubated in digestion buffer whitout enzyme. Ses i 2-ox is not resistant to reducing condition used in cathepsin B proteolysis, thus it was only subjected to proteolysis in presence of Cat.D (Figure 8B), and after 180 min of incubation about 80% of Ses i 2-ox is retained, this data demonstrate a slight stability of oxidized protein toward digestion of cathepsin D. Result is completely different at 24 h, Ses i 2-ox is digested and only 35% of intact protein is retained, while Ses i 2 is fully resistant at 24 h of incubation in presence of Cat.D. Data suggest a high resistance of native protein to the lysosomal proteolysis, and this result is in agreement with our hypothesis that oxidative damage is necessary to obtain a unfolded or partially unfolded antigen degradable in antigen processing.

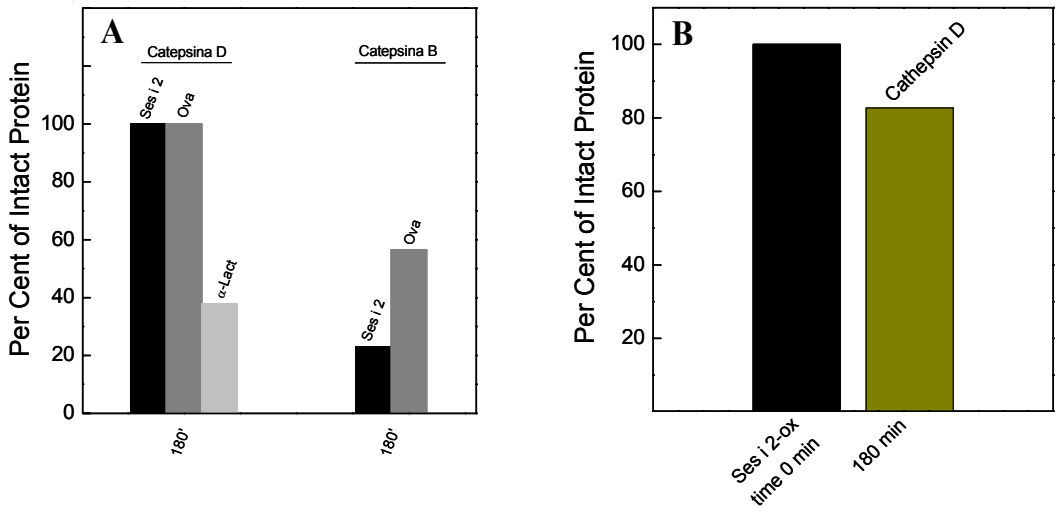

Figure 8. Enzymatic digestion of Ses i 2 and model proteins in the presence of cathepsin D and cathepsin B (A). Proteolysis was conduced in 0.2 mM sodium acetate pH 5.2 at 37°C. Proteolysis in presence of cathepsin B was conducted in reducing condition with 1 mM DTT. **Enzymatic digestion of Ses i 2-ox in presence of cathepsin D (B).** Proteolysis was conduced in 0.2 mM sodium acetate pH 5.2 at 37°C. The percent recovery of intact protein was determined as described under Material and Methods.

IgG-serum ELISA on immunized Ses i 2 or Ses i 2-ox mice

The identification of discrete sites in antigens that are recognized by particular antibodies or T-cell receptors is important for the characterization of allergens. Epitopes might be composed of sequential residues along the polypeptide chain (linear or continuous epitopes) or non-sequential residues from segments of the chain brought together by folded conformation of the protein (conformational or discontinuous epitopes). First step in the identification of Ig epitopes and correlation with oxidation of methionine residues is the detection of polyclonal antibodies against Ses i 2 and Ses i 2-ox in serum of immunized mice. With the intent to assess the levels of antibodies anti-Ses i 2 or anti-Ses i 2-ox in serum, high affinity and hydrophilic 96-well plates were coated with Ses i 2 or Ses i 2-ox (10 μg/ml; 100 μl/well). In the ELISA experiments were detected IgG antibodies in mice serum, in Figure 9A and 9B are reported values of absorbance in function of serum dilution. Data show high levels of IgG anti-Ses i 2 and a low quantity of anti-IgG Ses i 2-ox, also serum of mice immunized with Ses i 2 detects with low efficiency Ses i 2-ox. Results suggest that polyclonal antibodies anti-Ses i 2 may recognize with minor affinity epitopes in Ses i 2-ox, and this behaviour could be induced by structural changes in oxidized protein.

Early epitope mapping studies were carried out in major allergens of yellow (Sin a 1) and oriental mustard (Bra j 1); these studies provided the characterization of a common immunodominant IgE epitope (QGPHVISRIYQTAT) located in the hypervariable region

(Monsalve et al., 1993). Later on, Robotham and co-workers (Robotham et al., 2002) reported a peptide of twelve amino acids (QGL**RGEE**ME**E**MV), also located in the hypervariable region of Jug r 1, which showed the ability to bind strongly IgE from walnut-allergic patients´ sera. Mutational analysis demonstrated that **RGEE** and an additional **E** were necessary for maximum IgE recognition. Despite low sequence homology within the hypervariable region, the amino acid sequence RGGEMEE seems to be well conserved in 2S albumins from several plant species such as pecan nut, cashew nut (*Anacardium occidentale*), Brazil nut or castor bean. On the other hand, Ses i 2 is the only 2S allergen reported to date which does not contain any linear IgE-binding epitopes spanning the hypervariable region (Wolff et al., 2004). The epitope mapping of this allergen is characterized by several linear IgE-binding epitopes located between the helices Ia and Ib of the small subunit and at the helix II of the large chain. These linear IgE epitopes are: **SRQCQMRHCMQWMRSMRG** in light chain and **QFEHFRECCNELRDVK** in heavy chain.

Serum of mice immunized with Ses i 2 shows a low capability to recognize Ses i 2-ox and probably this is a consequence of the oxidation damage that compromises four methionine in LC of Ses i 2 and then linear epitopes in heavy chain (not Met residues) induce a minimal recognize. More important is the relationship between structural alterations in Ses i 2-ox and the low affinity of anti-Ses i 2 serum, in which are involved conformational epitopes. Hence, the behaviour of anti-Ses i 2 serum may be a consequence of alteration of conformational epitopes in the oxidized protein (Figure 9).

Also, the serum of mice immunized with Ses i 2-ox appears contain a very low levels of antibodies against Ses i 2-ox in fact the absorbance values are comparable with control. Moreover, native protein is not recognized by serum anti-Ses i 2-ox. Probably, in mice Ses i 2-ox is not stable to proteolytic process, consequently it is degraded in short peptides that are not immunogens. In order to confirm these data ELISA anti-IgG was carried out in hydrophilic plates (Figure 9B), in which is induced a increase of hydrophilic protein coating and results are in close agreement with previous data.

It is important to draw attention to the fact that most studies involving epitope characterization of 2S albumins are mainly based on mapping of linear epitopes. Unfortunately, largely unexplored in terms of allergen epitope characterization are those of conformational nature, comprised of amino acids distant in the proteins primary structure but adjacentonce the protein folds. (Moreno and Clemente, 2008).

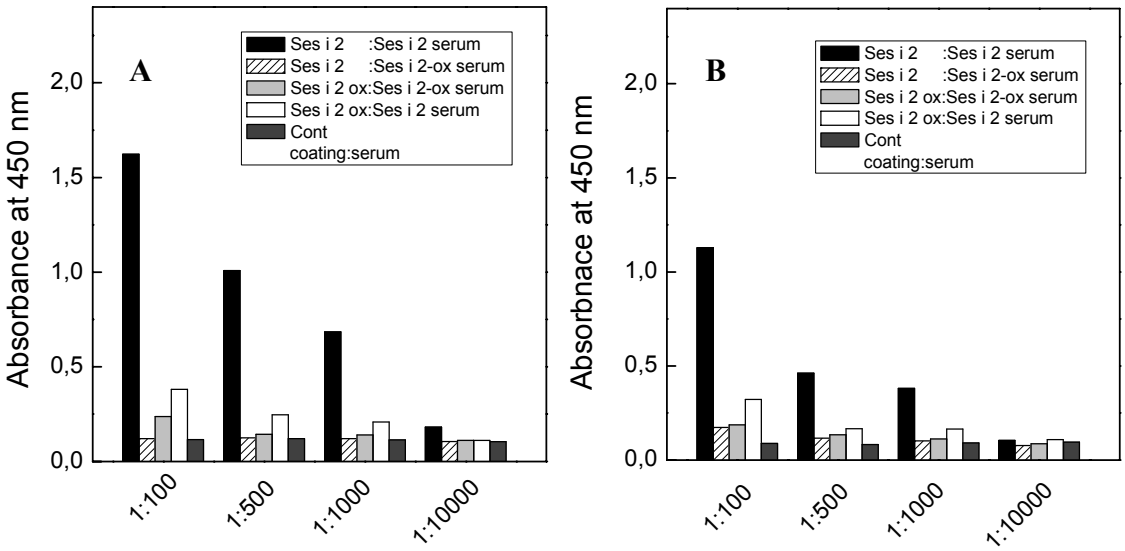

Figure 9. Detection of IgG anti-Ses i 2 and Ses i 2-ox in immunized mice serum. ELISA analysis were performed on to high affinity (A) and hydrophilic (B) 96-well plates.

The low Ses i 2 serum/Ses i 2-ox complexes levels implicate a strong contribution of conformation in IgG allergen recognition. At the same time the probable exposition of linear epitopes in Ses i 2-ox weakly stimulates an antibodies recognition.

Cytokines production and costimulatory molecules expression by DCs

Atopic disease are associate with elevated serum levels of both total and allergen-specific IgE. Production of IgE is controlled by T cells that provide cognate and non-cognate signals for B cells and that secrete various cytokines characteristic of the 'pro-allergenic' type 2 phenotype. In addition to inducing a humoral immune response, these cytokines control and modulate the functional state of effector cells, such as eosinophils, basophils and mast cells, which, upon activation produce additional amounts of cytokines including IL-4 and IL-5 and thus help to perpetuate the allergic immune response (Daser et al, 1995). The process of allergic sensitization is initiated by the presentation of allergens to T cell by antigen-presenting cells (APCs) as dentritic cells (DCs). CD4+ helper T cells recognized short peptides stably associated with class II MHC molecules displayed on the surface of APCs. Antigens that do not have access to DCs are ignored by T cells, while those that do have access to DCs can stimulate naïve T cells, driving their proliferation and differentiation or, in a special circumstances, their deletion (Lanzavecchia and Sallusto, 2001). The amount of signal that T cells receive is dependent on three factors: (1) the level of peptide-MHC complexes that initiate the signal transduction, (2) the level of costimulatory molecules that amplify the signal process, and (3) the stability of the synapse between CD4+ cells and DCs

that determines for how long the signaling process is sustained. T helper type 1 (Th1) and type 2 (Th2) cells represent terminally differentiated effector cell chacterised by different cytokine production and homing capacity. DCs promote Th1 and Th2 polarization by IL-12 and IL-4 production, respectively (Lanzavecchia et al, 2001). Other factors that contribute to the Th1-Th2 balance are the dose of antigen, strength of antigenic stimulation, duration of T cell receptor (TCR) engagement and nature of costimulatory molecules. MHC-peptide complexes that interact strongly with TCR favour type 1 responses, whereas weak interaction results in the priming of type 2 responses.

DCs in culture exist in two different functionally and phenotypically distinct states, immature and mature. Immature cells are adept at endocytosis and express relatively low levels of surface MHC calss I and class II products and costimulatory molecules. Abundant MHC class II molecules are synthesized, but they are mainly sequestered intracellulary il late endocytic compartments (lysosome). Antigen can be avidly taken up by immature DCs and targeted to MHC class II-positive lysosome. Most immature DCs exhibit three types of endocytosis: macropinocytosis, phagocytosis, and clathrin-mediated endocytosis. DCs maturation is typically triggered by production of microbial or viral phatogens, such as LPS, proinflammatory cytokines, such as TNFa and, by a variety of non inflammatory patogen-unrelated stimuli. The downregulation of endocytosis begins soon after the receipt of maturation signal, but clathrin-coated vescicle formation appears to continue, so mature DCs must not be considered as being completely incapable of endocytosis. One of the hallmarks of DC maturation is dramatic increased in surface MHC class II and costimulatory molecules. MHC class II products can increase some 5- to 20-fold while CD 86 (B7.2) increases up to 100-fold, these accessory molecules that interact with receptors on T cells to enhance adhesion and signalling (co–stimulation). Mature DCs synthesize high levels of IL-12 that enhance both innate and acquired immunity.

With the intent to elucidate a possible different stimulation of dendritic cells induced by genuine and oxidized 2S allergen we have qualitatively studied the cytokine production by DCs. When localized in peripheral blood or in nonlymphoid tissue, DC are considered to be functionally immature. This refers to the facts that DC in tissues are highly specialized for capturing and processing foreign or autologous protein antigens or haptens (Novak et al., 1999). Thus, we studied cytokines production such as IL-4, IL-12p70 and IL-10 by immature and mature DCs. Treatment of DCs with pathogen molecules such as bacterial LPS results in strong induction of maturation DCs. Immature cells are adept at endocytosis and express

relatively low levels of surface MHC class I and II products and costimulatory molecules (e.g., CD86) (Mellman and Steinman, 2001).

These cytokines were detected in the culture supernatant at 12 h or 24 h of stimulation with 10 µg of Ses i 2 or Ses i 2-ox. Previously, Ses i 2 and Ses i 2-ox were incubated in cell culture medium with the intent to demonstrate the proteins stability in the culturing conditions. Data confirmed the stability of both proteins during the stimulation period of DCs. Our results show that the absolute amounts of cytokines produced by DCs from different donors in response to stimulations varied considerably, but the trends are consistently superimposable.

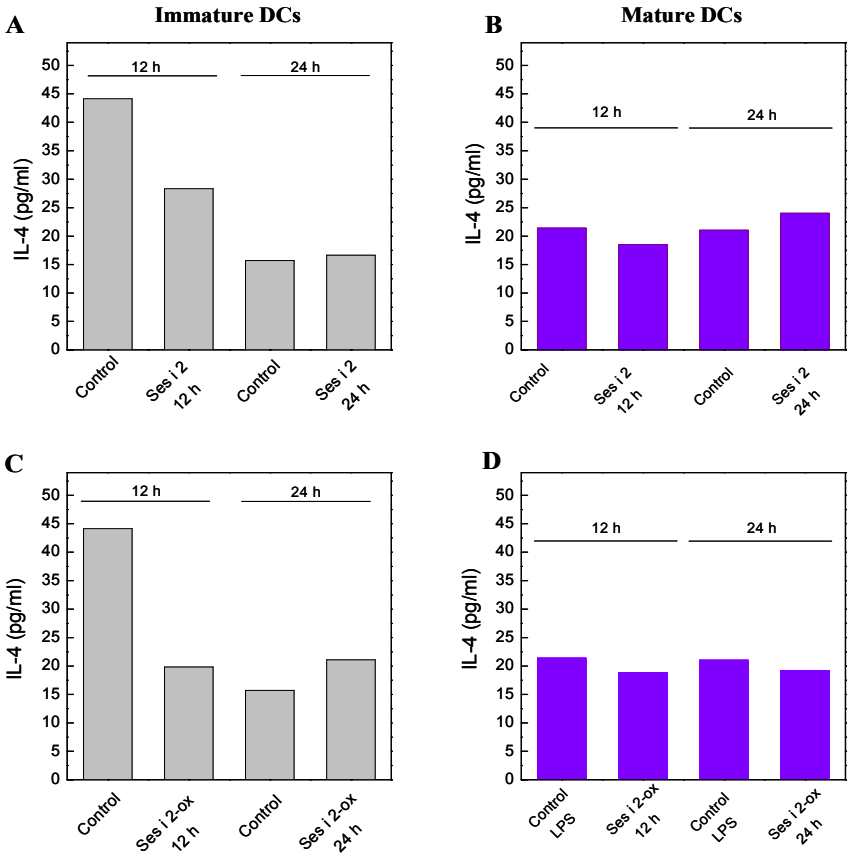

Figure 10. IL-4 production by immature (A-C) and mature DCs (B-D) stimulated with Ses i 2 and Ses i 2-ox. Concentration of IL-4 presents in the culture supernatants at 12 h or at 24 h, and after 24 h of stimulation with LPS for mature DCs, as determined by ELISA. Shown is one representative experiment of four conducted with different DC preparations. The ELISA values of production were comparable among different experiments, whereas the amounts varied among different donors.

IL-4 is a pleiotropic cytokine with a regulatory effects on B and T cells growth, function, immunoglobulin switching and is a critical factor for the development of type 2 immune response (Feghali et al., 1997). Data suggest that immature DCs have a low physiological production of IL-4, stimulation with Ses i 2 induces slight effect on IL-4 production with a

decrease in cytokine expression at 12 h, while at 24 h of stimulation is detectable a weak increment in IL-4 production (Figure 10A). Results in stimulation of immature DCs are in agreement with collected data in mature DCs that show a physiological decrease of the IL-4 expression, thus stimulation with Ses i 2 (Figure 10B) is not able to induce a strong effects on IL-4 production with a very weak decrease at 12 h and a limited increase at 24 h.

Incubation of immature DCs with Ses i 2-ox induces at 12 h a decrease in IL-4 level comparable with effect of Ses i 2. In the subsequent 12 h, IL-4 production physiologically decreases and stimulation in the presence of Ses i 2-ox induces a weak increase in IL-4 production (Figure 10C). Mature DCs show a physiological decrease of the IL-4 expression and stimulation with Ses i 2-ox (Figure 10D) does not induce a strong effects on IL-4 production with a very weak rise at 12 h and at 24 h. These data suggest that both proteins show appreciable effects on immature DCs, while in mature DCs the effect is minimized.

In contrast, Ses i 2 on immature DCs induces strong up-regulation of IL-10 secretion (Figure 11A); production of this cytokine follows a specific kinetic in which IL-10 accumulation is started at 6 h and its production is sustained and increased until at least 24 h (Langenkamp et al, 2000).

IL-10 induces a reduction of antigen-specific T-cell proliferation, inhibition of IL-2-incduced IFN-γ production by NK cells, and a inhibition of IL-4 and IFN-γ induced MHC class II expression on monocytes. Treatment of DCs with pathogen molecules as LPS results in a strong induction in the IL-10 basal expression with an accumulation at 24 h. The results reported above suggest that LPS interferes with capacity of Ses i 2 to induce a IL-10 production by mature DCs, thus LPS leads to generation of partially exhausted dendritic cells. Ses i 2-ox does not induce appreciable effects on immature DCs in the accumulation of IL-10, at 12 h after stimulation is possible to note a weak increment in IL-10 production, at 24 h IL-10 production is substantially comparable to the control, and the same behaviour is manifested by mature DCs (Figure 11 C and D).

Considering the accumulation kinetic data about IL-10, results indicate an incapacity by Ses i 2-ox to stimulate IL-10 production in DCs (Figure 11).

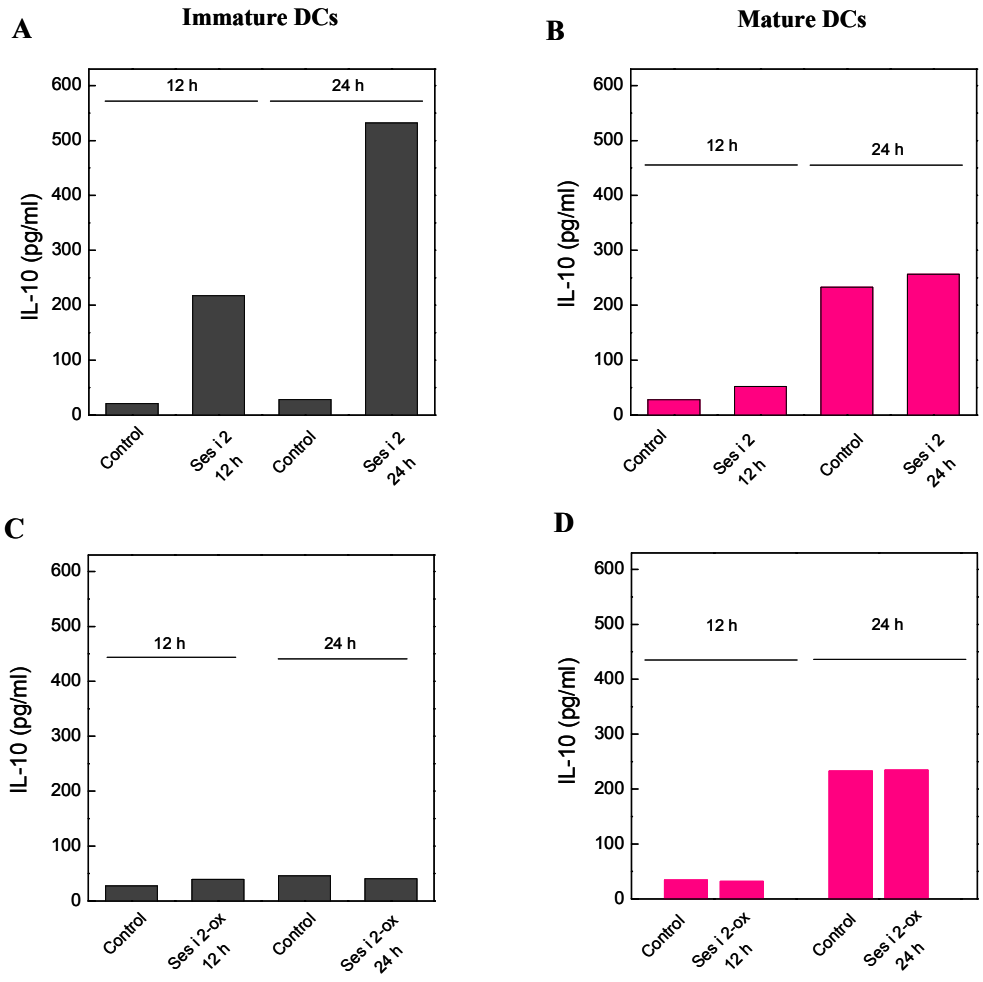

Figure 11. IL-10 production by immature (A-C) and mature DCs (B-D) stimulated with Ses i 2 and Ses i 2-ox. Concentration of IL-10 presents in the culture supernatants at 12 h or at 24 h, and after 24 h of stimulation with LPS for mature DCs, as determined by ELISA. Shown is one representative experiment of four conducted with different DC preparations. The ELISA values of production were comparable among different experiments, whereas the amounts varied among different donors.

Finally, we have measured the accumulation of IL-12p70 in culture medium at 12 h and 24 h of stimulation in the presence of Ses i 2 and Ses i 2-ox. IL-12 is a cytokine composed by two disulfide-linked subunits of 35 kDa (p35) and 40 kDa (p40). These associate to form the bioactive heterodimer of 70 kDa (p70). Many APCs produce some IL-12, but dendritic cells have been shown to be the major producers, and their intimate contact with T cells during initiation of a primary immune response implicates them as major inducers of Th1 versus Th2 polarization (Macatonia et al., 1995; Heufler et al., 1996).

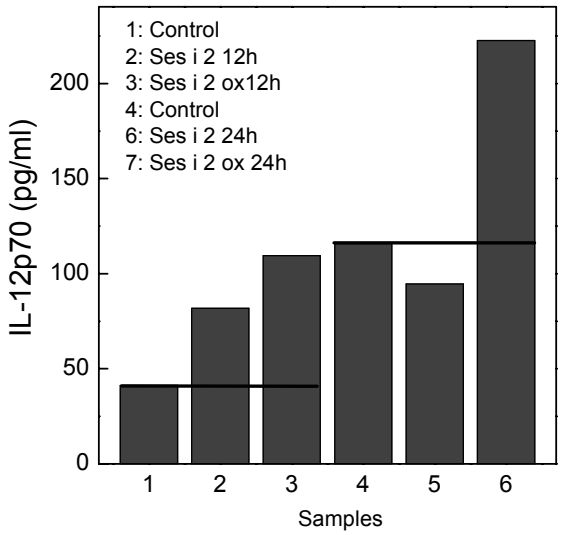

Figure 12. IL-12p70 production by immature DCs stimulated with Ses i 2 and Ses i 2-ox. Concentration of IL-12p70 presents in the culture supernatants at 12 h or at 24 h, and after 24 h of stimulation with LPS for mature DCs, as determined by ELISA. Shown is one representative experiment of four conducted with different DC preparations. The ELISA values of production were comparable among different experiments, whereas the amounts varied among different donors.

Genuine and oxidized allergens in immature DCs cultures are able to stimulate an accumulation of IL-12p70 at 12 h, while at 24 h Ses i 2-ox stimulates a strong increment in the IL-12 p70 production, while Ses i 2 is not able to stimulate an enhancement of IL-12p70 (Figure 12). Langenkamp and co-workers (Langenkamp et al, 2000) have demonstrated that IL-12p70 subunit is detectable only after 10 h but rapidly reached a plateau 12 to 18-24 h after stimulation. Maturation of DCs with LPS implies a dramatic decrease in IL-12p70 production, thus in our experiments the accumulation of IL-12 in mature was not measured DCs culture.

The polarization of T cell cytokine production patterns in to the Th1 or Th2 types has become important to elucidate the mechanism to the basis of allergic response. The above results might explain the pivotal role of IL-12p70 in the allergic response. There is a strong correlation among IL-4 expression and IL-12p70 production by DCs, in fact, IL-4 directly promotes Th2 differentiation from Th0 cells, also a low level of IL-4 has the potential to promote Th1 differentiation. This is an indirect effect, via the action of IL-4 on DCs to enhance the production and bioactivity of IL-12 by decreasing IL-10 expression. Nicoletti and co-workers (Temblay et al., 2007) have demonstrated that IL-4 loses the ability to induce the production of IL-12 by failing to instruct DCs (PPs obtained by C3H/HeJ sensitized mice) to produce less IL-10. Moreover, in atopy and hypersensivities, additional monocyte-derived factor, like a PGE_2, might contribute to the polarization into T-cell subset, and also acts

directly on B cells Ig production. This effects is partially modulated by IL-10 and IL-4: in the presence of IL-10, immunoglobulin secretion is enhanced, whereas in presence of IL-4, IgG and IgE production is inhibited (Daser et al, 1995). Our data are in close agreement with the above 'cytokines-phtaway'. Ses i 2 shows a low capability to stimulate the IL-4 production and at the same time it is strongly able to induce the accumulation of IL-10, overall these data may be related with a weak increment at 12 h and with the decrease at 24 h of the IL-12p70 expression. Ses i 2 enhances IL-10 and this cytokine through PGE_2 pathway may induce an increment in Ig production primary IgE in atopic individual. Ses i 2-ox demonstrates a very different behaviour with a slight rise in the IL-4 production at 24 h together with a substantial incapacity to stimulate IL-10 production. Results converge in extraordinary capacity of Ses i 2-ox to induce IL-12p70 production. The above data indicate a possible induction of Th2 response by Ses i 2, while Ses i 2-ox might induce a Th1 response. Overall our findings show a clear involvement of oxidative process in the balance of immune response, thus oxidative mechanisms in inflammation sites could be fundamental to develop a 'self-immune response' against allergens, this function can be explain by a close correlation between oxidative damage-protein unfolding and antigen processing pathway. These conclusion are in strong agreement with the observation whereby no difference in IL-12p70 production have been detected among DCs derived from atopic or non-atopic patients (Bellinghausen et al., 2000).

Indeed, the cytokines production is one way whereby DCs communicate and influence the T CD4+ response. The fundamental process or primary stimulus is complex formation between MHC-class II-peptide complexes and TCR. Other important mechanism is represented by co-stimulatory molecules, in fact, to become fully activated, T cells require additional signals by expression on the DCs surface of co-stimulatory molecules, that are the secondary stimulus in Th response. Co-stimulatory molecules cannot activate T-cells without concomitant TCR-MHC class II-peptide cross-linking. The dependence of T-cell activation on this "second signal" delivered by co-stimulatory molecules adds a second line of regulation to antigen-specific T-cell responses that reaches far beyond a mere "on-off" command. Co-stimulatory molecules interact with a specific receptor on the surface of T-cell and modify the effector phase of T-cell activation by inducing or suppressing the production of cytokine, by influencing cell survival or apoptosis, or by the up-regulation of the other cell surface molecules. In general co-stimulatory molecules are divided into main families: molecules from the B7:CD28 family that have a key roles in regulating T-cell activation and tolerance, such as CD80 (B7-1) and CD86 (B7-2), and from tumor necrosis factor receptor superfamily (TNFR) such as OX40 or CD27. Thus, we examined the effects of exposure to

Ses i 2 or Ses i 2-ox on the expression of DC co-stimulatory molecules by flow cytometry. Our experiments were focused on expression of CD80 (B7-1), CD86 (B7-2) and HLA-DR (MHC class II). The controls of our experiments show a high expression of co-stimulatory molecules, in fact, DCs are able to produce significant levels of B7-1 and B7-2 (Figure 13). Surprisingly, the expression of CD80 is not significantly altered after stimulation with Ses i 2, while the production of CD86 is slightly increased at 12 h. At the same time genuine allergen induces an appreciable decrease of HLA-DR (Figure 13). At 24 h of stimulation Ses i 2 is not able to induce effects on CD86 expression, but it slightly rises CD80 levels, while the HLA expression is down-regulated (Figure 13). In contrast, Ses i 2-ox treatment induces a marginal decreases of in MHC-class II, CD80 and CD86 at 12 h (Figure 13). Interestingly, at 24 h, Ses i 2-ox induces an increase of HLA-DR expression.

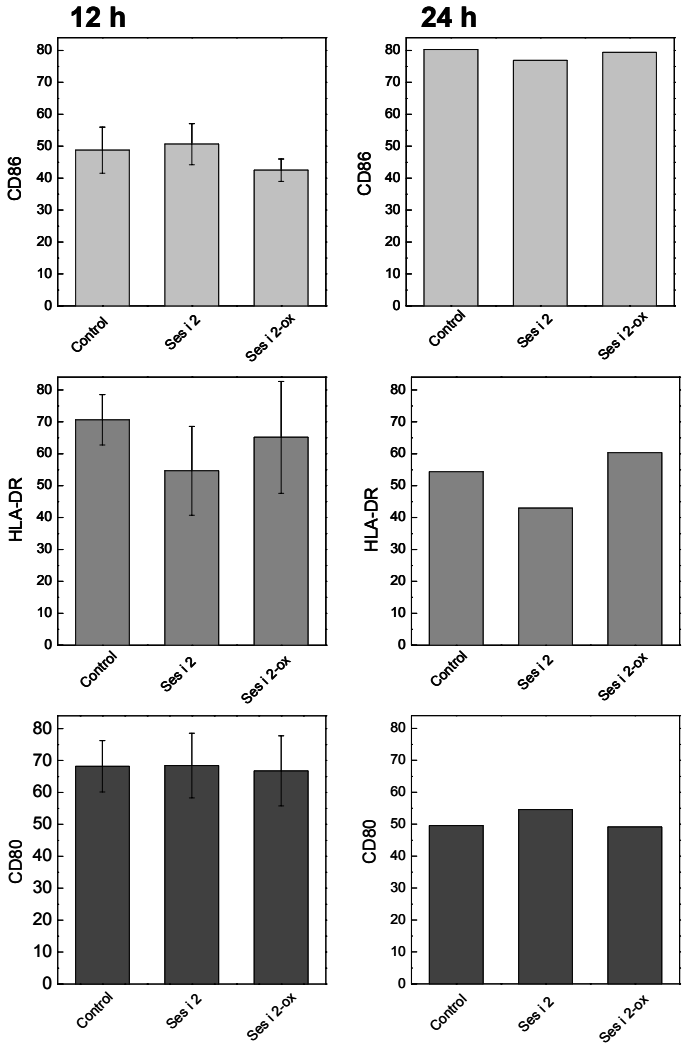

Figure 13.Percentage of co-stimulatory molecules expressed by DCs. DCs cells were treated with 10 µg Ses i 2 or Ses i 2-ox for 12 h or 24 h. Histograms reported the percentage of CD80, CD 86 and HLA of the CD1+ cell population analysed by flow cytometry. Results at 12 h of stimulation are expressed as the mean ± SD from four experiments.

In a simple stimulation model B7-1 and B7-2 may support the polarization of T cells in to type 1 or type 2 T cells, respectively (Kuchroo et al., 1995). The two molecules are constitutively expressed on the DCs surface with different kinetics, and they bind distinct regions of CTLA-4 molecule, and most likely to CD28 molecules. The outcome of co-stimulatory mediated by CD80 and CD86 is different: CD80 stimulates the production of IL-4, as well as IL-2 and IFN-γ production, thus provide an initial source of IL-4, and it acts as co-stimulus for generation of Th1 subset, while CD86 provides only a moderate signal for type 2 differentiation. The co-stimulatory effects are able to producing an effects on T cells only in presence of primary stimulus that is based on MHC-class II presentation pathway. Results show a inhibition in the expression of MHC-class II after stimulation with Ses i 2, while in presence of Ses i 2-ox the production of HLA-DR is enhanced at 24 h. These behaviours may be correlated with the Ses i 2-ox processing by DCs and the subsequent presentation in the complexes with MHC. Ses i 2 is not efficiently or correctly degraded and this compromises its MHC presentation. This effect is associated with the weak rise of CD86 expression together with no increased in the CD80 production and this co-stimulatory pathway may be correlated with incapacity by Ses i 2 to induce a mature phenotype of DCs. The low increment in CD86 expression could reflect the low levels of IL-4 production that favours the IL-10 expression (Ranger et al., 1996). In presence of Ses i 2-ox stimulus DCs show an increase in the HLA-DR production at 24 h without any stimulation in the CD80 or CD86 expression. These data may be correlated to hypothesis that the immature phenotype of DCs associated with the IL-12p70 production are key signals for Th1 response (Lanzavecchia et al., 2001).

CONCLUSION

Allergic response induces an inflammatory state in which MPOS system is able to oxidize Ses i 2 in the corresponding oxidized form. Ses i 2-ox is not stable to the neutrophil serine proteases, principal enzymes issued in extracellular matrix after PMN degranulation, while Ses i 2 is fully resistant to proteolysis. The high susceptibility to proteolysis may explain the low level of IgG anti-Ses i 2-ox in serum of mice immunized with Ses i 2-ox. Oxidation may be a main process in the degradation and modulation of immunogenicity of antigen, thus proteolysis of antigen and the generation of reactive oxidative damage are linked processes (Carrasco-Marin et al., 1995). Our data are in close agreement with this considerations, our ELISA and FACS experiments show a strong dependence among protein structure and immunogenicity of allergen. We examined the effects of genuine and oxidized

proteins on the co-stimulatory molecules and cytokines production by DCs, which are key regulators of the immune response. Our results demonstrate that Ses i 2 and Ses i 2-ox have very different effects on DCs function, particularly in the cytokine production and HLA-DR expression. Ses i 2 might induce a Th2 response by an increment in the expression of IL-10 that is correlated with a down-regulation in the IL-12p70 production. While, Ses i 2-ox might stimulate a Th1 immune response by an up-regulation of IL-12p70 correlated with an increase in the expression of MHC-class II at 24 h of stimulation. Overall data suggest that is possible to change the immunogenicity of an allergen through the introduction of covalent modification such as oxidation.

4.RESULTS

Preliminary Crystallographic Studies

Chapter 4.1

Preliminary Crystallographic Studies of a 2S Albumin Seed Protein Ses i 2 from *Sesamum Indicum*

INTRODUCTION

One of the most widespread groups of plant proteins is the prolamin superfamily, which comprises cereal seed storage proteins, a range of low-molecular-mass sulphur rich proteins (many of which are located in seeds) and some cell wall glycoproteins. This superfamily includes several major types of plant allergen: non-specific lipid transfer proteins, cereal seed, inhibitors of α-amylase and/or trypsin, and 2 S albumin storage proteins of dicotyledonous seeds (Shewry et al., 2002).

As occurs with other groups of storage proteins, the 2S albumins show a high level of polymorphism. These proteins are generally encoded by a multigene family leading to numerous isoforms subjected to post-translational modifications, mainly derived from proteolytic processing; these isoforms may show considerable differences in their structures and biological properties. Nevertheless, it is possible to define the protein structure of a "typical" 2S albumin. The conserved scaffold includes that the third and fourth cysteine residues are consecutive in the polypeptide chain (large subunit) and the fifth and sixth cysteine residues are separated by only one residue. Despite the skeleton of cysteine residues of 2S albumins being highly conserved, a relatively low amino acid sequence homology, within and among plant species, can be observed. As expected, regions spanning the cysteine residues showed the highest amino acid sequence homology whereas the regions showing the lowest amino acid sequence homology corresponded to i) the C-terminal of the small subunit, ii) the NH2-terminal of the large subunit and iii) that contained between the sixth and seventh cysteine residues within the large subunit. Overall, the degree of sequence homology of 2S allergens is low, ranging from 14 to 40 %.

2S albumins adopt a common and compact three dimensional structural scaffold comprising a bundle of five α-helices displayed in different regions (helices Ia, Ib, II, III and IV) and a C-terminal loop folded in a right-handed superhelix stabilized by four conserved disulphide bonds. Connecting the α-helices III and IV, there is an exposed and relatively short

segment known as “hypervariable region” which has been described to be the most important antigenic region of the 2S albumins. The structural homology within the protein family is high and such similarities have recently been exploited in protein modelling studies. Using the 2S albumin structures from rapeseed and castor bean as templates, structural models for the 2S albumins from Brazil nut and English walnut, and those from pecan nut (*Carya illinoinensis*) and peanut have been reported (Alcocer et al., 2002). Strikingly, the global fold is shown to be similar to that of other sulphur rich proteins from the prolamin superfamily like the non-specific lipid transfer proteins from wheat (various species of the genus *Triticum*) or the bifunctional α-amylase/trypsin inhibitor from ragi (*Eleusine coranaca*) (Strobl et al., 1995). The pattern of eight cysteines in specific order appears to be a structural scaffold of conserved helical regions that would form a network of disulphide bridges necessary for the maintenance of the tertiary structure.

In the previous chapter we have isolated and characterized mature form of Ses i 2 (SwissProt code Q9XHP1) the major allergen from white sesame seeds and belongs to the 2S albumin family. In this work, we have purified Ses i 2 in sufficiently large amounts (30 mg) for preliminary crystallization studies. Ses i 2 was purified to homogeneity (> 98%) in two consecutive chromatographic steps, involving size-exclusion chromatography on a sephacryl HR-100 column and semi-preparative RP-HPLC on a C18 coulmn. Subsequently, we have generated the structural homology model of Ses i 2 on the NMR structure of napin from Brassica napus (PDB code 1SM7), revealed that Ses i 2 is arranged in a four-helix bundle topology. Ses i 2 represents a suitable model to investigate the structural features that determine the allergenicity of antigen. Our approach is to investigate the role of Ses i 2 in allergenicity by its structural analyses by X-ray crystallography in order to establish a molecular basis for allergenicity.

Here, we used the x-ray crystallography approach to resolve the structure of Ses i 2. Small crystals of Ses i 2 have been obtained and preliminary diffraction data measured. In this chapter, we report the preliminary crystallographic studies of Ses i 2 from *S. indicum*.

The results have been obtained during my stage in the laboratory of Prof. Giuseppe Zanotti at the department of Biological Chemistry (University of Padua) collaboration with Dr. Laura Cendron. X-ray data collections were performed by Dr. Laura Cendron at the ID29 beamline of ESRF (Grenoble, France).

EXPERIMENTAL PROCEDURES

Extraction and purification of Ses i 2 from sesame seeds. To 1 g of coarsely ground sesame seeds were added 10 ml of 0.1 M Tris-HCl buffer, pH 8.0, containing 0.2 M NaCl. The mixture was gently stirred at room temperature for 24 h on a model 708 Asal (Milan, Italy) rotating stirred. Thereafter, the suspension was centrifuged at 13000 r.p.m. for 5 min and the supernatant filtered on 0.45-μm durapore filters (Millipore, Badford, MA, USA). 1 ml of the crude extract (~ 8 mg) was loaded onto a (1.6 x 60 cm) column (Pharmacia Fine Chemicals), packed in-house with Sephacryl HR-100 and eluted in the same Tris-HCl buffer at a flow-rate of 0.8 ml/min. In a second step, the fractions (1.5-2.0 ml each) corresponding to Ses i 2 eluted from the Sephacryl column were pooled, lyophilised and further purified by reversed-phase high-performace liquid chromatography (RP-HPLC) on a Grace-Vydac (The Separation Group, Hesperia, CA, USA) C18 semi-preparative column (1 x 25 cm, 5 μm, 300 Å porosity), eluted with a linear acetonitrile-0.1% TFA gradient, at a flow rate of 1.5 ml/min (see previous chapter).

Crystallization conditions. The purified protein was dialyzed to remove residual TFA impurity against a buffer containing 5 mM sodium acetate pH 5.5 for 24 h at 4°C (dialysis buffer was changed four times). The sample was finally concentrated to 5 mg/ml and used for crystallization trials, partially automated using an Oryx 8 crystallization robot (Douglas Instruments), working on 96 wells plates.

Solution of Ses i 2 (5 mg/ml) was crystallized by sitting-drop vapour-diffusion performed at 20°C. Drops containing equal volumes (0.6 μl) of protein solution (5 mg/ml) and precipitant solution were mixed and left equilibrating against 90 μl of the same precipitant solution, at 20°C. Initial crystallization experiments were set up using Crystal Screens I and II (Hampton Research) as well as many other independently designed conditions. Poorly diffracting crystals were obtained in in presence of 0.2 M K+/Na+ tartrate, 0.1 M sodium citrate, pH 5.6, and 2 M ammonium sulphate. Additionally, pH and precipitant variations were also tried with the intent to rise the crystals dimension and homogeneity. To improve the quality of these first crystals we performed many trials adjusting the concentration of the precipitant solution components, primarily concentration of ammonium sulphate was incremented to a final concentration of 2.22 M to facilitate the crystals growth. Then stock solution of precipitant agent was mixed with different amounts of co-solvents and additives such as glycerol, IPA, fos-choline-12, fos-choline-8, Octyl-glucoside, DDAO and zwitterionic agent.

Bunches of very thin and small platelets appeared after more then 1 month in the conditions were the protein was incubated with the precipitant agent in presence of 0.22 CMC fos-choline-12.

In order to obtain a major quality of crystals, Ses i 2 solution (5 mg/ml) in presence of fos-choline-12 (0.22 CMC) was subjected to other crystallization trials with PATC screen (Qiagen GmbH, Hilden, Germany). These crystallization trials were also performed by seeding techniques. Several datasets were collected on single crystals, under cryogenic conditions. The first small crystals available were measured at the ID29 beamline of ESRF (Grenoble, France).

Data collection. The best resolution data set (2.05 Å resolution) was collected at the ESRF beamline ID29 (Grenoble, France). An entire set of data was measured on a frozen crystal frozen in liquid N_2 at 100°K from a single crystal, with a wavelength of 0.97627 Å. Crystals belong to space group $P2_1$, with cell parameters a = 45.47 b = 56.65, c=61.02 Å, β=107.4°. The datasets were processed and scaled with programs MOSFLM and SCALA (Leslie A.G., 2006; Evans P., 2006) both included in the crystallographic package ccp4 (Collaborative Computational Project, Number 4 1994). The asymmetric unit dimensions are compatible with the presence of two monomers, corresponding to a V_M of 2.13 $Å^3$/Da and a solvent content of about 42% of the crystal volume, even if these data need to be confirmed only after the structure determination, which is still in progress.

PRELIMINARY RESULTS

The basic building block of a crystal is the unit cell which is a microscopic repeating unit within the crystal. This may be thought of as a box of six faces or sides, defined by three lengths a, b, c and three angles α, β, γ which are collectively referred to as lattice constants. The unit cell may contain part of a molecule, a single molecule or several molecules of the species under investigation. To arrive at a final structure, however, it is essential that the volume of unit cell is equal to or greater than the volume of one molecule. The unique part of the unit cell is called the asymmetric unit. A crystal may be thought of as a succession of symmetry operations around symmetry elements on the asymmetric unit of the unit cell to produce crystal lattice.

Our data demonstrate that biggest and less disorder plates are formed in precipitant agent in 0.2 M K+/Na+ tartrate, 0.1 M sodium citrate, pH 5.6, and 2 M ammonium sulphate added with 0.22 CMC fos-choline-12 after 1 month of incubation at 20°C (Figure 1).

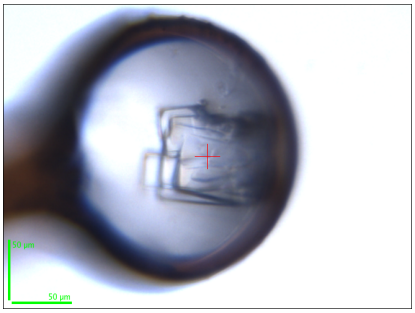

Figure 1. Plates of Ses i 2 crystal.

Data set of Ses i 2 crystal was collected and diffraction of X-ray results in a pattern which is mathematically related to the pattern of the crystal lattice. The diffraction patterns obtained contains information we use to calculate the molecular structure. In Figure 2 is reported a frame image of Ses i 2 crystal that represents a two-dimensional array of 'spot' of particular position and intensity (reflections). In order to convert this into three-dimensional structure it is necessary to collect a data set of many such diffraction patterns from a single Ses i 2 crystal. The data sets were processed and scaled with programs MOSFLM and SCALA and data collected are summarized in the table 1.

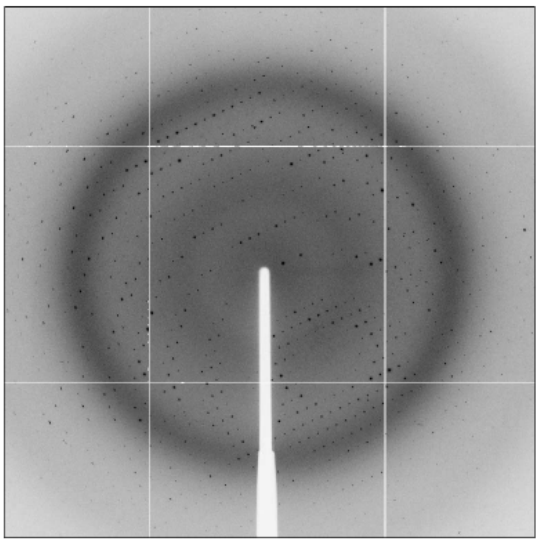

Figure 2. Image of a diffraction frame of Ses i 2.

Table I. Statistics on data collection and refinement.

X-ray data	
Wavelength [Å]	0.97627
Space group	$P2_1$
Cell parameters [Å, °]	a=45.47 b=56.65, c=61.02, β=107.4°
Resolution (Å)	43.39-2.00 (2.11 – 2.00)
Unique reflections	18935 (2745)
Multiplicity	3.3 (3.4)
Completeness (%)	99.8 (99.8)
<I/σ(I)>	6.2 (1.6)
Rmerge	0.079 (0.41)

In order to show the crystal symmetry in Figure 3 are reported images about the reciprocal space planes h0l and hk0.

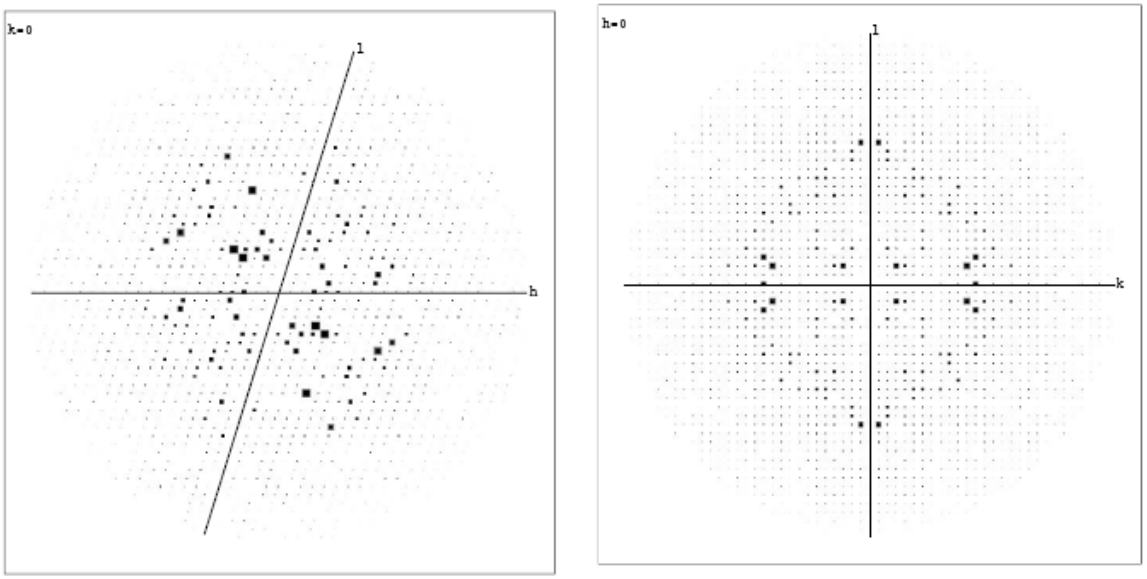

Figure 3. Lattice Planes h0l and hk0.

2s albumin family presents a low degree of sequence identity with a high degree of polimorfism in primary amino acid sequence (Figure 4).

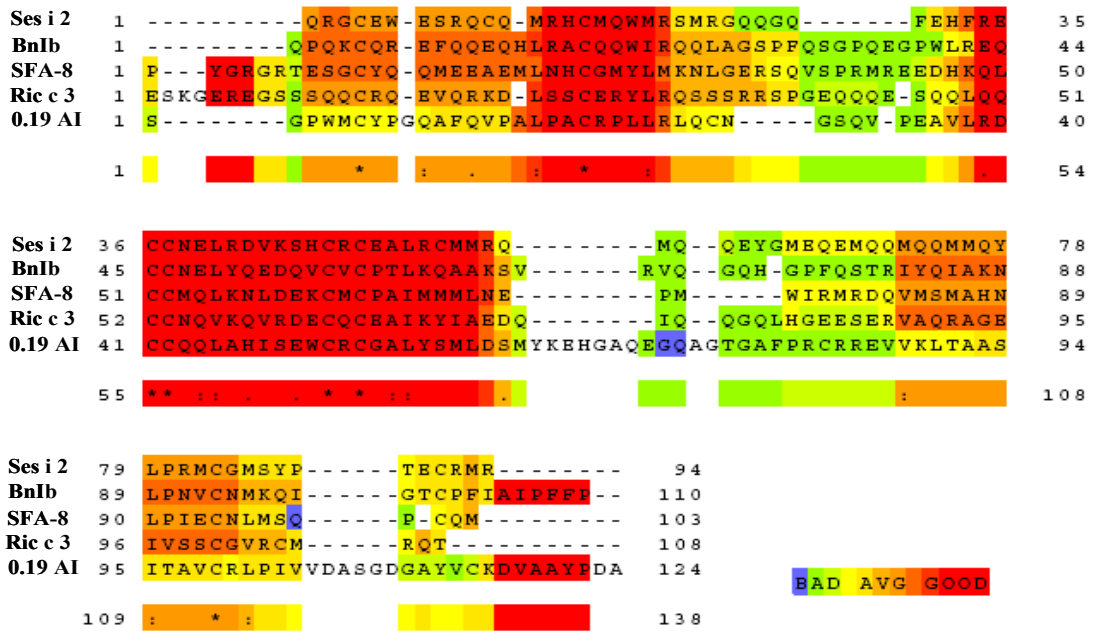

Figura 4. Multiple primary sequence alignment of allergenic 2S albumins from different species BnIb, Ses i 2, Ric c 3, SFA-8 and alpha-amylase inhibitor 0.19 AI. Alignment was performed using T-COFFEE (slow pair method) (Notredame et al., 2000). Numbers indicate the sequence position. Asterisks represent residue conservation among all the sequences.

These observations imply the molecular replacement method in the resolution of protein structure. Even when identity between pairs of proteins is limited or localized, molecular replacement can be carried out on fragments of their structures. Many trials of molecular replacement both using Phaser and MolRep software were performed using different models of the protein, derived from the 2s albumin family such as recombinant precursor of the 2S albumin BnIb (PDB code: 1SM7) from *Brassica napus,* SFA-8 *2s albumin from Helianthus annuus* (PDB code 1S6D), Ric c 3 *from Ricinus comunis* (PDB code 1PYS). Also, other trials were performed using models of alpha-amylase inhibitors of prolamin superfamily as 0.19 alpha-amylase inhibitor from wheat kernel *Triticum aestivum* (PDB code 1HSS). Unfortunately, till now, none of the models produced a reasonable experimental solution, most likely due to a slight shift of some the four helices or the flexible loops that connect the more structured core of the protein.

APPENDIX

Mass Data of Ses i 2

Light Chain

Mass (a.m.u)	Position	Peptide sequence	Modification
2455.0 (2438.1)	25-43	SRQCQMRHCMQWMRSMRGQ	Met ox (a,b,c)
890.3 (907.9)	18-24	QRGCEWE	Pyroglutamic acid

Heavy Chain

Mass (a.m.u.)	Position	Peptide sequence	Modification
3259.3 (3259.9)	98-123	MQQMQQMMQYLPRMCGMSYPTECRMR	
2712.1 (2713.2)	98-119	MQQMQQMMQYLPRMCGMSYPTE	
2004.8 (2005.3)	80-95	ALRCMMRQMQQEYGME	
1523.6 (1524.8)	80-91	ALRCMMRQMQQE	
1345.6 (1345.5)	69-79	LRDVKSHCRCE	
1159.5 (1177.2)	56-64	QGQFEHFRE	Pyroglutamic acid
1037.2 (1037.01)	61-68	HFRECCNE	
756.2 (755.2)	92-97	YGMEQE	
591.2 (607.6)	56-60	QGQFE	Pyroglutamic acid
587.3 (587.6)	61-64	HFRE	

Abbrevations

Å	Angstrom
Da	Dalton
DTT	Dithiothreitol
DC	Dendritic Cell
PMN	Polymorphonuclear cell
EDTA	Ethylene Diamino Tetracetic Acid
Ig	Immunoglobulin
SDAP	protein allergen databan
TCR	T cell receptor
MHC	Major Histocompatibility compelx
IL	interleukin
PEG	PolyEthyleneGlycol
LC	light chain
HC	heavy chain
FITC	fluorescein isothiocyanate
TFA	Trifluoroacetic Acid
Tris	Tris(hydroxymethyl)aminomethane
PBS	phosphate buffer saline
TOF	Time of flight
UV	ultraviolet
SDS	Sodium Dodecyl Sulfate
SDS-PAGE	SDS-polyacrylamide gel Electrophoresis
ESI	Elettrospray Ionization
HPLC	High-Pressure Liquid Chromatography
Th1	T cell subtype 1
Th2	T cell subtype 2

Amino Acids

Alanine	Ala	A
Arginine	Arg	R
Aspartic acid	Asp	D
Asparagine	Asn	N
Cysteine	Cys	C
Glutamine	Gln	Q
Glutamic	Glu	E
Glycine	Gly	G
Histidine	His	H
Isoleucine	Ile	I
Leucine	Leu	L
Lysine	Lys	K
Methionine	Met	M
Phenylalanine	Phe	F
Proline	Pro	P
Serine	Ser	S
Threonine	Thr	T
Tryptophan	Trp	W
Tyrosine	Tyr	Y
Valine	Val	V

References

Aalberse R.C. Structural biology of allergens. J Allergy Clin Immunol. (2000) **106**(2):228-38.

Abraham G.N. and Podell D.N. Pyroglutamic acid. Non-metabolic formation, function in proteins and peptides, and characteristics of the enzymes effecting its removal. *Mol Cell Biochem.* (1981) **38** Spec No(Pt 1):181-90.

Abraham G.N., Podell D.N. Pyroglutamic acid. Non-metabolic formation, function inproteins and peptides, and characteristics of the enzymes effecting its removal. *Mol Cell Biochem.* (1981) **38** Spec No(Pt 1):181-90.

Agizzio A.P., Carvalho A.O., Ribeiro Sde F., Machado O.L., Alves E.W., Okorokov L.A.,Samarão S.S., Bloch C. Jr, Prates M.V., Gomes V.M. A 2S albumin-homologous protein frompassion fruit seeds inhibits the fungal growth and acidification of the medium by Fusarium oxysporum. *Arch Biochem Biophys.* (2003) **416**(2):188-95.

Ahrsad S.H., Suresh Babu K., Holgate S.T. Anti-IgE therapy in asthma and allergy. (2001) ed. Martin Dunitz LTD, London.

Alcocer M. J. C., Murtagh G. J., Bailey K., Dumoulin M., Sarabia Meseguer A., Parker M. J., Archer D. B. The disulphide mapping, folding and characterisation of recombinant *Ber e* 1, an allergenic protein, and SFA8, two sulphur-rich 2 S plant albumins. *J. Mol. Biol.* (2002) **324**, 165-175.

Astwood J. D., Leach J. N., Fuchs R. L. Stability of food allergens to digestion in vitro. *Nat. Biotechnol.* (1996) **14**, 1269-1273.

Baud F, Pebay-Peyroula E., Cohen-Addad C., Odani S., Lehmann M.S. Crystal structure of hydrophobic protein from soybean; a member of a new cysteine-rich family. *J Mol Biol.* (1993) **231**(3):877-87.

Becktel W.J. and Schellman J.A. Protein stability curves. Biopolymers. (1987) **26**(11):1859-77.

Beeby M., O'Connor B.D., Ryttersgaard C., Boutz D.R., Perry L.J., Yeates T.O. The genomics of disulfide bonding and protein stabilization in thermophiles. *PLoS Biol.* (2005) **3**(9):e309.

Beier K.C, Kllinich T. and Hamelmann E. Master switches of T-cell activation and differentiation. *Eur. Respir.J*. (2007) **29**: 804-812.

Beier KC, Kallinich T, Hamelmann E. T-cell co-stimulatory molecules: novel targets for the treatment of allergic airway disease. *Eur Respir J.* (2007) **30**(2):383-90.

Bellinghausen I., Brand U., Knop J., Saloga J. Comparison of allergen-stimulated dendritic cells from atopic and nonatopic donors dissecting their effect on autologous naive and memory T helper cells of such donors. *J Allergy Clin Immunol.* (2000) **105**(5):988-96.

Berezovsky I.N., Zeldovich K.B., Shakhnovich E.I. Positive and negative design in stability and thermal adaptation of natural proteins. *PLoS Comput Biol*. (2007) **3**(3):e52.

Beyer K., Grishina G., Bardina L., Grishin A., Sampson H.A. Identification of an 11S globulin as a major hazelnut food allergen in hazelnut-induced systemic reactions. *J Allergy Clin Immunol* (2002) **110**: 517-523.

Bock S.A. and Atkins F.M. Patterns of food hypersensitivity during sixteen years of double-blind, placebo-controlled food challenges. *J Pediatr*. (1990) **117**(4):561-7.

Bousquet J., Björkstén B., Bruijnzeel-Koomen C.A., Huggett A., Ortolani C., Warner J.O., Smith M. Scientific criteria and the selection of allergenic foods for product labelling. *Allergy*. (1998) **53**(47 Suppl):3-21.

Brahms S., Brahms J. Determination of protein secondary structure in solution by vacuum ultraviolet circular dichroism. *J Mol Biol.* (1980) **138**(2):149-78.

Breiteneder H., Mills E.N. Molecular properties of food allergens. *J Allergy Clin. Immunol* (2005) **115**:14-23.

Breiteneder H., Mills E.N.C. Plant food allergens-structural and functional aspects of allergenicity. *Biotechnology Advances* (2005) **23**: 395-399.

Breiteneder H., Radauer C. A classification of plant food allergens. *J. Allergy Clin. Immunol*. (2004) **113**: 821-830.

Bennion B.J. and Daggett V. The molecular basis for the chemical denaturation of proteins by urea. *Proc Natl Acad Sci U S A.* (2003) **100**(9): 5142–5147.

Brot N. and Weissebach H. Biochemistry and physiological role of methionine sulfoxide in proteins. *Arch. Biochem. Biophy.* (1983) **223**: 271-281.

Brown R.E., Jarvis K.L., Hyland K.J. Protein measurement using bicinchoninic acid: elimination of interfering substances. *Anal Biochem.* (1989) **180**(1):136-9.

Brunner M., Walzer M. Absorption of undigested proteins in human beings: the absorption of unaltered fish protein in adults. *Arch Intern Med.* (1928) **42**:173-9.

Canutescu A.A., Shelenkov A.A., Dunbrack R.L. Jr. A graph-theory algorithm for rapid protein side-chain prediction. *Protein Sci.* (2003) **12**(9):2001-14.

Cardin A.D., Demeter D.A., Weintraub H.J. and Jackson R.L. Molecular design and modeling of protein-heparin interactions. *Methods Enzymol.* **203** (1991):556-83.

Cardoso C.R., Provinciatto P.R., Godoi D.F., Ferreira B.R., Teixeira G., Rossi M.A.,Cunha F.Q., Silva J.S. IL-4 regulates susceptibility to intestinal inflammation in murine food allergy. *Am J Physiol Gastrointest Liver Physiol*. (2009) **296**(3):G593-600.

Carrasco-Marín E., Paz-Miguel J.E., López-Mato P., Alvarez-Domínguez C., Leyva-Cobián F. Oxidation of defined antigens allows protein unfolding and increases both proteolytic

processing and exposes peptide epitopes which are recognized by specific T cells. *Immunology.* (1998) **95**(3):314-21.

Chambers S.J., Wickham M.S., Regoli M., Bertelli E., Gunning P.A., Nicoletti C. Rapid in vivo transport of proteins from digested allergen across pre-sensitized gut. *Biochem Biophys Res Commun.* (2004) **325**(4):1258-63.

Chao C.C., Ma Y.S., Standtman E.R. Modification of protein surface hydrophobicity and methione oxidation by oxidative system. *Proc. Natl. Acad. Sci. USA.* (1997) **94**: 2969-2974.

Chapman A.H. Endosomal proteolysis and MHC class II function. *Curr. Opin. Immun.* (1998) **10**: 93-102.

Chu W. and Trout B.L. On the mechanisms of oxidation of organic sulfides by H_2O_2 in aqueous solutions, *J. Am. Chem. Soc.* (2004) **126**: 900–908.

Chu W., Yin J., Wang D.I.C and Trout B.L. Molecular dynamics simulations and oxidation rates of methionine residues of granulocyte colony-stimulating factor at different pH values. *Biochemistry* (2004) **43**: 1019–1029.

Clarke J. and Fersht A.R. Engineered disulfide bonds as probes of the folding pathway of barnase: increasing the stability of proteins against the rate of denaturation. *Biochemistry.* (1993) **32**(16):4322-9.

Coons A.H., Creech H.J., Jones R.N., Berliner E. Demonstration of pneumoccocal antigen in tissues by use of fluorescent antibody. *J. Immunol.* (1942) **45**, 159-170.

Copeland R.A. Enzymes: a Practical Introduction to Structure, Mechanism and Data Analysis. (2000) 2nd ed., J.Wilye & Sons, New York.

Corbett R.J., Roche R.S. Use of high-speed size-exclusion chromatography for the study of protein folding and stability. *Biochemistry.* (1984) **23**(8):1888-94.

Creamer T.P. and Rose G.D. Side-chain entropy opposes alpha-helix formation but rationalizes experimentally determined helix-forming propensities. *Proc Natl Acad Sci U S A*. (1992) **89**(13):5937-41.

Creighton T.E. Proteins: Structures and Molecular Properties. (1993) 2nd ed., W.H. Freeman and Company, New York.

Dalal I., Binson I., Levine A., Somekh E., Ballin A., Reifen R. The pattern of sesame sensitivity among infants and children. *Pediatr Allergy Immunol* (2003) **4**:312-316.

Dalal I., Binson I., Reifen R., Amitai Z., Shohat T., Rahmani S., Levine A., Ballin A., Somekh E. Food allergy is a matter of geography after all: sesame as a major cause of severe IgE mediated food allergic reactions among infants and young children in Israel. *Allergy* (2002) **57**: 362-365.

Daser A., Meissner N., Herz U., Renz H. Role and modulation of T-cell cytokines in allergy. *Curr Opin Immunol.* (1995) **7**(6):762-70.

Davies K.J. Protein oxidation and proteolytic degradation. General aspects and relationship to cataract formation. *Adv Exp Med Biol.* (1990) **264**:503-11.

De Filippis V., Colombo G., Russo I., Spadari B., Fontana A. Probing the hirudin-thrombin interaction by incorporation of noncoded amino acids and molecular dynamics simulation. *Biochemistry*. (2002) **41**(46):13556-69.

De Filippis V., De Antoni F., Frigo M., Polverino de Laureto P., Fontana A. Enhanced Protein Thermostability by Ala --> Aib Replacement. *Biochemistry.* (1998) **37**(6):1686-96.

Delammare L., Pack M., Chang H., Mellman I., Trombetta E.S. Differential lysosomal proteolysis in antigen-presenting cells determinate antigen fate. *Science* (2005) **307**: 1630-1634.

Di Sansebastiano G.P., Paris N., Marc-Martin S., Neuhaus J.M. Regeneration of a lytic central vacuole and of neutral peripheral vacuoles can be visualized by green fluorescent proteins targeted to either type of vacuoles. *Plant Physiol.* (2001) **126**(1):78-86.

Dill K.A. and Shortle D. Denatured states of proteins. *Annu Rev Biochem.* (1991) **60**:795-825.

Douliez J.P., Michon T., Marion D. Steady-state tyrosine fluorescence to study the lipid-binding properties of a wheat non-specific lipid-transfer protein (nsLTP1). *Biochim Biophys Acta*. (2000) **1467**(1):65-72.

Duchardt F., Fotin-Mleczek M., Schwarz H., Fischer R., Brock R. A comprehensive model for the cellular uptake of cationic cell-penetrating peptides. *Traffic.* (2007) **8**(7):848-66.

Ebner C., Hirschwehr R., Bauer L., Breiteneder H., Valenta R., Ebner H., Kraft D.,Scheiner O. Identification of allergens in fruits and vegetables: IgE cross-reactivities with the important birch pollen allergens Bet v 1 and Bet v 2 (birch profilin). *J Allergy Clin Immunol.* (1995) **95**(5 Pt 1):962-9.

Eftink M.R. The use of fluorescence methods to monitor unfolding transition in proteins. *Biophysical J.* (1994) **66**: 482-501.

Esko J.D. and Lindahl U. Molecular diversity of heparan sulphate *J. Clin. Investig.* (2001) **108**:169–173.

Estévez R. and Jentsch T.J. CLC chloride channels: correlating structure with function. Curr. *Opin.Struct.Biol.* (2002) **12**: 531-539.

Evans P. Scaling and assessment of data quality. *Acta Cryst.* (2006) D**62**, 72-82

Fauchere, J., and Pliska V.. Hydrophobic parameters pi of amino-acid side chains from the partitioning of N-acetylamino-acid amides. *Eur. J. Med. Chem* (1983) **18**:369–383.

Fazeli N., Mohammadi N., Afshar Taromi F. A relationship between hydrodynamic and static properties of star-shaped polymers. *Polymer Testing.* (2004) **23**: 431–435

Feder J. A spectrophotometric assay for neutral protease. *Biochem Biophys Res Commun*. (1968) **32**(2):326-32.

Feghali C.A. and Wright T.M. Cytokines in acute and chronic inflammation. *Front Biosci.* (1997) **2**:d12-26.

Felton L. C. AND McMillon C.R. Chromatographically pure fluorescein and tetramethyl rhodamine isothiocyanates.(1961) *Ann.Biochem.* **2**:178-180.

Fernandez-Fuentes N., Zhai J., Fiser A. ArchPRED: a template based loop structure prediction server. *Nucleic Acids Res.* (2006) **34**(Web Server issue):W173-6.

Fittipaldi A., Ferrari A., Zoppé M., Arcangeli C., Pellegrini V., Beltram F., Giacca M. Cell membrane lipid rafts mediate caveolar endocytosis of HIV-1 Tat fusion proteins. *J Biol Chem*. (2003) **278**(36):34141-9.

Fontana A., De Laureto P.P., Spolaore B., Frare E., Picotti P., Zambonin M. Probing protein structure by limited proteolysis. *Acta Biochim Pol.*(2004)**51**(2):299-321.

Fontana A., Zambonin M., Polverino de Laureto P., De Filippis V., Clementi A., Scaramella E. Probing the conformational state of apomyoglobin by limited proteolysis. *J Mol Biol*. (1997) **266**(2):223-30.

Fremont S., Zitounl N., Kanny G., Veneri V., Metche M., Moneret-Vautrin D.A., Nicolas J.P. Allergenicity of some isoforms of white sesame proteins. *Clin Exp Allergy* (2002) **32**: 1211-1215

Fu T.J., Abbott U.R., Hatzos C. Digestibility of food allergens and nonallergenic proteins in simulated gastric fluid and simulated intestinal fluid-a comparative study. *J Agric Food Chem.* (2002) **50**(24):7154-60.

Furmonaviciene R., Ghaemmaghami A.M., Boyd S.E., Jones N.S., Bailey K., Willis A.C. The protease allergen Der p 1 cleaves cell surface DC-SIGN and DCSIGNR: experimental

analysis of in silico substrate identification and implications in allergic responses. Clin Exp Allergy (2007) **37**:231-42.

Gao J., Yin D.H., Yao Y., Sun H., Qin Z., Schoneich C.,Williams T.D., Squier T.C. (1998) Loss conformational stability in calmoldulin upon methionine oxidation. *Biophysical Journal* **74**:115-1134.

Gardner M. L. Absorption of intact proteins and peptides. *Physiology of the Gastrointestinal Tract*, (1994) ed. L. R. Johnson. New York: Raven.

Gekko K, Kimoto A, Kamiyama T. Effects of disulfide bonds on compactness of protein molecules revealed by volume, compressibility, and expansibility changes during reduction. *Biochemistry.* (2003) **42**(46):13746-53.

Gekle M., Drumm K., Mildenberger S., Freudinger R., Gassner B., Silbernagl S. Inhibition of Na+-H+ exchange impairs receptor-mediated albumin endocytosis in renal proximal tubule-derived epithelial cells from opossum. *J Physiol.* (1999) **520** Pt 3:709-21.

Glazer A.N. Specific chemical modification of proteins. *Annu Rev Biochem*. (1970) **39**:101-30.

Griffiths S.W. and Cooney C.L. Relationship between protein structure and methionine oxidation in recombinant human alpha 1-antitrypsin. *Biochemistry.* (2002) **41**(20):6245-52.

Halliwell B., Clement M.V., Long L.H. Hydrogen peroxide in the human body. *FEBS Lett.* (2000) **486**: 10-13.

Hara-Hishimura I., Takeuchi Y., Inoue K., Nishimura M. Vesicle transport and processing of the precursor to 2S albumin in pumpkin. *Plant J.* (1993)**4**(5):793-800.

Hara-Nishimura I.I., Shimada T., Hatano K., Takeuchi Y., Nishimura M. Transport of storage proteins to protein storage vacuoles is mediated by large precursor-accumulating vesicles. *Plant Cell*. (1998) **10**(5):825-36.

Harrison PM, Sternberg MJ. Analysis and classification of disulphide connectivity in proteins. The entropic effect of cross-linkage. *J Mol Biol.* (1994) **244**(4):448-63.

Hawkins C.L., Davies M.J. Inactivation of protease inhibitors and lysozyme by hypochlorous acid: role of side-chain oxidation and protein unfolding in loss of biological function. *Chem Res Toxicol*. (2005) **18**(10):1600-10.

Hawkins C.L., Pattison D.I., Davies M.J. Hypochloride-induced oxidation of amino acids, peptides and proteins. *Amino Acids* (2003) **25**:259-274.

Hefle S.L., Nordlee J.A., Taylor S.L. Allergenic foods. *Crit Rev Food Sci Nutr.* (1996) **36** Suppl:S69-89.

Heufler C., Koch F., Stanzl U., Topar G., Wysocka M., Trinchieri G., Enk A., Steinman R.M., Romani N., Schuler G. Interleukin-12 is produced by dendritic cells and mediates T helper 1 development as well as interferon-gamma production by T helper 1 cells. *Eur J Immunol*. (1996) **26**(3):659-68.

Heyman M., Crain-Denoyelle A.M., Nath S. K., and Desjeux J.F. Quantification of protein transcytosis in the human colon carcinoma cell line Caco-2. *J. Cell. Physiol*. (1990) **143**: 391–395.

Hiraiwa N., Kondo M., Nishimura M., Hara-Nishimura I. An aspartic endopeptidase is involved in the breakdown of propeptides of storage proteins in protein-storage vacuoles of plants. *Eur J Biochem.* (1997) **246**(1):133-41.

Hoofnagle AN, Resing KA, Ahn NG. Protein analysis by hydrogen exchange mass spectrometry. *Annu Rev Biophys Biomol Struct.* (2003) **32**:1-25.
Hooft RW, Vriend G. Improved coordinate reconstruction from stereo diagrams. *J Mol Graph*. (1996) **14**(3):168-72.

Jaenicke R. Stability and stabilization of globular proteins in solution. *J Biotechnol.* (2000) **79**(3):193-203.

Jensen PE. Antigen unfolding and disulfide reduction in antigen presenting cells. *Semin Immunol*. (1995) **7**(6):347-53 .

Johnson D. and Travis J. The oxidative inactivation of human alpha-1-proteinase inhibitor. Further evidence for methionine at the reactive center. *J Biol Chem.* (1979) **254**(10):4022-6.

Kean D.K., Goodbridge H.S, McGuinness S., Harnett M.M., Alcocer M.J.C. and Harnett W. Differential polarization of immune responses by plant 2S seed albumins, Ber e 1,and SFA8. *J Immunol*. (2006) **177**(3):1561-6.

Kelley L.A., Sutcliffe M.J. OLDERADO: on-line database of ensemble representatives and domains. On Line Database of Ensemble Representatives And DOmains. *Protein Sci.* (1997) **6**(12):2628-30.

Khan M.I., Surolia N., Mathew M.K., Balaram P., Surolia A. Fluorescence polarization as a tool to study lectin-sugar interaction. An investigation of the binding of 4-methylumbelliferyl beta-D galactopyranoside to Abrus precatorious agglutinin. *Eur J Biochem*. (1981) **115**(1):149-52.

Kim Y.H., Berry A.H., Spencer D.S., Stites W.E. Comparing the effect on protein stability of methionine oxidation versus mutagenesis: steps toward engineering oxidative resistance in proteins. *Protein Eng.* (2001) **14**(5):343-7.

Klonis, N. and W. H. Sawyer Spectral properties of the prototropic forms of fluorescein in aqueous solution. *J. Fluoresc.* (1996) **6 :** 147-157.

Klonisl N., Clayton A.H.A., Voss E.W., Sawyer W.H. Spectral Properties of Fluorescein in Solvent-Water Mixtures: Applications as a Probe of Hydrogen Bonding Environments in Biological Systems. *Photochemistry and Photobiology*. (1998) **67**(5): 500-51.

Klugerman M.R. Chemical and physical variables affecting the properties of fluorescein isothiocyanate and its protein conjugates. *J Immunol.* (1965) **95**(6):1165-73.

Kolopp-Sarda M.N., Moneret-Vautrin D.A., Gobert B., Kanny G., Brodschii M., Bene M.C., Faure G.C. Specific humoral immune responses in 12 cases of food sensitization to sesame seed. *Clin Exp Allergy* (1997) **27**: 1285-1291.

Koppelman S. J., Nieuwenhuizen W. F., Gaspari M., Knippels L. M. J., Penninks A. H., Knol E. F., Hefle S. L., de Jongh H. H. J. Reversible denaturation of Brazil nut 2S Albumin (Ber e 1) and implication of structural destabilization on digestion by pepsin. *J. Agric. Food Chem.* (2005), **53**, 123-131.

Kortt A.A., Caldwell J.B., Lilley G.G., Higgins T.J. Amino acid and cDNA sequences of a methionine-rich 2S protein from sunflower seed (Helianthus annuus L.). *Eur J Biochem.* (1991) **195**(2):329-34.

Kosuge M., Takeuchi T., Nakase I., Jones A.T., Futaki S. Cellular internalization and distribution of arginine-rich peptides as a function of extracellular peptide concentration, serum, and plasma membrane associated proteoglycans. *Bioconjug Chem*. (2008) **19**(3):656-64.

Kreis M. and Shewry P.R. Unusual features of cereal seed protein structure and evolution. *Bioessays*. (1989) **10**(6):201-7.

Kuchroo V.K., Das M.P., Brown J.A., Ranger A.M., Zamvil S.S., Sobel R.A., Weiner H.L., Nabavi N., Glimcher L.H. B7-1 and B7-2 costimulatory molecules activate differentially the Th1/Th2 developmental pathways: application to autoimmune disease therapy. *Cell.* (1995) **80**(5):707-18.

Lakowicz J.R. (1999). Principles of Fluorescence Spectroscopy 2nd ed. Kluwer Academic/Plenum New York.

Langenkamp A., Messi M., Lanzavecchia A., Sallusto F. Kinetics of dendritic cell activation: impact on priming of TH1, TH2 and nonpolarized T cells. *Nat Immunol.* (2000) **1**(4):311-6.

Laemmli U.K. Cleavage of structural proteins during the assembly of the head of bacteriophage T4. (1970) *Nature* **227**, 680-685.

Lanzavecchia A. and Sallusto F. Regulation of T cell immunity by dendritic cells. *Cell.* (2001) **106**(3):263-6.

Lanzavecchia A. and Sallusto F. The instructive role of dendritic cells on T cell responses: lineages, plasticity and kinetics. *Curr Opin Immunol.* (2001) **13**(3):291-8.

Lee W. and Downey G.P. Leukocyte Elastase Physiological Functions and Role in Acute Lung Injury. *Am J Respir Crit Care Med.* (2001) **164**: 896–904

Lehmann K., Schweimer K., Reese G., Randow S., Suhr M., Becker W.M., Vieths S., Rösch P. Structure and stability of 2S albumin-type peanut allergens: implications for the severity of peanut allergic reactions. *Biochem J.* (2006) **395**(3):463-72.

Lemanske R.F. Jr and Taylor S.L. Standardized extracts, foods. *Clin Rev Allergy.* (1987) **5**(1):23-36.

Lenzner S., Scholtes U., Peters J.H. Focussing human B cell specificity by immunoselection via antigen-presenting cells in vitro. *Immunobiology.* (1998) **198**(5):539-51.

Leslie A.G. The integration of macromolecular diffraction data. *Acta Crystallogr D Biol Crystallogr.* (2006) **62**(Pt 1):48-57.

Levine R.L., Federici M.M. Quantitation of aromatic residues in proteins: model compounds for second-derivative spectroscopy. *Biochemistry.* (1982) **21**(11):2600-6.

Levine R.L., Moskovitz J., Stadtman E.R. Oxidation of methionine in proteins: roles in antioxidant defense and cellular regulation. *IUBMB Life* (2000) **50**: 301-307.

Macatonia S.E., Hosken N.A., Litton M., Vieira P., Hsieh C.S., Culpepper J.A., Wysocka M., Trinchieri G., Murphy K.M., O'Garra A.. Dendritic cells produce IL-12 and direct the development of Th1 cells from naive CD4+ T cells. *J Immunol.* (1995) **154**(10):5071-9.

Marquez L.A., Huang J.T., Dunford H.B. Spectral and kinetic studies on the formation of myeloperoxidase compounds I and II: roles of hydrogen peroxide and superoxide. *Biochemistry.* (1994) **33**(6):1447-54.

Matter K., Stieger B., Klumperman J., Ginsel L., and Hauri H.P. Endocytosis, recycling, and lysosomal delivery of brush border hydrolases in cultured human intestinal epithelial cells (Caco-2). *J. Biol. Chem*. (1990) **265**: 3503–3512.

Mayer L. Mucosal immunity. *Pediatr* (2003) **11**:1595-600.

Mellman I. and Steinman R.M. Dendritic cells: specialized and regulated antigen processing machines. *Cell.* (2001) **106**(3):255-8.

Mills E.N., Jenkins J., Marigheto N., Belton P.S., Gunning A.P., Morris V.J. Allergens of the cupin superfamily. *Biochem Soc Trans.* (2002) **30**(Pt 6):925-9.

Monsalve R.I., Gonzalez de la Peña M.A., Menendez-Arias L., Lopez-Otin C., Villalba M., Rodriguez R. Characterization of a new oriental-mustard (Brassica juncea) allergen, Bra j IE: detection of an allergenic epitope. *Biochem J.* (1993) **293**(Pt 3):625-32.

Monsalve R.I., Lopez-Otin C., Villalba M., Rodríguez R. A new distinct group of 2 S albumins from rapeseed. Amino acid sequence of two low molecular weight napins.*FEBS Lett.* (1991) **295**(1-3):207-10.

Monsalve R.I., Menéndez-Arias L., López-Otín C., Rodríguez R. Beta-turns as structural motifs for the proteolytic processing of seed proteins. *FEBS Lett*. (1990) **263**(2):209-12.

Moreno F. J., Maldonado B. M., Wellner N., Mills E. N. C. Thermostability and in vitro digestibility of a purified major allergen 2S albumin (Ses i 1) from white sesame seeds (*Sesamum indicum L.*). *Biochim. Biophys. Acta* (2005), **1752**, 142-153.

Moreno F. J., Mellon F. A., Wickham M. S. J., Bottrill A.R., Mills E. N. C. Stability of the major allergen Brazil nut 2S albumin (Ber e 1) to physiologically-relevant in vitro gastrointestinal digestion. *FEBS J.* (2005) **272**, 341-352.

Moreno F.J. and Clemente A. 2S Albumin Storage Proteins: What Makes them Food Allergens? *Open Biochem J.* (2008) **2**:16-28.

Moreno F.J., Jenkins J.A., Mellon F.A., Rigby N.M., Robertson J.A., Wellner N., Clare Mills E.N. Mass spectrometry and structural characterization of 2S albumin isoforms from Brazil nuts (Bertholletia excelsa). *Biochim Biophys Acta.* (2004) **1698**(2):175-86.

Müntz K. Deposition of storage proteins. *Plant Mol Biol.* (1998) **38**(1-2):77-99.

Murén E., Ek B., Björk I., Rask L. Structural comparison of the precursor and the mature form of napin, the 2S storage protein in Brassica napus. *Eur J Biochem*. (1996) **242**(2):214-9.

Murtagh GJ, Archer DB, Dumoulin M, Ridout S, Matthews S, Arshad SH, Alcocer MJ. In vitro stability and immunoreactivity of the native and recombinant plant food 2S albumins Ber e 1 and SFA-8. *Clin Exp Allergy.* (2003) **33**(8):1147-52.

Murzin A.G., Brenner S.E., Hubbard T., Chothia C. SCOP: a structural classification of proteins database for the investigation of sequences and structures. *J Mol. Biol.* (1995) **247**(4):536-40.

Myers J.K., Pace C.N., Scholtz J.M. Denaturant m values and heat capacity changes: relation to changes in accessible surface areas of protein unfolding. *Protein Sci.* (1995) **4**(10):2138-48.

Nakase I., Niwa M., Takeuchi T., Sonomura K., Kawabata N., Koike Y., Takehashi M., Tanaka S., Ueda K., Simpson J.C., Jones A.T., Sugiura Y., Futaki S. Cellular uptake of arginine-rich peptides: roles for macropinocytosis and actin rearrangement. *Mol Ther.* (2004) **10**(6):1011-22

Navuluri L., Parvataneni S., Hassan H., Birmingham N.P., Kelly C., Gangur V. Allergic and anaphylactic response to sesame seeds in mice: identification of Sesi 3 and basic subunit of 11s globulins as allergens. *Int Arch Allergy Immunol*.(2006) **140**(3):270-6.

Nelson D.P., Kiesow L.A. Enthalpy of decomposition of hydrogen peroxide by catalase at 25ºC(with molar extinction coefficients of H_2O_2 solutions in the UV). *Anal Biochem*. (1972) **49**(2):474-478.

Nicoletti C. Unsolved mysteries of intestinal M cells. *Gut.* (2000) **47**(5):735-9.

Nishii I., Kataoka M., Goto Y. Thermodynamic stability of the molten globule states of apomyoglobin. *J Mol Biol.* (1995) **250**(2):223-38.

Notredame C., Higgins D.G., Heringa J. T-Coffee: A novel method for fast and accurate multiple sequence alignment. *J Mol Biol*. (2000) **302**(1):205-17.

Novak N., Haberstok J., Geiger E., Bieber T. Dendritic cells in allergy. *Allergy*.(1999) **54**(8):792-803.

Ogihara T., Tamai I., Takanaga H., Sai Y., and Tsuji A. Stereoselective and carrier-mediated transport of monocarboxylic acids across Caco-2 cells. *Pharm. Res*. (1996) **13**: 1828–1832.

Oliveberg M., Arcus V.L., Fersht A.R. pKA values of carboxyl groups in the native and denatured states of barnase: the pKA values of the denatured state are on average 0.4 units lower than those of model compounds. *Biochemistry.* (1995) **34**(29):9424-33.

Ortolani C., Ispano M., Ansaloni R., Rotondo F., Incorvaia C., Pastorello E.A. Diagnostic problems due to cross-reactions in food allergy. *Allergy.* (1998) **53** (46 Suppl):58-61.

Pace C.N. and Shaw K.L. Linear extrapolation method of analyzing solvent denaturation curves. *Proteins.* (2000);Suppl 4:1-7.

Pace C.N. Determination and analysis of urea and guanidine hydrochloride denaturation curves. *Methods Enzymol.* (1986) **131**:266-80.

Pace C.N., Grimsley G.R, Thomas S.T., Makhatadze G.I. Heat capacity change for ribonuclease A folding. *Protein Sci.* (1999) **8**(7):1500-4.

Pan B., Abel J., Ricci M.S., Brems D.N., Wang D.I., Trout B.L. Comparative oxidation studies of methionine residues reflect a structural effect on chemical kinetics in rhG-CSF. *Biochemistry.* (2006) **45**(51):15430-43.

Pantoja-Uceda D., Bruix M., Giménez-Gallego G., Rico M., Santoro J. Solution structure of RicC3, a 2S albumin storage protein from Ricinus communis. *Biochemistry.* (2003) **42**(47):13839-47.

Pantoja-Uceda D., Bruix M., Santoro J., Rico M., Monsalve R., Villalba M. Solution structure of allergenic 2 S albumins. *Biochem Soc Trans.* (2002) **30**: (Pt6):919-24.

Pantoja-Uceda D., Palomares O., Bruix M., Villalba M., Rodríguez R., Rico M., Santoro J. Solution structure and stability against digestion of rproBnIb, a recombinant 2S albumin from rapeseed: relationship to its allergenic properties. *Biochemistry.* (2004) **43**(51):16036-45.

Pardridge W.M. and Boado R.J. Enhanced cellular uptake of biotinylated antisense oligonucleotide or peptide mediated by avidin, a cationic protein. *FEBS Lett*. (1991) **288**(1-2):30-2.

Pastorello E.A., Incorvaia C., Pravettoni V., Ortolani C. Crossreactions in food allergy. *Clin Rev Allergy Immunol.* (1997) **15**(4):415-27.

Pastorello E.A., Varin E., Farioli L., Pravettoni V., Ortolani C., Trambaioli C., Fortunato D., Giuffrida M.G., Rivolta F., Robino A., Calamari A.M., Lacava L., Conti A. The major allergen of sesame seeds (Sesamum indicum) is a 2S albumin. *J Chromatogr B Biomed Sci Appl.* (2001) **756**(1-2):85-93.

Pattison D.I. and Davies M.J. Absolute rate constants for the raction of hypochlorous acid with protein side chains and peptide bonds. *Chem.Res.Toxicol*. (2001) **14**:1453-1464.

Perkins D.N., Pappin D.J., Creasy D.M., Cottrell J.S. Probability-based protein identification by searching sequence databases using mass spectrometry data. *Electrophoresis.* (1999) **20**(18):3551-67.

Pham C.T. Neutrophil serine proteases: specific regulators of inflammation. *Nat. Rev. Immunol*. (2006) **6**(7):541-50.

Pinto M., Robine-Leon S., Appay M.D., Kedinger M., Triadou N., Haffen K., Fogh J. and Zweibaum A. Enterocyte-like differentiation and polarization of the human colon carcinoma cell line Caco-2 in culture. *Biol. Cell* (1983) **47**: 323–330.

Privalov P.L. and Gill S.J. Stability of protein structure and hydrophobic interaction. *Adv Protein Chem.* (1988) **39**:191-234.

Prochiantz A. Messenger proteins: homeoproteins, TAT and others. *Curr.Opin.Cell.Bio.* (2000) **12**:400-406.

Radauer C., Bublin M., Wagner S., Mari A., Breiteneder H. Allergens are distributed into few protein families and possess a restricted number of biochemical functions. *J Allergy Clin Immunol*. (2008) **121**(4):847-52.

Ragone R., Colonna G., Balestrieri C., Servillo L., Irace G. Determination of tyrosine exposure in proteins by second-derivative spectroscopy. *Biochemistry.* (1984) **23**(8):1871-5.

Rahman S., Jolly C.J., Skerritt J.H., Wallosheck A. Cloning of a wheat 15-kDa grain softness protein (GSP). GSP is a mixture of puroindoline-like polypeptides. *Eur J Biochem.* (1994) **1**;223(3):917-25.

Ranger A.M., Das M.P., Kuchroo V.K., Glimcher L.H. B7-2 (CD86) is essential for the development of IL-4-producing T cells. *Int Immunol.* (1996) **8**(10):1549-60.

Rees M.D., Kennett E.C., Whitelock J.M., Davies M.J. Oxidative damage to extracellular matrix and its role in human pathologies. *Free Radic Biol Med.*(2008) **44**(12):1973-2001.

Regis W.C., Fattori J., Santoro M.M., Jamin M., Ramos C.H. On the difference in stability between horse and sperm whale myoglobins. *Arch Biochem Biophys.* (2005) **436**(1):168-77.

Rico M., Bruix M., González C., Monsalve R.I., Rodríguez R. 1H NMR assignment and global fold of napin BnIb, a representative 2S albumin seed protein. *Biochemistry* (1996) **35**(49):15672-82.

Riggs J.L., McAllister R.M., Lennette E.H. Immunofluorescent studies of RD-114 virus replication in cell culture. *J Gen Virol*. (1974) **25**(1):21-9.

Robotham J.M., Teuber S.S., Sathe S.K., Roux K.H. Linear IgE epitope mapping of the English walnut (Juglans regia) major food allergen, Jug r 1. *J Allergy Clin Immunol*. (2002) **109**(1):143-9.

Rost B. PHD: predicting one-dimensional protein structure by profile-based neural networks. *Methods Enzymol.* (1996) **266**:525-39.

Sai, Y., Kajita M., Tamai I., Kamata M., Wakama J., Wakamiya T., Tsuji A.. Intestinal absorption of fluorescencederivated cationic peptide 001-C8-NBD via adsorptive-mediated transcytosis. *Bioorg. Med. Chem* (1998) **6**: 1–8,.

Sampson H.A. Food allergy. Part 1: immunopathogenesis and clinical disorders. *J Allergy Clin Immunol*. (1999) **103**(5 Pt 1):717-28.

Sampson H.A. Food allergy. Part 2: diagnosis and management. *J Allergy Clin Immunol.* (1999) **103**(6):981-9.

Sampson H.A. Food hypersensitivity and dietary management in atopic dermatitis. *Pediatr Dermatol.* (1992) **4**:376-9.

Scheraga H.A. Theory of hydrophobic interactions. *J Biomol Struct Dyn.* (1998) **16**(2):447-60

Schmidt I., Renard D., Rondeau D., Richomme P., Popineau Y., Axelos M.A. Detailed physicochemical characterization of the 2S storage protein from rape (Brassica napus L.). *J Agric Food Chem*. (2004) **52**(19):5995-6001.

Schmidt J., Bosserhoff A.K. Processing of MIA protein during melanoma cell migration. *Int J Cancer.* (2009) **125**(7):1587-94.

Sharov V.S., Schöneich C. Diastereoselective protein methionine oxidation by reactive oxygen species and diastereoselective repair by methionine sulfoxide reductase. *Free Radic Biol Med.* (2000) **29**(10):986-94.

Shechter Y. Selective oxidation and reduction of methionine residues in peptides and proteins by oxygen exchange between sulfoxide and sulfide. *J Biol Chem.* (1986) **261**: 66-70.

Shechter Y., Burstein Y., Patchornik A. Selective oxidation of methionine residues in proteins. *Biochemistry* (1975) **14**: 4497-4502.

Shewry P.R. Plant storage proteins. *Biol Rev Camb Philos Soc.* (1995) **70**(3):375-426.

Shewry P.R., Beaudoin F., Jenkins J., Griffiths-Jones S., Mills E.N. Plant protein families and their relationships to food allergy. *Biochem Soc Trans.* (2002) **30**(Pt 6):906-10.

Shewry, P. R. and Pandya, M. J. (1999) in Seed Proteins (Shewry, P. R. and Casey, R., eds), pp. 563–586, Kluwer Academic Publishers, Dordrecht

Sjöback R., Nygren J. and Kubista M. Absorption and fluorescence properties of fluorescein. *Spectrochimica Acta Part A* (1995) **51**: L7-L21.

Smith D.L., Deng Y., Zhang Z. Probing the non-covalent structure of proteins by amide hydrogen exchange and mass spectrometry. *J Mass Spectrom.* (1997) **32**(2):135-46.

So A.L., Small G., Sperber K., Becker K., Oei E., Tyorkin M., Mayer L. Factors affecting antigen uptake by human intestinal epithelial cell lines. *Dig Dis Sci.* (2000) **45**(6):1130-7.

Stadtman E.R. Covalent modification reactions are marking steps in protein turnover. *Biochemistry*. (1990) **29**(27):6323-31.

Stadtman E.R., Van Remmen H., Richardson A., Wehr N.B., Levine R.L. Methionine oxidation and aging. *Biochimica et Biophysica Acta.* (2005) **1703**: 135-140.

Strickland E.H. Aromatic contributions to circular dichroism spectra of proteins. *CRC Crit. Rev. Biochem* (1974) **3**:113-75.

Strobel S. IgE-mediated (and food-induced) intestinal disease. *Clin Exp. Allergy.* (1995) **25** Suppl 1:3-6.

Strobl S., Mühlhahn P., Bernstein R., Wiltscheck R., Maskos K., Wunderlich M., Huber R., Glockshuber R., Holak T.A. Determination of the three-dimensional structure of the bifunctional alpha-amylase/trypsin inhibitor from ragi seeds by NMR spectroscopy. *Biochemistry.* (1995) **34**(26):8281-93.

Swanson J.A. and Watts C. Macropinocytosis. *Trends Cell Biol.* (1995) **5**(11):424-8.

Szuchman-Sapir A.J., Pattison D.I., Ellis N.A., Hawkins C.L., Davies M.J., Witting P.K. Hypochlorous acid oxidizes methionine and tryptophan residues in myoglobin. *Free Radic Biol Med.* (2008) **45**(6):789-98.

Tai S.S., Wu L.S., Chen E.C., Tzen J.T. Molecular cloning of 11S globulin and 2S albumin, the two major seed storage proteins in sesame. *J Agric Food Chem*. (1999) **47**(12):4932-8.

Taylor S.L., Lehrer S.B. Principles and characteristics of food allergens. *Crit. Rev Food Sci Nutr.* (1996)**36** Suppl:S91-118.

Taylor S.L., Lemanske R.F. Jr, Bush R.K., Busse W.W. Food allergens: structure and immunologic properties. *Ann Allergy.* (1987) **59**(5 Pt 2):93-9.

Temblay J.N., Bertelli E., Arques J.L., Regoli M., Nicoletti C. Production of IL-12 by Peyer patch-dendritic cells is critical for the resistance to food allergy. *J Allergy Clin Immunol*. (2007) **120**(3):659-65.

Tsan M. and Chen J. Oxidation of methionine by human plymorphonuclear leukocytes. *J.Cli.Invest.* (1980) **65**: 1041-1050.

Varela J., Navarro Pico M.L., Guerrero A., García F., Giménez Gallego G., Pivel J.P. Identification and characterization of the peptidic component of the immunomodulatory glycoconjugate Immunoferon. *Methods Find Exp Clin Pharmacol.* (2002) **24**(8):471-80.

Vender R.L. Therapeutic potential of neutrophil-elastase inhibition in pulmonary disease. *J Invest Med* (1996) **44**:531–539.

Vetter I., Kapitzke D:, Hermanussen S., Monteith G.R, Cabot P.R. The Effects of pH on Beta-Endorphin and Morphine Inhibition of Calcium Transients in Dorsal Root Ganglion Neurons. (2006) **7**: 488-499.

Vieille C., Zeikus G.J. Hyperthermophilic enzymes: sources, uses, and molecular mechanisms for thermostability. *Microbiol Mol Biol Rev.* (2001) **65**(1):1-43.
Vitale A. and Hinz G. Sorting of proteins to storage vacuoles: how many mechanisms? *Trends Plant Sci.* (2001) **10**(7):316-23.

Vivian J.T. and Callis P.R. Mechanisms of tryptophan fluorescence shifts in proteins. *Biophys J.* (2001) **80**(5):2093-109.

Vogt W. Oxidation of methionyl residues in proteins: tools, targets, and reversal. *Free Radic Biol Med.* (1995) **18**(1):93-105.

Walzer M. Allergy of the abdominal organs. *J Lab Clin Med.* (1941) **26**:1867-77.

Wan H., Winton H.L., Soeller C., Tovey E.R., Gruenert D.C., Thompson P.J. Der p 1 facilitates transepithelial allergen delivery by disruption of tight junctions. *J Clin. Invest* (1999) **104**:123-33.

Weber P.J., Bader J.E., Folkers G., Beck-Sickinger A.G. A fast and inexpensive method for N-terminal fluorescein-labeling of peptides. *Bioorg Med Chem Lett.*(1998) **8**(6):597-600.

Winterbourn C.C., Kettle A.J. Biomarkers of myeloperoxidase-derived hypochlorous acid. Free *Radic. Biol. Med*. (2000) **29**: 403-409.

Witting P.K., Wu B.J., Raftery M., Southwell-Keely P., Stocker R. Probucol protects against hypochlorite-induced endothelial dysfunction: identification of a novelpathway of probucol oxidation to a biologically active intermediate. *J Biol Chem*.(2005) **280**(16):15612-8.

Wolff N., Cogan U., Admon A., Dalal I., Katz Y., Hodos N., Karin N., Yannai S. Allergy to sesame in humans is associated primarily with IgE antibody to a 14 kDa2S albumin precursor. *Food Chem Toxicol.* (2003) **41**(8):1165-74.

Wolff N., Yannai S., Karin N., Levy Y., Reifen R., Dalal I., Cogan U. Identification and characterization of linear B-cell epitopes of beta-globulin, a major allergen of sesame seeds. *J Allergy Clin Immunol.* (2004) **114**(5):1151-8.

Wüthrich B., Stäger J., Johansson S.G. Celery allergy associated with birch and mugwort pollinosis. *Allergy.* (1990) **45**(8):566-71.

Yasukawa K, Inouye K. Improving the activity and stability of thermolysin by site-directed mutagenesis. *Biochim Biophys Acta*. (2007) **1774**(10):1281-8.

Yoram Shechter. Selective Oxidation and Reduction of Methionine Residuiens Peptides and Proteins by Oxygen Exchange between Sulfoxide and Sulfide. *JBC* (1986) **261**: 1.

Zeldovich K.B., Chen P., Shakhnovich E.I. Protein stability imposes limits on organism complexity and speed of molecular evolution. *Proc Natl Acad Sci U S A.* (2007) **104**(41):16152-7.

Zhang T., Maekawa Y., Hanaba J., Dainichi T., Nashed B.F., Hisaeda H., Sakai T., Asao T., Himeno K., Good R.A. and Katynuma N. Lysosomal cathepsin B plays an important role in antigen processing, while cathepsin D is involved in degradation of the invariant chain in ovalbumin-immunized mice. *Immunology* (2000) **100:** 13-20.

Ringraziamenti

Grazie al Prof. Vincenzo De Filippis per avermi introdotto nel mondo della ricerca dandomi in questi anni la possibilità di conoscere, scoprire e imparare.

Grazie al Prof. Daniele Dalzoppo che è sempre stato presente con la sua conoscenza infinita e la sua sorprendente simpatia.

Grazie ai "vecchi" del laboratorio che hanno reso possibile la magia di far passare cinque anni in un secondo grazie alla simpatia e all'entusiasmo dimostrato sempre anche nei momenti difficili.

Grazie al Prof. Giuseppe Zanotti per la disponibilità dimostrata nel progettare gli esperimenti di cristallografia.

Grazie alla Dott.ssa Laura Cendron del lab. del Prof. Zanotti per la collaborazione negli esperimenti di cristallografia e per le misure cristallografiche. Grazie Laura per la gentilezza, per avermi insegnato e per avere creduto nel cristallo Ses i 2.

Grazie al Prof. Ignazio Castagliuolo per il contributo fondamentale nello sviluppo e nella progettazione degli studi di immunoistochimica.

Grazie alla Dott.ssa Paola Brun del lab del prof. Castagliuolo per la collaborazione negli esperimenti di citofluorimetria e per la disponibilità dimostrata nell'affrontare con entusiasmo ogni idea.

Grazie a tutte le persone e sono davvero molte che hanno contribuito a rendere questi anni indimenticabili…non posso non sorridere se penso ad ogni uno di voi. Tra tutti un grazie particolare va a Chiara.

Grazie a mamma e papà, tanto di quello che ho fatto è merito vostro perché se non avessi avuto il vostro appoggio non sarei riuscita in tutto questo. Questo lavoro è dedicato a voi.